Advances in Polymer Science 246

Rangasamy Jayakumar
Shantikumar Nair *Editors*

Biomedical Applications of Polymeric Nanofibers

Springer

246

Advances in Polymer Science

Advances in Polymer Science

Recently Published and Forthcoming Volumes

Biomedical Applications of Polymeric Nanofibers
Volume Editors: Jayakumar, R., Nair, S.V.
Vol. 246, 2012

Synthetic Biodegradable Polymers
Volume Editors: Rieger, B., Künkel, A., Coates, G.W., Reichardt, R., Dinjus, E., Zevaco, T.A.
Vol. 245, 2012

Chitosan for Biomaterials II
Volume Editors: Jayakumar, R., Prabaharan, M., Muzzarelli, R.A.A.
Vol. 244, 2011

Chitosan for Biomaterials I
Volume Editors: Jayakumar, R., Prabaharan, M., Muzzarelli, R.A.A.
Vol. 243, 2011

Self Organized Nanostructures of Amphiphilic Block Copolymers II
Volume Editors: Müller, A.H.E., Borisov, O.
Vol. 242, 2011

Self Organized Nanostructures of Amphiphilic Block Copolymers I
Volume Editors: Müller, A.H.E., Borisov, O.
Vol. 241, 2011

Bioactive Surfaces
Volume Editors: Börner, H.G., Lutz, J.-F.
Vol. 240, 2011

Advanced Rubber Composites
Volume Editor: Heinrich, G.
Vol. 239, 2011

Polymer Thermodynamics
Volume Editors: Enders, S., Wolf, B.A.
Vol. 238, 2011

Enzymatic Polymerisation
Volume Editors: Palmans, A.R.A., Heise, A.
Vol. 237, 2010

High Solid Dispersion
Volume Editor: Cloitre, M.
Vol. 236, 2010

Silicon Polymers
Volume Editor: Muzafarov, A.
Vol. 235, 2011

Chemical Design of Responsive Microgels
Volume Editors: Pich, A., Richtering, W.
Vol. 234, 2010

Hybrid Latex Particles – Preparation with Emulsion
Volume Editors: van Herk, A.M., Landfester, K.
Vol. 233, 2010

Biopolymers
Volume Editors: Abe, A., Dušek, K., Kobayashi, S.
Vol. 232, 2010

Polymer Materials
Volume Editors: Lee, K.-S., Kobayashi, S.
Vol. 231, 2010

Polymer Characterization
Volume Editors: Dušek, K., Joanny, J.-F.
Vol. 230, 2010

Modern Techniques for Nano- and Microreactors/-reactions
Volume Editor: Caruso, F.
Vol. 229, 2010

Complex Macromolecular Systems II
Volume Editors: Müller, A.H.E., Schmidt, H.-W.
Vol. 228, 2010

Complex Macromolecular Systems I
Volume Editors: Müller, A.H.E., Schmidt, H.-W.
Vol. 227, 2010

Shape-Memory Polymers
Volume Editor: Lendlein, A.
Vol. 226, 2010

Polymer Libraries
Volume Editors: Meier, M.A.R., Webster, D.C.
Vol. 225, 2010

Polymer Membranes/Biomembranes
Volume Editors: Meier, W.P., Knoll, W.
Vol. 224, 2010

Organic Electronics
Volume Editors: Meller, G., Grasser, T.
Vol. 223, 2010

Biomedical Applications of Polymeric Nanofibers

Volume Editors: R. Jayakumar
Shantikumar V. Nair

With contributions by

V. Beachley · G. Brook · K.P. Chennazhi · L. Ghasemi-Mobarakeh · D. Hodde · R. Jayakumar · G. Jin · D. Kai · E. Katsanevakis · J.A. Kluge · A. Kriebel · E.J. Levorson · R.L. Mauck · J. Mey · A.G. Mikos · S.V. Nair · M. Prabaharan · M.P. Prabhakaran · S. Ramakrishna · P. Sangsanoh · K.T. Shalumon · S. Srinivasan · P. Supaphol · O. Suwantong · J. Venugopal · X. Wen · N. Zhang

Springer

Editors
Prof. R. Jayakumar
Amrita Center for Nanosciences
and Molecular Medicine
Amrita Institute of Medical Sciences
and Research Centre
Amrita Vishwa Vidyapeetham
Kochi 682 041
India
rjayakumar@aims.amrita.edu

Prof. Shantikumar V. Nair
Amrita Center for Nanosciences
and Molecular Medicine
Amrita Institute of Medical Sciences
and Research Centre
Amrita Vishwa Vidyapeetham
Kochi 682 041
India
shantinair@aims.amrita.edu

ISSN 0065-3195 e-ISSN 1436-5030
ISBN 978-3-642-27147-2 e-ISBN 978-3-642-27148-9
DOI 10.1007/978-3-642-27148-9
Springer Heidelberg Dordrecht London New York

Library Control Congress Number: 2011944818

Printed on acid-free paper

Springer is part of Springer Science+Business Media (www.springer.com)

Volume Editors

Prof. R. Jayakumar
Amrita Center for Nanosciences
and Molecular Medicine
Amrita Institute of Medical Sciences
and Research Centre
Amrita Vishwa Vidyapeetham
Kochi 682 041
India
rjayakumar@aims.amrita.edu

Prof. Shantikumar V. Nair
Amrita Center for Nanosciences
and Molecular Medicine
Amrita Institute of Medical Sciences
and Research Centre
Amrita Vishwa Vidyapeetham
Kochi 682 041
India
shantinair@aims.amrita.edu

Editorial Board

Advances in Polymer Sciences Also Available Electronically

Advances in Polymer Sciences is included in Springer's eBook package *Chemistry and Materials Science*. If a library does not opt for the whole package the book series may be bought on a subscription basis. Also, all back volumes are available electronically.

For all customers who have a standing order to the print version of *Advances in Polymer Sciences*, we offer free access to the electronic volumes of the Series published in the current year via SpringerLink.

If you do not have access, you can still view the table of contents of each volume and the abstract of each article by going to the SpringerLink homepage, clicking on "Browse by Online Libraries", then "Chemical Sciences", and finally choose *Advances in Polymer Science*.

You will find information about the

– Editorial Board
– Aims and Scope
– Instructions for Authors
– Sample Contribution

at springer.com using the search function by typing in *Advances in Polymer Sciences*.

Color figures are published in full color in the electronic version on SpringerLink.

Aims and Scope

The series presents critical reviews of the present and future trends in polymer and biopolymer science including chemistry, physical chemistry, physics and material science. It is addressed to all scientists at universities and in industry who wish to keep abreast of advances in the topics covered.

Review articles for the topical volumes are invited by the volume editors. As a rule, single contributions are also specially commissioned. The editors and publishers will, however, always be pleased to receive suggestions and supplementary information. Papers are accepted for *Advances in Polymer Science* in English.

In references *Advances in Polymer Sciences* is abbreviated as *Adv Polym Sci* and is cited as a journal.

Special volumes are edited by well known guest editors who invite reputed authors for the review articles in their volumes.

Impact Factor in 2010: 6.723; Section "Polymer Science": Rank 3 of 79

Preface

Electrospinning is a very attractive method used for the preparation of polymeric or composite fibers. During electrospinning, a high voltage is applied to a polymer solution to produce a polymer jet. With the fast evaporation of solvent combined with high extension ratios of the polymer solution, uniform diameter nanofibers can be produced. There has been an explosion of interest wherein these nanofibrous polymer mats are used for a variety of biomedical applications such as water treatment, biosensors, superhydrophobic surfaces, tissue engineering, wound healing and drug delivery.

The present volume entitled, "Biomedical Applications of Polymeric Nanofibers" attempts to provide a broad overview on the preparation techniques, structures and biomedical applications of different biopolymeric nanofibers. The book consists of 9 chapters:

Chapter 1 deals with the current designs of multiscale scaffolds and discusses their physico-chemical characteristics, as well as their potential applications in regenerative medicine. Chapter 2 focuses on the current state-of-the-art and future perspectives of stem cells and their differentiation on nanoengineered substrates for advanced tissue regeneration. Chapter 3 describes the methods utilized to create biomimetic structures for bone tissue engineering, as well as highlighting the advancements made in this field using these methods. Chapter 4 gives overviews of several tissue engineering approaches that have exploited composite design features and discusses new promising avenues for study. In addition, the drug- and growth-factor delivery capabilities of these systems will similarly be reviewed. Chapter 5 focuses on the development of artificial conduits for nerve regeneration using nanofibers as alternatives to the autograft. Chapter 6 deals with the fabrication of highly aligned nanofiber structures and their challenges and applications in the biomedical field. Chapter 7 summarizes the research and development related to the electrospinning of some common biocompatible polymers as well as an overview of their potential in many biomedical applications such as tissue engineering, wound dressing, carriers for drug delivery or controlled release, and enzyme

immobilization. Chapter 8 reviews the recent advances of electrospun nanofibrous scaffolds based on biodegradable and biocompatible polymers for controlled drug and biomolecule delivery applications. Chapter 9 summarizes the preparation and biomedical applications of silver nanoparticles incorporated into polymeric nanofibers.

Prof. R. Jayakumar
Prof. Shantikumar V. Nair

Contents

Adv Polym Sci (2012) 246: 1–20
DOI: 10.1007/12_2011_163

Published online: 3 November 2011

Multiscale Fibrous Scaffolds in Regenerative Medicine

Sowmya Srinivasan, R. Jayakumar, K.P. Chennazhi, Erica J. Levorson, Antonios G. Mikos, and Shantikumar V. Nair

Abstract In recent years, multiscale fibrous scaffolds containing a combination of micro- and nanoscale fibers have attracted a lot of attention in the tissue engineering field. The multiscale concept is inspired by the hierarchical structure of many tissues, such as bone. Fibrous scaffolds have been traditionally microscale; however, it has been determined that many physicochemical and biological properties are influenced by fiber scale. For this reason, in an effort to optimize tissue regeneration the use of multiple scales has been investigated for obtaining innovative property combinations not otherwise attainable with a single fiber scale. Multiscale architectures have been found to be favorable not only in bone regeneration but also in the regeneration of soft tissues including cardiovascular tissue, neural tissue, cartilage, and skin. The unique properties of multiscale scaffolds have been pivotal in better mimicking the extracellular matrix and promoting vascularization, a key step towards the development of engineered tissue. In this review, we present current designs of multiscale scaffolds and discuss their physicochemical characteristics, as well as their potential applications in regenerative medicine.

S. Srinivasan, R. Jayakumar (✉), K.P. Chennazhi, and S.V. Nair (✉)
Amrita Center for Nanosciences and Molecular Medicine, Amrita Institute of Medical Sciences and Research Centre, Cochin 682 041, India
e-mail: rjayakumar@aims.amrita.edu; shantinair@aims.amrita.edu

E.J. Levorson
Department of Bioengineering, Rice University, MS-142, P.O. Box 1892, Houston, TX 77251-1892, USA

A.G. Mikos
Department of Bioengineering, Rice University, MS-142, P.O. Box 1892, Houston, TX 77251-1892, USA

Department of Chemical and Biomolecular Engineering, Rice University, MS-362, P.O. Box 1892, Houston, TX 77251-1892, USA

Keywords Bone · Cardiovascular tissue engineering · Electrospinning · Microfibers · Multiscale fibrous scaffolds · Nanofibers · Neural

Contents

1 Introduction

Replacement of damaged tissues or organs by natural tissue instead of using synthetic implants is now seen as a realistic goal [1]. The emerging field of tissue engineering essentially involves engineering a suitably shaped biocompatible scaffold that has the potential to regenerate the host tissue when infused with the right mix of cells and other growth factors [2–7]. The regeneration can be conducted in vitro giving the opportunity to partially develop the host tissue extracorporeally, followed by implantation. An ideal scaffold must exhibit a porous, interconnected, and permeable structure to permit the infiltration of cells and nutrients and also should exhibit the appropriate surface structure and chemistry for cell adhesion and proliferation [8–12]. The ideal scaffold must also have mechanical properties comparable with the tissue being engineered and have just the right degree of biodegradability, such that it degrades to form soluble nontoxic products when the tissue is fully formed [13, 14].

The question of scale in this review is uniquely concerned with the scaffold structure. Early studies focused on scaffolds containing micrometer-sized interconnected pores to allow for infiltration of cells into the scaffold [15–19]. Since 2000, with advances in new nanomaterials and processing techniques a large number of studies [20–24] have focused on the role of the nanostructure of scaffolds in tissue regeneration. This was also prompted by the recognition that the environment of the cells in actual tissues (the extracellular matrix; ECM) is fundamentally nanostructured. On the other hand, microscale fibers allow the fabrication of scaffolds with controlled cell–cell interactions. Microfibers have the potential to be utilized as tissue engineering scaffolds in different forms for numerous applications such as wound dressings and bone regeneration [25, 26]. The appeal of nanofibers in tissue engineering is their structural similarity to native ECM;

however, ECM not only has a structural role but also a functional one. This network creates a dynamic, three-dimensional (3D) microenvironment in which cells are maintained. Signals are transmitted from cell surfaces in contact with ECM to the cell nucleus, enabling communication influencing cell adhesion, migration, growth, differentiation, programmed cell death, modulation of cytokine and growth factor activity, and activation of intracellular signaling [27]. Spun nanofibers also offer several advantages such as an extremely high surface-to-volume ratio, tunable porosity, flexibility with respect to scaffold size and shape, as well as the ability to control the nanofiber composition to achieve the desired results from its properties and functionality [27]. Though there are many studies that have proposed nanofibrous polymeric mats for tissue engineering, they have a limitation for 3D applications due to their pore size, which is smaller than a cellular diameter and restricts cell migration within the structure [28–30].

The use of toxic organic solvents for the fabrication of micro- and nanofibers is a major limitation of fibers obtained from synthetic polymers, which would require thorough washing or solvent evaporation treatment prior to use with cells. Natural polymers act as alternatives to synthetic polymers and offer a few advantages such as solubility in aqueous media due to their hydrophilic nature in addition to limited or nonexistent immunogenicity and cytotoxicity [31]. A variety of natural and synthetic polymers have been used to develop scaffolds; however, these scaffolds do not interact with cells in the desired manner. The growth of these cells may be affected by their interaction with the substrate [32–34]. In vivo, the complex structure of vasculature ensures a maximum nutrient diffusion distance of nearly 200 μm for the supply of nutrients to tissue. However, this distance exceeds 200 μm within in vitro constructs, resulting in reduced nutrient supply that compromises cell growth and differentiation [35–37]. Very few studies have looked at the vascularization of scaffolds, which is also of major concern [38]. Most of the current scaffolds lack an interconnected microcapillary network that would help cells to survive within these scaffolds. Also, the cells seeded onto larger and thicker scaffolds have limited success as the cells in the deeper layers are devoid of nutrients and oxygen. Hence, there are more cells at the surfaces of thick 3D scaffolds than in the deeper layers [39]. Therefore these scaffolds should be provided with an inbuilt nutrient distribution network to support the uniform growth of cells. Some fabrication techniques fail to form interconnected pores, which are an important requirement of tissue engineering scaffolds [40–43]. In addition, fabrication techniques in general fail to develop 3D constructs that mimic the complex natural tissues, specifically with regard to mechanical properties [38, 44, 45].

To overcome the current limitations, one approach developed mainly in the last 5 years has been to study multiscale scaffolds in an attempt to mimic hierarchical tissue structures. This review essentially focuses on studies involving multiscale fibrous scaffolds, their development, use of different fabrication methods, their properties, and specific applications in tissue engineering.

2 Multiscale Scaffolds: Principles and Fundamentals

ECM is a hierarchical structure comprised of both micro- and nanoscale structures. The micrometer scale offers a porous structure large enough for the migration of cells through the construct, whereas the nanoscale allows for enhanced protein adsorption, thus improving protein-mediated interactions with the cell surface and so favoring cell adhesion and improving cell viability [46]. The nanoscale fiber meshes exhibit high porosity and reduced pore sizes. Fiber diameter plays an important role in adhesion of cells to the fibers. Reports have suggested that nanofibers may serve as suitable biomaterials for tissue engineering since they can be used to enhance cell differentiation, adhesion, and proliferation [47]. Cells attach at multiple focal points, extend filopodia along the length of the fibers, and spread throughout the nanofiber matrix [48]. However, the effect of fiber diameter on tissue regeneration still remains unknown. Scaffold architecture and design are key factors in determining vascularization and nutrient supply, which are crucial for the development of regenerating tissue [49]. Studies have shown that pores of 100–300 μm favor vascularization and nutrient supply [50]. However, the relatively small pore size of nanoscale fibrous scaffolds compared to cell diameter (5–20 μm) limits cell migration and infiltration within the scaffold, leading to the formation of a monolayer of cells on the scaffold surface rather than a 3D cellular construct. For this reason, nanoscale fibrous scaffolds cannot mimic the natural thickness of certain tissues such as human articular cartilage, which ranges from 0.5 to 7.1 mm thick [51].

Microfiber scaffolds could be potentially advantageous because they are comprised of larger pores than nanofiber scaffolds. These larger pores could facilitate cellular infiltration and/or diffusion of nutrients during in vitro culture. To study the mechanism of interaction between cells and nanofibers, it is important to control the architecture of nanofibers to minimize the interaction of a single cell with neighboring fibers [47]. Controlling the nanofiber to microfiber ratio can easily vary the porosity of multiscale scaffolds. Pham et al., who developed a bimodal scaffold consisting of a top nanofiber layer and a bottom microfiber layer, demonstrated this [52]. These scaffolds were developed by a sequential electrospinning technique wherein the multiscale layers were electrospun using the same polymer with different morphologies. These scaffolds were characterized to evaluate the extent of nanofiber deposition as a function of duration of electrospinning time. Electrospinning for longer periods increased the amount and thickness of the nanofibrous layer. Hence, thickness and coverage of nanofibrous layer could be controlled by modulating the electrospinning time. Cross-sectional images helped in distinguishing the alternating layers, even in the presence of a thin nanofiber layer. Also, scaffolds with different densities of nanofiber layers were considered to investigate the effect on cellular infiltration into these bimodal scaffolds. Cell attachment at different intervals of time was found to be similar; however, cell spreading was affected by the presence of nanofibers. The cells initially appearing to exhibit rounded morphologies became

more spread with time, with the greatest amount of spreading being observed on scaffolds with nanofibers. Complete infiltration of cells was only observed in the presence of a flow perfusion bioreactor. Thus the presence of nanofibers was found to hinder cell migration due to the presence of smaller pores, but at the same time influenced cell spreading, proliferation, and differentiation [52]. However, these 3D scaffolds combining nano- and microscale fibers (nano/microfiber scaffolds) have a layered nanofibrous structure instead of a randomly mixed structure composed of nanofibers and microfibers. Therefore, the nanofibrous layers, which were formed in sheet-like structures over microfibers, can prevent the cells from infiltrating adequately into the scaffolds.

3 Mechanical, Physicochemical, and Biological Properties of Multiscale Scaffolds

The success of a tissue engineering scaffold ultimately depends on the interplay of various biological, mechanical and physicochemical properties. For every successful application, these tissue engineered constructs must satisfy the essential requirements of biological, mechanical, and physical properties. The scaffold architecture should support and withstand compressive forces and contraction in vivo. The scaffold should provide adequate support for cell attachment and growth in vitro and facilitate mass transfer of nutrients and oxygen when implanted in vivo. For biodegradable scaffolds, the rate of degradation should balance the rate of neo-tissue formation and remodeling, wherein the degree of remodeling depends on the type of tissue. Shalumon et al. prepared multiscale poly(ε-caprolactone) (PCL) fibrous scaffolds [46]. Various processing parameters such as viscosity, applied voltage, and flow rate influence the fiber diameter and result in the formation of a simultaneous micro/nanofiber matrix. The presence of nanofibers embedded in the microfiber matrix was found to enhance the mechanical strength in comparison to microfibers alone. Also, the strain values were increased, which may be attributed to the cumulative elongation effect in the presence of the nano/microfiber combination. The incorporation of nanocrystalline hydroxyapatite (nHA) into these multiscale fibers did not alter the fiber morphology; however, the fiber diameter was slightly larger. This was probably due to the increase in polymer viscosity. The cellular activity on multiscale scaffolds, regardless of the incorporation of nHA, was higher than on microfibers or nanofibers alone. Cells attached to the multiscale fibers were flattened, laterally stretched, and extended (Fig. 1) [46].

Similarly Shalumon et al. also fabricated electrospun porous poly(lactic acid) (PLA) multiscale scaffolds and evaluated their physicochemical and biological properties in detail [53]. These multiscale scaffolds were developed through a bimodal fiber fabrication system. The three main solution properties, solution viscosity, conductivity, and surface tension, were determined to be the governing

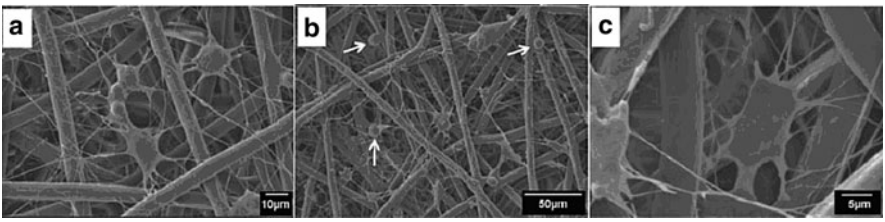

Fig. 1 SEM images of cell attachment after 12 h of incubation. (**a**) Cell attachment on multiscale scaffold. (**b**) Cell growth into the multiscale scaffold; *arrows* indicate spherical morphology of cells attached to microfibers. (**c**) Cell access to the interior of the multiscale scaffold through the pores in the microfibers (Adapted from [46])

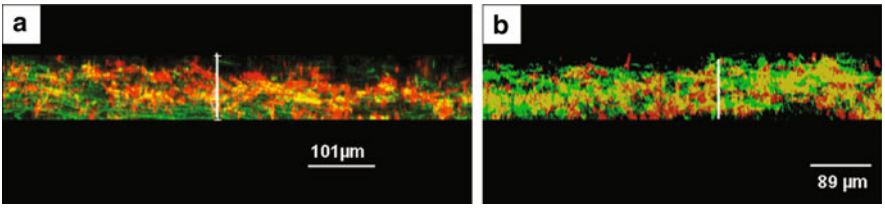

Fig. 2 3D projection images of cell infiltration behavior into (**a**) micro/nanofibrous scaffolds and (**b**) micro/nano/nHAp fibrous scaffolds (Adapted from [53])

factors in the formation of multiscale fibers. Cells seeded on the multiscale scaffold displayed a well-flattened and laterally stretched morphology over the scaffold surface. Cell penetration and proliferation on multiscale scaffolds was enhanced in comparison to nano- or microscale scaffolds (Fig. 2). This was due to the combined effect of porosity and low contact angle offered by the microfibers and the capacity for spreading offered by nanofibers. Increased cell penetration also resulted in homogenous distribution of the cells throughout the multiscale scaffold [53].

Santos et al. elucidated the importance of endothelial cell (EC) colonization and angiogenic potential of nano/microfibrous combined scaffolds [54]. The ECs spanned between microfibers with the support of nanobridges formed by the nanofibers, yielding a higher density of adherent ECs. This spanning of cells between the fibers was absent in the microfiber control. This could be due to the presence of a nanonetwork that induced a different cytoskeletal arrangement, which was reflected in the stretched shape with numerous cellular extensions. Besides improving the interconnectivity, these nano/micro scaffolds provided a means of physical support for the enhanced growth of ECs, thus showing close resemblance to morphology of a capillary-like network [54]. Edwards et al. also described similar work wherein a multiwalled carbon nanotube–PLGA nanofiber composite presented ideal pore spanning, allowing uniform distribution of fibroblast-like cells throughout the scaffold surface [55]. With an increase in cell spanning and stretching, the receptors also get stretched and activated. Tuzlakoglu et al.

developed polymeric micro/nanofiber scaffolds from a blend of starch and PCL. The results indicated changes in cell morphology and cytoskeletal rearrangement. The cell receptors were stretched and activated, leading to the expression of different genes in comparison to the unstretched cells [48]. Mota et al. developed dual-scale scaffolds consisting of aligned PCL microfilaments and PLGA nanofibers [32]. They observed that in the dual-scale scaffolds, cells were able to colonize the interfilament gap caused by the microfilaments. This was due to the effect of the guidance in cellular adhesion exerted by the electrospun nanofibers, which were also responsible for the morphological changes between cells adhered on fibers with different orientations. These dual-scale scaffolds are also characterized by fiber alignment and high spatial connectivity capable of directing cell orientation and migration [32]. The interaction of cells with ECM is not only an anisotropic behavior, but is also dependent on the chemical changes experienced from the surrounding environment. The cells endure chemical stimulation by direct contact with the surrounding ECM or the neighbors, which greatly depends on the spatial concentration distribution of the fibers. By altering the composition of nanofibers while electrospinning, multilayered scaffolds with specified chemistry, thickness, and morphology can be obtained [56].

Porosity and pore size are among the key factors responsible for the success of tissue engineered scaffolds. Optimum porosity enhances cell spreading and migration while supporting the exchange of nutrients between the scaffold and the surrounding environment. Porosity and pore size in electrospun scaffolds are mainly dependent on the fiber diameter and their packing density. Soliman et al. developed a bio-inspired multiscale 3D scaffold for soft tissue engineering wherein the fiber distributions were intermixed into a single, multimodal layer [57]. They also stated the importance of combining nano- and microfibers in a single scaffold wherein cell motility and adhesion was improved by the network of nanofibers. The web of nanofibers helped in bridging the cells across the microfibers, thus colonizing the entire scaffold, while the microfibers produced larger pores to accommodate the cells. This is a valuable characteristic because in a single-scale scaffold the cells are frequently confined to a single fiber due to the absence of bridging across microfibers that are far apart. The multimodal scaffold also exhibited superior strength and stiffness in comparison with the controls [57].

Multiscale scaffolds composed of nano- and microscale fiber meshes using two different electrospinning techniques, multilayer electrospinning and mixing electrospinning, were reported by Kidoaki et al. [58]. Initially, four different polymers were individually electrospun: type I collagen, styrenated gelatin (ST-gelatin), segmented polyurethane (SPU), and poly(ethylene oxide). Then, these individual fiber meshes were deposited layer-by-layer to form a trilayered electrospun mesh and mixed electrospun fiber mesh. A bilayered tubular construct composed of a thick SPU microfiber mesh as an outer layer and a thin type I collagen nanofiber mesh as an inner layer was fabricated as a prototype scaffold of artificial grafts and may provide compliance matching with native arteries and tissues. Further insights into detailed in vitro and in vivo studies are essential to visualize the functioning of the fiber mesh after implantation [58]. Thus, the

synergistic combination of micro- and nanofiber hierarchical scaffolds developed using combinations of a wide variety of biopolymers showed unique mechanical, biological, and physicochemical properties that are suitable for diverse tissue engineering applications and are absent in single-scale scaffolds.

4 Applications of Multiscale Scaffolds in Tissue Engineering

4.1 Bone

Bone tissue engineering is a branch of tissue engineering that aims to repair and/or regenerate bone using scaffolds with cell-based therapies and growth supplements. It may be used to restore skeleton function in the field of orthopedic and oral-maxillofacial surgery [59–61]. Scaffolds for bone tissue engineering are developed with the primary aim of closely mimicking the biophysical structure of natural ECM. Tuzlakoglu et al. developed nano- and microfiber combined scaffolds from starch/PCL-based biomaterials to support bone cells [48]. The nanofibers were electrospun in a random manner between the microfibers, thereby providing nanobridges similar to those found in ECM. In the presence of nanofibers, a well-spread cellular morphology and cytoskeletal organization of the SaOs-2 human osteoblast-like cell line and rat bone marrow stromal cells was observed. Osteoblasts were directed to bridge between microfibers and this resulted in scaffolds completely filled with cells after 2 weeks of culture. With cell stretching, the receptors also got stretched and activated, resulting in the expression of various genes in comparison to the unstretched cells. Cell viability and alkaline phosphatase (ALP) activity for both of the cell types was found to be enhanced in nano/microfiber combined scaffolds as compared to control scaffolds based on fiber meshes without nanofibers. Consequently, the developed structures are believed to have a great potential for the 3D organization and guidance of cells that are important for engineering 3D bone tissues. Their unique architecture, which supports and guides the cells, makes them suitable candidates for bone tissue engineering applications [48]. Martins et al. also developed bone ECM-inspired structures by conjugating electrospun chitosan (Cht) nanofibers within biodegradable polymeric microfibers [poly(butylene succinate) (PBS) and PBS/Cht], assembled in a fiber mesh structure [62]. The physical properties of these scaffolds could be enhanced by developing a highly connected porous framework. The osteogenic differentiation of human bone marrow mesenchymal stem cells (hBMSCs) produced an increased amount of calcium phosphates on these nanofiber-reinforced composite scaffolds, confirming ECM deposition and mineralization, mainly in the PBS/Cht-based fiber meshes. The osteogenic genotype of the cultured hBMSCs was confirmed by the expression of osteoblastic genes, namely those coding for ALP, osteopontin, bone sialoprotein and osteocalcin, and the transcription factors Runx2 and Osterix, all involved in different stages of osteogenesis [62]. Osathanon et al.

fabricated micro- and nanoporous fibrin/calcium phosphate composite scaffolds with tightly controllable pore size and interconnected pores using sphere-templating methods [63]. Murine calvarial cells attached, spread and showed a polygonal morphology on the surface of the scaffold. Multiple cell layers and fibrillar matrix deposition were observed. Cells seeded on mineralized fibrin scaffolds exhibited significantly higher ALP activity as well as osteoblast marker gene expression compared to fibrin scaffolds and nHA-incorporated fibrin scaffolds. The scaffolds also promoted bone formation in a mouse calvarial defect model, and the bone formation was enhanced by addition of recombinant human bone morphogenetic protein-2 (rhBMP-2) [63]. These works have demonstrated the combination of micro- and nanofiber scaffolds to be a feasible option for the design and development of hierarchical, fully functional, synthetic ECM substitutes.

Vascularization following implantation is a major concern in bone regeneration as well as tissue engineering as a whole because diffusion limitations are a major barrier to the production of 3D engineered tissues. Strategies that include seeding ECs on biomaterials and promoting their adhesion, migration, and functionality might be a solution for the formation of vascularized bone. Nano/microfiber combined scaffolds have a unique characteristic inspired by ECM, the nano-dimensions, which promote cell adhesion, together with a microfiber mesh that provides the mechanical support. Santos et al. described a work showing the influence of a nanonetwork on growth pattern, morphology, inflammatory expression profile, expression of structural proteins, homotypic interactions, and angiogenic potential of human ECs cultured on a scaffold made of a blend of starch and PCL [54]. These nanonetworks on microfiber meshes not only increased the adhesion surface area and interconnectivity in the constructs but also provided structural and organizational stability for ECs. As mentioned earlier, the human dermal microvascular ECs (HDMECs) spanned between the microfibers using the nanobridges formed by the nanofibers, thus favoring high levels of cell adhesion. On the microfibers, the cells exhibited a flattened morphology characteristic of their location inside larger blood vessels and an extremely stretched shape reminiscent of the angiogenic phenotype, with multiple cellular protrusions anchoring them to several nanofibers (Fig. 3). The cells also covered the entire surface of the scaffold without hampering the scaffold porosity. Furthermore, on nanofibers as well as on microfibers, ECs maintained the physiological expression pattern of the structural protein vimentin and platelet EC adhesion molecule (PECAM-1) between adjacent cells. In addition, ECs growing on the nano/microfiber combined scaffold were sensitive to pro-inflammatory stimulus. Under pro-angiogenic conditions in vitro, the ECM-like nanonetwork provided the structural and organizational stability for migration and organization of ECs into capillary-like structures with branching. The architecture of nano/microfiber combined scaffolds, thus, elicited and guided the 3D distribution of ECs without compromising the structural requirements for bone regeneration [54].

Multiscale scaffolds thus satisfy the required criteria of an ideal bone regenerating scaffold, namely biocompatibility. Likewise, they promote cellular adhesion, growth, and migration. The bone-specific cells align themselves along the

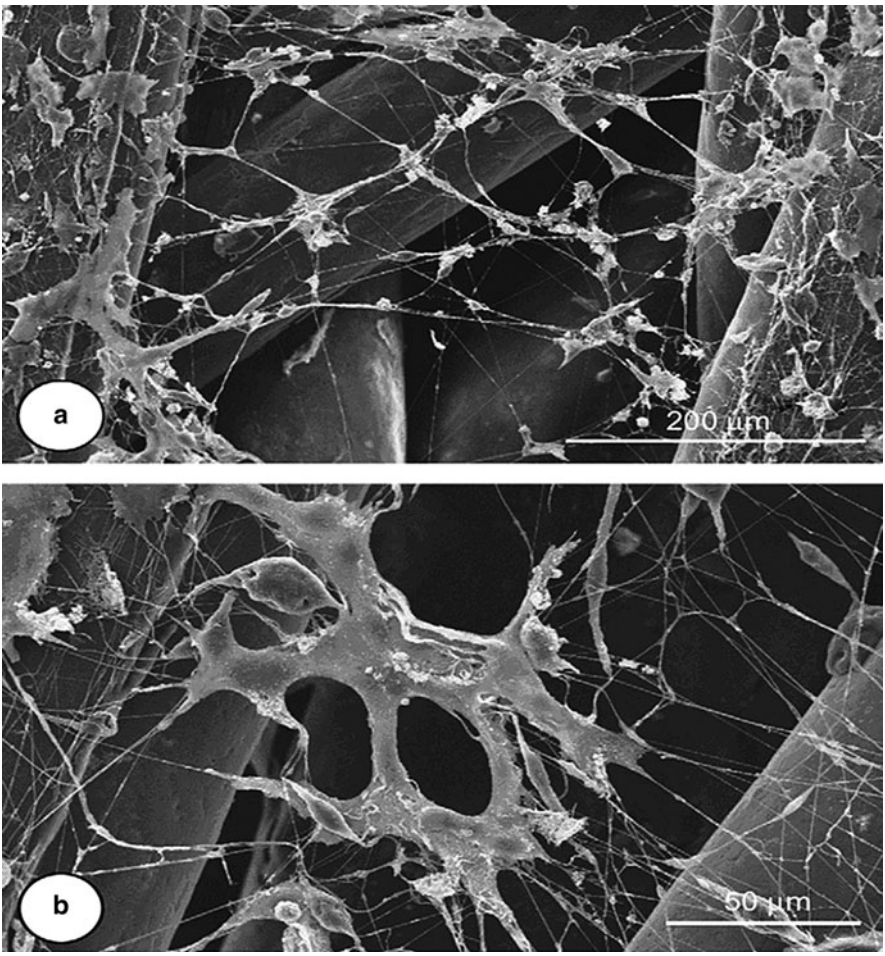

Fig. 3 (**a**, **b**) SEM micrographs of HUVEC cells on fibronectin-coated starch/PCL scaffolds, showing the nano/microfiber combined scaffold after 3 days of culture. Note the ability of the ECs to use the nanofibers to span across the microfiber structure (Adapted from [54])

long axis of the micro- and nanofibers, bond to the existing bone surface facilitated by the presence of nanoscale structures, and stimulate osteogenesis. The presence of microfibers in the construct provides the necessary porous structure for the cells to migrate easily, enable the supply of nutrients and oxygen, and enhance vascularization. These constructs are biodegradable and have a controlled degradation rate. They also exhibit mechanical and physicochemical properties that match the native bone. The architecture, properties, and biological requirements can be tuned during fabrication to obtain a construct of desired morphology and characteristics. All these factors should be further confirmed with in vivo studies to ensure that multiscale scaffolds are a suitable option for bone tissue engineering.

4.2 Cartilage

Cartilage is a tissue in which the ECM plays a very important role in both the biological and mechanical function of the tissue. For this reason, it follows that a well-designed scaffold that mimics the structure of native ECM could potentially lead to more successful development of engineered cartilage. Park et al. fabricated highly functionalized polymeric 3D scaffolds by a combination of direct polymer melt deposition (DPMD) and electrospinning [64]. Between the microfiber layers formed by DMPD, PCL/collagen nanofiber matrices were deposited via electrospinning. The hybrid scaffold showed a 3D woodpile structure composed of layers of PCL microfibers with a PCL/collagen nanofiber matrix (Fig. 4). This stacked structure was thought to be beneficial for the penetration of cells, also leading to increased cell migration through the side channels. Results confirmed enhanced chondrocyte attachment and proliferation on the hybrid scaffold. An increase in cell number was noted with an increase in culture duration. This could be due to direct reaction of cells to the nanofibrous topography such as groove, ridge, pore, step, and node topographies. Hence, the nanofibrous topography could be easily sensed by the seeded chondrocytes thereby influencing cellular interactions. The nanofibrous structure can also enhance serum protein adsorption

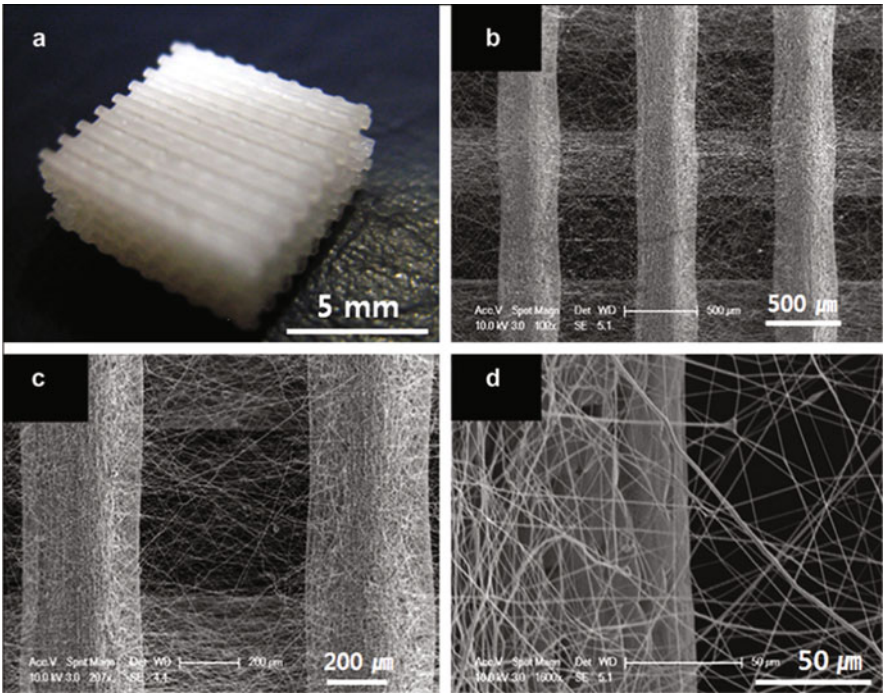

Fig. 4 (**a**) Photograph of the overall 3D woodpile structure with dimensions of 9 × 9 × 3.5 mm. (**b**) Hybrid basic unit layer composed of microfibers and the electrospun nanofiber matrix. (**c**, **d**) Magnified images of (**b**) (Adapted from [64])

on the surface of the hybrid scaffold. An increase in serum protein adsorption further enhances cell adhesion. With the exposure of collagen on the surface of the hybrid scaffold, cells were provided with a suitable environment for growth and differentiation. Hence, the surface nanotopography enhanced the cytocompatibility of the scaffold to make it more suitable for cartilage tissue regeneration [64].

4.3 Skin

Kim et al. reported the development of 3D scaffolds with randomly mixed interconnected network of micro- and nanofibers [65]. The hybrid process was designed by combining melt electrospinning and solution electrospinning. This hybrid structure with a randomly mixed network of micro- and nanofibers also had similar pore dimensions to microfiber scaffolds, and the scaffold thickness could also be varied to the centimeter scale making it adaptable for 3D culture of various tissues. The mechanical properties of the poly(D,L-lactic-*co*-glycolic acid) (PLGA) nano/microfiber composite scaffold were assessed using tensile testing. The PLGA nano/microfiber composite scaffold had higher tensile strength and elongation at break than the PLGA microfiber scaffolds, which may be due to the entangled structure of nanofibers with the microfibers. The nanofibers in the nano/microfiber scaffolds can provide more contacts and/or physical junctions with the microfibers or nanofibers, and thus act as physical crosslinks. The response of normal human epidermal keratinocytes (NHEKs) and primary normal human epidermal fibroblasts (NHEFs) forming this tissue was analyzed in vitro. The attachment of NHEF cells was significantly higher on PLGA micro/nanofiber scaffolds in comparison to NHEK cells. Regardless of culture duration, NHEKs did not spread well on the PLGA microfiber scaffolds. Conversely, NHEFs spread and spanned across the pores between fibers in the PLGA microfiber scaffolds within a single day of culture, yet cell contacts appeared broken in these scaffolds after 3 days, which could negatively influence further construct development. Nano/microfiber scaffolds seeded with either NHEK or NHEF cells displayed spreading and cellular infiltration after only 1 day of culture. Since the PLGA scaffolds possess similar tensile properties to human skin, and due to the increased cell spreading and infiltration of nanofiber containing constructs, it was anticipated that multiscale PLGA scaffolds would be a suitable tissue engineering scaffold for skin regeneration [65].

4.4 Neural

Neural tissue repair in order to treat nerve damage or neuropathy arising from a spinal cord or cerebral injury essentially requires the intervention of tissue engineering because axons are unable to regenerate on their own. Hence, recent advances in neural tissue engineering provide suitable and promising substitutes

for nerve regeneration [66, 67]. Wang et al. developed chitosan bilayered tubes and micro/nanofiber mesh tubes [68]. These tubes were prepared using the electrospinning technique. Bilayered tubes were formed by combining an inner nano/microfibrous tube with a chitosan film outer coating. These nano/microfiber mesh tubes, bilayered tubes, and film tubes were tested as bridge grafts in injured rat sciatic nerves. Although the mechanical properties of micro/nanofiber mesh tubes were inferior in comparison to the bilayered tubes, these properties were sufficient to serve as a nerve conduit preserving permeation of the mesh tube. Both function recovery and nerve regeneration were enhanced as a result of good permeation ability, thereby enabling the exchange of nutrients and metabolic wastes. The micro/nanofiber mesh also had the ability to interact with the ECM on both sides of the amputated nerve and to promote Schwann cell migration into the lesion area to provide a suitable environment for the growth of the nerve into the lesion site. The graft may also approximate the two sides of the lesion [68]. Panseri et al. used tubes made of biodegradable polymers (a blend of PLGA/PCL) fabricated by electrospinning to regenerate a 10-mm nerve gap in a rat sciatic nerve in vivo [69]. The flexible fibrous structure was easily sutured to the proximal and distal ends of the nerve stump. The graft also showed a porous structure allowing the passage of nutrients, and a necessary barrier to prevent the infiltration of unwanted tissue into the conduit. Four months after surgery, the electrospun tubes were found to induce neural tissue regeneration and functional reconnection of the two severed sciatic nerve tracts in comparison to the untreated control. Myelination and collagen deposition were detected in accordance with the newly regenerated nerve fibers. Thin fibrous tissue capsule formation around the surface of the conduit and negligible inflammatory response proved the biocompatible nature of the conduit. These results effectively showed that the prosthesis did not produce any mechanical stress-related nervous degeneration and favored the reestablishment of functional neuronal connections evoking re-innervation of the target muscles in the majority of treated animals [69]. The results from these studies confirmed the efficacy of multiscale scaffolds as suitable constructs for neural tissue engineering. Some of the remarkable features such as the migration of Schwann cells into the injury site favoring the growth of nerve, functional innervation, nerve regeneration as a result of good permeation ability with exchange of nutrients, and graft approximation clearly satisfy the needs of neural tissue engineering.

4.5 Cardiovascular

Regenerative medicine is of paramount importance for treating patients with severe cardiac diseases. Various strategies for regenerating the damaged myocardium are under investigation with varying degrees of success. These strategies include cell therapies, gene or protein therapy, and the application of passive or bioactive materials or a combination of cells, growth factors, and scaffolds to repair or regenerate cardiac tissues [4, 7, 70]. Kwon et al. fabricated nano/microstructured

biodegradable poly(L-lactic acid-*co*-ε-caprolactone) (PLCL) fabrics of different compositions by electrospinning [71]. Different architectures of the elastomeric copolyester, the equimolar PLCL copolymer, were prepared using different solvents. The decrease in the fiber diameter of the fabric resulted in a decrease in porosity and pore size, as well as an increase in fiber density and mechanical strength. Human umbilical vein endothelial cells (HUVECs) were well attached and proliferated on the small fiber diameter fabrics. Results suggest that these electrospun elastomeric fibers could be combined into multiscale scaffolds to yield more advantageous responses in cardiovascular and muscular tissue engineering endeavors by harnessing the positive characteristics of the differently scaled fibers in a single scaffold [71]. Further in vivo studies are essential to confirm its application for cardiac tissue engineering.

5 Logistics and Limitations

Often when nanofibers are incorporated into a microscale scaffold you see increased cellular attachment and spreading because nanofibers more closely resemble the scale of ECM than do microfibers and in turn act as cellular bridges across larger pores. While this is often a positive result for a multiscale scaffold, when the density of nanofibers is too great cellular infiltration of the scaffold is also limited, which is a detriment to the development of larger 3D tissues. Previous studies have shown that dense layers of nanofibers formed by as little as 300 s of electrospinning can significantly hinder the infiltration of cells into a scaffold [52]. For this reason, it is important to optimize the proportion of nanofibers to microfibers in multiscale scaffolds in order to maximize the beneficial effects of nanofibers while still harnessing the positive attribute of larger pore sizes usually associated with microscale scaffolds.

Due to the nature of the electrospinning process it is very difficult to independently vary the proportions of two differently scaled fiber diameters while maintaining consistent fiber characteristics. This is due to the fact that one of the primary ways to regulate fiber proportions is by adjusting the polymer extrusion flow rate. Consequently, flow rate also has a major influence on fiber diameter. Another strategy for controlling the relative proportion of different fiber scales is by interrupting the flow of one polymer stream to reduce the relative amount of that particular fiber. However, in order to interrupt the flow of a polymer stream while electrospinning, one must: (1) interrupt the voltage source, thus stopping the propulsion of the polymer solution; or (2) pause the extrusion of the polymer solution, this halts polymer flow yet a small amount of polymer may still be drawn out of the spinnerette due to the active electrical field; or (3) physically block the fibers from reaching the target, which may be difficult to do if other scaled fibers are being electrospun in close proximity to the fibers being manipulated. Furthermore, all of these methods of controlling fiber proportions generate issues regarding reproducibility. A summary of the tissue engineering applications of the multiscale fibrous scaffolds discussed in this review is given in Table 1.

Table 1 Applications of multiscale fibrous scaffolds for tissue engineering

Tissue	Diameter	Fiber fabrication	Application	Key results	Ref.
General tissue engineering	10 μm, 3–5 μm, and 500 nm	Aligned electrospun PGA/collagen fibers	In vitro culture of NIH-3T3 fibroblast-like cells	Increased cellular adhesion and spreading on nanofibers as compared to microfibers, regardless of fiber composition	[47]
	8 μm, 9–9.5 μm, 700–750 nm, 850–980 nm	Electrospun PLA micro/nanofibers without and with nHA	In vitro culture of MG-63 osteoblast-like cells	Cell penetration and proliferation on multiscale scaffolds was higher than for the control. Cells were dispersed throughout the scaffold. The addition of nHAp further improved the bioactivity	[53]
	34.1 ± 2.9 μm yarn and nanoscale fibers	Knitted tube of carbon nanotube yarn coated with electrospun PLGA nanofibers	In vitro culture of NR6 fibroblast-like cells	Electrospun nanofibers supported cell spanning across large pores while limiting infiltration of the tube	[55]
	3.3 μm and 600 nm	Electrospun PCL micro/nanofibers	In vitro culture of murine MSCs	Compared to monoscale micro- and nanocontrols, multiscale scaffolds led to increased adhesion, viability, and scaffold infiltration	[57]
Bone	365.4 ± 18.3 μm and 1 μm	Aligned melt-extruded PCL microfibers and electrospun PLGA fibers	In vitro culture of MC3T3 preosteoblast-like cells	Compared to extruded microfiber controls, dual-scale scaffolds led to increased cell viability and adhesion	[32]
	6.8 ± 0.4 μm with 244.7 ± 18.8 nm or 11.3 ± 1.9 μm with 269.5 ± 42.2 nm	Electrospun PCL micro-, nano-, and multiscale fibrous scaffolds with and without nHA	In vitro culture of MG-63 osteoblast-like cells	Cell activity, proliferation, and total protein adsorption were higher on scaffolds containing nanofibers than on those containing microfibers	[46]

(continued)

Table 1 (continued)

Tissue	Diameter	Fiber fabrication	Application	Key results	Ref.
	160 μm and 400 nm	Starch/PCL fiber bonded microscaffolds with electrospun nanofibers	In vitro culture of SaOs-2 osteosarcoma-like cells and rat MSCs	Compared to microfiber scaffolds, multiscale scaffolds displayed higher cell viability, ALP activity, and stretched cell morphology	[48]
	Bilayered scaffolds of 5 μm and 600 nm	Electrospun PCL micro/nanofibers	In vitro culture of rat MSCs	Nanofibers increased cell spreading and decreased infiltration while having little to no effect on attachment	[52]
	160 μm and 400 nm	Starch/PCL fiber bonded microscaffolds with electrospun nanofibers	In vitro culture of HUVECs and HDMECs	Cells on nanofibers spanned adjacent microfibers and adopted capillary-like morphologies while remaining sensitive to pro-inflammatory stimuli	[54]
	460 μm or 500 μm and nanoscale fibers	Melt-extruded PBS or PBS/Cht microfiber structures with electrospun Cht	In vitro culture of human bone marrow MSCs	Nanofibers led to increased deposition of calcium phosphate, especially in combination with PBS/Cht microfibers	[62]
	200–250 μm pore size and 40–80 nm	Fibrin, mineralized fibrin, or fibrin/nHA microporous, nanofibrous scaffolds	In vitro culture of murine calvarial cells and in vivo implantation of acellular scaffolds	Mineralized fibrin scaffolds showed higher ALP activity than fibrin and fibrin/nHA scaffolds. Scaffolds promoted bone formation in a mouse defect model	[63]
Cartilage	405 ± 15 μm and 431 ± 148 nm or 325 ± 128 nm	DPM deposited PCL microfiber structures with electrospun PCL or PCL/collagen nanofibers	In vitro culture of bovine chondrocytes	Cell attachment and proliferation was improved by the addition of electrospun nanofibers, with the largest increase due to PCL/collagen nanofibers	[64]

Skin	28 μm and 530 nm	Hybrid electrospun PLGA micro/nanofibers	In vitro culture of human epidermal keratinocytes and fibroblasts	Compared to microfiber controls, the cell attachment, spreading, and infiltration were higher in micro/nanofiber composite scaffolds	[65]
Nerve	Microscale fibers and 200–600 nm	Electrospun Cht nano/microfibrous tubes with or without Cht film outer coat	In vivo implantation in rat sciatic nerve	The Cht nano/microfiber mesh tubes effectively maintained defect space and enabled superior cell migration, permeation, and functional recovery	[68]
	Bilayered tubes of 7.5 ± 2.0 μm and 279 ± 87 nm	Electrospun PCL microfibers with PCL/PLGA nanofibers	In vivo implantation in rat sciatic nerve	Implants led to nerve regeneration, muscle re-innervation, as well as some evidence of myelination	[69]
Cardiac	7.0 ± 1.0 μm, 1.2 ± 0.2 μm, and 320 ± 80 nm	Electrospun PLCL nano- to microfiber fabrics	In vitro culture of HUVECs	Cell attachment and proliferation was higher on the highly packed nano- and 1-μm-scaled-fiber fabrics in comparison to the control	[71]

ALP alkaline phosphatase, *Cht* chitosan, *DPM* direct polymer melt, *HDMECs* human dermal microvascular endothelial cells, *HUVECs* human umbilical vein endothelial cells, *MSCs* mesenchymal stem cells, *nHA* nanocrystalline hydroxyapatite, *PBS* poly(butylene succinate), *PCL* poly(ε-caprolactone), *PGA* poly (glycolic acid), *PLA* Poly(lactic acid), *PLGA* poly(D,L-lactic-*co*-glycolic acid), *PLCL* poly(L-lactide-*co*-ε-caprolactone)

Conversely, it is also challenging to alter fiber diameters while keeping the relative fiber scale proportions constant, for the same list of reasons. This makes it challenging to design effective studies to examine the effect of fiber size or relative fiber type proportions on cellular responses within multiscale scaffolds. It would be easier to alter the fiber diameter or relative proportions of micro- to nanoscale features if electrospun nanofibers were coupled to a different fabrication technique such as polymer melt deposition. However, it can be argued that this might not produce a reasonably homogenous scaffold with an even mixing of nano- and microfeatures throughout the entire scaffold, which could in turn influence results.

6 Conclusions and Future Directions

Techniques to produce multiscale biomaterial scaffolds with designer geometries are 'the need of the hour' to provide improved biomimetic properties for functional tissue replacements. While micrometer fibers generate an open pore structure, nanofibers support cell adhesion and facilitate cell–cell interactions. This was further proven by cell penetration studies, which showed superior ingrowth of cells into hierarchical structures. Mixed bimodal scaffolds of two different polymers are another promising approach, because they exhibit hierarchical pore/surface systems and combine the beneficial properties of both polymers at two different scales. Various 3D micro- and nanoscale multiscale scaffolds have been fabricated through various techniques and were found to have the potential to essentially recreate natural bone, cardiac, neural, and vascular tissues.

The multiscale system also appears to be capable of providing more enhanced biological functionality, particularly for vascularization, which is favored by the interaction of ECs with the nanofibrous networks that allow suitable cell architecture and orientation for microtubule formation. Thus, the synergistic effect of micro- and nanoscales could successfully regenerate natural tissues in vivo in the near future. Future work should focus on optimizing this process to better recapitulate key features of the native ECM, including its mechanical and biochemical properties, which would enhance the functionality of these 3D multiscale scaffolds in order to fabricate functional tissue engineered constructs.

Acknowledgements The authors are grateful to Nanomission, Department of Science and Technology (DST), India, which partially supported this work, under the Nanoscience and Nanotechnology Initiative program. We also thank the Indo-US Science and Technology Forum for funding a joint R&D network center enabling collaborative research with international partners. We further acknowledge the support by the National Institutes of Health (R01 AR57083) for work on fabrication of multiscale fibrous scaffolds for regenerative medicine applications. R. Jayakumar is grateful to Department of Biotechnology (DBT), India (Ref. No. BT/PR13585/NNT/28/474/2010) and SERC Division, DST, India, for providing the fund under the scheme "Fast Track Scheme for Young Investigators (Ref. No. SR/FT/CS-005/2008)". E.J. Levorson also acknowledges the support of the Biotechnology Training Grant (NIH T32 GM08362) of the Rice Institute of Biosciences and Bioengineering.

References

1. Gomes ME, Reis RL (2004) Macromol Biosci 4:737
2. Novosel EC, Kleinhans C, Kluger PJ (2011) Adv Drug Deliv Rev 63:300
3. Stock UA, Vacanti JP (2001) Annu Rev Med 52:443
4. Levenberg S, Langer R (2004) Curr Top Dev Biol 61:113
5. Ikada Y (2006) J R Soc Interface R Soc 3:589
6. Baar K (2005) Exp Physiol 90:799
7. Marler JJ, Upton J, Langer R, Vacanti JP (1998) Adv Drug Deliv Rev 33:165
8. Ramakrishna S, Mayer J, Wintermantel E, Leong K (2001) Compos Sci Technol 61:1189
9. Archer R, Williams DJ (2005) Nat Biotechnol 23:1353
10. Bhatia SN, Chen CS (1999) Biomed Microdevices 2:131
11. Cao Y, Croll T, O'Connor AJ, Stevens GW, Cooper-White JJ (2006) J Biomater Sci Polym 17:369
12. Chen GP, Ushida T, Tateishi T (2001) Mater Sci Eng C 17:63
13. Cooper JA, Lu HH, Ko FK, Freeman JW, Laurencin CT (2000) Biomaterials 26:1523
14. Freyman TM, Yannas IV, Gibson LJ (2001) Prog Mater Sci 46:273
15. Hutmacher DW (2000) Biomaterials 21:2529
16. Yang S, Leong KF, Du Z, Chua CK (2001) Tissue Eng 7:679
17. Madihally SD, Matthew HWT (1999) Biomaterials 20:1133
18. Freed LE, Vunjak-Novakovic G, Biron RJ, Eagles DB, Lesnoy DC, Barlow SK, Langer R (1994) Nat Biotechnol 12:689
19. Karageorgiou V, Kaplan D (2005) Biomaterials 26:5474
20. Pham QP, Sharma U, Mikos AG (2006) Tissue Eng 12:1197
21. Frenot A, Chronakis IS (2003) Curr Opin Colloid Interf Sci 8:64
22. Mikos AG, Sarakinos G, Leite SM, Vacanti JP, Langer R (1993) Biomaterials 14:323
23. Whang K, Thomas CH, Healy KE, Nuber G (1995) Polymer 36:837
24. Liu H, Webster TJ (2007) Biomaterials 28:354
25. Min B, Lee SW, Lim JN, You Y, Lee TS, Kang PH, Park WH (2004) Polymer 45:7137
26. Maeda Y, Jayakumar R, Nagahama H, Furuike T, Tamura H (2008) Int J Biol Macromol 42:463
27. Liao S, Li B, Ma Z, Wei H, Chan C, Ramakrishna S (2006) Biomed Mater 1:45
28. Filippo C, Paolo AN, Luigi A (2007) Biomaterials 28:5093
29. Gregory FP, Srinivasa RR (2007) Soft Matter 3:521
30. Liu C, Xia Z, Czernuszka JT (2007) Trans I Chem E Part A Chem Eng Res Des 85:1051
31. Ohkawa K, Cha D, Kim H, Nishida A, Yamamoto H (2004) Macromol Rapid Commun 25:1600
32. Mota C, Dario P, Dinuccio D, Cesare E, Paulo B, Federica C (2011) Materials 4:527
33. Mouriño V, Boccaccini AR (2010) J R Soc Interface 7:209
34. Puppi D, Detta N, Piras AM, Chiellini F, Clarke DA, Reilly GC, Chiellini E (2010) Macromol Biosci 10:887
35. Leong KF, Cheah CM, Chua CK (2003) Biomaterials 24:2363
36. Heydarkhan-Hagvall S, Schenke-Layland K, Dhanasopon AP, Rofail F, Smith H, Wu BM, Shemin R, Beygui RE, MacLellan WR (2008) Biomaterials 29:2907
37. Kim G, Son J, Park S, Kim W (2008) Macromol Rapid Commun 29:1577
38. Yoon H, Ahn S, Kim G (2009) Macromol Rapid Commun 30:1632
39. Papenburg BJ, Liu J, Higuera GA, Barradas AM, de Boer J, van Blitterswijk CA, Wessling M, Stamatialis D (2009) Biomaterials 30:6228
40. Harini GS, Robert BM, Jason AB (2010) Macromol Biosci 10:265
41. Gomes ME, Sikavitsas VI, Behravesh E, Reis RL, Mikos AG (2003) J Biomed Mater Res 67:87
42. Sachlos E, Czernuszka JT (2003) Eur Cell Mater 5:29
43. Bong GC, Lifeng K, Ali K (2007) Expert Opin Drug Discov 2:1

44. Cioffi M, Küffer J, Ströbel S, Dubini G, Martin I, Wendt D (2008) J Biomech 41:2918
45. Teo WE, Ramakrishna S (2006) Nanotechnology 17:R89
46. Shalumon KT, Binulal NS, Deepthy M, Jayakumar R, Manzoor K, Nair SV (2011) J Macromol Sci A 48:21
47. Tian F, Hosseinkhani H, Hossenkhani M, Khademhosseini A, Yokoyama Y, Estrada GG, Kobayashi HJ (2008) Biomed Mater Res A 84:291
48. Tuzlakoglu K, Bolgen UN, Salgado AJ, Gomes ME, Piskin E, Reis RL (2005) J Mater Sci Mater Med 16:1099
49. Capes JS, Ando HY, Cameron RE (2005) J Mater Sci Mater Med 16:1069
50. O'Brien FJ, Harley BA, Yannas IV, Gibson LJ (2005) Biomaterials 26:433
51. Sung JK, Da HJ, Won HP, Byung-Moo M (2010) Polymer 51:1320
52. Pham QP, Sharma U, Mikos AG (2006) Biomacromolecules 7:2796
53. Shalumon KT, Chennazhi KP, Tamura H, Kawahara K, Nair SV, Jayakumar R (2011) IET Nanobiotechnology (in press) doi : 10.1049/iet-nbt.2011.0028
54. Santos MI, Tuzlakoglu K, Fuchs S, Gomes ME, Peters K, Unger RE, Piskin E, Reis RL, Kirkpatrick CJ (2008) Biomaterials 29:4306
55. Edwards SL, Church JS, Werkmeister JA, Ramshaw JAM (2009) Biomaterials 30:1725
56. Cima LG, Vacanti JP, Vacanti C, Ingber D, Mooney D, Langer RJ (1991) J Biomech Eng 113:143
57. Soliman S, Pagliari S, Rinaldi A, Forte G, Fiaccavento R, Pagliari F, Franzese O, Minieri M, Nardo PD, Licoccia S, Traversa E (2010) Acta Biomater 6:1227
58. Kidoaki S, Kwon IK, Matsuda T (2005) Biomaterials 26:37
59. Arafat MT, Lam CFX, Ekaputra AK, Wong SY, Li X, Gibson I (2011) Acta Biomater 7:809
60. Jang JH, Castano O, Kim HW (2009) Adv Drug Deliv Rev 61:1065
61. Rezwan K, Chen QZ, Blaker JJ, Boccaccini AR (2006) Biomaterials 27:3413
62. Martins A, Pinho ED, Correlo VM, Faria S, Marques AP, Reis RL, Neves NM (2010) Tissue Eng A 16:3599
63. Osathanon T, Linnes ML, Rajachar RM, Ratner BD, Somerman MJ, Giachelli CM (2008) Biomater 29:4091
64. Park SH, Kim TG, Kim HC, Yang DY, Park TG (2008) Acta Biomater 4:1198
65. Kim SJ, Jang DH, Park WH, Min BM (2010) Polymer 51:1320
66. Langer R, Vacanti JP (1993) Science 260:920
67. Schmidt CE, Leach JB (2003) Ann Biomed Eng 5:293
68. Wang W, Itoh S, Matsuda A, Ichinose S, Shinomiya K, Hata Y, Tanaka J (2008) J Biomed Mater Res A 84:557
69. Panseri S, Cunha C, Lowery J, Carro UD, Taraballi F, Amadio S, Vescovi A, Gelain F (2008) BMC Biotechnol 8:39
70. Bouten CVC, Dankers PYW, Driessen-Mol A, Pedron S, Brizard AMA, Baaijens FPT (2011) Adv Drug Deliv Rev 63:221
71. Kwon IK, Kidoaki S, Matsuda T (2005) Biomaterials 26:3929

Adv Polym Sci (2012) 246: 21–62
DOI: 10.1007/12_2011_113

Published online: 23 April 2011

Stem Cells and Nanostructures for Advanced Tissue Regeneration

Molamma P. Prabhakaran, J. Venugopal, Laleh Ghasemi-Mobarakeh, Dan Kai, Guorui Jin, and Seeram Ramakrishna

Abstract Stem cells are a promising alternative for cell therapy applications because of their self-renewing capability and potential to differentiate into a wide range of specialized cell lineages, including osteoblasts, chondrocytes, cardiomyocytes, and neuronal cells. Different kinds of stem cells are considered for cell-based tissue engineering approaches, of which bone-marrow-derived mesenchymal stem cells (BM-MSCs), adipose-derived stem cells (ADSCs) and embryonic stem cells (ESCs) are frequently utilized for advancement of new tissue engineering strategies. Nanostructures created by natural, synthetic, or composite polymeric biomaterials provide artificial templates of the extracellular matrix (ECM). They possess a high surface area to volume ratio, are porous with good mechanical properties, are sufficient to serve as a biomimetic platform to attract stem cells, cause differentiation, and provide functioning of the tissues. Nanoscale features such as fibers, pits, and grooves modulate cell behavior and might even stimulate the differentiation of stem cells to specific lineages; for example, the nanotopographical cues combined with chemical cues influence the neuronal induction of MSCs, resulting in high microtubule-associated protein expressions. Scaffolds can also be impregnated with several ligands for adhesion of receptors to the cells, or with other regulatory molecules and growth

M.P. Prabhakaran (✉) and J. Venugopal
E3-05-12, Health Care and Energy Materials Laboratory, Nanoscience and Nanotechnology Initiative, Faculty of Engineering, National University of Singapore, 2 Engineering Drive 3, Singapore 117576, Singapore
e-mail: nnimpp@nus.edu.sg

L. Ghasemi-Mobarakeh
Islamic Azad University, Najafabad Branch, Isfahan, Iran

D. Kai
NUS Graduate School for Integrative Sciences and Engineering, National University of Singapore, 2 Engineering Drive 3, Singapore 117576, Singapore

G. Jin and S. Ramakrishna
Department of Mechanical Engineering, National University of Singapore, 2 Engineering Drive 3, Singapore 117576, Singapore

factors for designed cell behavior or controlled cell differentiations. Different polymeric blends or fibers incorporated with nanoparticles (such as hydroxyapatite) in aligned or custom-made patterns can induce specific differentiation of stem cells for bone, cartilage, cardiac, nerve, and skin tissue regeneration. In this review, we will discuss the current state of the art and future perspectives on stem cells and their differentiation on nanoengineered substrates for advanced tissue regeneration.

Keywords Bone · Cardiac · Cartilage · Electrospinning · Mesenchymal stem cells · Nerve

Contents

1 Introduction

The basic functional units of cells and tissues are of nanoscale dimensions, and nanotechnology promises an important area of study in regenerative medicine. Cells are typically of tens of micrometers in diameter, and cellular structures such as the cytoskeletal elements and transmembrane proteins too exist in nanoscale proportions [1]. The supporting tissues form an intricate network of cues on the nanoscale (5–200 nm), and this network consists of a complex mixture of pores, pits, projections, etc., showing the complexity of the structures present in vivo [2]. Nanostructures are therefore important cues at the cellular level, and cells regulate and function depending on the topographical features and the type of surface molecules. The nanotopographical features are known to induce or disrupt the focal adhesion and spreading of cellular populations, which is mediated via the perturbation of integrin activation and clustering [1]. An ideal strategy in tissue engineering (TE) or regenerative medicine is to identify and utilize the right combination of biomaterial scaffolds, cells, and biological factors that assist cells to adhere, organize, and behave similarly to native tissue [3]. Polymeric biomaterials fabricated in various

structures, designs, and forms serve as provisional scaffolds for cells to attach, grow, and maintain differentiated functions.

This review provides an introduction to the different methods utilized for the fabrication of nanostructures, the different kinds of nanotopographies, and the major stem cell types studied in the field of tissue regeneration. Emphasis is given to the attachment and differentiation of mesenchymal stem cells (MSCs), embryonic stem cells (ESCs), and adipose-derived stem cells (ADSCs) on biomimetic nanomaterials for advancing the field of bone, cartilage, cardiac, nerve, and skin tissue regeneration.

1.1 Nanotechnology in Tissue Regeneration

Nanotechnology refers to one of the rapidly growing scientific disciplines studying and developing objects and materials with characteristic dimensions to resolve disease-related organ damage using tissue engineering. Nanotechnology could be a powerful tool for deciding the cell–biomaterial communications, inducing stem cell differentiation in a desired fashion (tissue). Nanotechnology aims to create structures at the atomic and molecular levels with a size range of 10–500 nm. It is also known that highly organized fibers (specific spatial organization) are present in native tissues such as ligaments and bone, providing sufficient mechanical strength. For example, collagen fiber bundles are aligned in parallel in native tendons and ligaments and are found as concentric waves in bone [4, 5]. Stem cells contribute to the organized tissue architecture of bone and cartilage to a certain extent, and aligned extracellular matrix (ECM) might be crucial for their differentiation behavior [6]. Cells come in contact with the ECM via integrins and transmembrane proteins, which interact with certain amino acid sequences found in the ECM proteins. The cell cytoskeleton becomes tethered to the fibrous structure of the ECM through these receptors and it activate a series of intracellular signaling pathways that affect cellular behavior such as cell adhesion, proliferation, and differentiations [7]. The fate of stem cells is decided by the signals and biophysical clues found in the cellular microenvironment. These signals are mainly the ECM molecules, soluble factors, biophysical factors, and intercellular contacts. Scaffolds can be engineered with suitable substrate moieties (high density epitopes) to assist or control the stem cell behavior in tissue assembly.

Stem cell nanotechnology has gained huge momentum and it is currently being applied for the treatment, repair, and regeneration of cells and tissues. Cells can interact with features as small as 5 nm and, hence, nanotopographies influence the cell behavior in addition to the type of substrates used for cell growth [8]. Nanoscale topographies are created by various fabrication methods such as electrospinning, polymer phase separation, photolithography, chemical vapor deposition, electron beam lithography etc. [9]. The morphological similarity of electrospun nanofibers to native ECM signifies the application of these scaffolds as a supportive matrix for stem cell attachment and differentiations. Nanofibrous scaffolds mimic the fibrous ECM of native tissue and could provide mechanical, biological, and

chemical cues to cells. Studies on the controlled release of basic-fibroblast growth factor (bFGF) from nanofibrous scaffolds and induced angiogenesis indicate the role of environmental factors required for the survival of cells in enhancing tissue regeneration [10]. By providing the appropriate biological cues, cell receptors can bind to signaling biomolecules and transmit the signals intracellularly by activating signaling cascades, which further modulate gene expression and decide the cell fate or the differentiation module. Cell alignment could be important for the treatment of nerve, cardiac, and even muscle tissue regeneration. Cells probe the topographical features of the ECM to proliferate and differentiate, whereby the "filapodia" gather the topographical, spatial, and chemical information from the material surfaces [11]. When engineering tissues such as ligaments, articular cartilage, and blood vessel walls, the principle of contact guidance dominates, mainly because these tissues possess highly anisotropic cellular organization [12]. The formation of elongated focal adhesion points is important in osteospecific differentiation of MSC, and the adhesion elongation relies on enhanced integrin clustering [1]. With focal adhesion corroborations, increased focal adhesion kinase (FAK) is recruited and subsequently activated to initiate the downstream signaling cascades. Moreover, limited focal adhesion points can also cause reduced mechanosensitive signaling events [1]. Substrate topography together with electrical conductivity has also been shown to contribute to nerve stem cell differentiation to specific neuronal lineages [13]. Among the various ECM-derived cell binding motifs, the scaffolds used in TE are mainly modified with peptides such as RGD, IKVAV, YIGSR, PHSRN and GFOGER [14]. There is an urgent need to evaluate and understand the particular cell behavior of stem cells on nanostructures, which might eventually help us to design a scaffold for enhanced tissue regeneration.

1.1.1 Nanostructure Fabrication Methods

Electrospinning is a simple, versatile, and affordable method for producing nanofibers with defined geometry by electrically charging a suspended droplet of polymer melt or solution. Natural, synthetic, and composite polymeric materials are electrospun to obtain fibers, and the diameter of the fibers can be adjusted by varying the polymer concentrations, solvents used, or by modulating the spinning conditions [15, 16]. Electrospun nanofibers provide a high surface area for cell attachment, and functionalization of fibers is possible by chemical conjugation of ECM molecules or by protein coatings (composite scaffolds). A variety of topographical patterns such random, aligned, porous, and core–shell nanofibers have been studied extensively for various TE applications. Figure 1 shows the nanofibrous architectures created by various electrospinning methods. Advanced and modified technologies such as multilayered electrospinning and simultaneous electrospin–electrospray methods have also been studied recently for obtaining scaffolds with multifunctional properties [17].

Phase separation is utilized for the fabrication of porous membranes and it allows for the generation of three-dimensional (3D) porous networks within the scaffolds. Considering the relationship of specific cells and pore sizes, polymeric

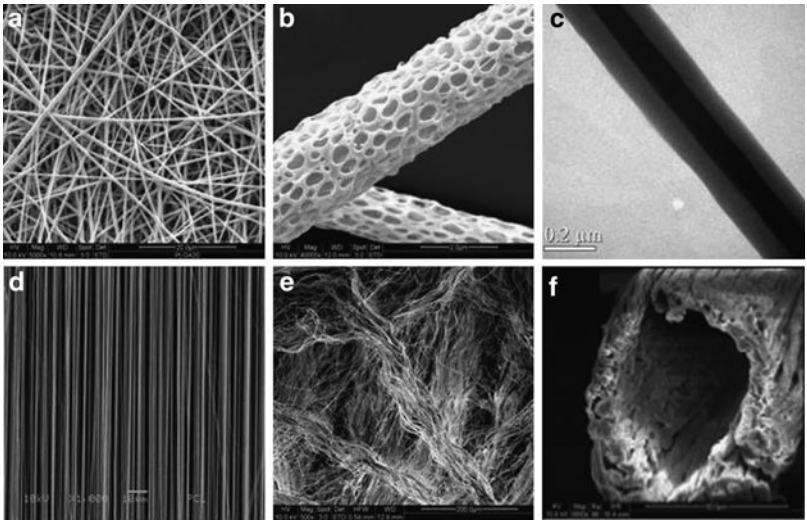

Fig. 1 Nanofibrous architectures created by electrospinning: (**a**) random nanofibers, (**b**) porous nanofibers, (**c**) core–shell nanofibers, (**d**) aligned nanofibers (**e**) nano-yarn, (**f**) hollow nanotubes

scaffolds should be designed not only with high degree of porosity but also with greater control over the pore size and morphology [18, 19]. The phase separation method is based on the thermodynamic de-mixing of a homogenous solution of polymer in solvent into polymer-rich and polymer-poor phases by exposure to another immiscible solvent or by cooling the solution below the glass transition temperature (*T*g) of the polymer. Processing variables such as the polymer type, concentration, solvent, and temperature are critical parameters that affect the morphology of the fabricated scaffolds.

Self-assembly involves the autonomous organization of individual components in an ordered structure or pattern without human intervention. It occurs through non covalent forces such as hydrogen bonding, electrostatic forces, or hydrophobic forces. Control of self-assembly in the design of peptide systems is carried out by switching the pH, or by varying the temperature, concentration etc. [20]. Cell-adhesive peptide ligands are commonly exposed to the self-assembled nanofibrous structures to enhance the bioactivity of the scaffolds for convenient applications in tissue regeneration [21].

Physical patterning techniques such as reactive ion etching, polymer molding etc. create microgrooves for designated cellular orientations [22, 23]. Patterned surfaces provide cues for cellular attachment, migration, orientation, and function. Soft lithographic techniques have been used to generate exquisite control over protein and cells in spatially defined patterns. Cell shape has been regulated at the microscale, and even the temporal and spatial distribution of biomolecules has been performed to direct explicit cell behavior and functions. Methods such as imprint lithography, photo or electron beam lithography, or microcontact printing are also carried out for patterning biological molecules or for constructing geometrically

designed substrates suitable for cellular interaction on a nanoscale [24, 25]. The Imprint lithography method utilizes a silicone rubber stamp (made by casting silicone rubber into a patterned die) inked with molecules to transfer the agent to a prepared surface. It is possible to provide specific cues, potentially suitable for a particular cell type or for specific differentiation modulation by this method. Grids, honeycomb networks, dots etc. are a few patterns created using the microcontact printing method to mimic the basement membrane structures of nanometer-sized pores and ridges [26]. Microcontact printing also has advantageous over other patterning methods as it does not involve the usage of harsh solvents and high temperatures [27]. Nanoimprint lithography is capable of creating patterns of sub-10 nm features and uses very simple equipment with convenient processing steps [28]. On the other hand, atomic force microscopic etching involves scratching the material surface with a nanosized pyramidal tip, but has limitations in application over a large surface area [29]. Design of nanotopographical patterns based on the specific needs of a particular tissue regeneration is therefore possible by application of the above-mentioned methods.

1.1.2 Substrate Stiffness and Effect of Mechanical Stretch

Stiffness of substrate plays an important role in cell adhesion, especially towards the lineage-specific differentiation of stem cells [30]. Hydrogels have the ability to simulate the nature of soft tissues and are highly attractive materials for developing synthetic ECM analogs [31]. Three-dimensional biomaterial constructs not only act as a mechanical support, but also provide a suitable structure and well-defined array of macromolecular signals to direct the de novo tissue development [32]. Moreover, cell infiltration can be improved using 3D structures, whereas the mechanical properties of the gels, release of biomolecules, transport and degradation kinetics can also be tuned for improving the cytocompatibility of encapsulated cells or towards stem cell differentiation [33, 34]. Engler and coworkers demonstrated that the differentiation of human mesenchymal stem cells (hMSCs) was dependent on the mechanical stiffness of 2D culture platforms [35]. Soft gels were demonstrated to support MSC differentiation to neuronal cells, while stiffer gels supported an osteoblast-like phenotype. Figure 2 shows the differentiation of stem cells on substrates with varying elasticity. Moreover, it is also possible to incorporate other inducing factors during matrix design to bestow lineage specificity [35]. Control of the biochemical and mechanical properties of the scaffolds will help us to understand the effect of specific cell–ECM interactions in 3D tissue models, and could used to dictate that cells behave in a desired fashion in vivo for tissue development [31].

Mechanical stretching of cell membranes can be achieved by nanotechnological approaches and it can direct and control the intracellular signaling and differentiation of stem cells [36]. Modifications made to the spatial distribution or cytoskeletal re-organization provide physical impetus, whereby the mechanical deformation becomes translated into biochemical responses [37]. When the cells encounter

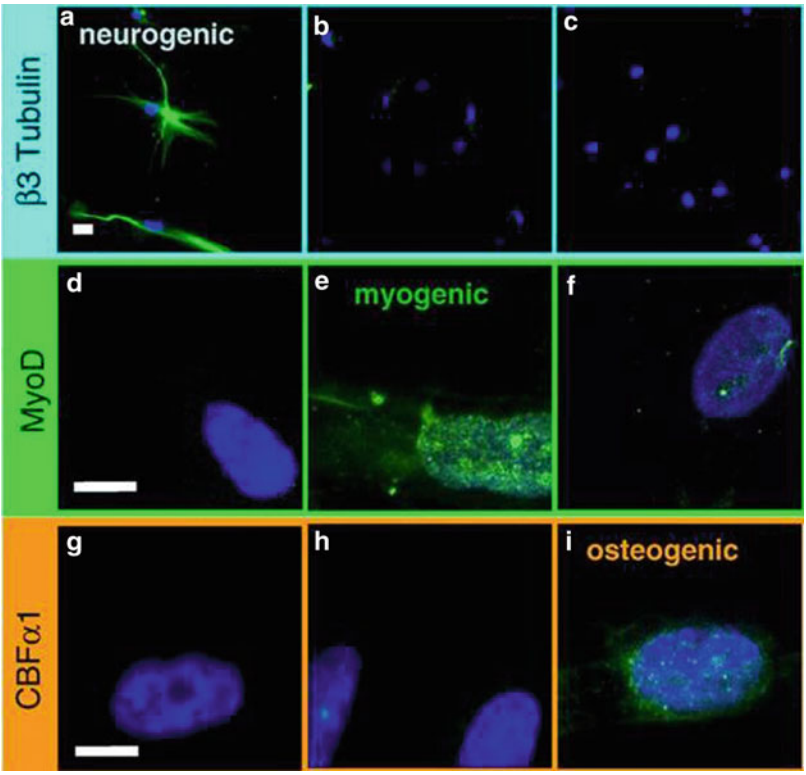

Fig. 2 Mesenchymal stem cell differentiation on substrates with different elasticity: (**a–c**) neurogenic differentiation on soft matrices; (**d–f**) myogenic matrices showing upregulated muscle transcription factor; (**g–i**) osteogenic differentiation on stiffer matrices. Reproduced with permission from Engler et al. [35]

topographic discontinuity, such as a groove or a cliff, re-organization of the microfilament occurs and cell activation can be further related to specific gene expressions compared to its growth on flat surfaces [38]. Studies using defined arrays of bound peptide fragments showed that the protein recruitment to focal adhesions requires an integrin spacing of less than 60 nm. A higher spacing between the integrins (70–300 nm) facilitates integrin clustering and focal adhesion formation [39]. Grooved substrates can provide an elongated morphology and alignment of cells, thus influencing cells including the MSCs to respond and upregulate the expression of ECM components and proteins pertaining to cellular adhesions [40]. On grooved surfaces, the cell microfilament bundles align predominately along the edges of the grooves [24]. It is known that the FAK-mediated ERK1/ERK2 signaling pathway is an important modulator of osteo- and adipo-specific differentiation of MSCs. Topographical information of a tissue-engineered graft regulates cellular adhesion and differentiation because an increase in integrin–substratum

interaction has been shown to upregulate the expression of FAK and ERK1/ERK2 in osteoprogenitor cells [41].

1.2 Stem Cells: Origin and Multipotency

Stem cells are present in every type of tissue, and smart engineered scaffolds loaded with stem cells can differentiate into specific cell lineages for effective tissue regeneration. "Stem" refers to the ability of progenitor cells to self-renew, meaning to divide and retain a daughter cell that does not differentiate, while also producing another daughter cell that differentiates or divides and then differentiates. Various organs, including the peripheral blood, bone marrow, pancreas, muscle, skin, fat, and neuronal system contain stem cells [42, 43]. "Differentiation" is the major cellular event that forms the basis for utilization of stem cells in regenerative medicine, and it is the microenvironmental cues that define the kind of differentiation [44]. Control of cell behavior by ligand density and/or specificity, nanopatterning, material architecture, mechanical properties of the material etc. are possible, aiming towards specific lineage differentiations. Distinct cell culture conditions or nanoenvironments, in conjunction with ECM molecules such as laminin, collagen, gelatin, cytokines or other growth factors, are utilized for the differentiation of stem cells to specific functional progeny [45].

Stem cells are mainly classified as adult stem cells and ESCs. ESCs are obtained from embryonic blastocysts, and adult stem cells are derived from various tissues of developed (adult) or developing individuals. The most commonly studied adult stem cells are the bone-marrow-derived mesenchymal stem cells (BM-MSCs) and the adipose-tissue-derived stem cells (ADSCs), discussed in this review.

1.2.1 Mesenchymal Stem Cells

MSCs are non-hematopoietic progenitor cells that have the potential to differentiate into various lineages of mesenchymal origin. They are attractive cell types for TE applications, relatively privileged in terms of immune compatibility, and can be easily isolated [46]. They are isolated from bone marrow (BM), immobilized blood, umbilical blood, cord blood, deciduous teeth, and even placenta. However, BM is relatively accessible and it serves as the main source of MSC. The advantage of using BM-MSC in regenerative medicine is because they are naturally poised to generate a particular tissue, which might consist of several cell types such as adipocytes, chondrocytes, osteoblasts, tenocytes, myoblasts, neurocytes etc. MSCs constitute approximately 2–3% of the total nuclear cell fraction of the BM [47]. Isolation of these cells involves seeding the mononuclear cell layers obtained from Ficoll density gradient centrifugations. MSCs have a spindle-shaped fibroblast-type morphology and adhere to the base of the culture flask, while the non-adherent hematopoietic cells are washed off. MSCs are positive to a variety of

surface markers such as CD44, CD105, and CD29 and are negative to markers such as CD45, CD34, and CD14 [48, 49]. However, the specificity of these markers is relatively weak, which means that they are not exclusively markers for MSCs. Under in vitro conditions, MSCs do not expand indefinitely unlike ESCs, and several agents including hormones, ECM molecules, and growth factors tightly determine the differentiation possibility of MSCs.

BM-MSCs possess high plasticity and have been differentiated into various cell lineages and contribute much to the regeneration of tissues at injured sites [50, 51]. It is reported that scaffolds loaded with different ratios of hydroxyapatite/tricalcium phosphate (HA/TCP) with MSCs showed different degrees of bone formation in vivo. Optimal composition of HA/TCP ratios within the composites were designed to match tissue deposition with scaffold degradation so as to promote the greatest ectopic bone formation [52]. Physical or mechanical forces are also suggested to regulate the stem cell differentiation process, and the latest trend is the "functional tissue engineering approach," where bioreactors are designed to reiterate certain segments of the in vivo and in vitro cell culture system [53].

1.2.2 Embryonic Stem Cells

ESCs are cells derived from the inner cell mass of blastocyst-stage embryos. ESCs have indefinite self-renewing capacity and possess pluripotency or the ability to differentiate to cells from three germ layers (endoderm, mesoderm, and ectoderm). ESCs differ from other tissue-specific stem cells in that they can be readily expanded in culture over an extensive period of time [54]. Their isolation involves treating day 5 blastocysts with pronase, transferring the zona-free blastocysts onto irradiated or mitomycin-C-treated mouse embryonic fibroblast (MEF) feeder cells or human adult fibroblasts, and then culturing in media containing bFGF and insulin-transferrin-selenium (ITS). The inner cell mass (ICM) lump is mechanically detached using capillary pipettes, cut into smaller pieces and transferred to fresh irradiated or mitomycin-C-treated MEFs and incubated with culture media [55]. OCT4 and telomerase are better-accepted markers for ESCs, but their expression in adult stem cells is less certain [56, 57]. ESC self-renewal versus differentiation is regulated via interactions with other cells, ECM components, soluble factors, and the physicochemical environment [58]. However, concerns exist regarding the immune reactions of ESCs along with the potential of undifferentiated ESCs towards teratoma development, which hamper the clinical applications of ESCs [59].

1.2.3 Adipose-Derived Stem Cells

Adipose tissue is the most abundant and accessible source of stem cells and ADSCs are demonstrated to possess multiple differentiation capacity. ADSCs originate from the stromal vascular fraction of adipose tissue. Liposuction is being undergone

by many people to remove excess adipose tissue, which could serve as a source of ADSCs. The contaminating hematopoietic cells are removed by washing the minced fat pads and the tissue fragments incubated with enzyme collagenase; then the contents are centrifuged and the mature adopicytes separated from the pelleted stromal vascular fraction [60]. ADSCs adhere to plastic surfaces and display fibroblastic characteristics, with abundant endoplasmic reticulum and large nucleus relative to the cytoplasmic volume [61]. Immunophenotypical studies suggest that the glycoprotein CD34 is present during early passage of human ADSCs and has not been found on MSCs [62]. At passage 0 (cells cultured for 72 h), less than 10% of human or murine ADSCs express CD31 [63]. Recent studies by Traktuev et al. [64] suggested that ADSCs can be defined by coexpression of CD34 and CD140b. ADSCs are suggested to contribute towards the angiogenic properties because they secrete angiogenic cytokines such as vascular endothelial growth factor (VEGF) and hepatocyte growth factor (HGF) [65]. Due to its angiogenic capabilities, ADSC-augmented nanostructures could be utilized for effective regeneration of vascular tissue. However, for clinical use, health care professionals should be educated with regard to the unique properties of ADSCs in order to avoid their inappropriate use (and ensure correct application).

2 Strategies for Advanced Tissue Regeneration

The efficiency of stem cell transplantation might be enhanced by encapsulating the cells in biocompatible scaffolds that provide a temporary 3D matrix for cell adhesion, migration, and differentiation. There is great interest in the ex vivo and in vivo differentiation capability of stem cells on nanomaterials for regeneration of injured tissues and organs. Here, we focus on recent developments in the mimicking of cell–matrix interactions representative of the stem cell niche, with an emphasis on nanostructures for modulating the stem cell differentiation for advancing the field of cardiac, bone, cartilage, nerve, and skin regeneration.

2.1 Osteogenesis

Orthopedics is a multibillion dollar industry and every year millions of people suffer from bone defects arising from cancer, fractures, periodontitis, osteoporosis, and infectious disease and many people die due to insufficient bone substitute. The functional treatment of fracture nonunion and bone loss associated with trauma and revision joint arthroplasty has become increasingly common and it remains a significant challenge to the field of musculoskeletal injury [66]. Bone grafts are increasingly used; however, they are plagued by high-failure rates of 16–50% [67]. The replacement of diseased bone tissue has taken a variety of forms: metals, ceramics, polymers, and bone itself, but none has proven ideal for TE. Biomaterials

can be either permanent or biodegradable, and need to be biocompatible, osteoinductive, osteoconductive, integrative, and mechanically compatible with native bone to fulfill the desired functionality in bone TE. These materials provide cell anchorage sites, mechanical stability, structural guidance, in vivo milieu, and an interface to respond to the physiological and biological changes in order to remodel ECM and integrate with the surrounding tissue [68]. Therefore, polymeric nanofibrous scaffolds applied for bone TE should be biocompatible with the surrounding biological fluids and tissues, biodegradable, and highly porous with interconnected spaces favorable for the diffusion of nutrients and the migration of a large number of cells.

Recently, 3D scaffold materials have become a crucial element for bone TE. These scaffold materials are designed to mimic one or more bone-forming components of autograft, in order to facilitate the growth of vasculature into material and provide an ideal environment for bone formation. The formation of bone can be roughly divided into three phases: (1) proliferative phase, during which collagenous matrix is deposited, (2) maturation phase, which is characterized by the activity of alkaline phosphate, and (3) mineralization phase, when the newly formed matrix begins to calcify. These phases are influenced by an increased amount of collagen type III coating, giving rise to an increase in cell proliferation and synthesis of collagen, both of which are characteristics of the early phase of bone formation. Collagen provides an inherently good biocompatibility with cells, and collagen-based implants are well known for their feasibility in promoting tissue regeneration. HA [$Ca_5(PO_4)_3OH$] is considered to be a structural template for the bone mineral phase. It is a major inorganic mineral component of bone and is commonly used as a bioceramic filler in polymer-based bone substitute because of its high bioactivity and biocompatibility [69]. Calcium phosphate biomaterials such as HA and TCP with appropriate 3D geometry are able to bind and concentrate endogenous bone morphogenetic proteins (BMP) in circulation, and may become osteoinductive [70] and effective carriers of bone cells.

2.1.1 Stem Cells and Nanomaterials for Bone Regeneration

Silk is an attractive material for osteochondral TE since its mechanical properties are favorable for engineering of load-bearing tissues and it displays a higher elastic modulus and tensile strength than other natural and synthetic biomaterials [71]. RGD-coupled silk films and scaffolds improved osteogenesis, stimulating increased osteogenic gene expression, calcification, and formation of bone-like trabeculae compared to unmodified silk materials [72]. Functionalization of silk films by covalent conjugation of bone morphogenetic protein-2 enhanced the osteogenic differentiation of MSCs compared to soluble delivery of bone morphogenetic protein-2 [73]. Another attractive ECM-mimicking biomaterial for creating tissue-specific microenvironments that facilitate synthetic cell–ligand interactions is composed of peptide amphiphiles (PAs). PAs are a broad class of molecules that self-assemble into nanofibrous supramolecular formations, emulating the native ECM architecture. These molecules consist of a peptide sequence covalently linked

to a hydrophobic alkyl chain [74]. The RGD ligand is prevalent in many ECM molecules, including fibronectin, laminin, and osteopontin, which have been well documented to increase cell adhesion [75]. Recent studies have shown that inclusion of RGD ligand can potentially increase osteogenic differentiation [76, 77]. Anderson et al. observed the osteoconductive potential on RGD-modified PA scaffolds independent of stimulatory aid, though not to the same phenotypic levels as the supplemented scaffolds [78]. However, PAs offer a promising regenerative tool for the continued development of bone TE applications.

Osteogenic activation of MSC requires the presence of β-glycerophosphate, ascorbic acid, and dexamethasone [79]. Yoshimoto et al. cultured rat MSC on poly(ε-caprolactone) (PCL) nanofibrous scaffolds of 400 nm diameter and observed ECM production (collagen) and multiple cell layer formation within a short span of one week [80]. Salerno et al. reported a novel approach for the design of porous PCL scaffolds with well-controlled microarchitectures, by combining gas formation and selective polymer extraction methods for osteogenic differentiation of hMSCs in vitro [81]. Hosseinkhani et al. investigated MSC behavior on self-assembled PA nanofibers and they found significantly enhanced osteogenic differentiation of MSCs in 3D PA scaffolds compared to 2D static tissue culture [82]. Dalby et al. [83] demonstrated the use of nanoporous topography to stimulate hMSCs to produce bone mineral in vitro, in the absence of osteogenic supplements. Their results demonstrated that highly ordered nanoporous topographies produce negligible cellular adhesion and osteoblastic differentiation. Dynamic bioreactor culture systems are essential for the in vitro cultivation and maturation of TE bone grafts, especially for larger grafts where the core of the scaffold is more than 200 μm [84]. The dynamic media flow causes mechanical stimulus to the cells, enhancing cellular osteogenesis and mineralization through triggering of mechanotransduction signaling pathways. In yet another study, the dynamic culture and osteogenic priming of hMSC-mediated macroporous PCL/TCP scaffolds in biaxial rotating bioreactors generated an effective TE bone graft for healing a critically sized defect [85].

Lyons et al. fabricated freeze-dried collagen/glycosaminioglycan (CGAG) and collagen/calcium phosphate scaffolds (CCP) for the culture of bone marrow stromal cells (BMSCs) for bone TE [86]. These researchers created a 7-mm transosseous calvarial defect in rats, and implanted it with either CGAG scaffold, TE-CGAG construct, CCP scaffold, TE-CCP construct, or with no scaffold (empty control), and the suture was closed. Animals were sacrificed after 4 and 8 weeks of follow-up study for the analysis of bone tissue regeneration. Results showed that the empty control group defects are filled with structurally and morphologically organized fibrous tissue consistent with failure to heal the bone defect (Fig. 3ai), demonstrating the critical size of the defect. Fibrous tissue was clearly seen extending from the defect margin (Fig. 3aii) with a few small areas of the new bone formation visible immediately adjacent to the host bone, indicating unsuccessful attempts at regeneration. CGAG scaffold-filled defects did exhibit signs of healing with woven bone formation visible around the defect periphery, with most found at the interface with the host bone (Fig. 3bii, biiii). Qualitative spectrum of newly formed bone was

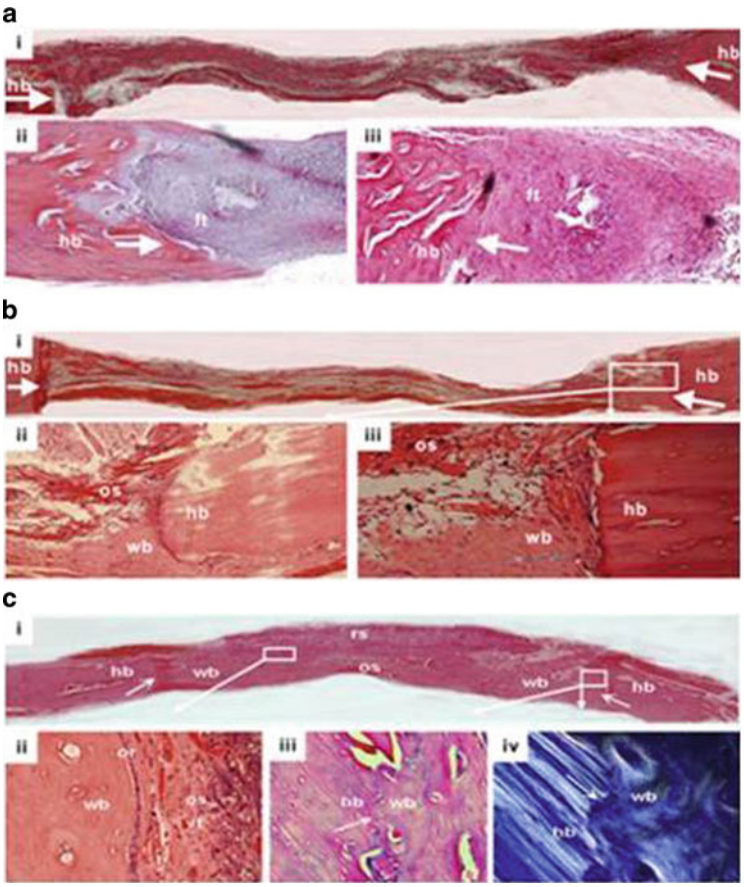

Fig. 3 Histological images (stained with hematoxylin and eosin) of bone tissue regeneration after implantation of a transosseous calvarial defect with CGAG or CCP scaffold. (**a**) Empty control group (no scaffold implant) at 8 weeks shows no healing of the defect: (**ai**) full-size image of the specimen, with the original host bone at the edges; higher magnifications (**aii** 20×, **aiii** 40×) shows fibrous tissue filling the defect and original host bone at the periphery. (**b**) CGAG group at 8 weeks post-surgery: (**bi**) full specimen; at higher magnifications (**bii, biii**), healing is seen extending from the host bone into the defect. (**c**) CCP group at 8 weeks post-surgery: (**ci**) shows progressive areas of healing across the defect and large areas of the defect filled in with healing woven bone and osteoid. The remnant of the scaffold can be seen heavily infiltrated with host cells. High magnification images (**cii**, **civ**) show a vertical rim of osteoblasts at the interface of new woven bone, and unmineralized osteoid with vascular tissue also present. (**ciii**) demonstrates the interface between the host bone and areas of new woven bone filling the defect. (**civ**) Epifluorescence microscopy image shows the interface between host bone and woven bone in the defect. *Arrows* indicate original host bone margins, *ft* fibrous tissue, *hb* host bone, *wb* woven bone, *os* unmineralized osteoid, *rs* remnanat of scaffold, *or* rim of osteoblasts, *vt* vascular tissue. Reproduced with permission from Lyons et al. [86]

visible bridging the defect in the CCP group at 8 weeks (Fig. 3ci), with woven bone advancing from the defect-host interface (Fig. 3ciii and civ). Staining of the immunomodulatory and tissue remodeling (M2 phenotype) marker CD163 at 4 weeks demonstrated active M2 mononuclear cell activity in the scaffold substance, particularly at the site of new bone formation and the host–scaffold interface in cell-free scaffolds (Fig. 4a). In the TE-CGAG and TE-CCP constructs, M2 phenotype mononuclear cells (MNC) were evident at 8 weeks, suggesting an advanced stage of remodeling process (Fig. 4a). In the TE-CGAG and TE-CCP constructs, M2 phenotype MNCs was evident at both 4 and 8 weeks predominantly at the periphery of the scaffold, especially in the fibrous/inflammatory capsule seen previously on

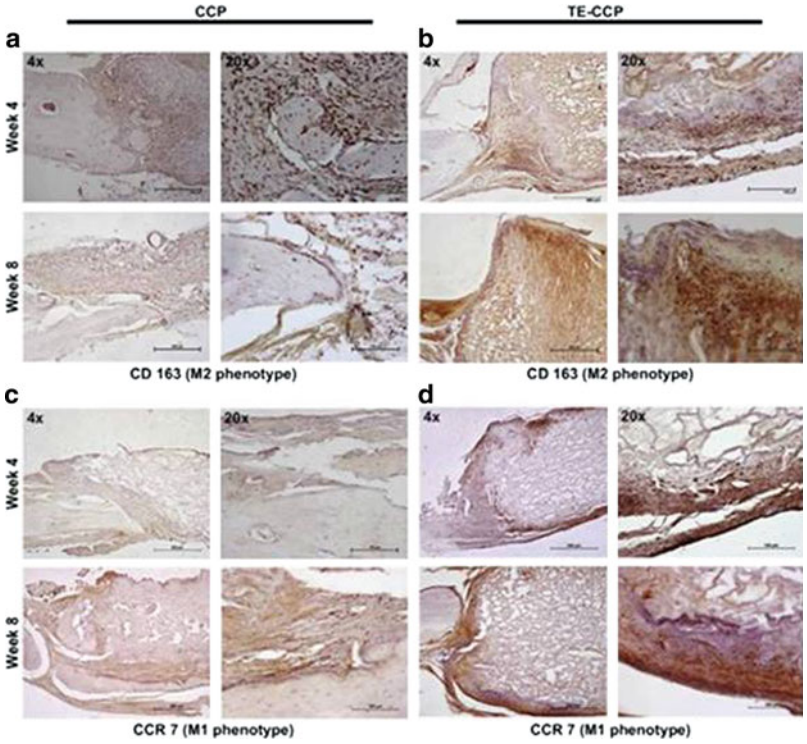

Fig. 4 Immunohistochemistry results for cell-free CCP and TE-CCP scaffolds at 4 and 8 weeks. (**a**) Staining for the immunomodulatory and tissue remodeling (M2 phenotype) marker CD163 at 4 weeks demonstrated active M2 macrophage activity in the scaffold substance, particularly at sites of new bone formation and the host–scaffold interface in cell-free scaffolds. These cells were less evident by 8 weeks, suggesting an advanced stage of the remodeling process. (**b**) In the TE scaffolds, M2 phenotype macrophages were evident at both 4 and 8 weeks predominantly at the periphery of the scaffold, especially in the fibrous/inflammatory capsule seen previously on histological examination. (**c**) The proinflammatory (CCR7) marker demonstrated little M1 macrophage cell activity in unseeded scaffolds at either 4 or 8 weeks. (**d**) There was marked population of these cells at the periphery of TE scaffolds at both 4 and 8 weeks. Reproduced with permission from Lyons et al. [86]

histological examination (Fig. 4b). The pro-inflammatory (CCR7) marker demonstrated little M1 phenotype MNC activity in unseeded scaffolds at either 4 or 8 weeks (Fig. 4c) but a marked population of such inflammatory cells at the periphery of the TE-CGAG constructs at both 4 and 8 weeks (Fig. 4d). These results proved that the collagen/calcium phosphate (CCP) scaffolds provided increased stiffness and accelerated new bone formation in the defect compared to a non-mineralized CGAG scaffold.

2.1.2 Embryonic Stem Cells on Nanostructures for Bone Regeneration

ESCs represent a potential advance in cell sourcing for TE because they proliferate for longer than other types of stem cells and possess the ability to differentiate to any tissue type within the body. The cell–cell interactions and BMPs secreted by primary bone-derived cells stimulated human ESCs (hESCs) into osteogenic lineages in a direct co-culture system [87]. Cell extracts derived from hESC-derived osteogenic cultures induced undifferentiated hESCs into osteogenic lineage [88]. Human ESC-derived embryoid body cells were cultured in the presence of osteogenic supplements such as ascorbic acid and β-glycerophosphate (BGP) for 14 days, and dexamethasone was added to this medium for another 24 h. The stimulated cells were further seeded onto poly(lactic acid) (PLA) scaffolds and implanted subcutaneously to the back of immunodeficient mice for 5 weeks. Discrete areas of mineralization were observed, and osteocalcin was expressed by the implanted cells [89]. Implantation in the peripheral cavity of osteogenic and control hESC-derived embryoid body cells in injection chambers for 11 weeks resulted in the formation of mineralized areas [90]. However, the osteogenic supplementation for 4 days before implantation was not sufficient to enhance osteogenic differentiation of hESCs to levels higher than spontaneous osteogenic differentiation.

Recent advances made in the field of nanotopography-mediated stem cell regeneration provide optimism that bone TE can create a permissive environment for bone regeneration. Progress has been made over the last few years for bone TE, but usage of ESCs still remains in its infancy. We are optimistic about the future perspectives in bone TE, though stem-cell-based therapy involves many legal and social questions that must be addressed before stem-cell-based therapies become clinically available.

2.2 Chondrogenesis

Developing artificial articular cartilage to repair cartilage has been an ongoing battle for scientists and surgeons for decades. Articular cartilage defects can be caused by congenital and metabolic diseases as well as trauma or injury, or from degeneration due to osteoarthritis. Articular cartilage damage leads to disability, morbidity, and dependence, consequently giving rise to healthcare expenditures

and loss of work [91]. Articular cartilage is a thin layer of hyaline cartilage that covers the surface of bones at large articulating diarthrodial joints. Its function is to enable low-friction movement whilst being able to bear high tensile forces and resist deformation. Its uniquely dense ECM is produced and maintained by a single type of specialized cell, the chondrocytes [92]. Mature joint cartilage is free of blood vessels and enervation, is composed of ECM rich in proteoglycans and collagen type II, and about 5% of the tissue volume is occupied by chondrocytes. These cells are spherical, embedded in lacunae filled with pericellular matrix, and have no contact to the distant neighbor cells. Although human cartilage can reach a thickness of up to 7–8 mm, its supply with nutrients and oxygen is constrained to diffusion which is, however, facilitated by compressive cyclic loading that provides a pumping mechanism during joint movements. The cartilage ECM is abundant in collagens that provide a network of proteoglycans and other biomolecules. The negatively charged proteoglycans are responsible for high osmotic swelling pressure, resulting in a large proportion of water within the tissue [93]. It is through the interactions between collagen, proteoglycans, and water that hyaline cartilage becomes a resilient tissue capable of lasting a lifetime.

The ability of clonally expanded human BM cells to differentiate towards the osteogenic, chondrogenic, and adipogenic lineages was demonstrated by Pittenger et al., thereby making it possible to develop treatments with human autologous cells for the repair of mesenchymal tissues such as bone, cartilage, and adipose tissues [50]. Cellular differentiation is characterized by increased synthesis of transcription factors sox-5 and sox-6, and the appearance of cartilage transcription factor sox-9 [94, 95]. In the growth plate, hypertrophy and calcification of the cartilage tissue precede vascular invasion, finally leading to tissue replacement by bone. Collagen type I and fibronectin are synthesized in the ECM prior to condensation and reach a maximum density at the time of cellular differentiation [96]. Chondrogenic differentiation of the condensing cells is characterized by the appearance of collagen types II, IX, and XI, the characteristic component of the collagen network of cartilage tissue. Mixed collagen type I and type II formation result in mechanically inferior fibrocartilage, and it is assumed to be an intrinsic property of MSCs that cannot be avoided in mesenchymal cartilage repair [97].

Chondrogenic differentiation, as described by Johnstone et al., requires a 3D environment, and the addition of various combinations of growth factor [98]. Several 3D cultures are being used for this purpose, including a micromass pellet culture system, high-density bridge cultures, and alginate bead cultures [99]. Zhou et al. demonstrated how transforming growth factor β (TGF-β) signals the Wnt signaling pathway to enhance the proliferation of MSCs towards chondrogenic lineages, and suggested that the process might be mediated by smad3 and β-catenin [100]. Dexamethasone has been shown to be a powerful supplement for inducing chondrogenesis via the glucocorticoid receptor by enhancing stimulation of the TGF-β superfamily, and subsequent collagen type II and cartilage-specific proteoglycan production [101]. Lee et al. postulated that hyaluronic acid facilitates the migration and adherence of MSCs to the defect, and demonstrated how this treatment was effective in inducing a repair response in a porcine model [102].

2.2.1 Mesenchymal Stem Cells on Nanomaterials for Cartilage Regeneration

Cartilage TE shows great promise, with application of 3D scaffolds seeded with cells. Porous scaffolds of PLA and poly(lactic-*co*-glycolic acid) (PLGA) have been demonstrated to be suitable substrates due to their good mechanical properties and degradation behavior [103]. These scaffolds create a 3D environment in which chondrocytes can be loaded before being re-implanted in the defect and must, therefore, be reabsorbable and non-toxic to the cells [104]. Li et al. investigated the chondrogenesis of MSCs on a PCL nanofibrous scaffold in the presence of TGF-β1 in vitro [105]. The differentiation of stem cells to chondrocytes on nanofibrous scaffold was comparable to an established cell pellet culture. It was advantageous to use nanofibers rather than cell pellet system, owing to their better mechanical properties, oxygen/nutrient exchange and ease of fabrication. PCL nanofibrous scaffold is a practical carrier for MSC transplantation and could be a suitable scaffold for cell-based tissue engineering for cartilage repair. Cheng et al. reported that human cartilage cells attached and proliferated on hyaluronic acid nanocrystals homogeneously dispersed in PLA, and that collagen fibers of 110 nm–1.8 μm diameter supported chondrocyte growth and infiltration [106, 107]. Chondrogenesis of MSCs was supported on 3D porous aqueous-derived silk scaffolds, forming cartilage-like tissue with spatial distribution of cells and ECM, with expression of chondrogenic genes, and zonal architecture resembling the native tissue [108, 109]. Chondrogenesis was improved in silk scaffolds compared to collagen scaffolds in terms of cell attachment, metabolic activity, proliferation, ECM deposition, and glycosaminoglycan (GAG) content [110, 111]. Results have also been encouraging using Hyalograft C, a hyaluronan-based scaffold, that demonstrated the formation of 96.7% of the repair tissue similar to hyaline cartilage [112].

Basically, two types of scaffolds have been employed for cartilage TE, i.e., porous sponges and hydrogels. Diao et al. employed pDNA-TGF-β1-activated 3D chitosan/gelatin scaffolds to improve the efficiency of rabbit cartilage in vivo [113]. The gene-enhanced-matrix (GEM) might provide stimuli to guide the differentiation of stem cells and is suggested for in vivo applications. On the other hand, the vector for gene delivery is crucially important to achieve high transfection efficiency and low toxicity. Particularly, a cationized chitosan derivative, i.e., *N*,*N*,*N*-trimethyl chitosan chloride (TMC) has a strong ability to condense DNA and facilitate cellular uptake in vitro, resulting in a higher cell transfection efficiency and lower cytotoxicity compared to polyethylenimine [114, 115]. Wang et al. fabricated three types of constructs for animal experiments: group A [PLGA sponge/fibrin gel/BMSCs/(TMC/pDNA-TGF-β1 complexes)] and two control groups, group B (without gene), and group C (without BMSCs) to study the cartilage repair [116]. Group A resulted in better chondrogenesis of BMSCs with hyaline cartilage formation and subchondral bone connection compared to both control groups. The cartilage matrices, GAGs, and collagen type II were abundantly stained in the neocartilage. Figure 5 shows histological images of the neocartilage after 12 weeks of transplantation in rabbit knees. Group A showed better restoration

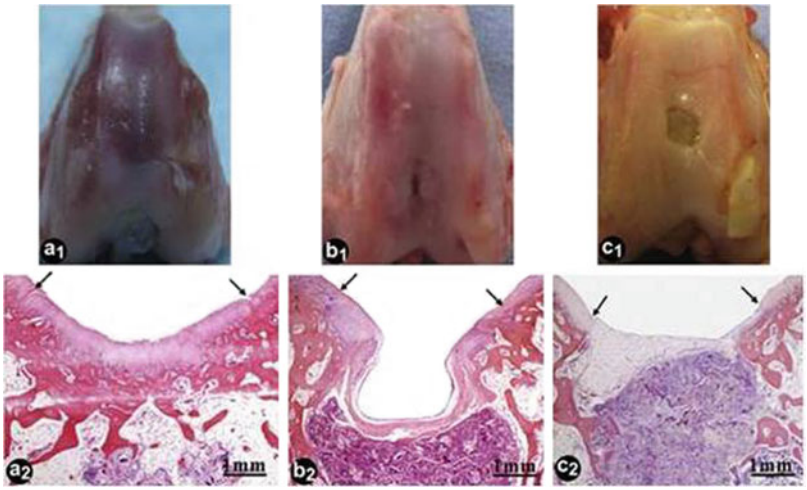

Fig. 5 Gross view (*top row*) and histological images (*bottom row*) of the neocartilage after transplantation for 12 weeks in rabbit knees. (**a1**, **a2**) PLGA/fibrin gel/BMSCs/(TMC/pDNA-TGF-β1 complexes), (**b1**, **b2**) Control group without gene, PLGA/fibrin gel/BMSCs, and (**c1**, **c2**) Control group without BMSCs, PLGA/fibrin gel/(TMC/pDNA-TGF-β1 complexes). *Arrows* indicate the boundaries between the grafts and host tissue. Reproduced with permission from Wang et al. [116]

of the cartilage defect and group C resulted in fibrous tissue formation and poor cartilage restoration. The bioactive construct (Group A) showed effective repair of osteochondral defect within a short period of 12 weeks. The gene complexes had a transfection efficiency in vitro of 9% to BMSCs, which could express TGF-β1. Transplantation of the constructs into full-thickness cartilage defects (diameter of 4 mm and depth of 4 mm) of rabbit knees resulted in hyaline cartilage, better chondrogenesis of BMSCs, subchondral bone connection, as well as deeper zone remodeling with histological score of 2.83, the best values obtained so far. The neocartilage contained abundant ECM of GAGs and collagen type II, in which chondrogenic genes such as those encoding collagen type II and aggrecan were also up-regulated, implying the efficient chondrogenic differentiation of BMSCs for cartilage regeneration.

2.2.2 Embryonic Stem Cells on Nanomaterials for Cartilage Regeneration

The use of mature cell types such as chondrocytes and osteoblasts is associated with several drawbacks including their limited availability, donor site morbidity, dedifferentiation, and limited proliferative capacity. These problems have urged researchers to study the chondrogenic and osteogenic lineage differentiation of ESCs and adipose stem cells. Human embryoid body cells were combined with Matrigel and seeded onto thin PLGA/PLA scaffolds. The hESC proliferation

medium was supplemented with TGF-β1 to direct the cells into the chondrogenic lineage, and cartilaginous tissue was formed [117]. Human embryoid body-derived mesenchymal-like cells were seeded in functionalized polyethylene glycol (PEG) hydrogels and cultured in chondrogenic medium containing TGF-β1. The addition of collagen type I or hyaluronic acid did not result in chondrogenic differentiation, but the addition of RGD peptides induced the formation of a cartilaginous matrix by hESC-derived mesenchymal-like cells [118]. It is also known that mechanical compression enhance chondrogenic differentiation [119]. The efficiency and stability of in vitro and in vivo cartilage formation should be improved further to obtain clinically relevant amounts of cartilage for TE applications [120, 121]. The current evidence, based primarily on large cartilage defects, suggests that BM stimulation procedures and whole tissue transplantation of allografts or autografts can achieve favorable outcomes when used for the management of focal chondral defects of the knee. Cell-based techniques performed with or without biocompatible elastomeric scaffolds have demonstrated early promise in animals, but additional human trials are required to validate the successful clinical outcomes and to save human life.

2.3 Tendon and Ligament Tissue Engineering

Tendon and ligament are connective tissues with closely packed collagen fiber bundles that connect bone to muscle and bone to bone, respectively. Tendon and ligament injuries caused by work- and sports-related activities are about half of the musculoskeletal injuries associated with pain and suboptimal healing [122]. TE offers the possibility of creating functional tissue grafts to treat tendon and ligament injuries without any of the undesirable side effects often associated with reconstructive methods. The lack of immunogenicity of MSCs makes them more suitable for allogeneic implants, and the application of a suitable scaffold containing biological signals could encourage the proliferation and differentiation of these cells. A cyclic mechanical stretch or addition of specific growth factors (e.g., bFGF, insulin-like growth factor IGF) could promote the matrix formation and differentiation of MSCs to fibroblastic cells specific for tendon and ligament lineages [123].

PLGA nanofibers were blend electrospun with bFGF by Sahoo et al. [122] to release the growth factor over a week, so as to mimic the ECM of injured tendon or ligament and to provide a topographical cue and required bioactivity for BM-MSC differentiation to tendon or ligament fibroblasts. The released bFGF activated tyrosine phosphorylation signaling, which proliferated and induced tendon- and ligament-like fibroblastic differentiation, suggesting its potential for tendon and ligament TE. In another study, microporous silk mesh was braided around a silk cord to produce a tightly wound shaft, and in vitro studies showed the expression of collagen types I and III, and tenascin-C gene expression of the MSC differentiated fibroblastic cells [124]. The scaffold was seeded with MSC and implanted into pig model in vivo to regenerate the anterior cruciate ligament [125]. Indirect ligament bone insertion with three zones (bone, Sharpey's fibers, and ligament) and the

production of key ligament-specific ECM components were observed during this study. Gelatin/silk fibroin hybrid scaffold was also used to provide a 3D cell culture environment after co-culturing MSCs with ligament fibroblasts [126]. MSCs showed faster proliferation in the co-culture system, and the specific regulatory signals produced by the fibroblasts were found to enhance the differentiation of MSCs for ligament tissue engineering.

The effects of nanofiber alignment on the differentiation of human tendon stem/progenitor cells (hTSPCs) was studied recently by Yin et al. [127], who fabricated both random and aligned poly-L-lactic acid (PLLA) nanofibers. The tendon-specific genes were highly expressed by hTSPCs grown on aligned nanofibers, while the results of alkaline phosphatase and alizarin red staining showed hindered osteogenesis on aligned substrates compared with that on random fibers. However, in vivo studies showed spindle-shaped cell and tendon-like tissue formation, hinting at the positive influence of topographical control in tendon TE. On the other hand, studies by Qiu et al. [128] suggested the application of hydrogels of oligo[poly(ethylene glycol) fumarate]/acrylated poly(ethylene glycol)-dithiothreitol hydrogels as a carrier for dosed delivery of MSCs for tendon regeneration. A composite PLGA knitted scaffold containing MSC-incorporated alginate gel was implanted in a 1-cm long defect in rabbit tendon. After 13 weeks of implantation, the regenerated tendons were found to possess higher elastic modulus (60%) than naturally healed (40%) tendons and showed vascularization [129]. Exploring the sensitivity of MSCs to gel stiffness, hydrogels functionalized with different substrates (fibronectin or collagen type I) were utilized by Sharma et al. [130] to probe the mitogen activated protein (MAP) kinase activity relative to tendon cell differentiation. These researchers found expression of tenoblast markers on collagen-containing substrates within a narrow range of stiffness. However, osteoblastic differentiations were observed on substrates impregnated with fibronectin, suggesting that the osteogenic differentiation decreased on substrates with low stiffness and ligand density. The above studies show the possibility of development of desirable engineered tendons composed of optimal stem cells and bioengineered scaffolds that could bring a bright future to the healing outcome of tendon and ligament injuries.

2.4 Cardiac Regeneration

The heart is an important organ, which pumps and circulates oxygenated blood through both the central and peripheral circulation of the body, providing nutrition to all the cells of the body. However, with increasing age of the population, together with smoking and alcohol abuse, heart failure and myocardial infarction are becoming the most challenging diseases or threat to the human population. Myocardial infarction occurs due to the interruption of blood supply to heart, resulting in the blockage of the coronary artery, causing the cardiomyocytes to die. Heart failure and myocardial damage has long been considered irreversible because adult cardiac myocytes are terminally differentiated and do not proliferate.

Moreover, cardiac muscle cannot replicate and regenerate by itself after injury [131, 132]. Heart transplantation is a treatment option for end-stage heart failure, but it has endured a slow and somewhat troubled evolution to transform itself into a more validated and useful therapy for patients, mainly because of the limited availability of donor organs and potential complications involved in its use [133]. Stem cell therapy and TE might solve the problem of how to treat thousands of patients who survive myocardial infarction and heart failure.

In native tissue, cells interact with 3D micro- or nanoscaled structures. Cardiomyocytes and fibroblasts disperse in a dense supporting vasculature and collagen-based ECM in the myocardium, producing mechanical contractions to pump blood forward to the body under physiological electrical signals. Scaffolds with appropriate nanostructures are able to control cell mechanics and shapes, which are crucial for cellular functions such as growth, differentiation, migration, and gene expression [134]. The response of cardiomyocytes to micro- and nanostructures has been examined by many researchers and interesting results have been reported. For example, Alperin et al. prepared polyurethane (PU) films coated with ECM proteins such as gelatin, laminin, or collagen type IV for cardiac TE [135].

Artificial cardiac patch is a tissue-engineered approach for the treatment of myocardial infarction, and it serves two functions: cell delivery and mechanical support. Therefore the biomaterials used in this approach should possess suitable nanostructures providing mechanical support and biological cues that promote cell attachment and growth. Chung et al. investigated the effects of silk fibroin/chitosan and silk fibroin/chitosan/hyaluronic acid hybrid patches on cardiomyogenic differentiation of induced rat MSCs, and observed significant improvement in the expression of selected cardiac muscle genes (such as those encoding Tnnt2 and Acta1) and of selected cardiac proteins (such as cardiotin and connexin 43) on the cardiac patches incorporating GAG microspheres [136, 137].

Multiple stem cell types have been identified and reported to have the capability to differentiate into cardiomyocytes, including MSCs, ESCs, ADSCs, hematopoietic stem cells (HSCs) and induced pluripotent stem cells (IPSCs). Although direct injection of stem cell suspensions into the injured heart has produced some promising results, with improved cardiac performance in animal models, this approach remains limited because of the difficulties in cell retention and transplantation survival. It has been reported that almost 90% of the cells were lost or leaked out during the injection, and even the 10% that successfully entered cells had a high death ratio of up to 90% within the first week [138]. Cardiac patches composed of sliced porous acellular bovine pericardium incorporated with multilayered MSC sheets were designed by Sung et al., and in vitro studies showed that MSCs tightly adhered to the fibronectin meshwork and redistributed throughout the scaffold. In vivo results showed that the cells together with neo-muscle fibers and neo-microvessels filled the pores of the scaffolds and the patch became well integrated within the host tissue [139]. Later, these researchers sandwiched ESC sheets into the sliced porous tissue scaffold and found that the mechanical properties of the engineered tissue were significantly increased [140]. Cultured in vitro for weeks, ESCs in the scaffolds were driven to cardiomyogenic lineages, and expressed

cardiac-specific proteins such as α-actinin and connexin 43. Miyahara et al. fabricated ADSC sheets as a cardiac patch to repair scarred myocardium and found newly formed vessels and engraftment of cardiomyocytes within the sheets after implantation; wall thinning in the scar area was reversed and cardiac function was improved [141]. The key challenge in cardiac TE is to create an engineered heart muscle that integrates well with the phenotypically stable cardiac cells and forms a native-like cardiac tissue [142]. The above-mentioned stem cells together with nano-architectured polymeric biomaterials might have the capability to differentiate into cardiomyogenic cells and could be promising alternatives for advanced cardiac TE.

2.4.1 Stem Cell Differentiation to Myocytes on Polymeric Nanomaterials

The functional multipotency of MSCs includes cardiac muscle formation, and several studies have suggested that BM-MSCs could differentiate into cardiomyocytes both in vitro and in vivo. Treatment of MSCs with 5-azacytidine, an analog of cytidine, has been the commonest strategy for inducing cardiac differentiation in vitro. Other strategies and treatments, including the addition of bone morphogenetic protein 2 (BMP-2) and fibroblast growth factor 4 (FGF-4) to the cardiomyogenic differentiation medium containing insulin, dexamethasone, and ascorbic acid, or co-culture using matured cardiomyocytes, have been successfully utilized for differentiation of MSCs to cardiomyocytes. Xiang et al. fabricated an injectable sponge-like material with collagen type I and GAG, and the scaffold was found to be highly porous with an average pore size of 120 ± 18 mm [143]. The material was used as a cell carrier to transplant adult BM-MSCs to the infarct region of rat heart, and results of their study showed that the grafted MSCs survived and even migrated into the heart walls. A substantial amount of neovascularization was observed in the infarct region and within the scaffold itself. This study demonstrated that collagen type I/GAG scaffolds are able to deliver BM-MSCs into the infarct region of the heart with a high survival ratio, further driving the differentiation of MSCs to induce neovascularization. Lee et al. encapsulated hMSCs to RGD peptide-modified alginate microspheres for myocardial repair [144]. Results showed that the modified alginate microspheres could improve MSC attachment and growth, and promote the expression of angiogenic growth factor in vitro. In vivo studies demonstrated that the encapsulation of hMSCs in alginate microbeads significantly increased the cell survival, reduced the infarct size, and enhanced arteriole formation compared with phosphate-buffered saline control or cells alone. Biehl et al. investigated the proliferation of mouse MSC progeny on poly(dimethyl siloxane) membranes with microprojections and they found that the proliferation of mouse MSC progeny was attenuated by 15-μm, but not 5-μm, high microprojections [145].

Guo et al. designed a novel self-assembling peptide (RGDSP) nanofiber as cell carrier to deliver BM-derived cardiac stem cells (CSCs) to repair infarct myocardium [146]. In vitro studies showed that the RGDSP scaffolds supported

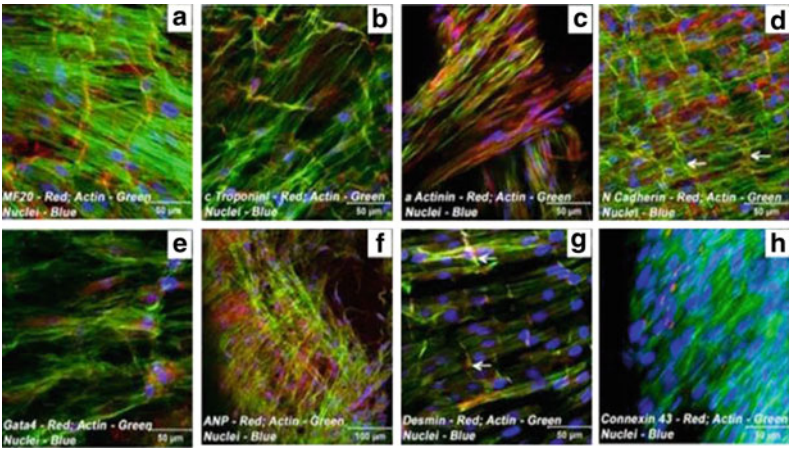

Fig. 6 Localization of key cardiac myocyte phenotypic markers of day 21 ECMs and BMSCs tube co-cultured in basal medium. Images demonstrate the expression of (**a**) sarcomeric myosin heavy chain (MF20), (**b**) cardiac troponin I, (**c**) α-actinin, (**d**) N-cadherin, (**e**) Gata4, (**f**) atrial natriuretic peptide (ANP), (**g**) desmin, and (**h**) connexin 43. Reproduced with permission from Valarmathi et al. [147]

the growth of CSCs and protected them from apoptosis and necrosis caused by anoxia. CSCs in RGDSP scaffolds differentiated into cardiomyocytes and expressed cardiac troponin T and connexin 43, and the viability of the grafted cells was improved during the in vivo studies. The RGDSP nanofibers were able to provide a suitable microenvironment for the survival and differentiation of CSCs, and it further increased the efficacy of CSC transplantation and improved cardiac function. Valarmathi et al. used a different approach by co-culturing rat ventricular embryonic cardiomyocytes and BMSCs on 3D aligned collagen type I fibrous scaffolds [147]. After 21 days, BMSCs were found to differentiate into cardiomyocyte lineages, and expressed transcripts coding for cardiomyocyte phenotypic markers and cardiomyogenic lineage-associated proteins (see Fig. 6). The 3D co-culture system provided a helpful in vitro model to exploit the mechanism of cardiomyogenic differentiation for myocardium regeneration.

Hydrogels, because of their high porosity and capability to exchange nutrients and oxygen with surrounding tissues, often serve as scaffolds for cell growth and delivery. Wang and coworkers prepared an injectable α-cyclodextrin/methoxypoly (ethylene glycol)–polycaprolactone-(dodecanedioic acid)-polycaprolactone–methoxypoly(ethylene glycol) (α-cyclodextrin/MPEG–PCL–MPEG) self-assembled hydrogel with a pore size of 50 μm, and encapsulated BM-MSCs in the supramolecular hydrogel to investigate the efficiency of cell transplantation for cardiac regeneration [148, 149]. The injection of BM-MSCs with hydrogel increased the cell retention and vessel density around the infarct region, and improved the left ventricle ejection fraction compared with the cell injection alone.

Cardiomyogenic differentiation of ESCs is regulated by certain soluble factors and signaling molecules interacting with cardiac-specific transcription factors. BMP-2 plays a central role in the induction of cardiac formation in vertebrate embryos, and expression of BMP-2 is mediated by GATA-4 and Nkx-2.5 [150]. It is also been reported that GATA-4 and Nkx-2.5 are essential for cardiac development. Other growth factors and soluble chemicals, such as FGF, IGF-1, and dimethyl sulfoxide, have also been proven to be involved in heart formation of vertebrates [150]. At the same time, strategies such as co-culture with cardiomyocytes or electrical stimulation can promote ESC differentiation to cardiomyogenic lineages. Akasha et al. used commercial CultiSpher-S microspheres (Percell Biolytica, Sweden) as a cell carrier to deliver ESC-derived cardiomyocytes for heart repair. CultiSpher-S, made from crosslinked porcine gelatin, is composed of macroporous and degradable microbeads with diameters of 130–380 μm. Results showed that the graft cells not only attached on the outer surface, but also invaded the inner pores of the microspheres, and expressed action potentials similar to normal cardiomyocytes [151]. ESC-derived cardiomyocytes cultured on polyurethane (PU) films for 30 days, showed that the cells exhibited preferential attachment and greater beating activity on PU films coated with laminin and collagen type IV [151]. ESC-derived cardiomyocytes also showed significant proliferation on poly(dimethyl siloxane) microprojections and had increased beating rates compared with cells grown on flat substrates [145].

2.4.2 Other Stem Cell Sources Used for Cardiomyogenic Differentiation

ADSCs have been demonstrated to be able to differentiate to cardiomyocytes, and induced pluripotent stem (IPS) cells that overcome the ethical issue of ESCs have opened a new gate for regenerative health care applications including the cardiac repair. Reprogramming the IPS cells for cardiac TE research still remains a huge challenge. For a long time, the heart was considered to be an organ beyond self-repair and regeneration, until the discovery of cardiac stem cells (CSCs) [152]. Compared to other stem cells, CSCs are a logical source of treatment for myocardial regeneration due to their likelihood of being intrinsically programmable to generate cardiac tissue. However, technical difficulties in collecting the cells and low cell numbers upon harvest still remain the main reasons limiting their application in cardiac tissue regeneration.

In summary, there are many stem cell types that have the potential for cardiac repair, but more sophisticated cell culture and TE approaches need to be developed. In addition, the main obstacle influencing cell therapeutic efficacy is the high death rate of donor stem cells after transplantation. Fabrication of biomaterial scaffolds with suitable nanostructure could be a feasible strategy for optimizing stem cell therapy for cardiac regeneration.

2.5 *Neurogenesis*

Nerve injuries occur by a variety of mechanisms, including traumatic wounds, thermal or chemical damage, myelin or axonal degeneration, and acute compression. Injury typically results in the loss of motor and sensory function, or both [153]. Neural diseases represent a very complicated and significant clinical problem; for example, in the USA alone, there are about 250,000–400,000 people living with spinal cord injury and nearly 13,000 additional people suffer spinal cord injuries each year [154]. Peripheral nerve lesions are serious injuries affecting 2.8% of trauma patients annually, leading to lifelong disability [155]. Moreover, each year this number grows by an estimated of 11,000 people in the USA, and in Europe more than 300, 000 cases of peripheral nerve injury are reported annually [156, 157]. Numerous strategies have been applied for the repair of peripheral nerve lesions, with the common goals of directing the regenerating nerve fibers into the distal endoneurial tubes and to improve axonal regeneration and functional recovery [158]. Implantation of autografts, allografts, and xenografts (providing graft from patient, cadavers, and animals, respectively) are some of the strategies applied in this field. Allograft and xenografts have certain disadvantages such as disease transmission and immunogenicity. The other disadvantages of autograft nerve repair systems include the loss of function at the donor nerve graft site and mismatch of damaged nerve and graft dimensions. TE offers promising strategies and provides viable alternatives to surgical procedures for harvested tissues and implants [159]. The fundamental approach in neural TE involves the fabrication of polymeric scaffolds with nerve cells to produce a 3D functional tissue suitable for implantation [160]. There is a growing research interest towards the application of stem cells in nerve TE and regenerative medicine to treat various neurological disorders [154]. Stem cell transplantation using a polymer scaffold might facilitate nerve regeneration more effectively than transplantation of stem cells alone [161].

2.5.1 Mesenchymal Stem Cell Differentiation on Nanostructures for Nerve Regeneration

MSCs obtained from BM are non-hematopoietic progenitor cells with the potential for multilineage differentiation into tissues of ectodermal (neural), endodermal (hepatocytes), and mesenchymal (adipocytes, chondrocytes) origin and have been used in nerve TE. Many researchers have attempted to regenerate nerve tissue by combining scaffolds with MSCs, and it has also been shown that the chemical composition of scaffolds influences the differentiation of MSC to nerve cells. Prabhakaran et al. compared the potential of hMSCs for in vitro neuronal differentiation on poly(L-lactic acid)-*co*-poly(ε-caprolactone)/collagen (PLCL/collagen) and PLCL nanofibrous scaffolds. Figure 7 shows SEM images of the morphology of MSC differentiated neuronal cells (Fig. 7a) and their expression of proteins, neurofilament (NF200), and nestin on the electrospun PLCL/collagen scaffolds.

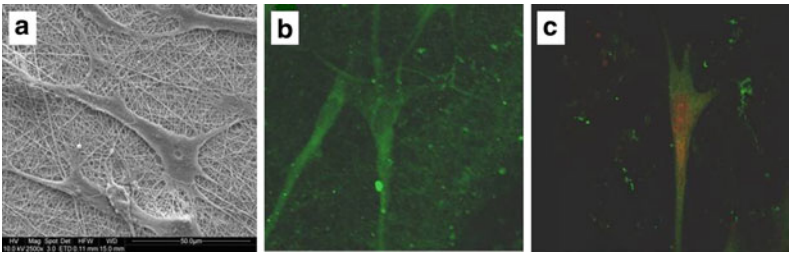

Fig. 7 MSC differentiated neuronal cells on electrospun PLCL/collagen scaffolds: (**a**) cell morphology by SEM, (**b**) expression of neurofilament protein, and (**c**) expression of nestin. Reproduced (Fig7b, 7c) with permission from Prabhakaran et al. [162]

Their findings showed that PLCL/collagen nanofibrous scaffolds serve as better substrates for differentiation of MSCs to nerve cells than the PLCL scaffolds [162]. In yet another study, Wang et al. synthesized terpolyesters of 3-hydroxybutyrate, 3-hydroxyvalerate and 3-hydroxyhexanoate (PHBVHHx), and compared them with PLA and copolyester of 3-hydroxybutyrate and 3-hydroxyhexanoate (PHBHHx) scaffolds for their respective functions in the differentiation of hMSCs to nerve cells. Their results showed that PHBVHHx films had better adhesion, proliferation, and differentiation of MSCs compared to PLA, thereby demonstrating the effect of substrate composition on MSC differentiation. The influence of pore size on the differentiation of MSCs to nerve cells was explained by these researchers, whereby a smaller scaffold pore size was found to increase the differentiation of MSCs to nerve cells [163]. On the other hand, Kuo et al. functionalized PLGA/chitosan scaffolds with collagen type I and investigated the differentiation of MSCs to nerve cells seeded on the scaffold. Their results showed that functionalized PLGA/chitosan/collagen scaffolds are promising substrates for differentiation of MSCs compared to PLGA/chitosan scaffolds [164]. Cho et al. immobilized nerve growth factor (NGF) on the surface of aligned PCL/PCL–PEG nanofibrous scaffolds and compared the neuronal differentiation of MSCs on NGF-immobilized nanofibrous scaffolds and physically adsorbed NGF nanofibrous scaffolds. Their results revealed higher expression of the neuronal cell marker proteins on NGF-immobilized nanofibrous scaffolds compared to its expression on physically adsorbed NGF scaffolds. Furthermore, the alignment of nanofibrous scaffolds also increased the expression levels of neuronal makers compared to random nanofibrous scaffolds, indicating that the NGF-conjugated aligned nanofibrous scaffolds significantly increased the neuronal differentiation of MSCs due to synergetic nanotopographical cues and the presence of NGF [165]. Wang et al. fabricated an injectable biodegradable hydrogel by blending gelatin and 3,4-hydroxyphenylpropionic acid and showed that the rate of MSC proliferation and neurogenesis of MSCs increased with a decrease in the stiffness of the hydrogel [166].

Substrate topographical patterns have also been shown to affect the differentiation of MSCs to nerve cells. Yim et al. investigated the differentiation and proliferation of hMSCs on nanogratings of 350 nm width and found alignment and elongation of

cytoskeleton and nuclei of MSCs along the nanogratings with higher expression of neuronal markers on patterned surfaces compared to unpatterned and micropatterned controls. Their results also showed that the combination of nanotopography and biochemical cues (retinoic acid) caused upregulation of neuronal protein expressions, but that nanotopography showed a stronger influence than retinoic acid alone [167].

Despite the capacity for spontaneous axonal regeneration, recovery after severe peripheral nerve injury remains variable and often very poor [168]. MSCs have been shown to have an important regenerative potential after transplantation into the stumps of transected sciatic nerves. Lopes et al. evaluated the regeneration of peripheral nerve using a tubular nerve guide of resorbable collagen filled with MSCs. Their results showed that the biodegradable collagen tube filled with MSCs induced better regeneration of peripheral nerve fibers across a nerve gap than did collagen tube without cells [169]. Oliveira et al. fabricated PCL conduits for regeneration of transected mouse median nerves and investigated the effect of MSCs on nerve regeneration by seeding MSCs on PCL nerve conduit before grafting of PCL conduits. The animals treated with MSCs had a significantly larger number of myelinated and unmyelinated nerve fibers and blood vessels compared to the control group (PCL conduit alone), indicating the possibility of improving regeneration and function of median nerve after a traumatic lesion [170]. Hou et al. differentiated MSCs into cells expressing characteristic markers of Schwann cells, and used PLGA nerve conduit along with differentiated MSCs for bridging a 10-mm-long sciatic nerve defect [171]. Ao et al. fabricated chitosan conduits and seeded them with MSC-derived Schwann cells and used the conduit to bridge the critical gap length of 12 mm in sciatic nerves of adult rats. Their results showed significantly higher axonal re-growth and re-myelination in nerves bridged with MSC-derived Schwann cells than in those bridged with cell-deprived conduits [172].

2.5.2 Embryonic and Adipose-Derived Stem Cells on Nanopatterns for Nerve Regeneration

Considerable attention has been given to the potential of ESC or their derivatives for the repair of nerve injury [173]. Willerth et al. incorporated neurotrophin 3 (NT-3) and platelet-derived growth factor (PDGF) into fibrin scaffolds and investigated the differentiation of ESCs into mature neural phenotypes, specifically neurons and oligodendrocytes. Their results showed that the controlled delivery of NT-3 and PDGF simultaneously increased the fraction of neural progenitors, neurons, and oligodendrocytes while decreasing the fraction of astrocytes compared to ESC seeded with unmodified fibrin scaffolds [174]. Chao et al. grafted poly (acrylic acid) thin films with carbon nanotubes (CNTs) and investigated the neural differentiation of hESC. Their results revealed higher neuronal differentiation potential of ESC on CNT-grafted poly(acrylic acid) compared to un-grafted poly (acrylic acid) thin films [175]. Carlberg et al. evaluated in vitro neuronal differentiation of hESC on electrospun PU nanofibrous scaffolds and demonstrated that

physical cues induced by the nanofibrous scaffolds induced stem cell differentiation to neuronal cells [176]. Xie et al. compared the differentiation of ESC seeded on electrospun random and uniaxially aligned PCL nanofibers. Their results demonstrated that aligned nanofibrous substrates discouraged the differentiation of ESC to astrocytes, which is very desirable in therapies targeting spinal cord injuries, as they may limit possible glia scar formation. They also demonstrated that the aligned electrospun fibers could guide the neurite outgrowth generated by the differentiated neurons [173]. Lee et al. constructed nanoscale ridge/groove pattern arrays using UV-assisted capillary force lithography on polyurethane acrylate (PUA) and showed that the nanoscale ridge/groove pattern arrays can rapidly and efficiently induce the differentiation of hESC into neuronal lineages, even in the absence of differentiation-inducing agents [177]. Figure 8 shows the expression of human neuronal proteins C and D (HuC/D, an RNA-binding protein), microtubule-associated protein 2 (MAP2, marker of mature neuronal cells) and glial fibrillary acidic protein (GFAP, marker of intermediate filament proteins of mature astrocytes) on patterned PUA films. Cells were co-immunolabeled with class III β-tubulin (Tuj1, neuronal cell marker) and 4,6-diamidino-2-phenylindole (DAPI, DNA marker). As can be seen in Fig. 8c,f no staining for GFAP was observed, indicating ESC differentiation into mature neurons without differentiation into a glial lineage such as astrocytes [177].

ADSCs are a clinically applicable source for cell therapy. Tse et al. fabricated a PCL/PLA scaffold using the solvent-cast method, and the scaffolds were found to

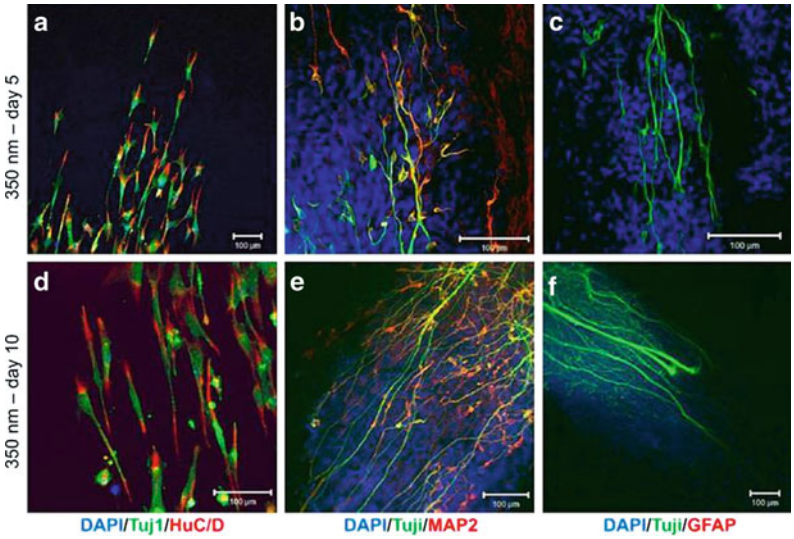

Fig. 8 Immunofluorescence staining of hESCs with neural and glial markers. (**a**, **d**) hESCs were immunolabeled for DAPI, Tuj1, and HuC/D. (**b**, **e**) hESCs immunolabeled for DAPI, Tuj1, and MAP2. (**c**, **f**) hESCs immunolabeled for DAPI, Tuj1, and GFAP. hESCs were cultured for 5 days (**a**–**c**) and 10 days (**d**–**f**) on 350-nm ridge/groove pattern arrays on PUA films. Reproduced with permission from Lee et al. [177]

support the differentiation of ADSCs into a Schwann-cell-like phenotype. A higher neurite length of dorsal root ganglion (DRG) by co-culturing with ADSCs was observed by these researchers, suggesting the possibility of enhancing nerve regeneration by seeding the nerve conduit with ADSCs before transplantation of nerve conduit to the site of nerve injury [178].

2.5.3 Alternative Stem Cells on Nanostructures for Nerve Regeneration

Neural stem cells (NSCs) are known to have both self-proliferation potential and multiple differentiation potential and can differentiate into various cell types such as neurons, astrocytes, oligodendrocytes, and Schwann-cell-like supportive cells when exposed to different conditions. Recently, NSCs has been used experimentally for both spinal cord and peripheral nerve injuries as a transplantation source with promising results [179]. NSCs exist not only in the developing mammalian nervous system but also in the adult nervous system of all mammalian organisms, including humans [180]. Dental pulp and peridontium have also been shown to be sources of NSCs, as well as olfactory mucosa, which are readily harvested by nasal biopsy [181]. With an ultimate goal of replacing damaged or injured neural tissues, introduction of NSCs to the site of neural tissue damage has been proposed due to their regenerative and neuroprotective potency [182]. Aijun et al. cultured NSCs on chitosan film and their results revealed that the NSCs proliferated on chitosan films and differentiated into neuron-like cells after 4 days of culture [179]. Bini et al. evaluated the suitability of biodegradable PLGA scaffolds for the differentiation of NSCs to nerve cells [183]. Numerous natural and synthetic polymers have been used as scaffolds for peripheral and central nerve regeneration in vitro or in vivo and these studies showed that the chemical nature of the substrates have a significant effect on both proliferation and differentiation of NSCs to nerve cells [184–186].

Functionalizing biomaterials with bioactive molecules such as ECM-derived cell adhesive molecules to impregnate guiding cues on the scaffolds is an emerging research interest and can provide an instructive extracellular microenvironment for NSCs [182, 187–189]. Yang et al. fabricated aligned PLLA nano- and microfibrous scaffolds to investigate the effect of nanofiber diameter on NSC proliferation and differentiation. Their findings showed a higher differentiation rate of NSCs on nanofibers than on microfibers, regardless of the fiber alignment [190]. He et al. fabricated aligned PLLA fibers by electrospinning and showed variable differentiations of NSCs depending on their fiber diameter and alignment. They reported longer neuritis on aligned fibers than on random fibers within the same diameter range [191]. Christopherson et al. cultured rat NSCs on electrospun polyethersulfone (PES) fibers with varying fiber diameters and demonstrated that the fiber diameter of PES fibers significantly influenced NSC differentiation. However, under the differentiation conditions, NSCs showed a 40% increase in oligodendrocyte differentiation on small diameter (283 nm) fibers and 20% increase in neuronal differentiation on high diameter (749 nm) fibers, in comparison to tissue culture on

polystyrene surfaces [192]. Results of our studies using PCL/gelatin nanofibers showed that the biocomposite PCL/gelatin (70:30) nanofibrous scaffolds enhanced NSC proliferation and differentiation compared to PCL nanofibrous scaffolds, and acted as a positive cue to support neurite outgrowth. Our results also showed that the direction of nerve cell elongation and neurite outgrowth on aligned nanofibrous scaffolds was parallel to the direction of orientation of the nanofibers [193]. Studies using conductive nanofibrous scaffolds of polyaniline/PCL/gelatin and applied electrical stimulation showed significantly enhanced cell differentiation and neurite outgrowth on stimulated scaffolds than on the non-stimulated scaffolds [194]. Lim et al. investigated the effect of aligned topography of substrates on cell morphology and neuronal differentiation. Their results showed that NSCs elongated along the major fiber axis on aligned fibers and that a higher fraction of cells on aligned fibers exhibited neuronal differentiation markers compared with cells on random fibers [195].

Topographical surface patterns such as steps, grooves, pillars, and pits (or pores) have been demonstrated to affect cell morphology, differentiation, motility, and function [196]. Hsu et al. fabricated micropatterned PLA conduits by microlithography and solvent-casting, and seeded the conduit with adult mouse NSCs for peripheral nerve regeneration. Their results showed that the seeded NSCs aligned on the micropatterned conduits and actin microfilaments oriented along the micropatterrned PLA scaffolds, whereas such defined orientations were not observed on non-patterned PLA substrates. The micropatterned surface facilitated the synthesis of neurotrophic factors and higher gene expression of NSCs [197]. Recknor et al. micropatterned polystyrene substrates and seeded them with NSCs. The micropatterned surfaces exhibited more than 75% cell alignment along the groove direction and enhanced neuronal differentiation and neurite alignment on topographically different regions of the same substrate [198]. In conclusion, nanostructures can be effective for the differentiation of stem cells to nerve cells due to their major role as a biomimetic interface between the scaffolds and cells in nerve TE.

2.6 Skin Tissue Engineering

Skin, the largest organ in the body, has a surface area of about 1.8 m^2 and occupies 8% of the total body mass of an adult. Skin comprises two layers: the outer protective epidermis and the inner corium or dermis, which provides the mechanical stability for skin and includes several important structures, such as the blood and lymph vessels, nerves, and appendages [199]. The most common skin injuries or skin wounds are categorized on the basis of the depth of the skin injury: epidermal or full-thickness skin wound. Skin can regenerate itself from minor epidermal injury; however, when the injury is a full-thickness skin wound (loss of both epidermis and dermis), the damaged skin cannot regenerate spontaneously [200]. Natural repair of wound healing is slow compared with the rapid wound cover needed to reduce

infection. At present, the use of cultured keratinocytes is limited by the length of time needed to grow epithelial sheets in vitro, during which time the patient is susceptible to infection. The epithelial sheets are also extremely fragile and do not adhere well to burned surfaces [201]. Stem cells can accelerate the re-epithelialization of skin wounds and bring the possibility of skin appendage regeneration.

2.6.1 Mesenchymal Stem Cells for Skin Regeneration

Stem cells are thought to be a powerful tool for treatment of a wide spectrum of diseases that are ineffectively treated by traditional approaches [201]. BM-derived stem cells have been shown to differentiate into epithelial cells of the liver, lungs, gastrointestinal tract and skin [202]. Systemic transplantation and local implantation of MSCs are promising treatment methods for skin wounds, especially for chronic wounds [203, 204]. The mechanisms by which BM-MSCs participate in cutaneous wound healing is by either differentiating into phenotypes of various damaged cells [205] or by enhancing the repair process by creating a microenvironment that promotes the local regeneration of cells endogenous to the tissue [206]. Wu et al. proved that BM-MSC-treated wounds exhibited significantly accelerated wound closure with increased re-epithelialization, cellularity, and angiogenesis [207]. Paunescu et al. examined the capability of human BM-MSCs to differentiate in vitro to functional epithelial-like cells [208]. To induce epithelial differentiation, they cultured MSCs using EGF, keratinocyte growth factor (KGF), HGF, and IGF-II. Their results demonstrated that hMSCs isolated from human BM can differentiate into epithelial-like cells and may serve as a cell source for TE and cell therapy of epithelial tissue.

Electrospun nanofibrous scaffolds can be prepared with high degree of control over their structure to create highly porous meshes of ultrafine fibers that resemble the ECM topography. The scaffolds are amenable to various functional modifications targeted towards enhancing stem cell survival and proliferation, directing their fates and promoting tissue organization [12]. Kobayashi and Spector investigated the clinical effects of mechanical stress on the behavior of BM-MSCs in a collagen type I/GAG scaffold matrix for 1 week under cyclic stretch loading conditions [209]. Their results suggested that mechanical stress may affect the proliferation and differentiation of stem cells and, subsequently, the wound healing process, via interactions between the stem cells and scaffold matrix. Delivery of growth factors and chemicals can also be mediated using degradable particles, entrapped within the biomaterial scaffold, which could provide temporal release kinetics for signaling biomolecules over a prolonged period of time [210–213]. Fan et al. [126] studied the differentiation of MSCs towards fibroblasts on silk-cable-reinforced gelatin/silk fibroin hybrid scaffold. Their results demonstrated that MSCs were distributed uniformly throughout the scaffold and showed good viability. MSCs in a co-culture system were proved to differentiate into ligament fibroblasts by synthesis of key ligament ECM components. Recently, Rustad et al. studied the effect of hydrogel microenvironment on stem cells in wound healing [214]. They placed

BM-MSC seeded hydrogels within wild-type excisional wounds and the results demonstrated that hydrogel delivery of MSCs improved cell survival following implantation compared to local injection, and that MSC-seeded hydrogels accelerated normal wound healing and are promising cell-scaffold constructs for skin regeneration.

2.6.2 Embryonic Stem Cells for Skin Regeneration

ESCs can potentially maintain a normal karyotype infinitely on culture in vitro and can differentiate into any cell type under appropriate conditions. The differentiation potential of murine ESCs into keratinocytes has been studied in vitro and results show that mouse ESC-derived keratinocyte-like cells expressed cytokeratin, keratin 14, and keartin18 (proposed markers for epidermal keratinocytes) [215]. The ability of hESC differentiation to epithelial lineages has also been studied in recent decades. Dabelsteen and Iuchi et al. found that hESCs can differentiate into keratinocyte-like cells expressing p63, K14, and involucrin [216, 217]. However, hESC-derived keratinocytes are different from postnatal keratinocytes due to their much lower proliferative potential in culture. The frequency with which they terminally differentiate was reduced compared with keratinocytes cultured from postnatal human epidermis. In contrast to previous results, Hind et al. showed that hESC-derived keratinocytes gave rise to packed and cohesive colonies and had an astounding proliferative potential [218]. They assessed the capability of the keratinocyte progeny of hESCs differentiating into full-functional keratinocytes and found that hESCs generate a homogeneous population of epithelial cells expressing keratins 5/14, keratin 10, involucrin, filaggrin, integrins α6/β4, collagen type VII, and laminin 5 at levels similar to those expressed by postnatal keratinocytes of squamous epithelia. Human ESC-derived keratinocytes were similar to human keratinocytes, both phenotypically and functionally. After 10 days of air–liquid differentiation, haematoxylin-eosin staining of the cryosection of organotypic hESC-derived keratinocyte cultures showed a pluristratified epithelium with a basal layer, stratum spinosum, stratum granulosum containing keratohyalin granules, and stratum corneum as superposed layers of dead squamous enucleated cells (Fig. 9).

2.6.3 Stem Cell–Scaffold Constructs for Skin Tissue Engineering

Altman et al. utilized a composite silk fibroin/chitosan scaffold for seeding and in vivo delivery of human ADSCs in a murine cutaneous wound model, and the delivery technique conferred physiological benefits to accelerated wound closure. ADSC seeded on a silk fibroin/chitosan scaffold differentiated into fibrovascular, endothelial, and epithelial components of restored tissue and enhanced the wound healing process [219].

Human umbilical cord blood (HUCB) stem cells have also been studied for skin TE. Kamolz et al. evaluated the potential of using HUCB stem cells to differentiate

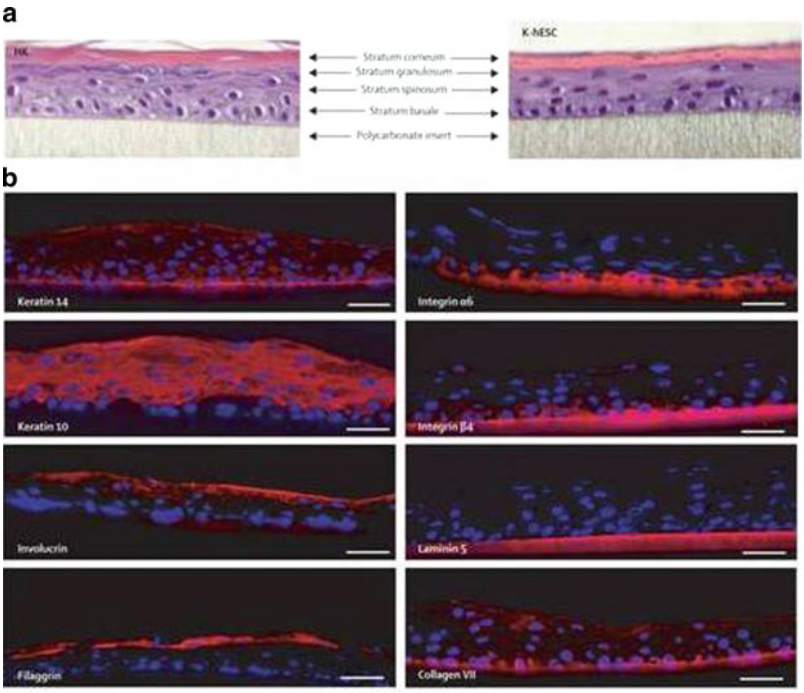

Fig. 9 Reconstruction of a pluristratified epidermis with keratinocytes derived from human embryonic stem cells (K-hESCs; SA01 cell line): (**a**) Haematoxylin-eosin staining of organotypic cultures of human primary keratinocytes (*left*) and K-hESCs (*right*). (**b**) Immunofluorescence analysis of the expression and localization of keratin 14, keratin 10, involucrin, filaggrin, integrin α6, integrin β4, laminin 5, and collagen type VII in the K-hESC organotypic epidermis. Scale bars: 50 μm. Reproduced with permission from Hind et al. [218]

into epithelial cells in vitro. Their results demonstrated three to four layers of regular epithelial sheet formation. The HUCB stem cells differentiated into epithelial cells under in vitro conditions, thereby serving as a starting material for isolation and expansion of cells for transplantation in patients with large skin defects [220]. Schneider et al. analyzed the possible epidermal differentiation of HUCB stem cells on dermal equivalents (DEs) consisting of collagen types I and III with dermal fibroblasts under culture conditions [221]. HUCB stem cells were further modified by pretreating the cells with 5-azacytidine or by supplementing the media with all-*trans*-retinoic acid. These researchers also demonstrated that HUCB stem cells can differentiate into myofibroblasts. Studies by Luo et al. showed that isolated HUCB stem cells could enhance the healing of mice skin defect wounds, and it was found that the implanted HUCB stem cells could differentiate into keratinocytes in the wound tissue [222]. Cultured ADSCs can also contribute to wound healing and can be added to engineer a trilayered skin substitute featuring the skin's deepest layer, the adipocyte-containing hypodermis, along with both dermis and epidermis [223]. ADSCs secrete various growth factors

that control and regenerate damaged skin-type cells, a function that has been termed essential for the regenerative mechanisms of ADSCs [224].

Salem et al. seeded pancreatic stem cells (PSCs) on "matriderm" and used the matrix to replace the bilateral full-thickness skin wounds made on the dorsum of Nu/Nu nude mice [225]. The vascularization rate showed a significant increase in the PSC-seeded scaffolds, and the morphology and immunohistochemistry showed new skin-like structures positive to epidermal markers of healing wound. The combined use of PSCs with matriderm as a matrix for dermal regeneration increased the epidermalization, vascularization, and healing of full-thickness wounds. Cell microenvironment is known to play a significant role in determining the progenitor cell function [226]. Different kinds of stem cells have been applied for wound healing using a biomimetic "stem cell niche" and most of the studies showed promising results. With further investigations towards understanding the mechanism of micro- and nanoenvironmental effects on stem cell behavior, we expect that the stem cell/biomaterial niche will play a vital role in advanced skin regeneration in the near future.

2.7 Other Tissue Regeneration Using Stem Cells and Nanomaterials

2.7.1 Vascular Regeneration

Cardiovascular disease is a leading cause of morbidity and mortality worldwide, with approximately 34% of all deaths in the USA being due to cardiovascular disease. Autologous grafts including the radial artery bypass grafts and saphenous vein are important therapeutic options for treatment of coronary artery disease. Tissue-engineered vascular grafts should mimic the native ECM structure and serve as a bridge to guide the cell-mediated remodeling of vascular tissue. Such tissue-engineered blood vessels should be non-immunogenic and non-thrombogenic to allow for high blood flow rate, with viscoelastic properties similar to the native vessel [227]. Wang et al. attempted to engineer a suitable blood vessel by differentiating ADSCs to smooth muscle cells (SMCs) through stimulation with BMP4 and TGF-β [228] and seeding the cells on poly(glycolic acid) (PGA) mesh. Subjected to pulsative stimulation for an 8 week period, the vessels showed high amounts of collagen deposition, similar to that of native vessels during this study. $Flk1^+$ (positive for VEGF receptor 2) progenitors derived from mouse ESCs differentiated to endothelial cells (ECs) on collagen type IV micropatterns immobilized with VEGF, while differentiation to SMCs was preferentially attained on unseeded collagen type IV scaffolds [229]. This phenomenon was also similar to that described for MSC differentiation on patterned surfaces with regard to the geometric and tractional mechanisms. Enhancing endothelial differentiation with VEGF might provide a suitable platform for vascular TE [230]. Collagen gel containing hESC-derived ECs were implanted into infarcted rat hearts in vivo by Nourse et al.

and robust networks of patient vessels filled with host blood cells were observed [230].

Blood vessel engineering using electrospun nanofibers might benefit from their mechanical strength, good cell attachment properties for endothelium formation, and directional alignment of SMCs along aligned nanofibers. Ex vivo stem cell expansion was carried out on nanofibers and the expanded cells then modified using pro-angiogenic growth factors to induce differentiation to ECs and SMCs and enhance vasculogenesis. Das et al. [231] demonstrated this method as a potential stem cell/biomaterial-based therapy for ischemic disease. Other factors such as the application of shear stress, bioreactors, and growth or biological factors might also assist in the development of a suitable blood vessel substitute with good mechanical strength.

3 Comments and Future Perspectives

Despite several advances in the field of stem cell research, the availability of stem cells remains a huge challenge for clinicians and scientists in the field of regenerative medicine [232]. The heterogeneity and differences between various tissue sources of MSCs and the factors that can influence MSCs to differentiate completely to a desired lineage all require further elucidation. ESCs encounter a range of ethical and legislative problems that differ from country to country [233]. Skepticism in terms of cell–cell fusion rather than stem cell plasticity has also been raised and further studies are required to explore and fully understand the mechanism of stem cell differentiation and stem cell behavior on nanostructures [234, 235]. The concerted efforts of engineers, biologists, and clinicians might advance the field of tissue regeneration and improve the quality of a patient's life using a synergistic stem cell/biomaterial approach.

Stem cell migration and differentiation in response to different nanotopographies can help in the engineering of materials to resemble the structural continuum of ECM. Specific scaffold properties affect cell function differently and hence "designer scaffolds" for precise tissue regeneration should be created and can offer the great potential of stem cell/nanotechnology to help advance the field of tissue regeneration. Approaches to the incorporation of nanopatterns on scaffold surfaces could be useful for guided tissue regeneration via the influence of exogenous or endogenous stem cells. Design of delivery systems or nanocarriers for the release of biomolecules into the nuclear compartments could be effective for the differentiation of stem cells. The fate of stem cells can be decided using novel engineering of stem cell technologies, with the aim of advancing their therapeutic use for human health care. The differentiation of stem cells can also be influenced by chemical signals such as cytokines, hormones, or other soluble factors within the nanomaterials and by physical and mechanical cues such as stimulation of receptors, cell stretch through contact with mechanically stimulated nanostructures, and electrical signals. The interdisciplinary field of stem cell and TE creates a platform for engineers, scientists, and clinicians to work together and advance the field of regenerative medicine.

4 Conclusion

Stem cell applications for tissue regeneration, especially on nanoengineered surfaces and structures, are still in the early stages of development. MSCs for bone repair on nanomaterials remains the most advanced field compared to others with respect to its potential for clinical application. This review describes the response of stem cells to topographical structures, molecules, and modifications in vitro, and the scientific information could be employed to regulate stem cell differentiations in vivo. Topographically modified materials might enhance the differentiation potential of stem cell populations, with crucial implications in tissue repair and clinical translations. Challenging achievements in the field of stem cell/nanomaterials for advances in tissue regeneration can certainly be expected in the next decade.

Acknowledgement This study was supported by NRF-Technion grant (R-398-001-065-592), and Nanoscience and Nanotechnology Initiative, Faculty of Engineering, National University of Singapore, Singapore.

References

1. Biggs MJP, Richards G, Dalby MJ (2010) Nanomed Nanotech Biol Med 6:619
2. Karuri NW, Liliensiek S, Teixeira AI, Abrams G, Campbell S, Nealey PF, Murphy CJ (2004) J Cell Sci 117:3153
3. Shekaran A, Garcia AJ (2011) Biochim Biophys Acta 1810:350
4. Elliott DH (1965) Biol Rev Camb Philos Soc 40:392
5. Weiner S, Traub W (1992) FASEB J 6:879
6. Lanfer B, Seib FP, Freudenberg U, Stamov D, Bley T, Bornhauser M, Werner C (2009) Biomaterials 30:5950
7. Sniadecki NJ, Desai RA, Ruiz SA, Chen CS (2006) Ann Biomed Eng 34:59
8. Curtis A, Wilkinson C (2001) Trends Biotechnol 19:97
9. Norman JJ, Desai TA (2006) Ann Biomed Eng 34:89
10. Hosseinkhani H, Hosseinkhani M, Khademhosseini A, Kobayashi H, Tabata Y (2006) Biomaterials 27:5836
11. Triplett JW, Pavalko FM (2006) Am J Physiol Cell Physiol 291:C909
12. Lim SH, Mao HQ (2009) Adv Drug Deliv Rev 61:1084
13. Jan E, Kotov NA (2007) Nano Lett 7:1123
14. Shakesheff K, Cannizzaro S, Langer R (1998) J Biomater Sci Polym Ed 9:507
15. Sill TJ, von Recum HA (2008) Biomaterials 29:1989
16. Lin K, Chua KN, Christopherson GT, Lim S, Mao HQ (2007) Polymer 48:6384
17. Prabhakaran MP, Ghasemi LM, Ramakrishna S (2011) J Nanosci Nanotec 11:3039
18. Rezwan K, Chen QZ, Blaker JJ, Boccaccini AR (2006) Biomaterials 27:3413
19. Guarino V, Ambrosio L (2008) Acta Biomater 4:1778
20. Kyle S, Aggeli A, Ingham E, McPherson MJ (2009) Trends Biotechnol 27:7423
21. Jayaraman K, Kotaki M, Zhang Y, Mo X, Ramakrishna S (2004) J Nanosci Nanotech 4:52
22. Miller C, Shanks H, Witt A, Rutkowski G, Mallapragada S (2001) Biomaterials 22:1263
23. Miller C, Jeftnija S, Mallapragada S (2002) Tissue Eng 8:367
24. Gadegaard N, Martines E, Riehle MO, Seunarine K, Wilkinson CDW (2006) Microelectron Eng 83:1577

25. Schmidt RC, Healy KE (2009) J Biomed Mater Res 90A:1252
26. Truskett VN, Watts MPC (2006) Trends Biotechnol 24:312
27. Schmalenberg KE, Uhrich KE (2005) Biomaterials 26:1423
28. Guo LJ (2004) J Phys D Appl Phys 37:R123–R141
29. Aguilar CA, Lu Y, Mao S, Chen S (2005) Biomaterials 26:7642
30. Mironov V, Kasyanov V, Markwald RR (2008) Trends Biotechnol 26:338
31. Tibbit MW, Anseth KS (2009) Biotechnol Bioeng 103:655
32. Holly SP, Larson MK, Parise LV (2000) Exp Cell Res 261:69
33. Griffith LG, Naughton G (2002) Science 295:1009
34. Saha K, Pollock JF, Schaffer DV, Healy KE (2007) Curr Opin Chem Biol 11:381
35. Engler AJ, Sen S, Sweeney HL, Discher DE (2006) Cell 126:677
36. Dobson J et al (2006) IEEE Trans Nanobiosci 5:173
37. Ingber D (1997) Annu Rev Physiol 59:575
38. Dalby MJ, Yarwood SJ, Riehle MO, Johnstone HJH, Affrossman S, Curtsi ASG (2002) Exp Cell Res 276:1
39. Selhuber-Unkel C, Lopez-Garcia M, Kessler H, Spatz JP (2008) Biophys J 95:5424
40. Dalby MJ, McCloy D, Robertson M, Wilkinson CD, Oreffo RO (2006) Biomaterials 27:1306
41. Biggs MJ, Richards RG, Gadegaard N, McMurray RJ, Affrossman S, Wilkinson CD (2009) J Biomed Mater Res A 91:195
42. Zuk PA, Zhu M, Mizuno H, Huang J, Futrell JW, Katz AJ, Benhaim P, Lorenz HP, Hedrick MH (2001) Tissue Eng 7:211
43. Bottai D, Fiocco R, Gelain F, Defilippis L, Galli R, Gritti A, Vescovi LA (2003) J Hematother Stem Cell Res 12:655
44. Cheng T (2008) Gene Ther 15:67
45. Yao S, Chen S, Clark J, Hao E, Beattie GM, Hayek A, Ding S (2006) Proc Natl Acad Sci USA 103:6907
46. Le Blanc K (2003) Cytotherapy 5:485
47. Caplan AI (1991) J Orthop Res 9:641
48. Baksh D, Song L, Tuan RS (2004) J Cell Mol Med 8:301
49. Gregory CA, Prockop DJ, Spees JL (2005) Exp Cell Res 306:330
50. Pittenger MF, Mackay AM, Beck SC, Jaiswal RK, Douglas R, Mosca JD, Moorman MA, Simonetti DW, Craig S, Marshak DR (1999) Science 284:143
51. Otto WR, Rao J (2004) Cell Prolif 37:97
52. Arinzeh TL, Tran T, Daculsi G (2005) Biomaterials 26:3631
53. Butler DL, Goldstein SA, Guilak F (2000) J Biomech Eng 122:570
54. Dellatore SM, Garcia AS, Miller WM (2008) Curr Opin Biotech 19:534
55. Thomson JA, Itskovitz-Eldor J, Shapiro SS et al (1998) Science 282:1145
56. Ratajczak MZ, Machalinski B, Wojakowski W, Ratajczak J, Kucia M (2007) Leukemia 21: 860
57. Hiyama E, Hiyama K (2007) Br J Cancer 96:1020
58. McDevitt TC, Palecek SP (2008) Curr Opin Biotechnol 19:527
59. Wu DC, Byod AS, Wood KJ (2007) Front Biosci 12:4525
60. Kurita M, Matsumoto D, Shigeura T, Sato K, Gonda K, Harii K, Yoshimura K (2008) Plast Reconstr Surg 121:1033
61. Strem BM, Hicok KC, Zhu M, Wulur I, Alfonso Z, Schreiber RE, Fraser JK, Hedrick MH (2005) Keio J Med 54:132
62. McIntosh K, Zvonic S, Garrett S, Mitchell JB, Floyd ZE, Hammill L, Kloster A, Halvorsen YD, Ting JP, Storms RW, Goh B, Kilroy G, Wu X, Gimble JM (2006) Stem Cells 24:1245
63. Planat-Benard V, Silvestre JS, Cousin B, Andre M, Nibbelink M, Tamarat R, Clergue M, Manneville C, Saillan-Barreau C, Duriez M, Tedgui A, Levy B, Penicaud L, Casteilla L (2004) Circulation 109:656
64. Traktuev DO, Merfeld-Clauss S, Li J, Kolonin M, Arap W, Pasqualini R, Johnstone BH, March KL (2008) Circ Res 102:77

65. Rehman J, Traktuev D, Li J, Merfeld-Clauss S, Temm-Grove CJ, Bovenkerk JE, Pell CL, Johnstone BH, Considine RV, March KL (2004) Circulation 109:1292
66. Datamonitor (2002) Market Dynamics: bone substitutes and growth factors. Datamonitor, New York
67. Stevenson S, Emery SE, Goldberg VM (1996) Clin Ortho Rel Res 324:66
68. Rose FR, Oreffo RO (2002) Biochem Biophys Res Commun 292:1
69. Hong Z, Zhang P, He C, Jing X (2005) Biomaterials 26:6296
70. Yuan Y, Yang YH, Li Y, Zhang X (1998) J Mater Sci Mater Med 9:723
71. Altman GH, Diaz F, Jakuba C, Calabro T, Horan RL, Chen J (2003) Biomaterials 24:401
72. Meinel L, Karageorgiou V, Hofmann S, Fajardo R, Snyder B, Li C (2004) J Biomed Mater Res A 71:25
73. Karageorgiou V, Meinel L, Hofmann S, Malhotra A, Volloch V, Kaplan D (2004) J Biomed Mater Res A 71:528
74. Hartgerink JD, Beniash E, Stupp SI (2001) Science (New York) 294:1684
75. Ruoslahti E (1996) Annu Rev Cell Dev Biol 12:697
76. Einhorn TA, Majeska RJ, Rush EB, Levine PM, Horowitz MC (1995) J Bone Mineral Res 10:1272
77. Arthur A, Zannettino A, Gronthos S (2009) J Cell Physiol 218:237
78. Anderson JM, Vines JB, Patterson JL, Chen H, Javed A, Jun HW (2011) Acta Biomat 7:675
79. Giovanni S, Brehm W, Mainil-Varlet P, Nesic D (2008) Differentiation 76:118
80. Yoshimoto H (2003) Biomaterials 24:2077
81. Salerno A, Guarnieri D, Lannone M, Zeppetelli S, Netti PA (2010) Tissue Eng A 16:2661
82. Hosseinkhani H, Hosseinkhani M, Tian F, Tabata Y (2006) Biomaterials 27:4079
83. Dalby MJ, Gadegaard NAJ, Tare R, Andar A, Riehle MO, Herzyk P, Wilkinson CDW, Oreffo ROC (2007) Nat Mater 6:997
84. Ishaug SL, Crane GM, Miller MJ, Yasko AW, Mikos AG (1997) Biomaterials 36:17
85. Zhang Z-Y, Teoh SH, Chan JKY (2010) Biomaterials 31:8684
86. Lyons FG, Al-Munajjed AA, Kieran SM, Toner ME, Murphy CM, Duffy GP, O'Brien FJ (2010) Biomaterials 31: 9232
87. Ahn SE, Kim S, Park KH (2006) Biochem Biophys Res Commun 340:403
88. Heng BC, Toh WS, Pereira BP (2008) Tissue Cell 40:219
89. Bielby RC, Boccaccini AR, Polak JM (2004) Tissue Eng 10:1518
90. Tremoleda JL, Forsyth NR, Khan NS (2008) Cloning Stem Cells 10:119
91. World Health Organization (2009) http://www.who.int/chp/topics/rheumatic/en/
92. Bora FW Jr, Miller G (1987) Hand Clin 3:325
93. Buckwalter JA, Mankin HJ (1998) Instr Course Lect 47:477
94. Ikeda T, Kamekura S, Mabuchi A, Kou I, Seki S, Takato T, Nakamura K, Kawaguchi H, Ikegawa S, Chung U (2004) Arthritis Rheum 50:3561
95. Ikeda T, Kawaguchi H, Kamekura S, Ogata N, Mori Y, Nakamura K, Ikegawa S, Chung U (2005) J Bone Miner Metab 23:337
96. Dessau W, von der Mark H, Fischer S (1980) J Embryol Exp Morphol 57:51
97. Johnstone B, Yoo JU (1999) Clin Orthop Relat Res 367:S156
98. Johnstone B, Hering TM, Caplan AI (1998) Exp Cell Res 238:265
99. Shakibaei M, De Souza P (1997) Cell Biol Int 21:75
100. Zhou S, Eid K, Glowacki J (2004) J Bone Miner Res 19:463
101. Derfoul A, Perkins GL, Hall DJ, Tuan RS (2006) Stem Cells 24:1487
102. Lee KB, Hui JH, Song IC (2007) Stem Cells 25:2964
103. Chung C, Burdick JA (2008) Adv Drug Deliv Rev 60(2):243
104. Trippel SB, Ghivizzani SC, Nixon AJ (2004) Gene Ther 11:351
105. Li WJ, Tuli R, Okafor C, Derfoul A, Hall DJ (2005) Biomaterials 26:599
106. Cheng L, Zhang SM, Chen PP, Huang SL, Cao RR, Zhou W, Liu J, Lou QM, Gong H (2006) Key Eng Mater 309–311:943
107. Matthews JA, Boland ED, Wnek GE (2003) J Bioact Compat Polym 18:125

108. Wang Y, Blasioli DJ, Kim HJ, Kaplan DL (2006) Biomaterials 27:4434
109. Wang Y, Kim UJ, Blasioli DJ, Kim HJ, Kaplan DL (2005) Biomaterials 26:7082
110. Hofmann S, Knecht S, Kaplan DL, Merkle HP (2006) Tissue Eng 12:2729
111. Meinel L, Hofmann S, Karageorgiou V, Zichner L, Langer R, Kaplan D (2004) Biotech Bioeng 88:379
112. Pavesio A, Abatangelo G, Borrione A (2003) Novartis Found Symp 249:203
113. Diao H, Wang J, Shen C, Xia S, Guo T, Dong L (2009) Tissue Eng Part A 15:2687
114. Mao Z, Ma L, Jiang Y, Yan M, Gao C, Shen J (2007) Macromol Biosci 7:855
115. Mao Z, Shi H, Guo R, Ma L, Gao C, Han C (2009) Acta Biomater 5:2983
116. Wang W, Li B, Li Y, Jiang Y, Ouyang H, Gao C (2010) Biomaterials 31:5953
117. Levenberg S, Huang NF, Lavik E (2003) Proc Natl Acad Sci USA 100:12741
118. Hwang NS, Varghese S, Zhang Z (2006) Tissue Eng 12:2695
119. Huang CY, Hagar KL, Frost LE (2004) Stem Cells 22:313
120. Jukes JM, van Blitterswijk CA, de Boe J (2010) J Tissue Eng Regen Med 4:165
121. Nelson L, Fairclough J, Archer CW (2010) Expert Opin Biol Ther 10:43
122. Sahoo S, Ang LT, Goh JCH, Toh SL (2010) Differentiation 29:102
123. Goh JC, Ouyang HW, Teoh SH, Chan CK, Lee EH (2003) Tissue Eng 9:S31
124. Liu H, Fan H, Tho SL, Goh JC (2008) Biomaterials 29:1443
125. Fan H, Liu H, Toh SL, Goh JCH (2009) Biomaterials 30:4967
126. Fan H, Liu H, Toh SL, Goh JCH (2008) Biomaterials 29:1017
127. Yin Z, Chen X, Chen JL, Shen WL, Nguyen TMH, Gao L, Ouyang HW (2010) Biomaterials 31:2163
128. Qiu Y, Lim JL, Scott L, Adams RC, Bui HT, Temenoff JS (2010) Acta Biomater (in press)
129. Vaquette C, Slimani S, Kahn CJ, Tran N, Rahouadi R, Wang X (2010) J Biomater Sci Polym Ed 21:1737
130. Sharma RI, Snedeker JG (2010) Biomaterials 31:7695
131. Weissberg P, Qasim A (2005) Br Med J 91:696
132. Leor J, Amsalem Y, Cohen S (2005) Pharmacol Ther 105:151
133. Stevenson L, Sietsema K, Tillisch J, Lem V, Walden J, Kobashigawa J, Moriguchi J (1990) Circulation 81:78
134. Kim D, Park J, Suh K, Kim P, Choi S, Ryu S, Park S, Lee S, Kim B (2006) Sens Actuators B Chem 117:391
135. Alperin C, Zandstra P, Woodhouse K (2005) Biomaterials 26:7377
136. Yang MC, Wang SS, Chi NH, Huang YY, Chang YL, Shieh MJ, Chung TW (2009) Biomaterials 30:3757
137. Yang MC, Chi NH, Chou NK, Huang YY, Chung TW, Chang YL, Liu HC, Shieh MJ, Wang SS (2010) Biomaterials 31:854
138. Wang H, Zhou J, Liu Z, Wang C (2010) J Cell Mol Med 14:1044
139. Wei H, Chen C, Lee W, Chiu I, Hwang S, Lin W, Huang C, Yeh Y, Chang Y, Sung H (2008) Biomaterials 29:3547
140. Huang C, Liao C, Yang M, Chen C, Hwang S, Hung Y, Chang Y, Sung H (2010) Biomaterials 31:6218
141. Miyahara Y, Nagaya N, Kataoka M, Yanagawa B, Tanaka K, Hao H, Ishino K, Ishida H, Shimizu T, Kangawa K (2006) Nat Med 12:459
142. Vunjak-Novakovic G, Tandon N, Godier A, Maidhof R, Marsano A, Martens T, Radisic M (2010) Tissue Eng B 16:169
143. Xiang Z, Liao R, Kelly M, Spector M (2006) Tissue Eng 12:2467
144. Yu JS, Du KT, Fang QZ, Gu YP, Mihardja SS, Sievers RE, Wu JC, Lee RJ (2010) Biomaterials 31:7012
145. Biehl J, Yamanaka S, Desai T, Boheler K, Russell B (2009) Dev Dyn 238:1964
146. Guo HD, Cui GH, Wang HJ, Tan YZ (2010) BBRC 399:42
147. Valarmathi MT, Goodwin RL, Fuseler JW, Davis JM, Yost MJ, Potts JD (2010) Biomaterials 31:3185

148. Wu DQ, Wang T, Lu B, Xu XD, Cheng SX, Jiang XJ, Zhang XZ, Zhuo RX (2008) Langmuir 24:10306
149. Wang T, Jiang XJ, Tang QZ, Li XY, Lin T, Wu DQ, Zhang XZ, Okello E (2009) Acta Biomater 5:2939
150. Sachinidis A, Fleischmann B, Kolossov E, Wartenberg M, Sauer H, Hescheler J (2003) Cardiovasc Res 58:278
151. Akasha A, Sotiriadou I, Doss M, Halbach M, Winkler J, Baunach J, Katsen-Globa A, Zimmermann H, Choo Y, Hescheler J (2008) Cell Physiol Biochem 22:665
152. Beltrami A, Barlucchi L, Torella D, Baker M, Limana F, Chimenti S, Kasahara H, Rota M, Musso E, Urbanek K (2003) Cell 114:763
153. Leach JB (2006) Tissue-engineered peripheral nerve. In: Akay M (ed) Wiley encyclopedia of biomedical engineering. Wiley, Hoboken, NJ
154. Tran PA, Zhang L, Webster TJ (2009) Adv Drug Deliv Rev 61:1097
155. Ciardelli G, Chiono V (2006) Macromol Biosci 6:13
156. Willerth SM, Sakiyama-Elbert SE (2007) Adv Drug Del Rev 59:325
157. Bueno FR, Shah SB (2008) Tissue eng Part B 14:219
158. Schmidt CE, Shastri VR, Vacanti JP, Langer R (1997) Proc Natl Acad Sci USA 94:8948
159. Schmidt CE, Leach JB (2003) Annu Rev Biomed Eng 5:293
160. Yang F, Xu CY, Kotaki M, Wang S, Ramakrishna S (2004) J Biomater Sci Polymer Edn 15:1483
161. Bhang SH, Lim JS, Choi CY, Kwon YK, Kim BS (2007) J Biomater Sci Polymer Edn 18:223
162. Prabhakaran MP, Venugopal JR, Ramakrishna S (2009) Biomaterials 30:4996
163. Wang L, Wang ZH, Shen CY, You ML, Xiao JF, Chen GQ (2010) Biomaterials 31:1691
164. Kuo YC, Yeh CF (2011) Colloids Surf B Biointerfaces 82:624
165. Cho YI, Choi JS, Jeong SY, Yoo HS (2010) Acta Biomater 6:4725
166. Wang L, Chung JE, Chan PP, Kurisawa M (2010) Biomaterials 31:1148
167. Yim EKF, Pang SW, Leong KW (2007) Exp Cell Res 313:1820
168. Kemp SWP, Walsh SK, Midha R (2008) Neurol Res 30:1030
169. Lopes FRP, Camargo de Moura Campos L, Dias Corrêa J Jr, Balduino A, Lora S, Langone F, Borojevic R, Blanco Martinez AM (2006) Exp Neurol 198:457
170. Oliveira JT, Almeida FM, Biancalana A, Baptista AF, Tomaz MA, Melo PA, Martinez AM (2010) Neuroscience 170:1295
171. Hou SY, Zhang HY, Quan DP, Liu XL, Zhu JK (2006) Neuroscience 140:101
172. Ao Q, Fung CK, Tsui AYP, Cai S, Zuo HC, Chan YS, Shum DKY (2011) Biomaterials 32:787
173. Xie J, Willerth SM, Li X, Macewan MR, Rader A, Sakiyama-Elbert SE, Xia Y (2009) Biomaterials 30:354
174. Willerth SM, Rader A, Sakiyama-Elbert SE (2008) Stem Cell Res 1:205
175. Chao TI, Xiang S, Chen CS, Chin WC, Nelson AJ, Wang C, Lu J (2009) Biochem Biophys Res Commun 384:426
176. Carlberg B, Axell MZ, Nannmark U, Liu J, Kuhn HG (2009) Biomed Mater 4:045004
177. Lee MR, Kwon KW, Jung H, Kim HN, Suh KY, Kim K, Kim KS (2010) Biomaterials 31:4360
178. Tse KH, Sun M, Mantovani C, Terenghi G, Downes S, Kingham PJ (2010) J Biomed Mater Res Part A 95A:701
179. Aijun W, Qiang AO, Qing HE, Xiaoming G, Kai G, Yandao G, Nanming Z, Xiufang Z (2006) Tsinghua Sci Tech 11:415
180. Gage FH (2000) Science 287:1433
181. Brignier AC, Gewirtz AM (2010) J Allergy Clin Immunol 125:S336
182. Lee YB, Polio S, Lee W, Dai G, Menon L, Carroll RS, Yoo SS (2010) Exp Neurol 223:645
183. Bini TB, Gao S, Wang S, Ramakrishna S (2006) J Mater Sci 41:6453
184. Young TH, Hung CH (2005) Biomaterials 26:4291
185. Cheng M, Deng J, Yang F, Gong Y, Zhao N, Zhang X (2003) Biomaterials 24:2871

186. ZhaoYang Y, LinHong M, HongMei D, XiaoGuang L (2010) Sci China Life Sci 53:215
187. He L, Liao S, Quan D, Ngiam M, Chan CK, Ramakrishna S, Lu J (2009) Biomaterials 30:1578
188. Leipzig ND, Wylie RG, Kim H, Shoichet MS (2011) Biomaterials 32:57
189. Chung TW, Yang MC, Tseng CC, Sheu SH, Wang SS, Huang YY, Chen SD (2011) Biomaterials 32:734
190. Yang F, Murugan R, Wang S, Ramakrishna S (2005) Biomaterials 26:2603
191. He L, Liao S, Quan D, Ma K, Chan C, Ramakrishna S, Lu J (2010) Acta Biomater 6:2960
192. Christopherson GT, Song H, Mao HQ (2009) Biomaterials 30:556
193. Ghasemi-Mobarakeh L, Prabhakaran MP, Morshed M, Nasr-Esfahani MH, Ramakrishna S (2008) Biomaterials 29:4532
194. Ghasemi-Mobarakeh L, Prabhakaran MP, Morshed M, Nasr-Esfahani MH, Ramakrishna S (2009) Tissue Eng Part A 15:3605
195. Lim SH, Liu XY, Song H, Yarema KJ, Mao HQ (2010) Biomaterials 31:9031
196. Tsuruma A, Tanaka M, Yamamoto S, Shimomura M (2008) Colloids surf A Physicochem Eng Asp 313–314:536
197. Hsu SH, Su CH, Chiu IM (2009) Artif Organs 33:26
198. Recknor JB, Sakaguchi DS, Mallapragad SA (2006) Biomaterials 27:4098
199. MacNeil S (2007) Nature 445:874
200. Yannas IV, Kwan MD, Longaker MT (2007) Tissue Eng 13:1789
201. Zhang C-p, Fu X-b (2008) Chin J Traumatol 11:209
202. Krause DS, Theise ND, Collector MI, Henegariu O, Hwang S, Gardner R, Neutzel S, Sharkis SJ (2001) Cell 105:369
203. Badiavas EV, Falanga V (2003) Arch Dermatol 139:510
204. Falanga V, Iwamoto S, Chartier M, Yufit T, Butmarc J, Kouttab N, Shrayer D, Carson P (2007) Tissue Eng 13:1299
205. Sasaki M, Abe R, Fujita Y, Ando S, Inokuma D, Shimizu H (2008) J Immunol 180:2581
206. Spees JL, Olson SD, Ylostalo J, Lynch PJ, Smith J, Perry A, Peister A, Wang MY, Prockop DJ (2003) Proc Natl Acad Sci USA 100:2397
207. Wu Y, Chen L, Scott PG, Tredget EE (2007) Stem Cells 25:2648
208. Păunescu V, Deak E, Herman D, Siska IR, Tănasie G, Bunu C, Anghel S, Tatu CA, Oprea TI, Henschler R, Rüster B, Bistrian R, Seifried E (2007) J Cell Mol Med 11:502
209. Kobayashi M, Spector M (2009) Mol Cell Biomech 6:217
210. Holland TA, Tabata Y, Mikos AG (2005) J Control Release 101:111
211. Zahid L, Mark W, Eric MB, Antonios GM, Duke PJ (2003) J Oral Maxillofac Surg 61:1061
212. Park H, Temenoff JS, Holland TA, Tabata Y, Mikos AG (2005) Biomaterials 26:7095
213. Wake MC, Gerecht PD, Lu L, Mikos AG (1998) Biomaterials 19:1255
214. Rustad K, Wong VW, Sorkin M, Glotzbach JP, Nehama D, Major MR, Rajadas J, Longaker MT, Gurtner GC (2010) J Am Coll Surg 211:S91
215. Haase I, Knaup R, Wartenberg M, Sauer H, Hescheler J, Mahrle G (2007) Eur J Cell Biol 86:801
216. Iuchi S, Dabelsteen S, Easley K, Rheinwald JG, Green H (2006) Proc Natl Acad Sci USA 103:1792
217. Dabelsteen S, Hercule P, Barron P, Rice M, Dorsainville G, Rheinwald JG (2009) Stem Cells 27:1388
218. Hind G, Xavier N, Fernando L, Jessica F, Gilles L, Manoubia S, Marcela Del R, Christine CB, Francois-Xavier B, Marc P, Christine B, Gilles W (2009) Lancet 374:1745
219. Altman AM, Yan Y, Matthias N, Bai X, Rios C, Mathur AB, Song YH, Alt EU (2009) Stem Cells 27:250
220. Kamolz LP, Kolbus A, Wick N, Mazal PR, Eisenbock B, Burjak S, Meissl G (2006) Burns 32:16
221. Schneider RK, Püllen A, Kramann R, Bornemann J, Knüchel R, Neuss S, Perez-Bouza A (2010) Differentiation 79:182

222. Luo G, Cheng W, He W, Wang X, Tan J, Fitzgerald M, Li X, Wu J (2010) Wound Repair Regen 18:506
223. Paquet C, Larouche D, Bisson F, Proulx S, Simard-Bisson C, Gaudreault M, Robitaille H, Carrier P, Martel I, Duranceau L, Auger FA, Fradette J, Guérin SL, Germain L (2010) Ann N Y Acad Sci 1197:166
224. Lee EY, Xia Y, Kim WS, Kim MH, Kim TH, Kim KJ, Park BS, Sung JH (2009) Wound Repair Regen 17:540
225. Salem H, Ciba P, Rapoport DH, Egana JT, Reithmayer K, Kadry M, Machens HG, Kruse C (2009) Biomaterials 30:789
226. Dawson E, Mapili G, Erickson K, Taqvi S, Roy K (2008) Adv Drug Deliv Rev 60:215
227. Vara DS, Salacinski HJ, Kannan RY, Bordenave L, Hamilton G, Seifalian AM (2005) Pathol Biol 53:599
228. Wang C, Cen L, Yin S, Liu Q, Liu W, Cao Y, Cui L (2010) Biomaterials 31:621
229. Chiang CK, Chowdhury MF, Iyer RK, Stanford WL, Radisic M (2010) Acta Biomater 6:1904
230. Nourse MB, Halpin DE, Scatena M, Mortisen DJ, Tulloch NL, Hauch KD, Torok-Storb B, Ratner BD, Pabon L, Murry CE (2010) Arterioscler Thromb Vasc Biol 30:80
231. Das H, Abdulhameed N, Joseph M, Sakthivel R, Mao HQ, Polpili VJ (2009) Cell Trans 18:305
232. Gimble JM, Katz AJ, Bunnell BA (2007) Circ Res 100:1249
233. Rodriguez AM, Elabd C, Amri EZ, Ailhaud G, Dani C (2005) Biochimie 87:125
234. Wurmser AE, Gage FH (2002) Nature 416:485
235. Wurmser AE, Nakashima K, Summers RG (2004) Nature 430:350

Adv Polym Sci (2012) 246: 63–100
DOI: 10.1007/12_2011_131

Published online: 28 July 2011

Creating Electrospun Nanofiber-Based Biomimetic Scaffolds for Bone Regeneration

Eleni Katsanevakis, Xuejun Wen, and Ning Zhang

Abstract Bone defects due to trauma, congenital deformity, or disease are highly prevalent in today's society. Some 5–10% of these injuries result in a non-union and need surgical intervention. Currently, the main treatment method for these types of defects is a bone allograft or autograft. The main issues associated with these methods include pain, infection, and donor site morbidity. Bone tissue engineering is a diverse field that focuses on the regeneration of bone by combining cells, scaffolds, growth factors, and dynamic forces. Recently, tissue engineering methods that mimic the natural extracellular matrix (ECM) of bone have been utilized to better serve this need. One such method is the use of electrospinning, which allows for the creation of polymer nanofibers with diameters ranging from

E. Katsanevakis
Clemson-MUSC Bioengineering program; Department of Bioengineering, Clemson University, 173 Ashley Ave. CRI#609, Charleston, SC 29425, USA

X. Wen
Clemson-MUSC Bioengineering program; Department of Bioengineering, Clemson University, 173 Ashley Ave. CRI#609, Charleston, SC 29425, USA

Department of Orthopedic Surgery, Medical University of South Carolina, Charleston, SC 29425, USA

Department of Regenerative Medicine and Cell Biology, Medical University of South Carolina, Charleston, SC 29425, USA

N. Zhang (✉)
Clemson-MUSC Bioengineering program; Department of Bioengineering, Clemson University, 173 Ashley Ave. CRI#609, Charleston, SC 29425, USA

Department of Regenerative Medicine and Cell Biology, Medical University of South Carolina, Charleston, SC 29425, USA

Department of Microbiology and Immunology, Medical University of South Carolina, Charleston, SC 29425, USA
e-mail: nzhang@clemson.edu; zhangn@musc.edu

a couple microns down to a few nanometers. These nanofibers are very similar in structure and size to those of the natural collagen seen in bone ECM. Further, by combining certain biomimetic techniques along with electrospinning, it is possible to more closely mimic the mechanical properties and morphology of the ECM of bone, as well as enhance cell attachment, alignment, and proliferation. For these reasons, electrospinning is a biomimetic approach that has emerged as a choice candidate for the regeneration of native bone tissue. In this review, we will describe the methods utilized to create biomimetic structures for bone tissue engineering, as well as highlight the advancements made in this field using these methods.

Keywords Biomimetic · Bone · Electrospinning · Growth factors · Hydroxyapatite · Nanofibers

Contents

1 Introduction

Bone is composed of both organic and inorganic components, with the inorganic hydroxyapatite (HAp) forming between and elongating on the aligned organic collagen fibers. This structure is the building unit and lowest level in the hierarchical structural organization of bone. The many different levels allow bone to serve its numerous functions, as well as provide it with the necessary physical and mechanical characteristics. The macrostructure consists of both cortical and cancellous bone, with each of these types of bone having a very distinct microstructure. Whereas cancellous bone has a very irregular and porous microstructure, cortical bone's microstructure is very ordered and is composed of very tightly packed osteons, also called Haversian systems. These osteons are cylindrical structures that consist of lamellar sheets of aligned collagen fibers formed into concentric layers. Lower in the hierarchical structure of bone, these fibers are composed of aligned fibrils, which are self-assembled from triple-helical collagen molecules. These molecules are staggered in their long axis by 67 nm, generating a 35 nm

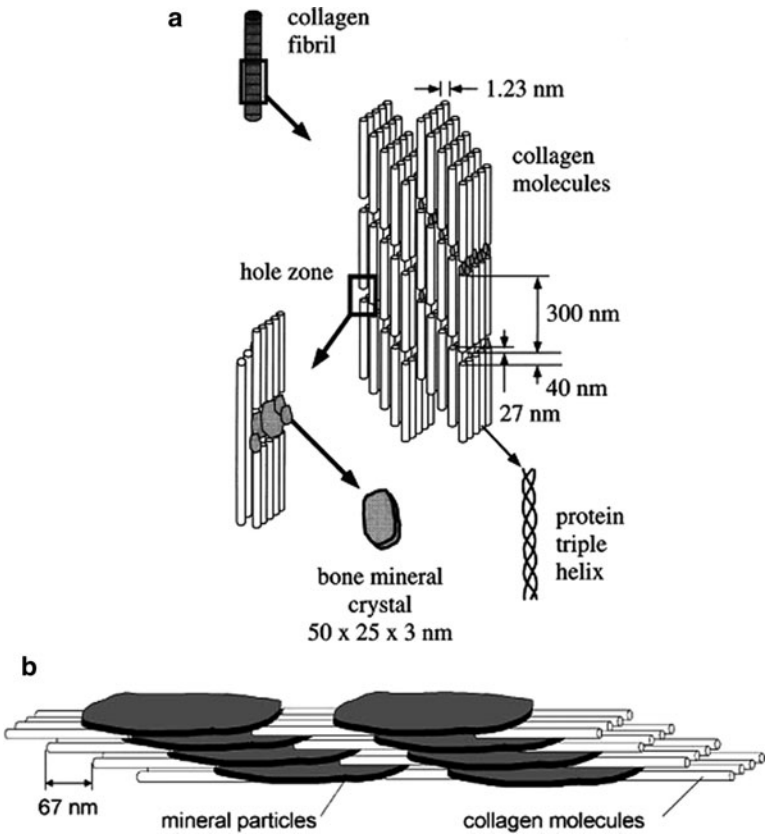

Fig. 1 Microstructure of bone, showing staggered structure of collagen molecules, which creates hole zones in which HAp is nucleated (**a**) [1]. The lowest level of hierarchical structure of bone, showing alignment and elongation of HAp crystals as a function of underlying aligned collagen fibrils (**b**) [2] (Reproduced by permission of The Royal Society of Chemistry)

anionic gap zone in which HAp is nucleated (Fig. 1a) [1, 2]. The size of these HAp crystals are in the range of 2–7 nm in thickness, 15–200 nm in length, and 10–80 nm in width [2, 3]. Once nucleated, these crystals align and elongate along with the aligned collagen fibrils (Fig. 1b). The HAp component in this precise nanostructure allows for enhanced mechanical properties that give bone its necessary high strength and fracture toughness. Yet, the highly crosslinked collagen framework maintains its load-bearing function, as well as viscoelasticity, which allows bone tissue to absorb shock [4]. This structure, however, also plays a significant role in cell behavior and response. Whereas osteoblasts and osteoclasts are present on the mineralized bone, osteocytes are embedded within the bone matrix. Specific cues and signals between the different cells allow for ECM secretion and resorption as well as mineralization of this matrix. The collagen matrix, which is secreted by the

osteoblasts, provides a substrate for the HAp to deposit as well as for the bone-forming cells to attach, align, and proliferate.

There are many different types of bone, including long bones, such as the tibia and femur, which have a cancellous interior and a dense cortical shell; and flat bones, such as the calvaria, which have a sandwich structure with dense cortical layers on the outside and a thin layer of cancellous bone on the inside [1]. Although the components remain the same, each type of bone has different macrostructures in order to serve different functions. These functions include structural support, protection, storing of healing cells, and mineral ion homeostasis [1]. The mechanical properties of bone also differ depending on the bone type, and can vary along and throughout the bone. Long bones, which consist of mostly cortical bone, have been shown to have a yield strength of 78–151 MPa in tension, 131–224 MPa in compression, and a modulus of elasticity of 17–20 GPa, when tested along the longitudinal axis. However, the mechanical properties of cancellous bones are much lower, with a strength of 5–10 MPa and modulus of 50–100 MPa [5–7]. This drastic change is due to the highly porous structure of cancellous bone [8]. The amount of mineralization, which can vary between bones and bone types, also has a great effect on the mechanical properties of bone [9]. Although the mechanical properties of bone have often been described, they are usually expressed in a range because the actual numbers can vary from specimen to specimen, as well as change depending on testing method and conditions [1]. Despite the superior mechanical properties described above, defects still occur very often in bone tissue.

Critically sized defects in bone are highly prevalent in today's society, due to trauma, congenital deformity, or disease [10]. Trauma can have many causes, including battlefield injury [11, 12], gunshot wound [13], or accident, such as falling and breaking a bone [14]. In about 5–10% of all traumatic bone injuries, bone cannot heal itself to form a union, and surgical intervention must take place [10, 15]. The most prevailing type of congenital deformity associated with bone that is seen today is a cleft palate [16, 17], in which, during development, the palatal shelves that form the palate do not fuse [18]. Surgical resection of large portions of bone can also need to be performed due to diseases such as cancer, with the most prevailing type being osteosarcoma [19]. With this case, a large amount of bone typically needs to be removed and replaced with a permanent prosthesis, if no other options exist. However, these prostheses often fail due to wear debris or deep infection over time [19]. Currently, autografts and allografts are the main treatment methods for critically sized defects in bone. However, issues associated with these methods are very common and include donor site morbidity [20, 21] and donor-to-recipient cross-infections [22, 23]. For these reasons, researchers have begun to steer more towards a tissue engineering approach in order to actually regenerate bone tissue. This would allow for new tissue in-growth that would take place while a temporary scaffold is degrading and would eventually replace it with the native tissue. This method would only require one surgical procedure and would be a drastic improvement on the methods currently being used.

2 Tissue Engineering for Bone Regeneration

Tissue engineering has been described as "an interdisciplinary field that applies the principles of engineering and life sciences toward the development of biological substitutes that restore, maintain, or improve tissue function or a whole organ" [24, 25]. The term tissue engineering first became known in the early to mid-1990s and since has become widespread and is considered by many to be the primary means for repairing or replacing tissue and organ defects in the future. The concept utilizes 3D scaffolds, cells, and growth factors or other biomolecules (Fig. 2) [26] in order to provide a temporary tissue construct for cells to grow on and produce ECM while new tissue forms and the scaffold degrades [27]. In theory, these scaffolds should be biocompatible, degradable, highly porous, and hydrophilic in order to allow for cell infiltration and attachment, as well as tissue in-growth [27, 28]. Depending upon the application, many other properties are also required, such as suitable elasticity and other mechanical properties [27]. Cells can then be seeded onto these scaffolds in order to attach and proliferate and produce new tissue, which will eventually take the place of the degraded scaffold. The type of cells used is extremely extensive and depends on the application and the tissue being regenerated. The cells can either be fully differentiated cells or progenitor cells,

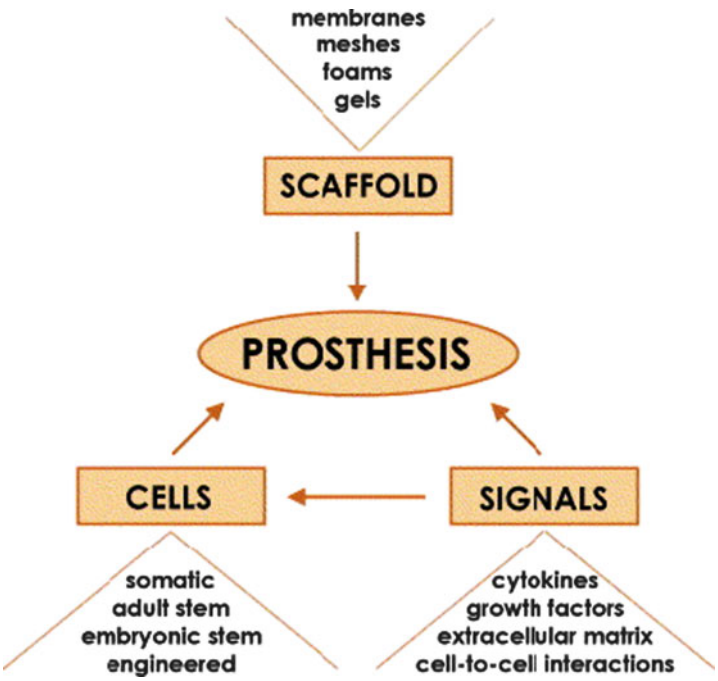

Fig. 2 Basic principles of tissue engineering [26]

such as stem cells, that can be induced to differentiate towards a certain lineage [29]. For example, specifically for bone tissue engineering, osteoblasts can be seeded onto matrices and implanted in order to secrete new bone tissue for regeneration of injured bone. However, certain stem cells can also be used. These cells can be directed to differentiate towards the desired lineage in order to regenerate the injured tissue. These types of cells, which can be of embryonic or adult origin, are often easier to use because one type of stem cell can be differentiated towards multiple cell lineages and be used for several applications. Though embryonic stem cells are useful due to their inherent ability to produce all cell lineages, adult stem cells are frequently used because there are no ethical considerations, plus they are usually very easy to acquire non-invasively. Such examples include adipose-derived stem cells (ADSCs) and dental pulp stem cells (DPSCs), which can be acquired from excess fat tissue or extruded molars/wisdom teeth, respectively. Both of these cell types have been shown to be multipotent, i.e., able to differentiate into multiple cell lineage pathways, including osteogenic pathways [30, 31]. There are many other stem cells that are capable of osteogenic differentiation, including mesenchymal stem cells (MSCs), a type of multipotent stem cells. MSCs are originally found in bone marrow, however, they can be isolated from many other

Table 1 Sources of adult mesenchymal stem cells (MSCs) [32]

Source tissue	Multilineage differentiation potential	Representative references
	Adipocyte	[26, 33]
	Astrocyte, neuron	[12, 34]
	Cardiomyocyte	[14, 15, 35–37]
	Chondrocyte	[26, 38–40]
	Hepatocyte	[6, 7, 41]
	Mesangial cell	[13]
	Muscle	[10, 42]
	Neuron	[11, 12]
	Osteoblast	[26, 43–47]
	Stromal cell	[48]
Bone marrow	Various embryonic tissue lineages	[49]
	Adiocyte, myotubes, osteocyte	[50]
	Endothelial cell, neuron	[20, 51]
	Chondrocyte	[52]
Muscle	Osteocyte	[20]
Trabecular bone	Adipocyte, chondrocyte, osteoblast	[27–29]
Dermis	Adipocyte, chondrocyte, muscle, osteoblast	[21]
	Chondrocyte, muscle, osteoblast	[16]
Adipose tissue	Stromal cell	[53]
Periosteum	Chondrocyte, osteoblast	[17, 18]
	Chondrocyte	[22]
Pericyte	Osteoblast	[23, 24]
Blood	Adipocyte, fibroblast, osteoblast, osteoclast	[25]
Synovial membrane	Adipocyte, chondrocyte, muscle, osteoblast	[18]

tissue sources as well (Table 1) [32]. As can be seen from Table 1, regardless of the tissue source, MSCs generally have osteogenic potential. In order to induce differentiation of these cells towards a desired lineage, such as an osteogenic lineage for bone tissue regeneration, the tissue engineering scaffolds can be loaded with growth factors or other biomolecules. This can be done by either incorporating them within the polymer scaffold or chemically attaching the biomolecules to the surface [42, 43, 54]. However, it is important to note that cell-free strategies are also prevalent for tissue engineering applications. These scaffolds do not involve the inclusion of any cells on the scaffold, but feature growth factors and other biomolecules either attached on the surface of the polymer or incorporated within the scaffold. The incorporated growth factors will be released from the scaffold in a controlled manner and may recruit endogenous stem cells and induce them to differentiate into a desired lineage in order to regenerate the injured tissue [55].

Specifically, the field of bone tissue engineering requires many of the same properties as other tissue engineering areas for scaffold materials, including biocompatibility, biodegradability, and high porosity, to name a few. Timely biodegradability and high porosity are especially important in order to allow for bone ingrowth and vascularization. Other requirements for bone tissue engineering scaffolds include: acting as substrate for osteoid deposition, supporting and promoting osteogenic differentiation, and promoting osseointegration [7]. Additional requirements can be seen in Table 2 [56]. However, since bone tissue is a type of load-bearing tissue, the scaffolds for bone regeneration need to possess sufficient mechanical properties. To this end, the concept of biomimicry has recently evolved to define the properties of scaffolds for bone regeneration. Biomimicry refers to structural, compositional, property, and functional similarities of an artificial structure to a natural tissue. Using an artificial structure that is both physically and chemically biomimetic, it is more possible for the body to regenerate a tissue in a manner that would occur naturally. By mimicking the structure, function, and chemical cues seen in natural tissue, an artificial tissue engineering scaffold can have the capability to regenerate tissue more efficiently and effectively. For this reason, biomimicry has been extensively used as a criterion to direct material choices and scaffold design for bone regeneration.

Table 2 Desirable qualities of a bone tissue-engineering scaffold [56]

Available to surgeon on short notice	Promotes bone ingrowth
Absorbs in predictable manner in concert with bone growth	Does not induce soft tissue growth at bone/implant interface
Adaptable to irregular wound site, malleable	Average pore size approximately 200–400 μm
Maximal bone growth through osteoinduction and/or osteoconduction	No detrimental effects to surrounding tissue due to processing
Correct mechanical and physical properties for application	Sterilizable without loss of properties
Good bony apposition	Absorbable with biocompatible components

Many different materials have been investigated for use in synthetic bone scaffolds. The most obvious choice would be ceramics, due to their similar structure and composition to natural bone. Ceramics have also been proven to have enhanced bioactivity, by bonding to bone easily and enhancing bone tissue formation. However, for tissue engineering applications, these materials are not suitable due to increased brittleness when creating a porous scaffold, as well as lack of biodegradability and osteoinductivity. This has led investigators to look more towards polymers as materials for synthetic bone scaffolds. Polymers are great for tissue engineering applications due to their biocompatibility, biodegradibilty, and versatility. However, these materials lack the mechanical properties to act as bone tissue substitutes. Recently, however, polymer/ceramic composites have emerged as the leading method for developing synthetic bone scaffolds [7]. These scaffolds are created by incorporating nanosized ceramic constituents, such as HAp, into polymer matrices to create a biomimetic structure and to improve the mechanical properties. These composite structures have been shown to enhance certain mechanical properties including strength, modulus, and crack resistance [7, 57–60]. Table 3 lists common fabrication methods for polymer/ceramic composites, as well as their advantages and disadvantages [61].

Table 3 Advantages and disadvantages of different fabrication methods for polymer/ceramic composites [61]

Fabrication route	Advantages	Disadvantages
Thermally induced phase separation [33, 37]	High porosities (~95%)	Long time to sublime solvent (48 h)
	Highly interconnected pore structures	Shrinkage issues
	Anisotropic and tubular pores possible	Small scale production
	Control of structure and pore size by varying preparation conditions	Use of organic solvents
Solvent casting/particle leaching [41, 45]	Controlled porosity	Structures generally isotropic
	Controlled interconnectivity (if particles are sintered)	Use of organic solvents
Solid free-form [46, 47]	Porous structure can be tailored to host tissue	Resolution needs to be improved to the microscale
	Protein and cell encapsulation possible	Some methods use organic solvents
	Good interface with medical imaging	
Microspher sintering [48]	Graded porosity structures possible	Interconnectivity is an issue
	Controlled porosity	Use of organic solvents
	Can be fabricated into complex shapes	
Scaffold coating [62]	Quick and easy	Clogging of pores
		Sometimes organic solvents used
		Coating adhesion to substrate can be too weak

There are many tissue engineering techniques currently being investigated as scaffold fabrication methods for bone tissue regeneration, including solvent casting/particulate leaching [38, 44, 63–66], phase separation [67–69], fiber bonding [70], freeze-drying [71–73], gas foaming [74, 75], and rapid prototyping methods [76–79]. Many of these methods, as can be seen in Table 3, can be combined with other techniques in order to create a polymer/ceramic composite scaffold. These differing fabrication methods can be used to achieve different structures of polymer/ceramic composites. Although these methods have all shown notable advances in this field, many are not adequate for bone tissue engineering because of the more complex requirements for this specific type of scaffold. These methods possess many downfall, including poor mechanical properties, low porosity, and poor degradation rates. One of the most promising methods, however, is electrospinning [80–85], which has the unique ability to create polymer nanofibers that can mimic the ECM of many tissues, including the lowest level in the hierarchical structure of bone. Using this method, nanofibers have been created that can be highly aligned and range from a few microns down to as small as several nanometers in diameter.

A wide variety of polymers can be used with electrospinning, including synthetic, natural, or a combination of both. This allows the tailoring of specific properties, including mechanical properties and degradation rates. Further, these electrospun scaffolds have the ability to be easily mineralized with HAp using a biomimetic technique. Available techniques for the mineralization of polymer fibers include electrospraying [86], co-precipitation [87, 88], blending [39, 40, 83, 89–97], simulated body fluid (SBF) immersion [98–101], and an alternate soaking process [102–106]. The resulting composite structures have a very similar microstructure to that of natural bone. In this case, the benefits of both polymers and ceramics can be utilized, while cutting down the drawbacks. Using just polymers would not give a high mechanical strength, whereas using just ceramics provides a material that is too brittle. Also, biodegradable polymers can be used to create these scaffolds so that the scaffolds can degrade over time in order to allow for new tissue infiltration. Further, the incorporation of polymers supports cell adhesion, alignment and proliferation, whereas the incorporation of HAp not only results in better mechanical properties, but also in better bioactivity and osteoconductivity of the scaffold.

It is highly evident that tissue engineering approaches for bone regeneration are necessary in order to produce an effective strategy for bone growth and repair. Biomimetic approaches seem to be the frontrunner when trying to achieve goals in this area. Concurrently, creating biomimetic structures by mineralizing electrospun scaffolds, loading them with growth factors or other biomolecules, and then creating 3D bone-like structures, represents a promising strategy for the regeneration of native bone tissue. In the following sections, we will review both the electrospinning and biomineralization techniques for the creation of polymer nanofiber array-based biomimetic scaffolds for bone regeneration.

2.1 Electrospinning

Electrospinning is a tissue engineering technique that has been used for many years to fabricate polymer nanofibrous scaffolds. It utilizes a high voltage power supply to electrically charge a polymer solution that is then extruded from a syringe through a metallic capillary outlet, using a syringe pump. The polymer droplet transforms into a Taylor cone due to the electrostatic charges, and when the voltage surpasses a threshold value, the polymer solution becomes a charged jet. This charged jet moves towards a metal collection plate, with the solvent evaporating in the process, and polymer nanofibers remain on the collection plate [107] (see Fig. 3). Nanofibers with diameters ranging from a couple microns down to a few nanometers, which can be compared to the ECM of many tissues in the body, have been created using this method.

Numerous physical traits of the scaffolds can be produced by varying the electrospinning conditions and parameters. Changing parameters such as the polymer concentration, solvent, voltage, flow rate, distance to the collection plate, and diameter of the needle, can drastically alter the morphology of the fibers. Also, by changing how the fibers are collected, the morphology of the scaffold can be affected, either producing randomly aligned mats, highly aligned scaffolds, or 3D structures [108]. These scaffolds are considered to be superior tissue engineering scaffolds because they are highly porous and have a high ratio of surface area to

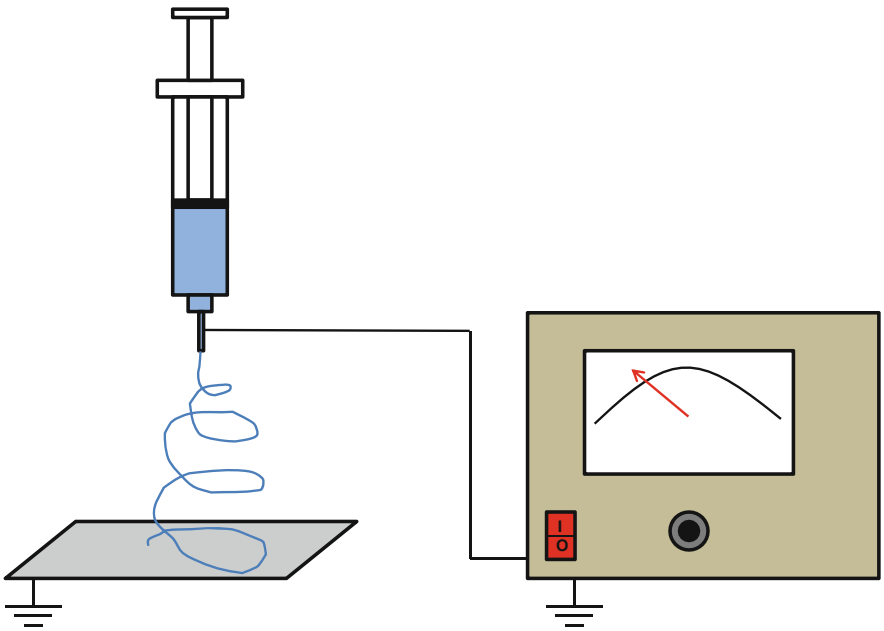

Fig. 3 Standard electrospinning setup

Table 4 Common examples of synthetic and natural polymers, as well as combinations of both, used for electrospinning

Type of polymer	Polymer	References
Synthetic	Poly(L-lactide)	[110–112]
	Poly(ε-caprolactone)	[113–115]
	Poly(lactide-*co*-glycodide)	[116–119]
	Poly(ethylene oxide)	[115, 120]
	Poly(vinyl alcohol)	[121, 122]
	Poly(ester urethane) urea	[123, 124]
	Poly(ethylene-*co*-vinyl alcohol)	[125]
	Poly(L-lactide-*co*-ε-caprolactone)	[126, 127]
Natural	Chitin	[52, 128]
	Chitosan	[52, 128–130]
	Collagen	[131–134]
	Cellulose	[128]
	Silk fibroin	[96, 135, 136]
	Hyaluronic acid	[128, 137]
	Fibrin	[138]
	Fibrinogen	[139–141]
	Gelatin	[132, 142]
	Elastin	[131, 132, 134]
Combination	Silk fibroin and poly(ethylene oxide)	[143]
	Hyaluronic acid and poly(ε-caprolactone)	[144]
	Collagen and poly(ε-caprolactone)	[35, 145]
	Chitosan and poly(ethylene oxide)	[36]

ratio [27, 109]. Electrospinning techniques are compatible with many types of polymers, natural or synthetic, or combinations of both. Table 4 lists some common types of polymers that can be electrospun. The ease of fabrication, and the low cost, plus the ability to tailor the scaffolds to specific needs, makes electrospinning an excellent candidate and popular choice for tissue engineering applications.

It is highly evident that electrospinning has many excellent qualities, which have made it one of the leading scaffold fabrication methods for tissue engineering applications, including bone tissue engineering. Many different approaches for bone tissue regeneration are being undertaken using this electrospinning technique. These approaches are typically designed to mimic the natural structure of bones, and include: creating aligned nanofibrous scaffolds, creating polymer/ceramic composites, biomolecule delivery using drug encapsulation, and creating 3D electrospun nanofiber-based biomimetic scaffolds. However, electrospinning can be considered a biomimetic technique in itself. With electrospun nanofibers ranging from a couple of microns down to several nanometers, these nanofibers mimic the collagen fibers found in bone's ECM. This similar morphology allows for superior mechanical properties, as well as increased cell attachment and proliferation [100, 110–112]. This enhanced cell attachment can most likely be attributed to the greater surface area provided by the 3D structure. Numerous studies also indicate that cells seeded onto polymer nanofibers, as compared to smooth controls, generally show

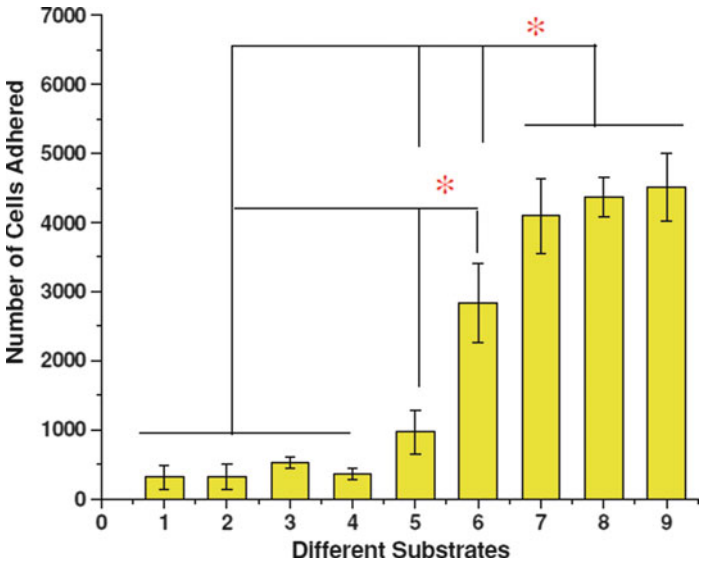

Fig. 4 Attachment of cells to different substrates: *1* TCP, *2* glass coverslip, *3* gelatin-coated coverslip, *4* collagen-coated coverslip, *5* P(LLA-CL) nanofiber, *6* air-plasma treated P(LLA-CL) nanofiber, *7* Collagen-coated P(LLA-CL) nanofiber, *8* collagen microfiber, *9* collagen nanofibers [114]

enhanced ECM production [113, 114]. In a study by Chan et al. [114], collagen electrospun nanofibers scaffolds were shown to significantly increase cell attachment as compared with collagen film used as the control. This shows the great importance of surface topography for cell attachment. This groups also compared other smooth materials to various polymer nanofibers, and determined that cells attached significantly better to nanofibers than to the controls (Fig. 4) [114]. Other groups have also conducted studies comparing electrospun scaffold to tissue culture polystyrene (TCP) and have indicated enhanced cell attachment, spreading, and proliferation [110–112]. Further, these scaffolds have also been shown to stimulate prostaglandin synthesis, osteocalcin (OCN) synthesis, and alkaline phoshatase activity in osteoblastic cells, as well as show increased collagen production and calcium deposition [85, 111]. However, many researchers are now focusing on using electrospinning combined with other biomimetic techniques, listed above, in order to more completely mimic the actual structure and composition of bone microstructure. These biomimetic methods are being tested in vitro using cell studies for attachment and proliferation, measuring alkaline phosphatase (ALP) activity, ECM production, as well as in vivo for new bone tissue formation. Mechanical testing is also being conducted in order to determine whether the mechanical properties of the scaffolds are improved and are suitable for this application.

2.2 *Creating Aligned Nanofibrous Scaffolds*

Aligned nanofibrous scaffolds, produced by electrospinning, have been gaining in popularity in recent years due to their increased ability to mimic the aligned collagen fibers in the ECM of many tissues of the body, including bone. This biomimetic method for bone tissue regeneration applications allows for bone-forming cells to attach and align along the aligned fibers and has been shown to demonstrate enhanced proliferation and ECM production [115, 116]. Currently, the main approach to the creation of aligned nanofibers uses a rotating collecting drum. This metal collecting drum is connected to a high speed motor so, as it rotates, the charged polymer solution travels towards it and the fibers collect on it in an aligned manner, in the tangential direction [89, 90, 113, 117–119]. This is a very simple and efficient way to create aligned nanofibers (Fig. 5). Lee et al. [115] used this rotating drum method and observed cell orientation parallel to the aligned fibers, whereas a random orientation was observed for the cells seeded onto films and randomly oriented fibers (Fig. 6a). The authors also observed a significant increase in proliferation (Fig. 6b), when comparing the aligned fibers to the TCP control, as well as ECM production (Fig. 6c) when comparing the aligned fibers to randomly oriented fibers. A significant increase was also seen in the mechanical properties of the aligned scaffolds (Fig. 6d) [115]. Similarly, Zhong et al. [116] also saw a significant increase in cell proliferation in aligned scaffolds compared to randomly oriented scaffolds. However, there are not many instances where aligned nanofibers have been used specifically for bone regeneration applications. In a related application, Bashur et al. [113], used this same method, and compared aligned scaffolds to unaligned scaffolds and spin-coated samples. It was determined that bone marrow stromal cells were oriented parallel to the aligned fibers and assumed a more spindle-like morphology on these scaffolds, whereas no orientation was observed for the controls. It was also observed that, as compared to the unaligned scaffolds, when cells were cultured on aligned nanofiber scaffolds, the relative expression of

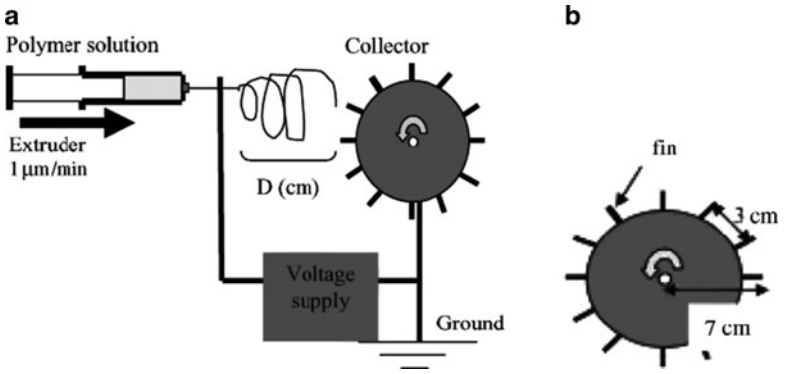

Fig. 5 Modified electrospinning setup utilizing a rotating drum (**a**). Typical dimensions of rotating drum (**b**) [146]

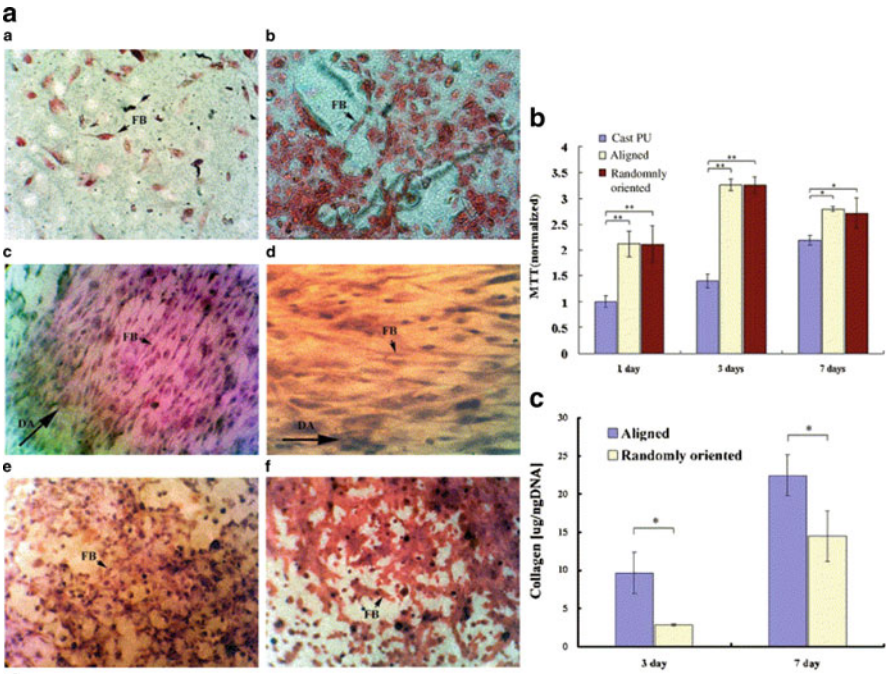

d

	E1 (kPa)	E2 (kPa)	Max strain	Ultimate strength (kPa)
Aligned	2500 ± 63 (ε < 0.1)	3550±28 (ε>0.1)	1.08±0.17	3520±30
Randomly oriented	540 ± 60 (ε < 0.4)	1630±11 (ε>0.4)	1.03±0.16	1130±21

Fig. 6 Cell alignment and ECM production on polyurethane films (*top*), aligned nanofibers (*middle*), and randomly oriented nanofibers (*bottom*) (**a**). Cell proliferation (**b**), collagen I production (**c**), and mechanical properties (**d**) of aligned and randomly oriented scaffolds [115]

four different ligament proteins was increased, though specific markers for bone tissue formation or bone cell differentiation were not assessed. In another study, Jose et al. [89, 90], used this same electrospinning method for bone tissue regeneration, but also incorporated HAp nanoparticles into the scaffolds. Preliminary studies have indicated greater mechanical properties, such as storage modulus for the aligned composite scaffold containing an optimal concentration of HAp; however, these parameters were not compared to unaligned nanofibrous scaffolds as a control. Cell studies do indicate that these scaffolds support cell adhesion, spreading, proliferation, and growth, and showed that the cells aligned along the direction of the fiber orientation.

Other techniques to attain highly aligned nanofibers are also employed, and are not quite as popular, but often demonstrate enhanced alignment of the nanofibers. These techniques typically rely on two parallel collecting plates, in which the polymer solution is extruded in between the two. Once a charge is applied to the polymer, it travels towards the plates and the electric field between the two plates triggers the fibers to align parallel to each other but perpendicular to the

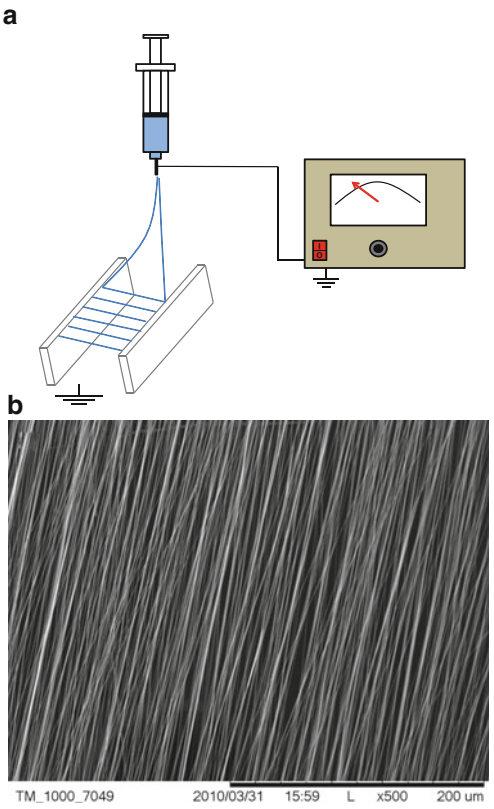

Fig. 7 Setup for parallel plate electrospinning (**a**). Aligned nanofibrous scaffold produced by this method (**b**)

plates (Fig. 7) [120, 121]. For instance, Li et al. [121, 122] used this method to develop highly aligned scaffolds with over 80% of the fibers being at the 0° angle. These results were determined by the measurement of over 150 fibers. No cell studies or mechanical testing was conducted at this time, but the researchers introduced this technique as an idea to create 3D structures with these aligned scaffolds for specific tissue engineering applications. Beachley et al. [120] used a similar parallel plate approach, but developed a system that utilizes parallel rotating plates (data not shown). Once the fibers align between the plates, they are moved down to a collection rack at the bottom by these rotating plates. This allows for increased alignment, as well as the ability to tailor the thickness and/or fiber density of the scaffolds. In vitro results indicate higher cell proliferation after 7 days of culture on aligned scaffolds than after culture on films. The cells were also observed to align parallel to the fiber direction, whereas a random orientation was demonstrated by the cells on the films (unpublished results). This method is beginning to be utilized more often, and allows the creation of highly aligned nanofibers, in which the fiber length, diameter, and uniformity can be altered.

Though few cell studies on aligned nanofibrous scaffolds have been specifically conducted for bone regeneration applications, preliminary data in other areas

suggest that these aligned nanofibrous scaffolds could potentially enhance bone tissue formation, and are thus good candidates for bone tissue regeneration applications. With literature reporting that nanofibrous scaffolds demonstrate enhanced attachment and proliferation as compared to smooth controls, and that aligned nanofibrous scaffold show enhanced ECM production and proliferation as compared to unaligned nanofibers, it is obvious that these scaffolds are superior to others currently being used for bone regeneration applications. With additional research in this area being focused specifically for bone regeneration efforts, many new milestones can be achieved in this field. By building on data previously reported in the literature, it will be possible in the future to regenerate bone using aligned nanofibrous scaffolds.

2.3 Creating Polymer/Ceramic Composites

For bone tissue engineering, the main method for creating a biomimetic structure utilizes a polymer and ceramic composite in order to not only enhance mechanical properties, but also create an osteoconductive scaffold. This is due to the inherent ability of the polymer/ceramic composite to mimic the mechanical and physical properties of the microstructure of bone, which consists of HAp nanoparticles forming between, and aligning on the collagen fibers of bone ECM. This exquisite structure has extraordinary mechanical properties that give bone its necessary high strength and fracture toughness, as well as the elasticity that allows bone tissue to absorb shock [4]. These unparalleled characteristics are highly centered on the role of the nanosize of the two main constituents, as well as their positioning, which allow the mineral phase to absorb the load while the protein matrix transfers the load between HAp minerals via shear (see Fig. 8) [2, 123, 124]. For bone regeneration applications, the mechanical properties of the scaffolds are also very important.

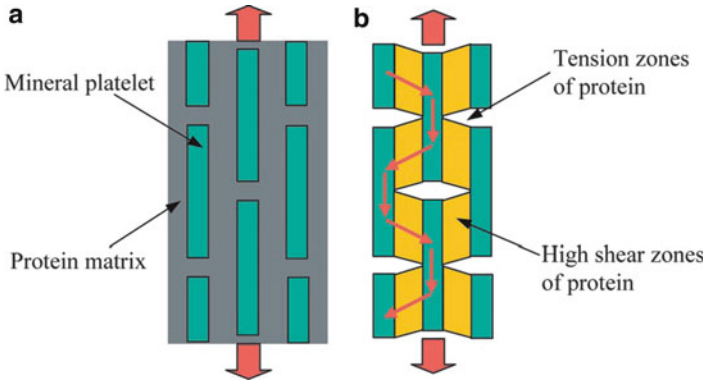

Fig. 8 Staggered structure of HAp embedded within protein matrix (a). The majority of the load is being carried by the mineral platelets as the protein matrix transfers the stress via shear (b). [124]

With load-bearing tissues, it is important for the scaffold to at least have sufficient mechanical properties to withstand the stresses and loading in the in vivo environment. These mechanical properties should be maintained for sufficient time for tissue to begin to in-grow and assume some of the load [125]. The inclusion of HAp nanoparticles within or on an artificial structure not only enhances mechanical properties and mimics the natural microstructure of bone, but also creates a bioactive material, which results in new tissue formation once incorporated inside the body as a scaffold for bone regeneration [126]. This has to do with chemical reactions, occurring at the surface of the polymer, in which dissolution products of the HAp on the surface of the construct (such as calcium and phosphate ions) upregulate gene expression that controls osteogenesis and the production of growth factors. This leads to ECM production and the formation of carbonated HAp, which allows the scaffold to create a bond with the natural tissue around it [52, 127]. For these reasons, the use of polymer/ceramic composites is increasingly being looked at as an alternative to current tissue engineering approaches.

There are many different ways to create a polymer/ceramic composite structure. Many methods rely on a biomimetic approach, often utilizing techniques that involve the immersion of polymer nanofibers into solutions that contain ion concentrations similar to that of human blood plasma. There are many different ways to do this, including the use of SBF, [98–101] alternating soaking in concentrated calcium and phosphate solutions, [102–106] and others [88, 128–130]. Oftentimes, with the first two methods, the surface of the polymer has to be functionalized with anionic functional groups in order for the positively charged calcium ions to have a place to bind to the surface of the polymer and initiate nucleation of HAp. These methods imitate what naturally occurs in the body when bone is forming. However, the most popular and easy way to create a polymer/ceramic composite with electrospun nanofibers is to simply add HAp nanoparticles into the polymer solution prior to electrospinning [39, 40, 83, 89–97]. This method is very straightforward and has been proven to improve the mechanical properties of the scaffold as well as enhance cell attachment and proliferation [91, 92]. Electrospraying HAp nanoparticles onto the polymer nanofiber surface is also an effective technique, but not utilized quite as often as the other methods [86].

One of the most common ways to create a HAp coating on polymer nanofibers is immersing them in SBF, which has ion concentrations similar to that of human blood plasma (Table 5) [131]. Though SBF immersion is often utilized as a method

Table 5 Ion concentration of different SBFs compared to human blood plasma [131, 167]

	Ion concentration (mM)							
SBF	Na^+	K^+	Mg^{2+}	Ca^{2+}	CT^-	HCO_3^-	HPO_4^{2-}	SO_4^{2-}
Human blood plasma	142.0	5.0	1.5	2.5	103.0	27.0	1.0	0.5
Original SBF	142.0	5.0	1.5	2.5	148.8	4.2	1.0	0
Corrected SBF	142.0	5.0	1.5	2.5	147.8	4.2	1.0	0.5
Revised SBF	142.0	5.0	1.5	2.5	103.0	27.0	1.0	0.5
Newly improved SBF	142.0	5.0	1.5	2.5	103.0	4.2	1.0	0.5

to determine scaffold bioactivity, it is also used to create a biomimetic coating on scaffolds, which also renders the scaffolds bioactive. The ease of fabrication, plus the low cost and effectiveness, makes this method one of the most popular for creating this biomimetic coating. Also, different concentrations of SBF, such as 1.5×, 5×, and 10×, can be used to shorten the mineralization time. When a material is immersed in SBF, the calcium ions present in the solution are attracted to anionic functional groups on the polymer chain, such as hydroxyl and carboxyl groups, to name a few, and chelation begins on the surface. The phosphate ions also begin to bind and this initiates the formation of a HAp coating on the surface. Depending on the conditions, both the composition and structure of the mineral formed can be almost identical to that of natural bone mineral. This method is very popular because it forms a biomimetic coating on the polymer's surface, which resembles the HAp that forms on the surface of collagen in bone ECM. This also creates an osteoconductive surface for implantation. Chen et al. [101] used this method to create a continuous mineral layer on the surface of an electrospun scaffold. Prior to immersion in SBF, however, the nanofibers were also subjected to a hydrolysis treatment in order to increase the functional groups on the polymer surface. Results indicate that scaffolds have an enhanced ability to mineralize if a hydrolysis treatment was performed prior to SBF immersion. However, no mechanical testing or cell studies were conducted. Yang et al. [98] conducted a similar study, including a hydrolysis treatment, but used 10× SBF instead. The optimal mineralization time was determined to be 2 h, during which time formation of a homogenous mineral coating was observable. No mechanical testing or cell studies were conducted in this study. Li et al. [99] also used SBF for bone tissue engineering applications, but did conduct cell studies on their mineralized electrospun scaffolds. It was determined that preosteoblasts attached, spread, and proliferated better on electrospun nanofibers mineralized by SBF than on non-mineralized nanofibers. Likewise, Ito et al. [100] used this mineralization method and compared polymer nanofibers and films, and found that cells not only attached to the nanofibers significantly better than on the films, but also attached onto the mineralized fibers just as well as onto the unmineralized fibers.

Immersing polymer nanofibers in alternating calcium and phosphate solutions is another method of creating a biomimetic HAp coating on polymer nanofibers (Fig. 9). This method is very similar to using SBF with respect to the mechanism by which the biomimetic coating is formed. There has, however, been some data that proves that this alternating soaking method actually works better than immersing in SBF. This is probably due to the introduction of larger amounts of calcium and phosphate ions since the solutions are highly concentrated. In one particular study by Yin et al. [103], though not polymer nanofibers, functionalized and unfunctionalized polymer scaffolds were immersed in either SBF or alternating $CaCl_2$ and Na_2HPO_4 solutions. Results indicated that SBF did not form apatite on the unfunctionalized polymer scaffold and barely formed apatite on the functionalized polymer scaffold, whereas both scaffolds that were immersed in alternating $CaCl_2$ and Na_2HPO_4 solutions showed extensive apatite formation and growth. For this method, the calcium solutions typically consist of $CaCl_2$ [102–105,

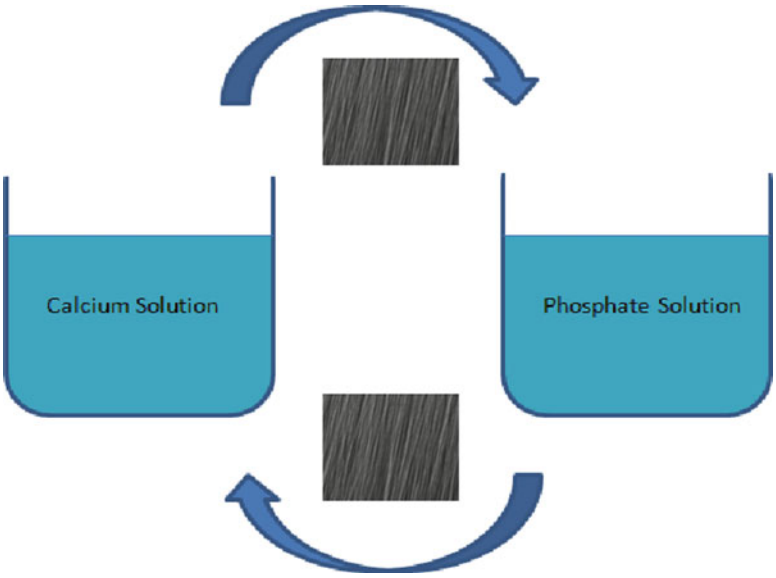

Fig. 9 Alternate soaking method

132–136], though other salts have been used. The phosphate solution typically used is dihydrogen sodium phosphate (Na_2HPO_4) [102, 103, 105, 133–136]; however, diammonium phosphate, $(NH_4)_2HPO_4$, [132] and monopotassium phosphate (KH_2PO_4) [104] are also used. This method works by introducing a large amount of calcium ions to the anionic functional groups present on the polymer chains, which initiates the nucleation and allows for mineral growth. Taguchi et al. [106] has demonstrated this method, though not on electrospun nanofibers. This method was used to create a HAp coating on poly (vinyl alcohol) (PVA) gels. The polymer samples were immersed in 200 mM $CaCl_2$ for 2 h and then soaked in 120 mM Na_2HPO_4 for 2 h. This cycle was repeated five times and X-ray diffraction (XRD) data showed that the sample peaks matched the five main peaks of HAp. Similarly, Madhumathi et al. [136] used this same method on chitosan hydrogels; energy dispersive X-ray spectroscopy (EDX), Fourier transform infrared spectroscopy (FTIR), and XRD data suggest that the coating produced was very similar to that of HAp. Further, this scaffold showed excellent biocompatibility as compared to the control. This same group, also used this method to create a biomimetic HAp coating on β-chitin membranes, and observed similar EDX, FTIR, and XRD data [135]. They also conducted in vitro cell studies and noticed significantly better cell attachment and spreading on the composite membranes as compared to the controls. However, this method is also very successful in forming a biomimetic HAp coating on electrospun nanofibers. Shalumon et al. [134] used this method to create a HAp coating on carboxymethyl chitin/PVA electrospun nanofibers. EDX data demonstrated a calcium to phosphorus ratio of 1.89, which is very similar to the

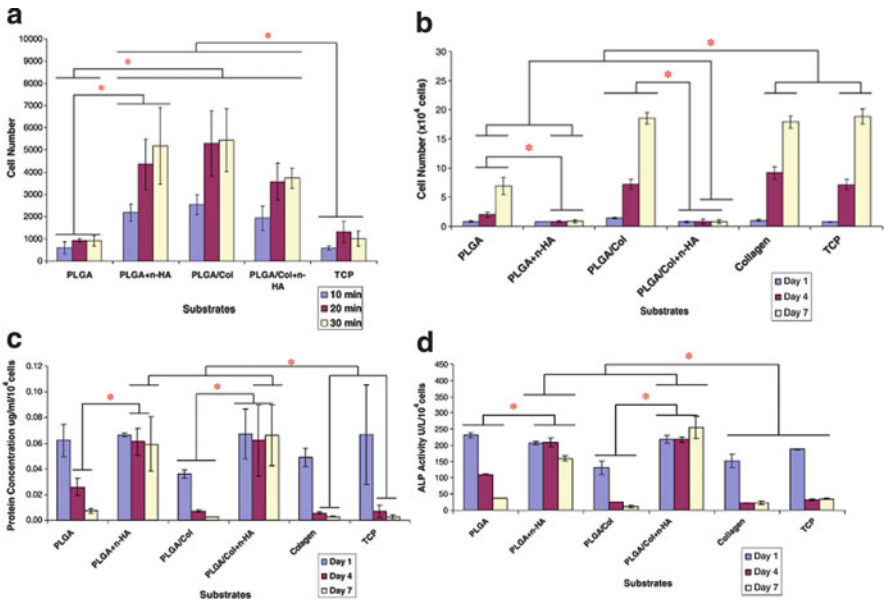

Fig. 10 Human fetal osteoblast (hFOB) attachment (**a**), proliferation (**b**), protein secretion (**c**) and ALP activity (**d**) on various mineralized and unmineralized nanofiber scaffolds [102]

theoretical value of the Ca:P ratio of HAp that is found in natural bone, often reported to be 1.67 [104, 137]. Ngiam et al. [102] used this same method and observed similar results. Alternate soaking in concentrate calcium and phosphate solution was used to create a HAp coating on two different types of polymer nanofibers, either poly(lactic-*co*-glycolic acid) (PLGA) or a PLGA/collagen copolymer. They determined that their coating had a Ca/P ratio of 1.67, which is equivalent to the theoretical value of the Ca/P ratio of HAp in natural bone. Data also demonstrated that scaffolds mineralized with this technique showed enhanced osteoblast attachment and spreading on the PLGA scaffolds (Fig. 10a), as well as enhanced protein secretion and ALP activity (Fig. 10c and d), though cell proliferation was significantly lower (Fig. 10b). This decline was attributed to the rough surface of the Hap-containing groups, which other researchers have also noticed [138–140]. Ngiam et al. [105] conducted another study using different polymers and observed the same results. An ALP assay was also conducted, but no significant difference between the mineralized and unmineralized groups was seen. Yang et al. [104] used $CaCl_2$ and KH_2PO_4 solutions to create a HAp coating on electrospun chitosan scaffolds. The concentrations and amount of each solution was specifically chosen to exhibit a Ca/P ratio of 1.67. SEM, EDX, and FTIR data showed a HAp coating similar to that of natural HAp. In vitro data suggests ideal cell morphology and enhanced viability with these scaffolds.

Another popular method for creating electrospun ceramic/polymer composites is to blend HAp nanoparticles directly into the polymer solution prior to

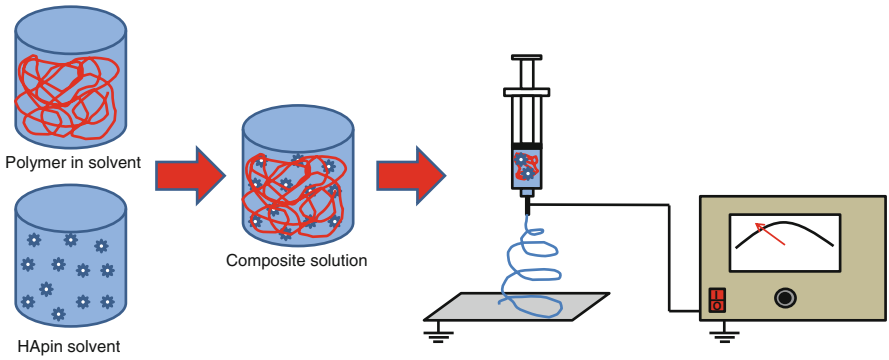

Fig. 11 Two-step blending method used to create polymer/ceramic composite fibers

electrospinning (Fig. 11). This method is by far the easiest and is very cost-effective. HAp nanoparticles, ranging in composition and size, can be incorporated into varying polymer solutions prior to electrospinning in order to create a composite material. Many polymers, including polycaprolactone (PCL) [39, 91], poly(D,L-lactide-*co*-glycolide) (PLGA) [89, 90, 93, 95], poly(D,L-lactic acid) (PLA) [94], and poly(L-lactic acid) (PLLA) [83, 92] can be used. These HAp nanoparticles are usually incorporated via a two-step method in order to ensure proper dispersion. This method is far simpler than immersion in SBF or alternating calcium and phosphate solutions because it not only saves time, but ensures that the proper composition of HAp is used. With other methods, the composition of the coating can never be guaranteed to be exactly similar to that of natural bone. Also, different concentrations of HAp can be added, with different groups coming up with different optimal concentrations of HAp in order to enhance the mechanical properties, cell attachment, and ECM production. For instance, Kim et al. [94] used this technique in order to produce composite nanofibers. These nanofibers showed significantly higher cell attachment, after 6 h, and proliferation, after 2 days. Significantly higher ALP activity was also observed with the composite scaffolds as compared to pure polymer scaffolds and TCP after 7 days. Jose et al. [89] also used this two-step blending method to determine the optimal HAp concentration. First, the polymer was dissolved in the solvent at the desired ratio. Then, the same solvent was used and the desired amount of HAp nanoparticles were dispersed into the solvent and sonicated for 90 min to break up any nanoparticle agglomerations. The two solutions were then combined at the desired ratio and stirred for 90 min. These solutions of either 0.0, 0.2, 0.5, 1.0, or 5.0 wt% HAp were created and used to determine the optimal HAp concentration. It was concluded that 0.5 wt% HAp allowed the best mechanical properties and showed an excellent cellular response. When specifically comparing this concentration of HAp to the samples that contained no HAp (0.0 wt%), the mechanical properties were significantly greater, though no in vitro or in vivo studies were conducted to compare these groups. Similarly, Yang at al. [91] utilized this same method, but actually synthesized their

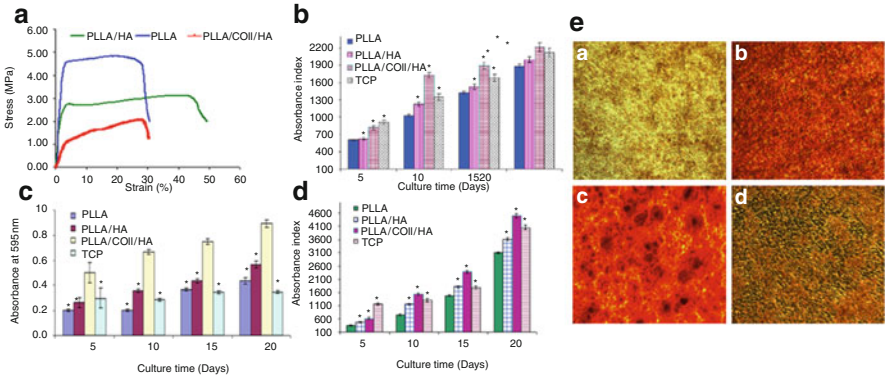

Fig. 12 Stress–strain curve of varying mineralized and unmineralized scaffolds (**a**). hFOB proliferation (**b**), ALP activity (**c**), and calcium deposition (**d**) on varying scaffolds. Alizaren Red staining of PLLA scaffold (*top left*), PLLA/HA scaffold (*top right*), PLLA/Col/HA scaffold (*bottom left*), TCP (*bottom right*) (**e**) [83]

HAp nanoparticles by a precipitation reaction. The creation of HAp nanoparticles was confirmed by XRD and FTIR. The nanoparticles were then included in the polymer solution in the same two-step process as previously described. Varying the amounts of HAp inclusion was also studied, and it was determined that there was a significant increase in mechanical properties and ALP activity of osteoblast-like cells after 1, 4, and 8 days with an increase HAp concentration. Prabhakaran et al. [83] also used this method, but did not use a two-step process. HAp particles were directly incorporated into the polymer solution at 20 wt% and then electrospun. When measuring mechanical properties of these fibers compared to pure PLLA controls, this group noticed significantly lower tensile strength for the composite fibers (Fig. 12a). The authors did not hypothesize why this occurred, but it might be due to HAp agglomerations in the nanofibers causing fiber breakage, and therefore lower mechanical properties. However, for in vitro cell studies, the proliferation rate (Fig. 12b), ALP activity (Fig. 12c), and calcium deposition (Fig. 12d) of human fetal osteoblasts was significantly higher at all times points in the HAp-containing group than in controls not containing HAp. Alizaren Red staining also proved higher mineral deposition for these scaffolds (Fig. 12e). Sui et al. [92] created polymer/HAp composite scaffolds in a similar manner, and showed that the HAp-containing nanofibers scaffolds had a significantly higher specific surface area, due to the HAp nanoparticles, and therefore greater cumulative pore volume, and theorized that this would allow for better cell penetration and growth of cells. It was later proved that these scaffolds actually did demonstrate enhanced osteoblast attachment, viability, and proliferation, as well as enhanced mechanical properties. Nie at al. [93] used similar method to the above-mentioned groups, and also compared different HAp concentrations. However, bone morphogenetic protein 2 (BMP-2) was also included in the scaffolds for enhanced bone tissue formation.

It was found that the scaffolds containing HAp showed significantly better cell attachment. Viability and proliferation were also enhanced, but were probably affected by the inclusion of BMP-2. Lastly, Lee et al. [95] conducted a similar study by seeding PLGA and PLGA/HAp composite scaffolds with human mesenchymal stem cells (hMSCs) and noticed that there was a significantly higher expression of osteogenic differentiation genes, such as ALP and OCN, for the cells seeded onto the composite scaffolds. A significantly higher amount of calcium was also observed on these scaffolds as compared to the control.

Other methods, though not as popular, have been shown to be very effective in creating a biomimetic HAp coating on polymer nanofibers. For example, electrospraying, as demonstrated by Gupta et al. [86], utilizes a charged jet of HAp nanoparticles simultaneously with electrospinning in order to produce a composite scaffold similar to that formed when HAP is blended into the polymer solution. The difference between the two methods, however, might be what makes electrospraying better, suggests Gupta et al. Electrospraying allows the HAp to remain on the surface of the nanofibers, whereas the blended method embeds the HAp nanoparticles within (Fig. 13). This makes a huge difference because the bioactivity and osteoconductivity of the scaffold rely on HAp being on the surface of the nanofibers. For this reason, Gupta et al. set out to prove that this method creates a composite scaffold that is better for bone regeneration applications. This group compared polymer scaffolds (control) with polymer/ceramic composites created by either the blending method or electrospraying method. Results indicate similar mechanical properties and proliferation rates for both composite scaffolds (significantly higher than the controls). However, when seeded with osteoblasts, there was significantly higher ALP activity and mineralization deposition on the electrosprayed scaffolds than on the blended composite scaffolds. This indicates

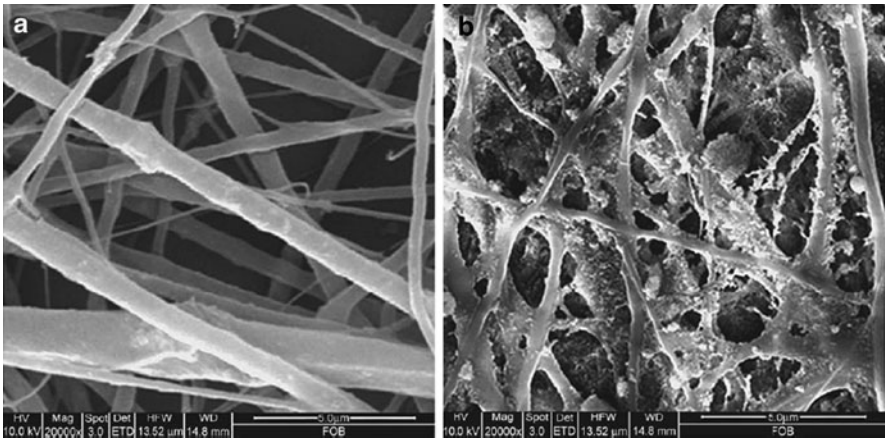

Fig. 13 Incorporation of HAp nanoparticles by blending (**a**) and electrospraying (**b**) [86]

that this method might create a more bioactive and osteoconductive scaffold than blending HAp nanoparticles into the polymer solution.

Another method used to create polymer/ceramic composites by electrospinning includes a co-precipitation method [87, 88], which works in a very similar manner to the blending method; however, both the organic and inorganic components are precipitated together prior to dissolving and electrospinning. Song et al. [87, 88] dissolved $Ca(OH)_2$ in cold distilled water and separately dissolved the polymer (collagen, in this case) in H_3PO_4. Both solutions were then added to a reaction vessel containing a TRIS-HCl buffer solution, and kept at pH 9. The amounts of Ca and P were predetermined to get the desired composition. The mixture was stirred vigorously for 48 h followed by washing and lyophilization. This dried polymer/HAp composite was then dissolved in an organic solvent and electrospun. Song et al. [88] found that by using scaffolds created by this method, as compared to pure polymer controls, cell proliferation was significantly greater after 2 days. Also, although at day 7 a decrease in ALP activity was seen, by day 14 a significant increase in ALP activity was seen in the composite scaffolds. Zhang et al. [130] used a very similar method, but used chitosan as the polymer. Similar results were found, indicating a significant difference in cell proliferation and mineral deposition at days 10 and 15 of the composite scaffold as compared to pure polymer scaffolds.

The last method to be discussed, which is used to form polymer/ceramic composites by electrospinning, is extremely different to the methods previously described, but worth mentioning. Zuo et al. [129] used a method to create a composite scaffold that is actually the reverse of what most people are doing. Instead of mineralizing the nanofibers, Zuo et al. actually incorporated electrospun polymer nanofibers into a ceramic bone cement in order to form a composite scaffold. It was found that by incorporating electrospun nanofibers into the cement, the scaffold became less brittle and actually behaved similarly to that of a ductile material because of the fibers. Composite scaffolds with different polymers and fiber diameters were then tested in order to determine which scaffold demonstrated the most ideal mechanical properties. However, no cell studies were conducted and this method would most likely be used for a bone substitute instead of for bone regeneration applications.

The methods discussed above that are used to create polymer/ceramic composites are all successful ways to create not only biomimetic scaffolds, but scaffolds that are also bioactive and osteoconductive. All of the methods have their downfalls, but the methods that create a HAp coating most similar to that of natural bone in both structure and composition are typically the most effective. Mechanical testing data indicate significantly improved mechanical properties for these types of scaffolds, which is very important in load-bearing tissue engineering applications. Also, cells studies show promising results, demonstrating enhanced cell attachment, proliferation, and ALP activity. However, many researchers have not attempted to combine this biomimetic method with other methods in order to more effectively regenerate bone.

2.4 Biomolecule Delivery

When bone tissue is injured, the body goes through a natural process in order to repair this tissue to its normal strength, structure, and function [141]. Immediately after a fracture, growth factors and cytokines can be instantly detected at the fracture site, and are secreted in order to recruit other cells to begin the repair process. These growth factors can include fibroblast growth factor (FGF-1 and FGF-2), platelet-derived growth factor (PDGF-AA, PDGF-AB, PDGF-BB), transforming growth factor-β (TGF-β1 and TGF-β2), and bone morphogenetic protein (BMP-2, BMP-3, BMP-4, and BMP-7) [141]. However, not all fractures can be repaired by this natural process. Some fractures result in a non-union, and surgical intervention must take place. However, for tissue engineering applications, these natural proteins that are normally expressed in the body can be utilized to help the bone regeneration process. Using electrospun scaffolds, these same biomolecules can be incorporated into the scaffolds in order to enhance bone regeneration when the body cannot heal the defect itself.

The growth factors mentioned above are expressed immediately after injury at the fracture site and are most often incorporated into scaffolds for bone regeneration applications. Biomolecules can be incorporated into nanofiber-based scaffolds by many means, including adsorption of the biomolecule onto the surface, encapsulating the biomolecule into the polymer solution prior to electrospinning, and the creation of biomolecule/polymer nanoparticles that can be encapsulated into the polymer solution prior to electrospinning [40]. Nie et al. [40] created biomimetic electrospun scaffolds by including both HAp nanoparticles as well as BMP-2. All of the methods of biomolecule incorporation were then compared in order to determine which was most effective (see Fig. 14 for schematic). It was discovered that all methods released BMP-2 and that the BMP-2 retained its bioactivity. However, it was determined that the scaffolds created by encapsulating BMP-2/polymer nanoparticles within electrospun nanofibers showed a better and more linear release curve than the other groups, which showed a strong initial burst release (Fig. 15a). These curves also corresponded to cytotoxicity data, where cells seeded onto scaffolds that showed an initial burst release showed significantly lower viability because of this burse release (Fig. 15b). Further, fibers encapsulating the BMP-2/polymer nanoparticles also demonstrated enhanced cell attachment (Fig. 15c). However, these samples were not compared to a control not containing BMP-2. Li et al. [96] conducted a study based on the encapsulation of BMP-2 in silk/PEO electrospun nanofibers that also contained HAp nanoparticles. It was also determined that the encapsulation of both HAp and BMP-2 enhanced calcium deposition after 31 days in culture and BMP-2 transcript levels after 14 days in culture. However, no significant difference was seen in bone sialoprotein (BSP) or collagen I production and no other cell studies were performed.

Fu et al. [97] also compared two of the methods for BMP-2 inclusion. The effects of adding different concentrations of HAp nanoparticles were studied when BMP-2 was either encapsulated within the fiber (F1–F3), or loaded after scaffold

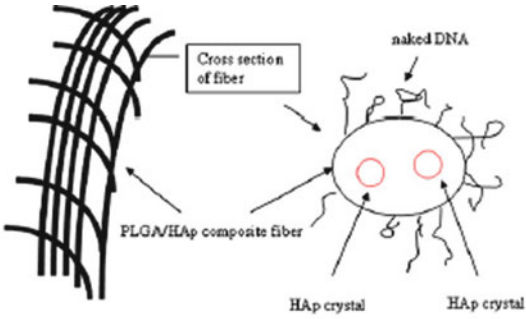

PLGA/HAp composite fiber with naked DNA coated outside

Mode A

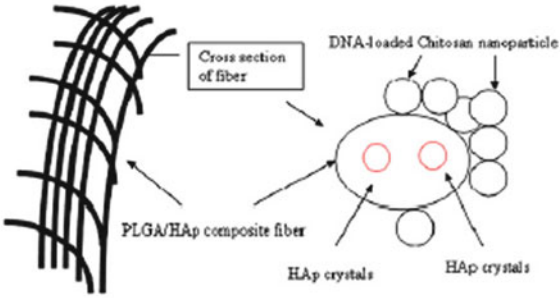

PLGA/HAp composite fiber with DNA-loaded Chitosan nanoparticle coated outside

Mode B

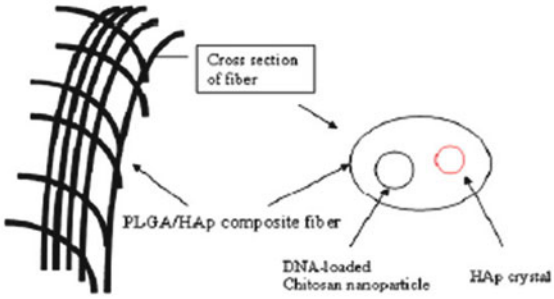

PLGA/HAp composite fiber with DNA-loaded Chitosan nanoparticles encapsulated inside

Mode C

Fig. 14 Methods for incorporating biomolecules into/on polymer nanofibers [40]

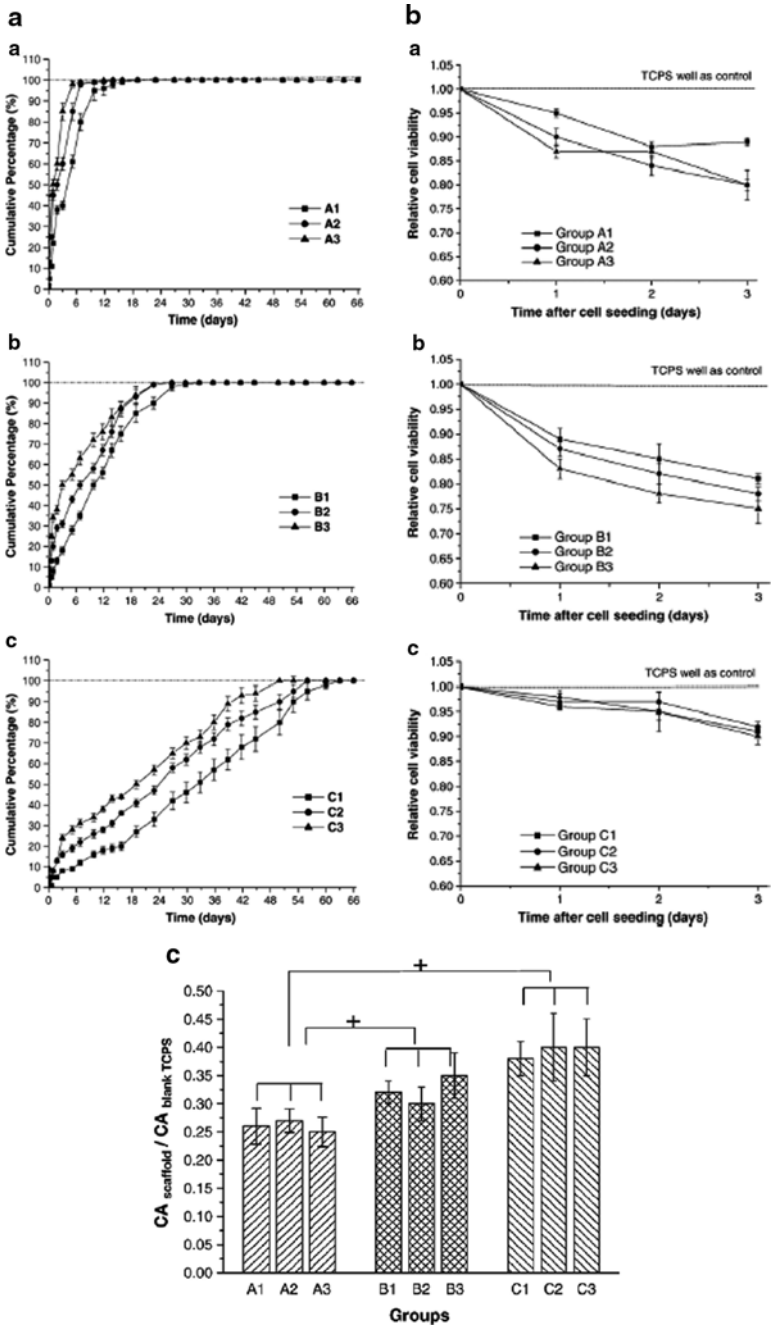

Fig. 15 DNA release over 60 days (**a**). Cytotoxicity of each scaffold (**b**). Cell attachment on each scaffold (**c**) [40]. Groups *A*, *B* and *C* refer to the method of incorporation shown in Fig. 14; the *numbers* of each group correspond to the amount of HAp inclusion (0%, 5%, and 10%)

fabrication (F4). Mechanical testing determined that the inclusion of a proper amount of HAp nanoparticles increased the tensile stress of the scaffolds. Release curves indicated a burst release for F4, which is to be expected since it can diffuse into the media without the fibers having to degrade. The other release profiles (F1–F3) were very similar, even though it is important to note that the samples not containing any HAp nanoparticles released the BMP-2 the slowest. These results correlated with the results for ALP activity of the seeded scaffolds, with F4 showing significantly higher ALP activity than the others in the first couple of weeks (due to the burst) then significantly lower in the last couple of weeks. In vivo studies indicate that the scaffolds that contain both BMP-2 and HAp are required to retain the bioactivity of BMP-2 and to have any effect on bone formation, yet it was not determined which method of BMP-2 incorporation and what concentration of HAp was best for bone regeneration applications. Schofer et al. [142] also incorporated BMP-2 into their electrospun scaffolds for bone regeneration applications. BMP-2 was incorporated by blending it into their polymer solution prior to electrospinning. When seeded with hMSCs, results indicate an increase in expression of genes associated with an osteoblast lineage, as compared to control that did not contain BMP-2.

Though BMP-2 and other growth factors are used most for this application, other biomolecules can also be incorporated into polymer nanofibers, including genes and pharmaceuticals. For instance, Pişkin et al. [143] incorporated simvastatin, a statin drug known to stimulate bone regeneration, into electrospun PCL nanofibrous scaffolds. The drug was incorporated by two different methods: by either blending it with the polymer solution prior to electrospinning or by loading it after electrospinning. The scaffolds were then spirally wound into a 3D structure and implanted into a critically size cranial defect in rats. Histological data and MicroCT results from the in vivo study indicate that the PCL scaffolds in which the simvastatin was incorporated prior to electrospinning showed significantly better ossification and mineralization of the defect area.

The methods discussed above for biomolecule inclusion in electrospun nanofibers have all been shown to be effective in maintaining the bioactivity of the biomolecules, as well as enhancing ALP activity and other genes associated with bone regeneration. In general, encapsulating biomolecules into the polymer solution prior to electrospinning, either alone or in nanoparticles, has been proven to be more effective than adsorbing onto the surface, due to the lack of a burst release. This method has sufficient encapsulation efficiency and has been shown to release the biomolecules steadily over a period of 60 days in vitro. Sustained controlled release of biomolecules is very important for bone regeneration since it is a slow process. Some groups have also combined this method with other biomimetic techniques, such as composite scaffolds and 3D scaffolds, and have seen very promising results. By creating a 3D bone-like structure using electrospun nanofibrous scaffolds, further advances in bone tissue regeneration will probably take place.

2.5 Creating 3D Electrospun Nanofiber-Based Biomimetic Scaffolds

Using electrospun nanofibrous scaffolds, it is also possible to create a 3D bone-like structure. This type of structure can be created in numerous ways, including stacking, rolling, or actually electrospinning a 3D structure. When combined with other biomimetic methods, such as growth factor delivery or aligned nanofibrous scaffolds, this method has been proven to be successful in inducing bone tissue formation in vivo [143]. The most common way to create a 3D bone-like structure is to stack seeded electrospun scaffolds on top of each other in a layer-by-layer approach. However, rolling scaffolds into cylinders is also popular, as is actually electrospinning 3D structures. For instance, Pişkin et al. [143], as mentioned above, created a 3D structure by rolling electrospun simvastatin-loaded PCL scaffolds into spirals. This biomimetic technique demonstrated enhanced bone formation and mineralization in vivo as compared to the control, in which the defect did not contain a scaffold. Ekaputra et al. [144] used a similar rolling technique, but formed a more tubular structure. PCL/collagen scaffolds of 2 cm $\times$ 2 cm were seeded on both sides with pig bone marrow mesenchymal cells (pBMMCs) then rolled into cylindrical shapes with a diameter of 6 mm. The scaffolds were then wrapped in sheets of osteogenic cells. When seeded with pBMMCs, these scaffolds demonstrated enhanced bone tissue formation, with higher production of calcium, OCN, osteopontin, and collagen I.

Li et al. [121, 122] used a different approach and stacked their aligned electrospun scaffolds using a layer-by-layer approach. This method is the one most often utilized to create 3D structures by electrospinning. This group introduced this method, and mentioned certain applications, such as controlling hierarchical structures for bone regeneration, but conducted no in vitro or in vivo studies with the scaffolds. Srouji et al. [145] also used a similar stacking method, but did not use aligned fibers, and therefore could not create patterned structures. Thirty electrospun scaffolds were seeded with cells and stacked on top of each other. When compared to a TCP control, cell viability was comparable and not significantly different for the 3D scaffold. Further, in vivo results indicate that the scaffolds support cell infiltration and neovascularization. McCullen et al. [35] also utilized this stacking method to create a 3D bone-like structure, but altered the technique slightly. First, the scaffolds were created by electrospinning, but then were laser ablated in order to create large pores in the scaffold. Cells were then seeded onto the scaffolds and the scaffolds were bonded in layers by polymerizing type I collagen to create thick 3D scaffolds. Results of in vitro cell studies after 21 days demonstrate significantly higher cell proliferation and significantly higher mineral production on the ablated scaffolds than on unablated controls. This most likely has to do with cellular infiltration into the scaffold due to the ablated pores. However, no in vivo studies were conducted. Inanç et al. [36] also used the stacking method to create 3D bone-like structures. First, PLGA nanofibrous scaffolds were created via electrospinning. These scaffolds were then seeded with human

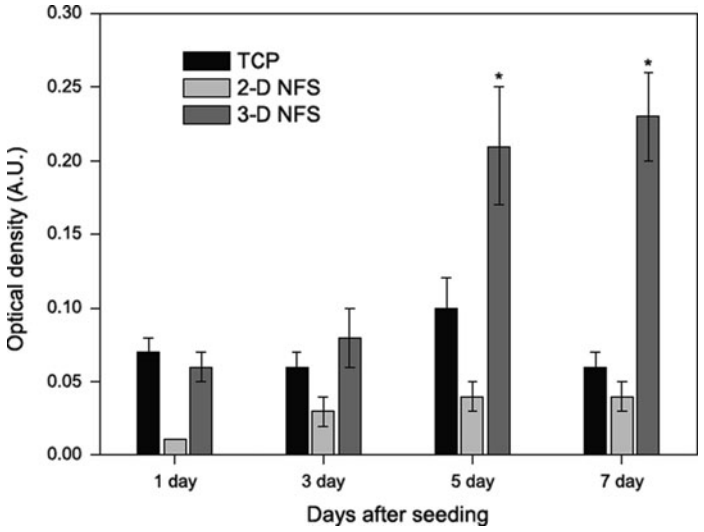

Fig. 16 Preosteoblast proliferation on TCP, 2D, and 3D nanofibrous fibroin scaffold (*NFS*) [37]

periodontal ligament (hPDL) cells. Additional layers were added to the scaffolds on days 3, 6, 9 and 12. No significant difference was seen in cell viability as compared to TCP controls. hPDL cells were observed to attach and spread very well on the 3D structure. Further, the cells showed significantly higher production of osteopontin and bone sialoprotein after 21 days in culture.

Others have electrospun 3D nanofibrous scaffolds, using a "wet-spinning" technique. This is most often done by collecting the nanofibers in a metal collecting bath that allows for a 3D "sponge-like" structure. For instance, Ki et al. [37] and Shin et al. [147] have used this method and collected 3D nanofibrous scaffolds in a metal collecting bath containing methanol. The first group, Ki et al. [37], also created 2D electrospun scaffolds in order to compare the two types. Physically, the 3D scaffold was 1.5 mm thick whereas the 2D scaffold was 0.15 mm thick; however, the pore size and porosity were also higher in the 3D scaffolds. This group performed cell studies that showed significantly higher proliferation of cells on the 3D scaffolds than on both 2D scaffolds and TCP after 5 and 7 days of culture (Fig. 16). The authors suggest that this is most likely due to the ability of cells to attach and migrate better on these scaffolds due to their structure and high porosity. Later, Shin et al. [147] used the same method to create 3D scaffolds (Fig. 17a) but used a different material and also measured proliferation and ALP activity. When compared to TCP, these 3D scaffolds showed significantly higher proliferation after 4 and 7 days of culture (Fig. 17b) as well as significantly higher ALP activity after 28 days (Fig. 17c).

Others have combined electrospun scaffolds with scaffolds created by other techniques to create a 3D bone-like scaffold for bone regeneration. For instance, Martins et al. [62] combined both electrospinning and rapid prototyping in order to create a 3D bone-like structure. This method is very similar to the layer-by-layer

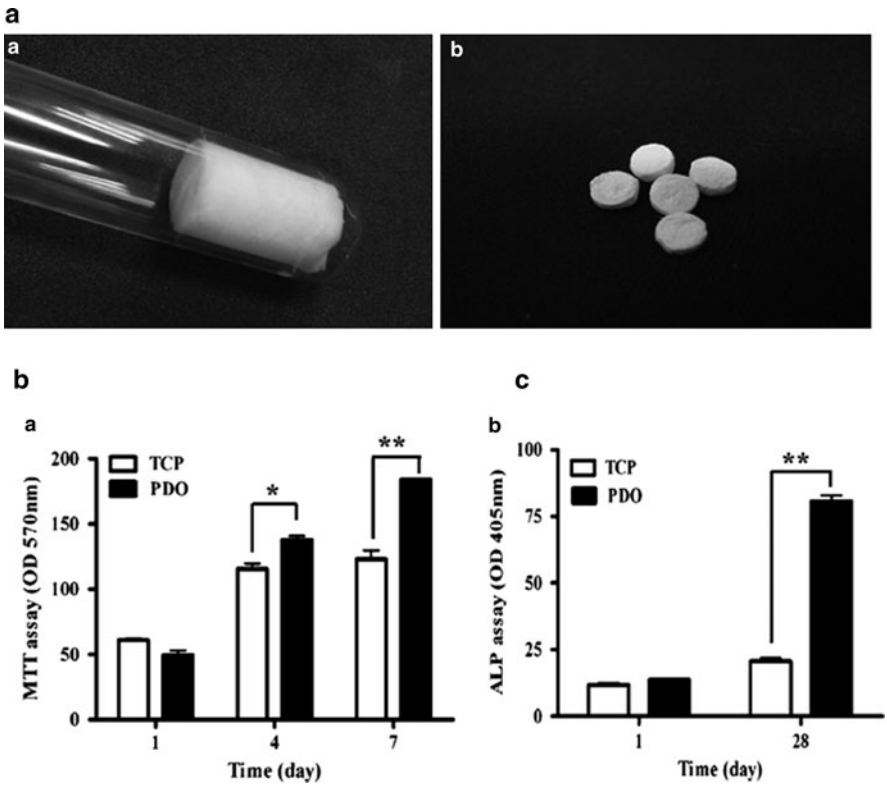

Fig. 17 Images of 3D nanofibrous structure produced by wet-spinning method (**a**). Preosteoblast proliferation on TCP and 3D scaffold (**b**). ALP activity of preosteoblasts on TCP and 3D scaffolds [147]

approach discussed above, but incorporates the layers of electrospun nanofiber scaffolds within the microfiber meshes created by rapid prototyping. The scaffolds created by rapid prototyping alone were then compared to the scaffolds with incorporated electrospun nanofibers and it was found that after 7 days in culture, the scaffolds that incorporated electrospun nanofibers showed significantly higher proliferation and ALP activity.

3D bone-like structures are the ultimate biomimetic technique that can eventually lead to bone regeneration. The techniques listed above have been proven to form new bone tissue in vivo. However, current strategies are not utilizing all of these biomimetic techniques to create the ultimate 3D bone-like structure. The lack of certain qualities that enhance bone cell response and mechanical properties, such as nanofiber alignment and a composite structure, does not allow for a 3D bone-like structure. By combining *all* of the biomimetic techniques discussed in this review, the resulting 3D scaffold would more closely mimic the structure and composition of bone, and regeneration of bone tissue would be more feasible.

2.6 Comparison of Nanofiber-Based Biomimetic Scaffolds with Other Types of Biomaterial Scaffolds for Bone Regeneration

Though emphasis has been placed on creating 3D biomimetic nanofibrous scaffolds for bone tissue regeneration, it is necessary to mention other tissue engineering methods that have shown great promise in this field. Modern methods are slowly gaining on tissue engineering methods investigated in the past, such as use of bioglass scaffolds [34, 49, 50, 148] and calcium-phosphate-based ceramic scaffolds [77, 149–151]. Although these conventional scaffolds have shown great promise due to their inherent osteoconductivity and osteoinductivity, disadvantages such as limited porosity and unsuitable biodegradation have forced the synthesis of a new generation of biomaterials for bone regeneration applications [33]. Although biomimetic electrospun scaffolds, as discussed above, are included in this new generation of biomaterials, other include, but are not limited to, hydrogels [41, 45–48, 51, 53], 3D foams [152–156], and microsphere-based scaffolds [157–161]. These biomaterials, as compared to conventional scaffolds, have attracted increasing interest due to their unique ability to be able to be injected into the defect site non-invasively, as we as possessing many other excellent properties.

Of these materials, hydrogels are of great interest, due to their many excellent qualities for this application, including the ease of loading growth factors and drugs, as well as possessing tunable degradation rates. Patterson et al. [41] created a hyaluronic acid (HA) hydrogel containing either BMP-2 and/or vascular endothelial growth factor (VEGF) with differing degradation rates in order to determine how this affected the collagen orientation of new bone formed under these conditions. The authors determined that the co-delivery of both of these growth factors from the HA hydrogels stimulated new bone formation and mineralization, but also showed that the orientation of the collagen fibers could be guided by the degradation rate. Others have combined the excellent properties of a hydrogel with ceramic beads in order to created an injectable composite structure [162, 163]. Zhao et al. [164] expanded on this approach and created an injectable calcium phosphate/alginate hydrogel paste seeded with umbilical cord MSCs. This paste had all the attractive properties of a hydrogel, such as injectability and the ability to load growth factors and seed cells, but also had greatly improved mechanical properties. Results have indicated mechanical properties similar to those reported for cancellous bone.

Use of 3D foams is also a popular method for bone regeneration applications, although they are most often employed for trabecular bone regeneration [152, 154]. There are a few methods utilized to create foams for this application, one of the most popular being a polymer foam replication technique, in which a polymer foam is either electrosprayed or immersed into a HAp/bioactive glass particle slurry in order to fully coat the foam and create a trabecular bone-like architecture. However, other methods are also utilized, including creating composite foam solutions that are injectable and form once inside the body [153]. Results of Fu et al. [152] have indicated mechanical properties similar to those of natural trabecular bone,

and Montufar et al. [153] demonstrated excellent cell viability, proliferation, and differentiation on these foams.

One last method that needs to be discussed and that has shown much promise is the use of microsphere-based scaffolds for bone regeneration [157–160]. These microspheres can be used in conjunction with many other materials, such as injectable hydrogels, pastes, or solutions and are a great way to incorporate growth factors and control their release. They are also often employed in order to take advantage of the properties of two different materials, such as polymers and ceramics, in order to enhance bone formation. Very promising in vitro results, such as enhanced proliferation, ALP activity, and calcium secretion, as well as in vivo results, such as new bone tissue formation, have been obtained using microspheres for bone regeneration [157–160].

Though not entirely similar, it is important to note that many of these methods also attempt to emulate the natural structure of bone by creating 3D biomimetic structures, including polymer/ceramic composites and growth factor inclusion. While these methods have shown promise for bone regeneration applications, nanofiber-based methods seem to be the most promising for regeneration of cortical bone. These other methods have shown great potential in forming trabecular bone in vivo, yet more structured and mechanically stable bone is required for cortical bone regeneration. The highly aligned structure of electrospun nanofibers direct cell alignment and can guide new tissue growth to form a structure more similar to that of natural cortical bone.

3 Conclusions, Current Challenges, and Future Directions

Biomimetic scaffolds with structural, compositional, and mechanical properties similar to those of natural bone hold great promise for bone tissue engineering. Mineralized electrospun nanofiber array-based biomimetic scaffolds are ideal substrates to support osteoblast or osteogenic stem/progenitor cell attachment, alignment, proliferation, and differentiation, and can offer osteoinductivity and osteoconductivity to promote bone tissue formation. Further incorporation of schemes for controlled delivery of biomolecules and growth factors would fine-tune cell response for bone tissue regeneration.

Current challenges facing bone tissue regeneration lie in the fact that there is an additional requirement for these scaffolds as opposed to other tissue engineering scaffolds, and that is sufficient mechanical properties. To date, there is little evidence of a material for bone tissue engineering scaffolds that can promote osteoconductivity and osteoinductivity and also support the necessary in vivo loads that are characteristic of this tissue. Further, although scaffolds have been able to promote new tissue formation they have not been able to successfully create bone that is “functional and mechanically competent” [165]. Often the bone tissue created is highly disorganized and the acquired tissue architecture is not like that of natural bone [166]. Another great challenge facing this field, as well as all tissue

engineering fields, is the ability to vascularize the new tissue. For tissues greater than 100–200 μm in thickness, there must be a blood vessel supply to deliver oxygen and nutrients to the tissue and to remove waste in order for the tissue to survive. Current strategies in this field have not been able to create functional blood vessels for this purpose. Other challenges relating to all tissue engineering fields, such as achieving proper degradation rates, are also evident in the field of bone tissue engineering.

References

1. Rho JY, Kuhn-Spearing L, Zioupos P (1998) Med Eng Phys 20:92
2. Fratzl P, Gupta HS, Paschalis EP, Roschger P (2004) J Mater Chem 14:2115
3. Rubin MA, Jasiuk I, Taylor J, Rubin J, Ganey T, Apkarian RP (2003) Bone 33:270
4. Barrere F, van Blitterswijk CA, de Groot K (2006) Int J Nanomedicine 1:317
5. Hayes WC (1991) Basic orthopedic biomechanics. Lippincott-Raven, New York, p 93
6. Cowin SC (1989) Bone biomechanics. CRC, Boca Raton, p 97
7. Porter JR, Ruckh TT, Popat KC (2009) Biotechnol Prog 25:1539
8. Martin RB (1991) J Biomech 24(Suppl 1):79
9. Currey JD (1984) Philos Trans R Soc Lond B Biol Sci 304:509
10. Horner EA, Kirkham J, Wood D, Curran S, Smith M, Thomson B, Yang XB (2010) Tissue Eng B Rev 16:263
11. Covey DC, Aaron RK, Born CT, Calhoun JH, Einhorn TA, Hayda RA, Levin LS, Mazurek MT, Murray CK, Powell ET, Schwarz EM, Wenke JC (2008) Instr Course Lect 57:65
12. Lew TA, Walker JA, Wenke JC, Blackbourne LH, Hale RG (2010) J Oral Maxillofac Surg 68:3
13. Pape HC, Pufe T (2010) Injury 41:553–554
14. Williamson DM, Lowdon MR (1988) Injury 19:9
15. Praemer A, Furner S, Rice DP (1992) Musculoskeletal conditions in the United States. American Academy of Orthopaedic Surgeons, Park Ridge
16. Ciminello FS, Morin RJ, Nguyen TJ, Wolfe SA (2009) Compr Ther 35:37
17. Gritli-Linde A (2007) Dev Biol 301:309
18. Meng L, Bian Z, Torensma R, Von den Hoff JW (2009) J Dent Res 88:22
19. Heare T, Hensley MA, Dell'Orfano S (2009) Curr Opin Pediatr 21:365
20. Silber JS, Anderson DG, Daffner SD, Brislin BT, Leland JM, Hilibrand AS, Vaccaro AR, Albert TJ (2003) Spine (Phila Pa 1976) 28:134
21. Banwart JC, Asher MA, Hassanein RS (1995) Spine 20:1055
22. Graham SM, Leonidou A, Aslam-Pervez N, Hamza A, Panteliadis P, Heliotis M, Mantalaris A, Tsiridis E (2010) Expert Opin Biol Ther 10(6):885
23. Mankin HJ, Hornicek FJ, Raskin KA (2005) Clin Orthop Relat Res 432:210
24. Langer R, Vacanti JP (1993) Science 260:920
25. Skalak R, Fox CF (eds) (1988) Tissue engineering. Liss, New York
26. Becker C, Jakse G (2007) Eur Urol 51:1217
27. Yang S, Leong K, Du Z, Chua C (2001) Tissue Eng 7:679
28. Cohen S, Bano MC, Cima LG, Allcock HR, Vacanti JP, Vacanti CA, Langer R (1993) Clin Mater 13:3
29. Heath CA (2000) Trends Biotechnol 18:17
30. Gimble JM, Katz AJ, Bunnell BA (2007) Circ Res 100:1249
31. Graziano A, d'Aquino R, Laino G, Papaccio G (2008) Stem Cell Rev 4:21
32. Tuan RS, Boland G, Tuli R (2003) Arthritis Res Ther 5:32

33. El-Ghannam A (2005) Expert Rev Med Devices 2:87
34. Chen QZ, Thompson ID, Boccaccini AR (2006) Biomaterials 27:2414
35. McCullen SD, Miller PR, Gittard SD, Gorga RE, Pourdeyhimi B, Narayan RJ, Loboa EG (2010) Tissue Eng Part C Methods 16(5):1095
36. Inanç B, Arslan YE, Seker S, Elçin AE, Elçin YM (2009) J Biomed Mater Res A 90:186
37. Ki CS, Park SY, Kim HJ, Jung HM, Woo KM, Lee JW, Park YH (2008) Biotechnol Lett 30:405
38. Ren J, Zhao P, Ren T, Gu S, Pan K (2008) J Mater Sci Mater Med 19:1075
39. Wutticharoenmongkol P, Sanchavanakit N, Pavasant P, Supaphol P (2006) Macromol Biosci 6:70
40. Nie H, Wang CH (2007) J Control Release 120:111
41. Patterson J, Siew R, Herring SW, Lin AS, Guldberg R, Stayton PS (2010) Biomaterials 31:6772
42. Mullen LM, Best SM, Brooks RA, Ghose S, Gwynne JH, Wardale J, Rushton N, Cameron R (2010) Tissue Eng Part C Methods 16:1439
43. Kanczler JM, Ginty PJ, White L, Clarke NM, Howdle SM, Shakesheff KM, Oreffo RO (2010) Biomaterials 31:1242
44. Cao H, Kuboyama N (2010) Bone 46:386
45. Takaoka R, Hikasa Y, Hayashi K, Tabata Y (2012) J Biomater Sci Polym Ed 22:1581–1589. doi: 10.1163/092050610X517095
46. Ishida K, Matsumoto T, Sasaki K, Mifune Y, Tei K, Kubo S, Matsushita T, Takayama K, Akisue T, Tabata Y, Kurosaka M, Kuroda R (2010) Tissue Eng A 16(10):3271
47. Asamura S, Mochizuki Y, Yamamoto M, Tabata Y, Isogai N (2010) Ann Plast Surg 64:496
48. Humber CC, Sandor GK, Davis JM, Peel SA, Brkovic BM, Kim YD, Holmes HI, Clokie CM (2010) Oral Surg Oral Med Oral Pathol Oral Radiol Endod 109:372
49. Chen QZ, Rezwan K, Francon V, Armitage D, Nazhat SN, Jones FH, Boccaccini AR (2007) Acta Biomater 3:551
50. Bretcanu O, Misra S, Roy I, Renghini C, Fiori F, Boccaccini AR, Salih V (2009) J Tissue Eng Regen Med 3:139
51. Reichert JC, Heymer A, Berner A, Eulert J, Noth U (2009) Biomed Mater 4:065001
52. Xynos ID, Edgar AJ, Buttery LD, Hench LL, Polak JM (2000) Biochem Biophys Res Commun 276:461
53. Guo X, Park H, Young S, Kretlow JD, van den Beucken JJ, Baggett LS, Tabata Y, Kasper FK, Mikos AG, Jansen JA (2010) Acta Biomater 6:39
54. Cushnie EK, Khan YM, Laurencin CT (2010) J Biomed Mater Res A 94A:568
55. Bueno EM, Glowacki J (2009) Nat Rev Rheumatol 5:685
56. Burg KJ, Porter S, Kellam JF (2000) Biomaterials 21:2347
57. Kaufman JD, Song J, Klapperich CM (2007) J Biomed Mater Res A 81:611
58. Yu H, Matthew HW, Wooley PH, Yang SY (2008) J Biomed Mater Res B Appl Biomater 86B:541
59. Wang J, Qu L, Meng X, Gao J, Li H, Wen G (2008) Biomed Mater 3:025004
60. Porter BD, Oldham JB, He SL, Zobitz ME, Payne RG, An KN, Currier BL, Mikos AG, Yaszemski MJ (2000) J Biomech Eng 122:286
61. Rezwan K, Chen QZ, Blaker JJ, Boccaccini AR (2006) Biomaterials 27:3413
62. Martins A, Chung S, Pedro AJ, Sousa RA, Marques AP, Reis RL, Neves NM (2009) J Tissue Eng Regen Med 3:37
63. Zhang P, Hong Z, Yu T, Chen X, Jing X (2009) Biomaterials 30:58
64. Pamula E, Filova E, Bacakova L, Lisa V, Adamczyk D (2009) J Biomed Mater Res A 89:432
65. Kim SS, Sun Park M, Jeon O, Yong Choi C, Kim BS (2006) Biomaterials 27:1399
66. Lin HR, Kuo CJ, Yang CY, Shaw SY, Wu YJ (2002) J Biomed Mater Res 63:271
67. Lo H, Ponticiello MS, Leong KW (1995) Tissue Eng 1:15
68. Jack KS, Velayudhan S, Luckman P, Trau M, Grondahl L, Cooper-White J (2009) Acta Biomater 5:2657

69. Liu X, Smith LA, Hu J, Ma PX (2009) Biomaterials 30:2252
70. Tuzlakoglu K, Bolgen N, Salgado AJ, Gomes ME, Piskin E, Reis RL (2005) J Mater Sci Mater Med 16:1099
71. Seol YJ, Lee JY, Park YJ, Lee YM, Young K, Rhyu IC, Lee SJ, Han SB, Chung CP (2004) Biotechnol Lett 26:1037
72. Cunniffe GM, Dickson GR, Partap S, Stanton KT, O'Brien FJ (2010) J Mater Sci Mater Med 21:2293–2298
73. Aboudzadeh N, Imani M, Shokrgozar MA, Khavandi A, Javadpour J, Shafieyan Y, Farokhi M (2010) J Biomed Mater Res A 94A:137
74. Wang L, Li Y, Zuo Y, Zhang L, Zou Q, Cheng L, Jiang H (2009) Biomed Mater 4:025003
75. Kim IY, Seo SJ, Moon HS, Yoo MK, Park IY, Kim BC, Cho CS (2008) Biotechnol Adv 26:1
76. Wettergreen MA, Bucklen BS, Sun W, Liebschner MA (2005) Ann Biomed Eng 33:1333
77. Warnke PH, Seitz H, Warnke F, Becker ST, Sivananthan S, Sherry E, Liu Q, Wiltfang J, Douglas T (2010) J Biomed Mater Res B Appl Biomater 93:212
78. Warnke PH, Douglas T, Wollny P, Sherry E, Steiner M, Galonska S, Becker ST, Springer IN, Wiltfang J, Sivananthan S (2009) Tissue Eng Part C Methods 15:115
79. Heo SJ, Kim SE, Wei J, Hyun YT, Yun HS, Kim DH, Shin JW, Shin JW (2009) J Biomed Mater Res A 89:108
80. Jang JH, Castano O, Kim HW (2009) Adv Drug Deliv Rev 61:1065
81. Stevens R (2009) Med Device Technol 20:32
82. Ashammakhi N, Wimpenny I, Nikkola L, Yang Y (2009) J Biomed Nanotechnol 5:1
83. Prabhakaran MP, Venugopal J, Ramakrishna S (2009) Acta Biomater 5:2884
84. Ramachandran K, Gouma PI (2008) Recent Pat Nanotechnol 2:1
85. Yoshimoto H, Shin YM, Terai H, Vacanti JP (2003) Biomaterials 24:2077
86. Gupta D, Venugopal J, Mitra S, Giri Dev VR, Ramakrishna S (2009) Biomaterials 30:2085
87. Song JH, Kim HE, Kim HW (2007) J Biomed Mater Res B Appl Biomater 83:248
88. Song JH, Kim HE, Kim HW (2008) J Mater Sci Mater Med 19:2925
89. Jose MV, Thomas V, Xu Y, Bellis S, Nyairo E, Dean D (2010) Macromol Biosci 10:433
90. Jose MV, Thomas V, Johnson KT, Dean DR, Nyairo E (2009) Acta Biomater 5:305
91. Yang F, Both SK, Yang X, Walboomers XF, Jansen JA (2009) Acta Biomater 5:3295
92. Sui G, Yang X, Mei F, Hu X, Chen G, Deng X, Ryu S (2007) J Biomed Mater Res A 82:445
93. Nie H, Soh BW, Fu YC, Wang CH (2008) Biotechnol Bioeng 99:223
94. Kim HW, Lee HH, Knowles JC (2006) J Biomed Mater Res A 79:643
95. Lee JH, Rim NG, Jung HS, Shin H (2010) Macromol Biosci 10:173
96. Li C, Vepari C, Jin HJ, Kim HJ, Kaplan DL (2006) Biomaterials 27:3115
97. Fu YC, Nie H, Ho ML, Wang CK, Wang CH (2008) Biotechnol Bioeng 99:996
98. Yang F, Wolke JG, Jansen JA (2008) Chem Eng J 137:154
99. Li X, Xie J, Yuan X, Xia Y (2008) Langmuir 24:14145
100. Ito Y, Hasuda H, Kamitakahara M, Ohtsuki C, Tanihara M, Kang IK, Kwon OH (2005) J Biosci Bioeng 100:43
101. Chen J, Chu B, Hsiao BS (2006) J Biomed Mater Res A 79:307
102. Ngiam M, Liao S, Patil AJ, Cheng Z, Chan CK, Ramakrishna S (2009) Bone 45:4
103. Yin YJ, Luo XY, Cui JF, Wang CY, Guo XM, Yao KD (2004) Macromol Biosci 4:971
104. Yang D, Jin Y, Zhou Y, Ma G, Chen X, Lu F, Nie J (2008) Macromol Biosci 8:239
105. Ngiam M, Liao S, Patil AJ, Cheng Z, Yang F, Gubler MJ, Ramakrishna S, Chan CK (2009) Tissue Eng A 15:535
106. Taguchi T, Kishida A, Akashi M (1998) Chem Lett 27:711
107. Zeng J, Xu X, Chen X, Liang Q, Bian X, Yang L, Jing X (2003) J Control Release 92:227
108. Ashammakhi N, Ndreu A, Yang Y, Ylikauppila H, Nikkola L, Hasirci V (2007) Eur J Plast Surg DOI 10.1007/500238-008-0217-3. pages 2265-2286
109. Doshi J, Reneker D (1995) J Electrostat 35:151
110. Badami AS, Kreke MR, Thompson MS, Riffle JS, Goldstein AS (2006) Biomaterials 27:596
111. Kang YM, Kim KH, Seol YJ, Rhee SH (2009) Acta Biomater 5:462

112. Ma K, Chan CK, Liao S, Hwang WY, Feng Q, Ramakrishna S (2008) Biomaterials 29:2096
113. Bashur CA, Shaffer RD, Dahlgren LA, Guelcher SA, Goldstein AS (2009) Tissue Eng A 15:2435
114. Chan CK, Liao S, Li B, Lareu RR, Larrick JW, Ramakrishna S, Raghunath M (2009) Biomed Mater 4:035006
115. Lee CH, Shin HJ, Cho IH, Kang YM, Kim IA, Park KD, Shin JW (2005) Biomaterials 26:1261
116. Zhong S, Teo WE, Zhu X, Beuerman RW, Ramakrishna S, Yung LY (2006) J Biomed Mater Res A 79:456
117. Katta P, Alessandro M, Ramsier RD, Chase GG (2004) Nano Lett 4:2215
118. Nerurkar NL, Elliott DM, Mauck RL (2007) J Orthop Res 25:1018
119. Pan H, Li L, Hu L, Cui X (2006) Polymer 47:4901
120. Beachley V, Wen X (2009) Mater Sci Eng C 29:663
121. Li D, Wang Y, Xia Y (2003) Nano Lett 3:1167
122. Li D, Wang Y, Xia Y (2004) Adv Mater 16:361
123. Jager I, Fratzl P (2000) Biophys J 79:1737
124. Gao H, Ji B, Jager IL, Arzt E, Fratzl P (2003) Proc Natl Acad Sci USA 100:5597
125. Hutmacher DW (2000) Biomaterials 21:2529
126. Hench LL (1998) Biomaterials 19:1419
127. Xynos ID, Edgar AJ, Buttery LD, Hench LL, Polak JM (2001) J Biomed Mater Res 55:151
128. Yang GL, He FM, Hu JA, Wang XX, Zhao SF (2009) Oral Surg Oral Med Oral Pathol Oral Radiol Endod 107:782
129. Zuo Y, Yang F, Wolke JG, Li Y, Jansen JA (2010) Acta Biomater 6:1238
130. Zhang Y, Venugopal JR, El-Turki A, Ramakrishna S, Su B, Lim CT (2008) Biomaterials 29:4314
131. Katsanevakis E, Wen X, Shi D, Zhang N (2010) Key Eng Mater 441:269
132. Iwatsubo T, Sumaru K, Kanamori T, Shinbo T, Yamaguchi T (2006) Biomacromolecules 7:95
133. Yamaguchi I, Itoh S, Suzuki M, Osaka A, Tanaka J (2003) Biomaterials 24:3285
134. Shalumon KT, Binulal NS, Selvamurugan N, Nair SV, Menon D, Furuike T, Tamura H, Jayakumar R (2009) Carbohydr Polym 77:863
135. Madhumathi K, Binulal NS, Nagahama H, Tamura H, Shalumon KT, Selvamurugan N, Nair SV, Jayakumar R (2009) Int J Biol Macromol 44:1
136. Madhumathi K, Shalumon KT, Rani VV, Tamura H, Furuike T, Selvamurugan N, Nair SV, Jayakumar R (2009) Int J Biol Macromol 45:12
137. Raynaud S, Champion E, Bernache-Assollant D, Thomas P (2002) Biomaterials 23:1065
138. Anselme K, Bigerelle M, Noel B, Dufresne E, Judas D, Iost A, Hardouin P (2000) J Biomed Mater Res 49:155
139. Martin JY, Schwartz Z, Hummert TW, Schraub DM, Simpson J, Lankford J Jr, Dean DD, Cochran DL, Boyan BD (1995) J Biomed Mater Res 29:389
140. Bacakova L, Stary V, Kofronova O, Lisa V (2001) J Biomed Mater Res 54:567
141. Barnes GL, Kostenuik PJ, Gerstenfeld LC, Einhorn TA (1999) J Bone Miner Res 14:1805
142. Schofer MD, Fuchs-Winkelmann S, Grabedunkel C, Wack C, Dersch R, Rudisile M, Wendorff JH, Greiner A, Paletta JR, Boudriot U (2008) ScientificWorldJournal 8:1269
143. Pişkin E, Isoglu IA, Bolgen N, Vargel I, Griffiths S, Cavusoglu T, Korkusuz P, Guzel E, Cartmell S (2009) J Biomed Mater Res A 90:1137
144. Ekaputra AK, Zhou Y, Cool SM, Hutmacher DW (2009) Tissue Eng A 15:3779
145. Srouji S, Kizhner T, Suss-Tobi E, Livne E, Zussman E (2008) J Mater Sci Mater Med 19:1249
146. Afifi AM, Nakajima H, Yamane H, Kimura Y, Nakano S (2009) Macromol Mater Eng 294:658
147. Shin TJ, Park SY, Kim HJ, Lee HJ, Youk JH (2010) Biotechnol Lett 32:877
148. Chen QZ, Efthymiou A, Salih V, Boccaccini AR (2008) J Biomed Mater Res A 84:1049

149. Detsch R, Schaefer S, Deisinger U, Ziegler G, Seitz H, Leukers B (2010). J Biomater Appl (in press) doi: 10.1177/0885328210373285
150. Verron E, Khairoun I, Guicheux J, Bouler JM (2010) Drug Discov Today 15:547
151. Komlev VS, Mastrogiacomo M, Pereira RC, Peyrin F, Rustichelli F, Cancedda R (2010) Eur Cell Mater 19:136
152. Fu Q, Rahaman MN, Fu H, Liu X (2010) J Biomed Mater Res A 95A:164
153. Montufar EB, Traykova T, Gil C, Harr I, Almirall A, Aguirre A, Engel E, Planell JA, Ginebra MP (2010) Acta Biomater 6:876
154. Muthutantri A, Huang J, Edirisinghe M (2008) J Mater Sci Mater Med 19:1485
155. Bertoldi S, Fare S, Denegri M, Rossi D, Haugen HJ, Parolini O, Tanzi MC (2010) J Mater Sci Mater Med 21:1005
156. Gorna K, Gogolewski S (2003) J Biomed Mater Res A 67:813
157. Wang Y, Shi X, Ren L, Yao Y, Zhang F, Wang DA (2010) J Biomed Mater Res B Appl Biomater 93:84
158. Jiang T, Nukavarapu SP, Deng M, Jabbarzadeh E, Kofron MD, Doty SB, Abdel-Fattah WI, Laurencin CT (2010) Acta Biomater 6:3457
159. Lee TJ, Kang SW, Bhang SH, Kang JM, Kim BS (2010) J Biomater Sci Polym Ed 21:635
160. Shi X, Wang Y, Ren L, Gong Y, Wang DA (2009) Pharm Res 26:422
161. Basmanav FB, Kose GT, Hasirci V (2008) Biomaterials 29:4195
162. Matsuno T, Hashimoto Y, Adachi S, Omata K, Yoshitaka Y, Ozeki Y, Umezu Y, Tabata Y, Nakamura M, Satoh T (2008) Dent Mater J 27:827
163. Haberstroh K, Ritter K, Kuschnierz J, Bormann KH, Kaps C, Carvalho C, Mulhaupt R, Sittinger M, Gellrich NC (2010) J Biomed Mater Res B Appl Biomater 93:520
164. Zhao L, Weir MD, Xu HH (2010) Biomaterials 31:6502
165. Rose FR, Oreffo RO (2002) Biochem Biophys Res Commun 292:1
166. Griffith LG, Naughton G (2002) Science 295:1009
166. Oyane A, Kim HM, Furuya T, Kokubo T, Miyazaki T, Nakamura T (2003) J Biomed Mater Res A 65:188

Adv Polym Sci (2012) 246: 101–130
DOI: 10.1007/12_2011_142

Published online: 21 September 2011

Synthetic/Biopolymer Nanofibrous Composites as Dynamic Tissue Engineering Scaffolds

J.A. Kluge and R.L. Mauck

Abstract Synthetic/biopolymer composite scaffolds can provide improved flexibility when designing optimized stem-cell-laden tissue repair devices for fiber-reinforced tissues. Composites enable a range of mechanical properties, rates of degradation, and other functional attributes of a degradable scaffold to be finely tuned by modifying polymer sources and their processing techniques. Furthermore, marrying synthetic fibers spun from harsh solvents with polymers spun from mild organic or aqueous-based solvents can allow for delivery of active molecular species in these composites. In the pre-processing fabrication steps, polymers can be selected and combined from traditional or newer high-throughput approaches into networks with properties that reflect the individual components or their interactions. These properties may also depend on the spinning solvents used. In post-processing steps, factors such as the ambient environmental conditions or crosslinking solvent treatments can differentially affect the constituent polymers chosen. Several case studies will be discussed in order to highlight the potential advantages of these approaches. For example, many studies have shown that the mechanical properties of composite mats can be designed with superior or more tissue-like properties than individual polymer sources alone. Further, it has been shown that the degradation rates of the temporary scaffold can be more finely tuned in composites by combining rapidly and slowly degrading systems. The drug and growth factor delivery capabilities of these systems will similarly be reviewed. We conclude with an overview of several tissue engineering approaches that have exploited composite design features and discuss new promising avenues for study.

Keywords Biopolymers · Composites · Mechanical properties · Synthetic · Tissue engineering

J.A. Kluge and R.L. Mauck (✉)
McKay Orthopaedic Research Laboratory, University of Pennsylvania, Philadelphia, PA 19104, USA
e-mail: lemauck@mail.med.upenn.edu

Contents

1 Overview and Principles of Nanofibrous Construct Fabrication

The field of tissue engineering has rapidly expanded due to the increasing need for implant therapies that can improve the quality of life for an aging population. Patients suffering from breakdown of soft tissues such as those from musculoskeletal or cardiovascular systems represent a large subset of this population, driving an equally large market for tissue replacements that can address significant clinical needs, both biologic and mechanical in nature. Therefore, for the past few decades, researchers have focused on designing tissue analogs with these (often conflicting) needs in mind, and many have turned to emerging biomaterial-based technologies for potential solutions. Researchers are meanwhile forced to consider that design targets set by native tissue benchmarks must comply with the demands of the surgical intervention and offer solutions that can meet the timeline for implant integration and longevity. To address these significant demands while still providing options for an iterative biomaterial-based design scheme, whereby constructs are evaluated first in vitro and then in a series of animal model experiments, it is therefore crucial that the overall design scheme entails sufficient versatility.

Electrospun nanofibers have been identified as an adaptable biomaterial that, as a tissue engineering scaffold or substrate, can direct cellular activity either through structural cues, release of signaling factors, or through innate surface chemistries based on the polymers selected [1]. Moreover, electrospinning is a technique that is well suited to handle most biocompatible polymers, and the resultant fibers are amenable to a wide diversity of post-processing techniques (See Fig. 1). With its increasing popularity, the library of available polymers to be utilized in this manner is extremely large and ever expanding. Blending of multiple polymers into the same spinning mixture (dope) enables an even greater variety of spinning options by overcoming limitations imparted by the electrospinning process. More recently, electrospun scaffolds have been designed with either the ability to incorporate a variety of polymer sources simultaneously (i.e., through multijet spinning) or

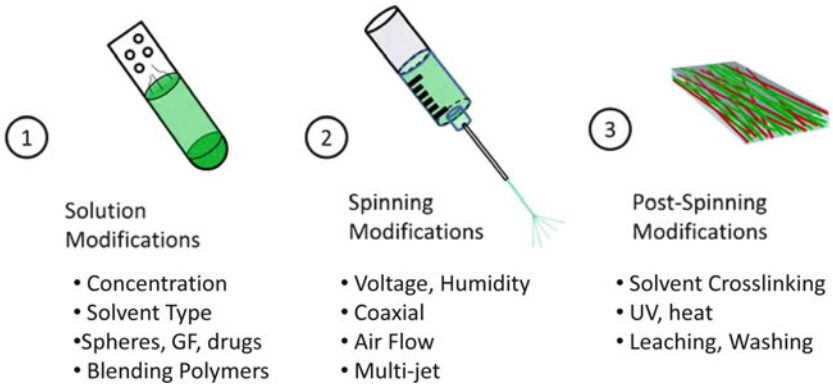

Fig. 1 Nanofiber modification strategies. In step *1*, many polymer and solution properties will affect the size, stability, and reactivity of nanofibers in the final mat, including multipolymer blending strategies, incorporation of soluble factors/drugs/spheres, and/or loading concentrations. In step *2*, during spinning, the ambient conditions and voltage applied must be tailored for each polymer source and can be dictated by the nature of the collector or the number of jets employed simultaneously. In step *3*, the as-spun mat can be modified by various crosslinking techniques to stabilize the polymers or, in the case of soluble or carrier polymers, these can be leached out by subsequent liquid washes

with the ability to be modified after polymer formation (i.e., through crosslinking and surface modification) in a manner that further diversifies the qualities of the scaffolds produced. In this work, the approaches taken to date to develop composite nanofibrous polymer materials for applications in tissue repair are summarized. Specifically, this review highlights electrospinning techniques that employ in some form or fashion both synthetic polymers and polymers derived from living organisms, the so-called biopolymers. A particular focus will be nanofibrous composite designs that have allowed advances in the field of tissue engineering by enabling unique and versatile options for property control. The challenges and opportunities specific to these composites will be overviewed so that new directions can be identified to stimulate future research endeavors.

2 Electrospinning Polymer Choices

2.1 Synthetic Polymers

Synthetic acrylic nanofibers were the first polymers to be electrospun by a process in which a grounded surface was used as a target to collect fibers emanating from a charged source [2]. Those conditions used some 40 years ago are still being employed today to enable the fabrication of almost all other polymer materials. There are a vast number of degradable synthetic polymer materials from which

to choose [3] and most can be dissolved in and spun directly from common solvents, making synthetic polymer electrospinning a highly powerful and versatile approach for tissue engineering [4, 5]. Among these synthetics, available materials can be further divided into several classes based on their derivation and resultant structure.

The most heavily explored degradable synthetic materials to date pertain to the following classes: poly(α-hydroxy esters) including poly(ε-caprolactone) (PCL), poly(glycolic acid) (PGA), poly(lactic acid) (PLA), and their copolymer poly (lactic-*co*-glycolic acid) (PLGA) [6]; poly(ethers) including poly(ethylene oxide) (PEO) and poly(ethylene glycol) (PEG) [7]; poly(vinyl alcohol) (PVA) [8]; polyurethane (PU) [9]; and poly(anhydrides) [10]. These are perhaps the most prominent examples, although many other synthetic materials are currently being pursued. Additionally, emerging synthetic polymers taken from combinatorial libraries, including poly(arylates) and poly(β-amino esters) (PBAEs) [11–13], indicate that the list of degradable synthetic polymers is rapidly expanding, many of which will be translated to the electrospun format [12]. The key processing features of and advantages/drawbacks of several of these polymer systems will be discussed in the following subsections.

2.1.1 Poly(α-hydroxy esters)

When electrospun scaffolds were first considered for tissue engineering applications, several poly(α-hydroxy esters) candidates were explored because of their degradability and their history of usage as sutures [14] and tissue engineering scaffolds [15, 16]. The most widely investigated of this group are PGA and PLA, the former being a more crystalline polyester with high (i.e., stiff) mechanical properties, and the latter a more hydrophobic and chiral polyester (whose stereoisomer content confers the degree of crystallinity) with lower (less stiff) properties than PGA [14]. PGA can be dissolved in highly fluorinated solvents such as hexafluoroisopropanol (HFIP) for electrospinning, whereas PLA (and its stereoisomer variants) can be spun from more common organic solvents such as tetrahydrofuran (THF) and *N*,*N*-dimethylformamide (DMF) [6]. The Bowlin group was the first to electrospin nanofibers of PGA, among many other degradable polymers, and they assessed the ability to control features of the mat such as fiber diameter and cell interactions [17]. They later showed that PGA can be "softened" by pretreatment with hydrochloric acid (HCl^-), resulting in a scaffold with higher cellularity in vitro and lower inflammatory response in vivo [18]. PLA was likewise one of the first degradable polymers to be electrospun. Early efforts focused on tailoring its degree of crystallinity by adjusting the ratio between D- and L- isomers, forming either amorphous poly(D,L-lactide) (PDLA) or semi-crystalline poly(L-lactide) (PLLA) [19]. PLA been spun by many groups, some using the fibers as drug delivery vehicles [20, 21].

PCL was also identified as a useful polymer for tissue engineering due to its very simple processing and impressive hydrolytic stability from intrinsic hydrophobic polymer properties [22–24]. When compared directly to the mechanical properties

of relatively stiff polymers such as PGA and PLA, PCL nanofibrous scaffolds are much softer but have a much greater range of elasticity [6]. PCL can be spun from DMF or THF and, while the resultant polymer remains highly hydrophobic, a hydrophilic surface more conducive for efficient cell attachment can be created via hydration in gradient ethanol [6]. This treatment can be used for all the polyester materials described herein, not only to alter surface features but also for sterilization; furthermore, this treatment does not alter the material's hydrolytic stability of up to several months in vitro [6, 25]. Due to the ease of use and impressive mechanical properties (including long-term hydrolytic stability), PCL has been highly pursued as a nanofibrous scaffold [26–28] and will be discussed further in Sect. 3.3.

Similar to other geometric forms of these polyester-based polymers investigated to date (i.e., foams and fibers), the choice of poly(α-hydroxy ester) subtype will determine hydrolytic stability and initial mechanical properties [6]. In general, fibers formed from hydrophobic polyesters such as PLLA and PCL are softer and will degrade more slowly than fibers from the more crystalline PGA polymers. However, with increased D-stereoisomers of lactic acid in PDLLA or by copolymerizing greater amounts of PGA into PLGA polymers, these mechanical properties can be tuned and hydrolytic susceptibility reduced [6, 29]. Along these lines, Zong et al. showed that PLGA 75:25 (ratio of polylactic to polyglycolic acid in the copolymer) and PDLLA degraded much faster than PLGA 10:90 and PLLA [30]. Furthermore, it was observed early on that PCL was an excellent "carrier" polymer to be blended with other synthetics, because greater solubility and thus mass loading of this polyester promote greater control of solution properties for spinning while resulting in a stiff and stable polymer mat [31].

2.1.2 Polyurethanes

PU materials have been used historically to form nondegradable biomaterials for applications requiring long-term stability, such as catheters and other prosthetic cardiovascular devices [14]. Segmented PU materials are composed of three basic components: (1) a polyol (a hydroxyl-terminated macromer, or so-called "soft segment"), (2) a diisocyanate (a reactive low M_W compound), and (3) a chain extender (usually a small molecule with hydroxyl or amine end groups) [14, 32]. Together, the diisocyanate and chain extender comprise the so-called "hard segment" of the polymer. Like PCL, pure PU can be purchased commercially and electrospun from DMF and THF. In this way, nanofibrous PU membranes were first introduced as a facile [33] but practically nondegradable scaffold for study of wound healing potential [9] or as a substrate to study the effects of fiber alignment and mechanical strain on gross changes in cell behavior (i.e., alignment and matrix production) [34].

Despite their apparent nondegradability, PU materials investigated in vivo show long-term wear patterns that result from unavoidable hydration imposed during upstream processing. Although the reaction is very slow, aliphatic ester linkages in poly(ester urethane) (PEU) materials are known to be susceptible to hydrolytic

degradation [32]. Biodegradable and biocompatible classes of PU biomaterials can be formed by removing aromatic diisocyanates (a toxic precursor) [35], thus eliminating their potential carcinogenicity [36, 37]. For example, these diisocyanates are often replaced by lysine-diisocyanates (LDI) so as to result in nontoxic lysine byproducts [38]. Furthermore, the polyol soft segment can be made from polyesters such as PLA/PGA and PCL [39] as well as PEO [40] to further hydrolytic susceptibility.

Several new types of "degradable urethanes" have thus been designed, formed by altering one of the core components: either the prepolymer formulation (typically the nature of the polyol) or the chain extension. These degradable PU materials were developed for tissue engineering and translated to the electrospun format, with some showing drug delivery capabilities [32, 35, 41–44]. For example, the Wagner group has explored nanofibrous PU materials formed from block copolymers PCL and 1,4-diisocyanatobutane (BDI), resulting in a specific class of PU referred to as poly(ether urethane)urea (PEUU) [39]. This formulation was later modified such that poly(ether ester) triblock copolymers (PCL–PEG–PCL) were synthesized with BDI and putrescine to form poly(ether ester urethane)urea (PEEUU) [44]. Since they are formed from the same precursors, PEUUs and PEEUUs show properties similar to those of pure PCL, such as hydrophobicity, hydrolytic stability, and elasticity comparable with native tissues [44–46]. PEEUU nanofiber scaffolds are differentially degradable by varying the lengths of polyester and triblock soft segment [44]. The Woodhouse group has also formed degradable nanofibrous PU scaffolds using the unique biocompatible LDI features described above as a target for enzymatic cleavage, along with either PEO or PCL polyol and an L-phenylalanine-based chain extender to promote hydrolysis [38, 47]. These variants show similar mechanical properties to the PEEUU systems above when a PCL polyol was utilized [48], but have also demonstrated enzymatic susceptibility to chymotrypsin in vitro [38]. The mechanism behind enzymatic breakdown of PU systems or block copolymers has been described elsewhere in greater detail [32].

2.1.3 Soluble Polymers: PEO, PEG, and PVA

Although several of the above described polymers and nanofibrous scaffolds are enzymatically and/or hydrolytically degradable, several other polymers including PEO, PEG (i.e., the low M_w version of PEO), and PVA have been utilized in order to induce more rapidly degrading or immediately soluble features into scaffold materials. PEO was initially pursued as a model polymer to aid in the study of the physics pertaining to electrospinning [49, 50], and studying PEO spinning helped to explain the bending instabilities encountered by the emergent polymer jet under sufficient applied voltage [51]. As PEO spinning was optimized, modifications of various processing parameters (e.g., solution viscosity, applied charge, collection distance, etc.) were shown to significantly affect the quality of the fiber produced [52]. These control features now provide practical guidelines for most other polymer systems. Due to its ease of use and handling (PEO is water- and ethanol-soluble), the polymer was soon identified as a suitable "carrier" molecule (as little as

2 wt%) to increase polymer viscosity and stabilize the resultant jet when mixed with other desired polymers [53]. As will be discussed in Sect. 3.1, blending of PEO with biopolymers has become a very popular tool for overcoming the processing limitations of less soluble or less available materials.

Rather than identifying their structural properties or fiber-forming abilities, researchers working with PEG and PVA have focused mostly on using the polymers for biomolecular release strategies [8, 54]. PVA is a semicrystalline polyhydroxy polymer and is one of the most widely available synthetics [55]; therefore, electrospinning of PVA is relatively cheap and easy to perform, utilizing water as the spinning solvent [56]. PVA nanofiber solubility is temperature-dependent and will proceed rapidly at 37 °C [8], but the polymer can be crosslinked to improve stability [57]. To study the stability of entrapped biomolecules within PVA nanofibers, fluorescein isothiocyanate-labeled bovine serum albumin (FITC-BSA) and Luciferase were each mixed with the PVA solution prior to spinning. The enzyme Luciferase remained active, and overall release profiles for both molecules were temperature-dependent, with or without a poly(*p*-xylylene) coating to retard the rate of release [8].

Likewise, PEG is a cheap biocompatible polymer typically used to increase the hydrophilicity of degradable biomaterials, with byproducts known to be easily cleared by the body [58]. The usage of PEG is similar to that of PEO because of its identical monomeric units, but the low M_w PEG has been more useful in generating block copolymer strategies [59, 60]. PEG was also used early on in the context of the core–shell technique (which will be discussed in greater detail in Sect. 3.5) whereby the solubility of the PEG molecules encased in a slow-degrading shell led to a gradual release of entrapped lysozymes [54]. Together, PEG, PEO, and PVA have become heavily utilized soluble polymer options that have enabled dynamic composite scaffold designs through a variety of processing options that will be discussed further in the following sections.

2.2 Biopolymers

Although synthetic polymers were the first to be electrospun, biopolymers have gained increasing attention because of their versatility and compatibility with other biological species including entrapped biologically relevant molecules and human tissues [61]. Some of the major biopolymers investigated to date will be reviewed, with specific attention paid to (1) features that can add versatility to composite schemes, and (2) methodologies that partnered synthetic/biopolymer blending or synthesis that allowed designers to overcome the limitations of the biopolymer systems alone. The first of these biopolymers include highly available protein systems including collagen and silk fibroin, and the lesser available or recombinantly produced elastin biomolecule. Also reviewed will be several other polysaccharide-based materials that play a natural role in tissue or plant structure and function and have also been heavily explored as electrospun biomaterials, e.g., alginate, hyaluronic acid, chitosan, and cellulose [62].

Although not covered here in detail, several other newly emerging biopolymer sources have been incorporated into electrospinning techniques and composite approaches, including urinary bladder matrix (UBM) [45] and platelet-rich plasma [63], which contain endogenous reservoirs of preserved growth factors. These newer platforms as well as water-based solvent approaches employing more traditional biopolymers will probably be incorporated into next-generation scaffolds used to deliver soluble factors that can promote enhanced regenerative pathways.

2.2.1 Collagen and Gelatin

Collagen protein is the most heavily explored naturally derived polymer because of its prevalence in connective tissues and its known biocompatibility [14]. Gelatin, on the other hand, contains an identical amino acid structure to collagen but is formed by heat denaturation and partial digestion of collagen, creating a soluble variant with less intermolecular crosslinks [64]. Two gelatin subtypes can be extracted from tissues: type A, processed by an acidic pretreatment, and type B, processed by an alkaline pretreatment [61]. Gelatin is also much less expensive and easier to prepare than intact collagen. Collagen was the first biopolymer to be electrospun using techniques adopted from synthetic spinning practices [65]. Although a PEO carrier was originally required for collagen spinning, it was later shown that pure collagen could be dissolved and spun from HFIP without a carrier [66]. Gelatin can likewise be spun without a carrier, in solvents such as HFIP and TFE, as well as formic acid (FA), acetic acid (AA), and water [67].

A range of different collagen subtypes have been successfully spun into nanofibrous meshes offering a wide range of constituent fiber diameters and structural features; however, the resultant mechanical properties of electrospun mats described to date are inferior to the properties of native tissues [61]. In the early attempts to spin pure type I collagen, the use of highly fluorinated alcohols (common to synthetic techniques) compromised some of the key load-bearing microstructural features of normal fibril-forming collagens [64, 68]. Electrospun acid-soluble type I collagen does show a quarter-staggered arrangement under transmission electron microscopy (TEM) and has shown improved enzymatic stability in vivo compared to electrospun gelatin [69]. However, it still lacks the normal second harmonic optical signature (derived from its microcrystalline content), and its circular dichroism (CD) spectra suggest a pronounced loss of triple helices in favor of random coils [64]. In addition to these marked differences in secondary structure, the denaturation of acid-soluble collagens during solubilization in fluoroalchohols results in a more water-soluble physical state [64]. On the other hand, when milder polar solvents such as ethanol are used, the triple helical structure of naturally derived collagen can be preserved [70]. This indicates that while collagen electrospinning is indeed possible, care must be taken to select proper spinning solvents and post-processing conditions in order to ensure high fidelity with native structure.

In order to crosslink the resultant collagen and gelatin nanofiber mats and prevent resolubilization, solvent and/or heat treatment are popular methodologies [61]. Glutaraldehyde (GA) is a common solvent that is proven to enhance the mechanical properties of collagen mats; however, there are associated risks of cytotoxicity and calcification if the scaffolds are used in vivo [68]. Gelatin and type I collagen scaffolds have also been crosslinked by methylene bis-(4-cyclohexylisocyanate) (HMDI) in isopropanol with the resultant gelatin mats being stiffer than those of collagen [71]. We have also explored the fabrication of collagen-based nanofibrous scaffolds and found that although GA treatments improve the mechanical performance of the scaffolds, genipin is a more favorable crosslinker due to improved dimensional stability and maintenance of fibrillar architecture (see Fig. 2) [72].

2.2.2 Silk

Like collagens, silks are also abundant, naturally derived proteins that are evolutionarily optimized to form high-strength fibers from soluble precursors through fairly simple biochemical processing methods [73–75]. Silks derived from the silkworm *Bombyx mori* have been used as sutures for decades and are FDA-approved biomaterials [76]. Through water-based processing methodologies, the core protein fibroin can be successfully extracted from the native cocoon, dissolved,

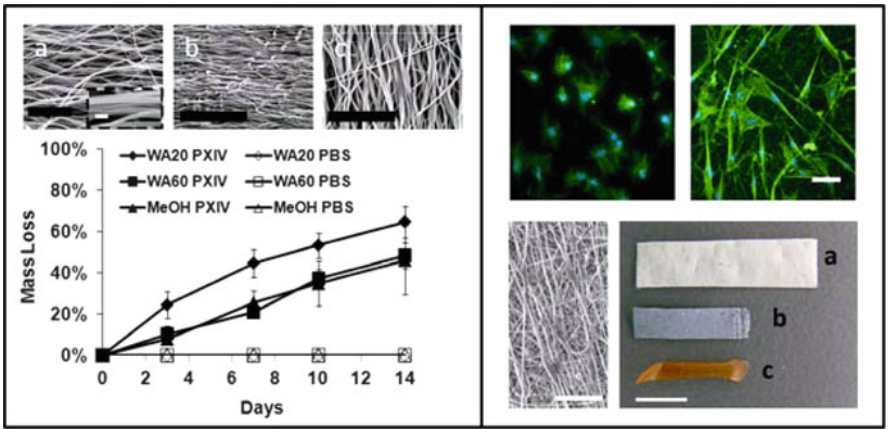

Fig. 2 Biopolymer design and post-processing. *Left panel*: SEM micrographs of silk mats formed on a rotating mandrel with post-processing: (a) as-spun, (b) methanol-treated, and (c) water annealed for 1 h at 37°C (black scale bar: 20 mm, white scale bar inset (a): 1 mm). *Left graph*: Silk mats treated by 37°C water annealing for 20 min. (*filled diamonds*), 60 min. (*filled squares*), or crosslinked by soaking in methanol for 5 min (*filled triangles*) were exposed to 0.1 mg/mL Protease XIV (or PBS control, *unfilled symbols*) for 14 days, rinsed, and weighed dry. *Right Panel*: DAPI/phalloidin staining of mesenchymal stem cells seeded on tissue culture plastic (*left*) compared to collagen nanofibrous mats (*right*) (scale bar: 50 mm). *Lower right panel*: Collagen nanofibrous scaffolds under SEM (scale bar: 50 mm) and gross images either (a) before crosslinking, or after crosslinking with (b) genipin and (c) glutaraldehyde (scale bar: 500 mm)

and purified to yield high M_w and high protein wt% solutions that are suitable for spinning [77]. The native silkworm and spider silk fibers are insoluble due to formation of well-characterized and pronounced β-pleated sheets that compliment lesser secondary structures such as α-helices and random coils in a multidomain hierarchy [78]. The high M_w and diverse amino acid sequences add additional flexibility into the potential structures formed by the soluble precursors [79, 80]. In addition to shielding the protein from interactions with water, these tight secondary structures impart impressive enzymatic stability to silk-based biomaterials [81].

Electrospinning silk has become quite commonplace [77] and, like many synthetics, was first conducted using an HFIP solvent [82, 83]. A completely water-based methodology employing PEO as a carrier was introduced shortly thereafter [7]. Several spinning conditions were varied during the systematic investigations that followed, including the effect of electric field characteristics, silk concentration, and spinning solutions (FA, HFIP, HFA-trihydrate) [84–86]. Although silk fibers electrospun from relatively large wt% solutions (5–15%) in FA at 3 kV/cm yielded small fiber diameters (<100 nm) in some studies [85, 86], others using the PEO carrier approach or HFIP solvents report much larger diameters (300–800 nm) [7, 84, 87]. However, spinning from HFIP can be potentially harmful towards other soluble non-silk species such as drugs, growth factors, or other delivered materials and can be toxic if not sufficiently removed. Therefore, while HFIP affords simpler control of initial mass loadings, most recent strategies geared towards tissue engineering employ all-aqueous approaches [88–91].

Once the electrospun silk mat has solidified, the protein is still water-soluble, with the exception of a few insoluble fibers or fragments formed because the physical shearing can cause minor β-sheet crosslinking [92]. In order to crosslink and form fully insoluble silk mats, very mild crosslinking conditions can be pursued including the use of methanol and other polar organic solvents [7, 84, 93, 94]. Interestingly, several groups have also investigated the role of water and organic solvent vapor treatments on the gradual crosslinking of silk mats [87, 95]. We have also recently studied the effect of water vapor-induced crystallinity compared to methanol solvent treatments as post-spinning modifications to modulate the functional properties of aqueous silk nanofibrous scaffolds (see Fig. 2) [96]. In concert with all of these crosslinking modalities, enzymes and growth factors can be safely entrapped to act as delivery stores for a variety of in vivo applications [93, 97].

2.2.3 Elastin

Elastin is a major structural protein element found in many connective tissues that is known to impart resiliency and elasticity to mechanically loaded tissues. It is therefore no surprise that the material has become an important tool in tissue engineering research [98]. Mature elastic fibers found in tissues contain structural subunits called tropoelastin, an amorphous 64 kDa monomer composed of 830 amino acids [14]. In the extracellular space, the cell-synthesized tropoelastin is exposed to lysyl oxidase-mediated oxidation at available lysine residues and then

self-associates by coacervation for crosslinking [99]. The remaining amino acid sequence is rich in glycine, valine, alanine, and proline, whose predominantly hydrophobic character give rise to mobile hydrophobic regions [71].

Bowlin's group was the first to demonstrate that functional electrospun constructs could be formed using solubilized elastin from ligamentum nuchae [100]. These elastin networks, formed from fibers of ~1 μm, did not contain the same crosslinking features as native elastin due to dissolution in HFIP and crosslinking in GA. Continued work by the Weiss group showed that electrospinning from the recombinantly produced precursor tropoelastin produced more wave-like fibers, similar to those found in larger elastin-rich arteries, suggesting that the source of elastin plays a major role in the resulting material properties [71]. Although alpha- and kappa-elastin are typically easier to obtain from fragments of mature elastin fibers, the materials formed directly from recombinantly produced soluble tropoelastin monomers continue to be the most heavily investigated [71]. Future efforts to improve these recombinant mimics and to uncover improved crosslinking methods for these elastin systems will aid in biomimetic fabrication strategies.

2.2.4 Hyaluronic Acid

Hyaluronic acid (HA) is a nonsulfated mucopolysaccharide, composed of alternating D-glucuronic acid and *N*-acetyl-D-glucosamine, that naturally provides many binding sites for proteoglycans in the form of long polymeric chains (up to 4 μm in length) [101]. As a result, HA can be of very large M_w (1–10,000 kDa) [102] and is highly hydrophilic due to the large concentration of polyanionic complexes [101]. These properties (size and hydrophilicity) impart a narrow electrospinning-specific processing window to HA because unusually high viscosity solutions require excessive field strength to overcome inherent surface tension, and hydrophilic polymers require longer evaporation time before solid fiber formation, otherwise fusion of fibers will occur at the collector surface [103]. These issues were confronted in the first reports of HA electrospinning, in which high electrical potentials (2–4 kV/cm) were employed to overcome the inherently high surface tension [102–104]. The authors of the first published HA electrospinning study were forced to use a 1.3–1.5 w/v%, 3,500 kDa HA solution, which resulted in very small fibers with diameters of ~50 nm [104]. Consequently, the authors found it necessary to lower the solution viscosity but maintain a high level of polymer concentration during spinning by introducing a fraction of lower M_w HA (45 kDa) in with the high M_w HA (3,500 kDa) polymer [104]. These modifications, however, did not markedly increase fiber diameter. Subsequently, higher M_w carriers including PEO [102], gelatin [103], zein [105], and collagen [106] were used to co-spin slightly lower-than-native M_w HA solutions (158 kDa HA-DTPH [102] and 2,000 kDa HA [103]), a blending strategy we have seen for many other polymeric systems. Finally, the use of ethanol and DMF as spinning solvents was effective in increasing solvent evaporation rates and decreasing surface tension, respectively, leading to vastly improved fiber morphologies [107].

Modifications of the carboxylic acid of the glucuronic acid moiety or the C-6 hydroxyl group of the *N*-acetylglucosamine sugar, through various synthetic chemical approaches, has lead to new and interesting adaptations of the backbone polysaccharide HA [108] that provide additional crosslinking methods [102], functional moieties [108, 109], and/or enzyme-cleavable sites [110]. Thiolated HA has been electrospun into nanofibrous scaffolds with a PEO carrier, and the fibers were crosslinked with PEG-diacrylate (PEGDA) prior to removal of PEO. PEGDA-crosslinked HA nanofibrous scaffolds were coated with fibronectin and supported fibroblast spreading [102]. Alternatively, HA macromers have been synthesized to include reactive methacrylate groups, which were later coupled to UV polymerizable side chains. These polymers can support photoinitiated radical polymerization to mediate attachment of crosslinkers (which could be extended by hydrolytically cleavable spacers [111]) and/or incorporate enzyme-degradable moieties. These photoinitiated HA polymers have been electrospun into scaffolds with spatially and temporally controllable crosslinking [109]. Spinning these methacrylated HA mats with a PEO carrier resulted in dry fibers of about 200–300 nm in diameter that swelled appreciably in solution. The long-term vision of these systems is that they be used for spatial control to pattern porosity into the fibrous scaffolds, which can then be used to enhance cellular infiltration and vascularization [109].

2.2.5 Alginate

Alginate is another anionic polysaccharide that is derived from brown seaweed and contains subunits of (1,4)-linked β-D-mannuronic acid (M) and α-L-guluronic acid (G). The presence of divalent cations (i.e., Ca^{2+}, Mg^{2+}, etc.) will cause the linear alginate polymers to ionically crosslink. Resultant biomaterials have excellent biocompatibility (a low to mild inflammatory response), are nontoxic, and nonimmunogenic [62]. Like HA, electrospinning the alginate polysaccharide is difficult; however, problems with alginate stem from a lack of chain entanglement due to the extended lengths of polymer segments. As a result, the first accounts of alginate spinning arrived late, and required PEO for spinning [112]. By mixing in glycerol, new interchain hydrogen bonds were facilitated [113]. Alternatively to PEO, PVA can be added to facilitate spinning in much the same way as for other systems previously described [114, 115]. These materials show good interactions with chondrocyte-like cells [112], but have not been extensively explored compared to other naturally derived polymer systems.

2.2.6 Chitosan

Chitin is another highly available polysaccharide biopolymer; it is derived from the exoskeleton of arthropods (specifically crab and shrimp shells) and formed from repeats of (1,4)-linked *N*-acetyl-β-D-glucosamine. In its natural form, the chains of

chitin form extended "ribbon" patterns composed of tight crystalline packing that is rich in interchain hydrogen bonding. This large degree of crystallinity imparts stiffness and brittle mechanical behavior to the natural polymer. The three isoforms of chitin (α, β, and δ) correspond to the degree of parallel versus antiparallel chain orientations in these ribbons [101].Chitosan can be formed in aqueous acid solutions when the degree of deacetylation in chitin reaches ~50% [62]. The first mats formed from chitosan were spun from AA, and a PEO carrier was again utilized [116]. Pure chitosan spinning was later investigated using a range of solvents including AA, DMF, and trifluoroacetic acid (TFA); however, only TFA and TFA mixed with dichloromethane were reported to form defect-free fibers, probably due to its volatility and its softening effect on the rigid chain interactions [117].

Mats spun from TFA will swell uncontrollably or solubilize in salt solutions, requiring neutralization [118] or crosslinking [119, 120] to maintain dimensional stability. These issues stem from chitosan's polycationic nature in solution, whereas polyanionic polysaccharides like HA will remain stable once introduced to a salt-rich environment. Nonetheless, both long-chain high M_w polymers demand large electric potentials to form pure insoluble fibers during electrospinning in order to overcome the large surface tension, requiring a very strict window of available solvents [117]. The use of toxic solvents to dissolve and spin chitosan (e.g., TFA) could lead to harmful residues post-spinning, thus AA or FA are typically employed as spinning solvents and, if crosslinking is undesirable, blending is typically pursued to mitigate swelling issues [116, 119, 121–124]. The nanofibrous mats that result are biocompatible and offer advantages such as controllable rates of degradability (dependent on levels of deacytalation)[125], cellular binding affinity [121, 126], as well as anti-thrombogenic [127–129] and anti-fouling capacities [130] that make them very useful for wound healing applications [131].

2.2.7 Cellulose

Cellulose is the most abundant natural polymer in the world, as it forms the structural backbone of nearly all plants. It is a linear homopolymer of D-glucose units that are linked by β(1→4)-glycosidic bonds, allowing the polymer to assume an extended conformation capable of intramolecular hydrogen bonding [101]. Tight packing confers a crystalline structure to cellulose that requires extremely high temperatures to melt. Like many of the other biopolymers reviewed herein, cellulose has limited solubility in common organic solvents; however, it is soluble in *N*-methyl-morpholine *N*-oxide/water (NMMO/water) and lithium chloride/dimethylacetamide (LiCl/DMAc). Cellulose derivatives, including cellulose acetate among others, have been used to enhance the solubility of the polymer for later electrospinning. Uses of these derivatives and control points (including PEO/PVA blends) have been extensively reviewed elsewhere [62].

3 Composites

Although the principles of the electrospinning impart processing limitations, there are nonetheless several means by which electrospun composite mats can be formed (see Fig. 3). The traditional and most heavily investigated technique blends selected polymers into a common spinning dope from which a single family of fibers is spun onto a collection target. In this case, polymer A is mixed to a given ratio with polymer B to yield properties dependent on the polymers chosen and their mixing ratios. An alternative method of composite mat formation is to utilize distinct spinning dopes for collection onto a common surface. This approach can be further distinguished into either coaxial spinning or multifiber spinning, the former resulting in fibers with polymer A coating polymer B, and the latter approach resulting in a mat containing distinct but interwoven fibers from polymer A and polymer B.

3.1 Blending

Blending of synthetic and biopolymer spinning dopes was initially introduced as a means of overcoming limitations in spinning capacity of certain biologically derived molecules. In a seminal work, Huang et al. were the first to use PEO as an agent to help increase solution viscosity in order to reach levels necessary to form defect-free type I collagen nanofibers [133]. This technique has become increasingly popular because of PEO's natural biocompatibility and solubility, making it a simple carrier material with limited adverse effects on the desired biopolymer fiber family [7, 115, 116, 124, 134–136]. Following work blending

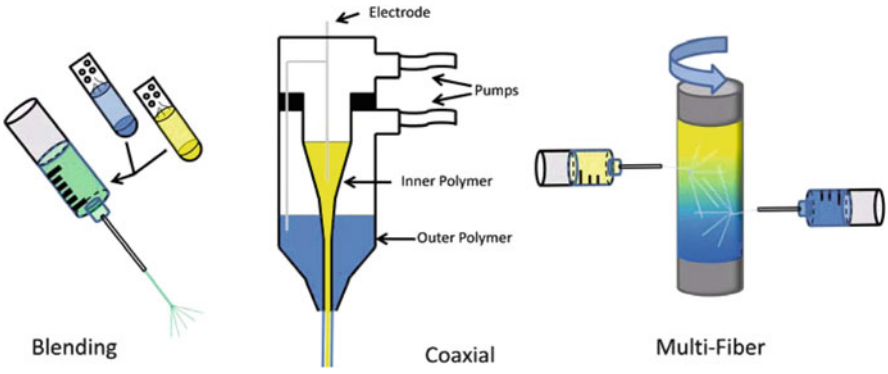

Fig. 3 Composite formation strategies. *Left*: Blending combines multiple polymers into a common spinning solution for use in traditional electrospinning procedures. *Center*: Coaxial spinning requires a custom-designed chamber, typically equipped with independent pumped polymer sources from designated chambers. These are often charged by a single electrode that can penetrate both chambers. Adapted from Sun et al. [132]. *Right*: Multifiber systems deliver two or more interspersed fiber populations to a common grounded rotating mandrel

PEO, other polymers such as PCL [66] and biopolymers such as elastin [100], were introduced to similarly aid in spinning feasibility [100, 137].

Although blending of polymer solutions can lead to improved spinning conditions, there are upper limits to solution viscosity (10–20 P has been reported, depending on the polymer [5]) such that not every blend ratio and mass loading of polymer is feasible. Higher viscosities and higher mass fractions of spinning dopes are associated with increased fiber diameters [2], which may have adverse effects on the cellular level [138]. Thus, rather than blend polymers (especially PEO) solely to enable spinning other desired materials, blending has continued to find use as a technique to impart greater versatility to mats in areas of mechanical performance, degradability, and even delivery of bioactive molecules.

3.1.1 Mechanically Improved Blends

Copolymerization has historically been used as a powerful method for exploring new and mechanically versatile polymer formulations. For instance, the synthesis of PLGA copolymers and subsequent formation into electrospun mats that vary in PLA (soft) and PGA (stiff) subunits will enable control of yield strength and strain characteristics according to the ratio of incorporation [6]. However, because synthesis and copolymerization are generally arduous endeavors [109], and may ultimately be incompatible for the majority of synthetic/biopolymer pairings, such blends are typically created by simple mixing in mutual solvents [139]. The Bowlin group has been at the forefront of blended electrospinning and were able to show that blended PLA and PGA systems operate in a similar fashion to their synthesized counterparts, demonstrating that various ratios of these polyester can achieve intermediate properties [140]. Nonetheless, the mechanical properties of blends are dependent on the nature of the polymers employed, their relative ratios, and any interfacial effects; taken together, property prediction is difficult without sufficient experimentation [141].

Most polymer blends are designed to allow softer or weaker biopolymers to be spun with stiffer and stronger synthetic fibers so as to preserve biocompatibility while remaining mechanically viable. The difficulty in preparing competent blends, however, is in the selection of mutually appropriate solvents that will both solubilize the synthetic component while at the same time not excessively denaturing the biopolymer component (see Table 1). Collagen and gelatin have been blended with various polyesters to provide composites with biocompatibility, combined with improved properties over collagen-based materials alone [141]. Gelatin and PCL composites, both spun from TFE, showed concentration-dependent properties when blended at different ratios [145]. Using only a 10% increase in collagen, PLCL/collagen blends in HFIP improved biocompatibility (HUVEC attachment and spreading) over PLCL alone without significantly diminishing construct stiffness; however, at higher ratios (30–50% collagen) the construct mechanics were significantly impaired and the dimensional stability of cell-laden constructs decreased significantly [148]. Powell et al. confirmed these findings using PCL/collagen

Table 1 Comparison of synthetic and biopolymer solvent compatibilities and post-spinning crosslinkers investigated to date

Polymer	Solvent										Post-spinning crosslinker					Refs
	DMF	THF	HFIP	DCM	NMMO	FA	AA	H_2O	EtOH	MeOH	GA	MeOH	H_2O	Genipin	UV	
PLA	■	■	■													[6]
PGA	■	■	■													[6]
PLGA	■	■	■						■							[6]
PCL	■	■	■													[6]
PEUU	■	■	■	■												[39, 43, 46]
PEEUU	■	■	■	■												[142]
PVA	■	■	■	■				■		■						[21, 56]
PEO	■	■	■	■				■	■							[52]
Collagen					■	■	■				■			■	■	[143, 144]
Gelatin	■	■	■		■	■		■	■		■	■		■	■	[145, 146]
Elastin			■								■					[100, 143]
Silk			■		■	■	■	■			■	■	■	■		[82, 85, 87]
HA	■	■	■					■	■						■	[103]
Alginate								■								[112]
Chitosan	■	■	■		■	■	■				■					[117, 121]
Cellulose				■							■					[62]

Shaded cells indicate compatibility of polymer with solvent or crosslinker: *PLA* poly(lactic acid), *PGA* poly(glycolic acid): *PLGA* poly(lactic-*co*-glycolic acid), *PCL* poly(ε-caprolactone), *PEU* poly(ester urethane), *PEEUU* poly(ester ether urethane), *PVA* poly(vinyl alcohol), *PEO* poly(ethylene oxide), *HA* hyaluronic acid, *DMF* *N*,*N*-dimethylformamide, *AA* acetic acid, *FA* formic acid, *DCM* dichloromethane, *HFIP* hexafluoroisopropanol, *THF* tetrahydrofuran, *GA* glutaraldehyde, *NMMO* *N*-methyl-morpholine *N*-oxide/water (NMMO/water)

blends for skin regeneration, showing that PCL additions of only 10% are capable of significantly improving the mechanical properties [149]. Along with these encouraging findings, it important to note that fluorinated solvent treatments such as those employed above will ultimately denature the once-intact collagen source, resulting in purely gelatin/synthetic composites [64].

Besides collagen, many other biopolymers (including silk, gelatin, elastin, chitosan, and UBM) have been blended, with the aim of balancing mechanics and biocompatibility. Increasing amounts of PEUU in PEUU/UBM composites led to linear increases in both ultimate tensile strength and ductility, while UBM was important for in vitro cell compatibility and remodeling potential [45]. The Bowlin group also showed that blends of a poly(dioxanone) (PDO) and elastin could help modify structural properties of electrospun tubes, such as adding compliance to the normally stiff and brittle behavior of crystalline PDO polymers [150]. These ideas were also extended to multiple blended biopolymers, demonstrated by the use of PLGA, gelatin, and elastin in the tuning of scaffold mechanics [20], and tri-component blends of elastin, collagen, and a combination of several polyesters used to tune structural properties of a vascular graft [143].

3.1.2 Blends to Modify Rates of Degradation

As we have seen, polymer selection and modifications can alter structural properties of the electrospun fibers, resulting in materials with different types of crosslinking modalities (i.e., covalent, ionic, or hydrogen bonding), M_w, or both. In turn, these features not only influence scaffold mechanical properties, but can also change the stability of the polymer in an aqueous, salt-rich environment. Additionally, certain naturally derived polymers and engineered synthetics (such as modified HAs or PEEUUs) contain native-like epitopes that are recognized by physiological enzymes and will be cleaved on the basis of their prevalence and availability. In this way, blending polymers of different hydrolytic or enzymatic stability (or both) can result in new tailorable designs that can serve a variety of application-specific remodeling needs.

To explore variable degradation strategies, Stankus developed blends of UBM with PEUU, and tested their cellular compatibility in vitro and remodeling potential in vivo. Interestingly, subcutaneous implantation of the PEUU/UBM blend scaffolds resulted in increased scaffold degradation and a large cellular infiltrate when compared with electrospun PEUU alone [45]. It was unclear, however, if the added enzymatic (matrix metalloproteinase) susceptibility of the UBM component, the interruption of normal intact PEUU structure, or the increased cell signaling due to the release of bioactive factors from the UBM component (growth factors, chemokines, and cytokines) were ultimately most influential towards increasing integration and turnover. Likewise, degradation of nanofibrous scaffolds based on chitin was shown to be faster than that of microfibers formed from the same solvents, and rapidly degraded in vivo [126]. These findings were then translated into blends of PLLA-PCL copolymers

blended with chitosan to advance their design [151, 152]. Results suggest that chitosan could foster a higher rate of cell proliferation in vitro, and will be useful in pore opening to facilitate cell ingress [152].

3.1.3 Blends to Facilitate Delivery

The highly hydrophobic polymer chemistry and the nature of solvents used for synthetic fiber spinning eliminate the ability to incorporate most bioactive entities into the spinning process. On the other hand, most biopolymers are readily soluble in water and/or salt solutions that are crucial for the stabilization of labile enzymes and delicate signaling molecules. Therefore, blending strategies have been developed to partner encapsulation-friendly polymers with other structural or permanent polymer aspects to facilitate application-specific delivery. Because chitosan is a valuable delivery vehicle but a poor load-bearing fiber type, blends of chitosan/synthetics have been extensively studied for a number of applications. As a case study, Jiang et al. showed early on that Ibuprofen-loaded composite membranes composed of PLGA and PEG-*graft*-chitosan (PEG-*g*-CHN) could be prepared by electrospinning [153]. The authors observed that electrospun membranes of PLGA alone shrank to ~20% of the original area, even after a brief incubation in buffer solution at 37 °C. In turn, shrinkage of the PLGA component dramatically reduced membrane porosity, cell ingress potential, and diffusional capacity of these scaffolds. The extent of shrinkage in PLGA/PEG-*g*-CHN electrospun membranes decreased with increasing PEG-*g*-CHN content. To explain this, the authors claimed that the high content of hydrophilic PEG-*g*-CHN component swelled in water, effectively preventing the shrinkage of the PLGA. Subsequently, more than 85% of Ibuprofen loaded into pure PLGA fibers was released after 4 days of incubation. In contrast, the addition of PEG-*g*-CHN greatly moderated the release rate of Ibuprofen from the electrospun PLGA/PEG-*g*-CHN membrane [153]. A number of other release studies focusing on drugs and growth factors in studies employing blended nanofibers have been reviewed elsewhere [154].

3.2 Coaxial Fibers

Instead of mixing two spinning solvents together into the same blend, researchers have also developed strategies to simultaneously spin a sheath or "shell" of one polymer coaxially around a central or "core" polymer during mat fabrication [132, 155–159]. Sun et al. were the first to publish on the technique, and showed that two spinnable polymer solutions formed of varying solvents could be spun into two distinct segments of the same fiber [132]. Shortly thereafter, Yu et al. showed that coaxially spun fibers composed of both synthetic and biopolymer constituents were feasible [156, 160]. Interestingly, they also showed that a core fluid could be either an electrospinnable fluid or a fluid that is, on its own, not readily fiber-forming by

electrospinning or hard to process into a fiber by conventional means, such as silk fibroin. This is possible because the process of fiber formation and collection happens very rapidly, and mixing of the two polymers is limited; furthermore, since the shell shields the core fluid from the vapor–liquid interface, surface tension and therefore Rayleigh instability of the stream is reduced [156]. A gelatin core coaxially spun with a PCL shell was also introduced shortly thereafter to highlight the ability to partner biopolymer and synthetic sources in order to tune mechanics and degradability, depending on the concentration of gelatin in the dope used to spin the core [157, 161].

These findings suggest that delivery of bioactive materials could also be facilitated by entrapment in a core, surrounded by a polymer of desired stability and thickness to tune rates of release. Zhang et al. were the first to show that this technique was viable for delivery of water-soluble entities, and did so by using bovine serum albumin (BSA) and lysozymes [54]. Following this finding, many other groups used this technique for a variety of other release strategies and molecules of interest: the release of BSA from dextran (another natural polysaccharide) ensheathed in PCL [162], release of model enzymes from PEO ensheathed in PCL [163], release of active nerve growth factor from BSA ensheathed in PLCL [164, 165], and release of angiogenic factors from poly(3-hydroxy butyrate) (a bacterially derived polyester) ensheathed in PLLA [166]. These studies all illustrate that either soluble or unstable encapsulates can be stabilized by the presence of the sheath, and that the properties of release are controlled by both core and shell properties. Chitosan is particularly well suited to this technology because of the difficulty in spinning pure solutions, while being a potentially valuable encapsulant [167]. Due to their general success so far, future studies will undoubtedly continue to utilize synthetic sheaths such as PLLA and PCL to protect and facilitate spinning of biopolymer core components such as chitosan, silk, and gelatin or soluble core polymers such as PVA or PEO.

3.3 Multifiber Scaffolds

Although the blending of polymers and coaxial spinning have enabled added versatility to nanofiber scaffold design, resultant constructs often fall short of structural and mechanical benchmarks set impressively high by native tissues [168]. One difficulty with blending polymers is control over the spatial distribution of mixed constituents in the final fiber, which can arise from incomplete mixing during spinning or the disassociation of these constituents as the fiber is drawn towards the collection target and the solvent evaporates. By comparing the various polymer types reviewed herein (see Table 1), another limitation of blending becomes clear: the use of some organic polymers and fluorinated alcohol solvents would denature the biopolymers; conversely, most biopolymer-friendly solvents are incapable of solubilizing many synthetics, with the exception of PEO and PVA carriers. Together, these shortcomings have undoubtedly limited the expansion of

the blended polymer palette. Additionally, coaxial spun fibers are well suited to enhance the delivery functionality of fibers but ultimately sacrifice mechanical properties by the slow loss of the core's structural integrity [157].

Therefore, an alternative approach at advancing electrospun polymer designs is to spin multiple distinct polymers from separate sources, but collect them concurrently on a common grounded surface. Our group and others have utilized these techniques to design multifiber scaffolds with diverse properties that reflect the contribution of the individual components (see Fig. 4) [25, 169–171]. This technique was first introduced by Gupta et al. [172], and later Ding et al. used the technique to prepare constructs of varying mechanical properties based on variations in PVA and cellulose content (see Fig. 4) [57]. Systems were later fabricated to incorporate PEO as a water-soluble and sacrificial fiber family to intersperse a second water-insoluble and stable family of PCL nanofibers [169]. In these studies, the ratio between PEO fiber and PCL fiber incorporation dictated the potential of stem cells to infiltrate the central portion of a thick (~1 mm) construct.

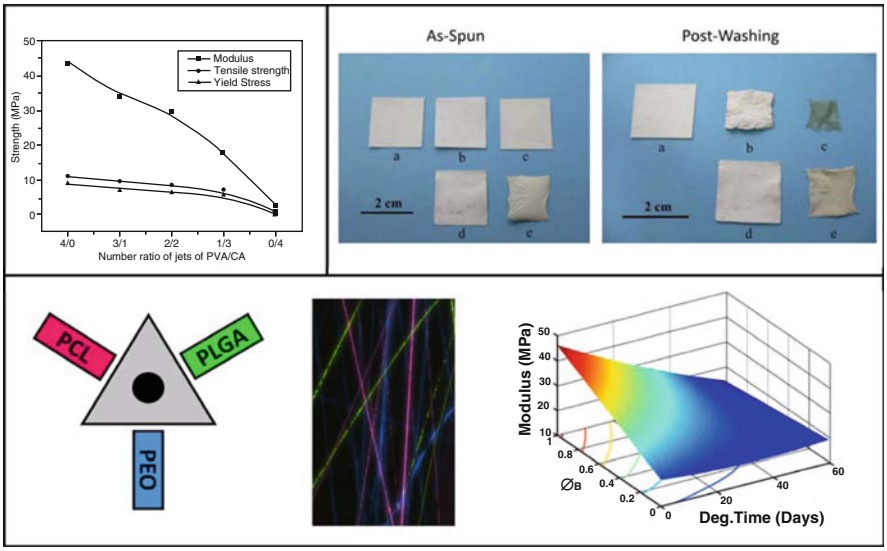

Fig. 4 Multifiber spinning and post-spinning modifications. *Top left*: Modulus, tensile strength, and yield stress of nanofibrous mats as a function of number ratio of jets of PVA solution to those of cellulose acetate (*CA*). Reprinted from Ding et al. [57] with permission. *Top right*: Optical images of as-formed mats and shrunken mats after incubation in PBS at 37 °C for 24 h: (*a*) chitosan/PVA, (*b*) PLGA, (*c*) PLGA–chitosan/PVA, (*d*) crosslinked PLGA–chitosan/PVA, (*e*) crosslinked chitosan/PVA. Reprinted from Duan et al. [121] with permission. *Bottom*: Multipolymer nanofibrous composites. Scaffold mechanics can be tuned with the integration of different polymers into nanofibrous composites, here PEO, PCL, and PLGA (*left*). The polymers were collected simultaneously to produce a fully interspersed fiber mixture (*center*). Using this approach, and based on the starting properties of each individual polymer, a wide range of scaffold properties such as degradation rate and elastic modulus can be generated (*right*). Data adapted from Baker et al. [25]

Furthermore, by adding multiple fiber jets of distinct polymer sources to be collected simultaneously, dynamic scaffolds with temporal degradative features and mechanical properties can be designed (see Fig. 4) [25].

One other important advantage of multifiber scaffolds is that crosslinking and other post-spinning modifications can be selectively applied to individual fiber families based on their responsiveness to environmental or solvent conditions. This fact can be appreciated by scanning the list of crosslinking solvents found in Table 1, comparing biopolymer choices with common synthetics, which are generally unaltered by crosslinking agents such as GA and methanol. As a case study, Duan et al. fabricated multifiber mats composed of PLGA (spun from THF/DMF) and chitosan (spun from AA with a PVA carrier) in order to identify a formulation suitable for wound dressing applications (see Fig. 4) [121]. From a reactivity standpoint, PLGA is a somewhat more hydrophobic synthetic polymer that, when sufficiently hydrated, will distort appreciably [25], whereas chitosan is a hydrophilic biopolymer requiring crosslinking to remain insoluble when exposed to water. The authors found that GA vapors, while unreactive towards PLGA alone, were effective in maintaining fibrillar chitosan nanofibers. When PLGA and chitosan were spun together into a multifiber composite scaffold, GA treatments resulted in a completely insoluble composite construct that had a balanced water uptake potential and dimensional stability as well as optimal cellular proliferation profiles [121]. These positive findings are the result of the proper selection, not only of polymer sources but also of discriminatory crosslinking conditions that highlight the power of multifiber spinning.

We have begun to capitalize on these multifiber design principles by co-spinning other versatile biopolymer sources with our synthetic (PCL or otherwise) nanofiber families in order to create mechanically robust, dynamic, and bioactive composites. As outlined above, we have demonstrated that both silk and collagen can be co-spun with synthetic nanofibers to create biopolymer composites with both mechanical integrity and flexibility in post-processing [72, 96, 173]. Collagen/PCL nanofiber composites are more biomimetic than pure PCL and can improve the initial cellularity of composites [173]. The Wagner group also established that multifiber mats can be functionalized to release drugs or growth factors by using one family to act as a stable template (PEUU nanofibers), while a second family (PLGA) can be used to deliver active antibiotics [42]. We have introduced this concept to the biopolymer domain by creating multifiber families where the enzymatically degradable biopolymer component (silk) can be used to deliver active growth factors, while the synthetic component (PCL) can be used to mechanically stabilize the component [174]. Additionally, a third water-soluble component (PEO) has been added to enhance cell ingress into these silk/PCL composites [174], while also providing the opportunity to deliver yet another microsphere-based delivery modality with different release kinetics than from the fibers themselves [175]. Taken together, these seemingly limitless design options permit evolutionary design options to fabricate dynamic, tissue-specific structures (see Fig. 5) that will potentially address a number of disease states through functional tissue engineering [168].

4 Future Outlook

In this chapter, we have highlighted the many potential formulations involving synthetic and biosynthetic nanofibrous elements for the fabrication of tissue engineering scaffolds for the repair or replacement of damaged or diseased tissues. Vascular tissue engineering, for example, has seen the incorporation of a number of polymer options and fabrication techniques to move directly into animal models to further functional repair [176]. We have fabricated higher-ordered structures including wedge-shaped and concentric bilayers to mimic the complex architecture of fiber-reinforced tissues such as the meniscus and the intervertebral disc, respectively (see Fig. 5). Future translation of biopolymer/

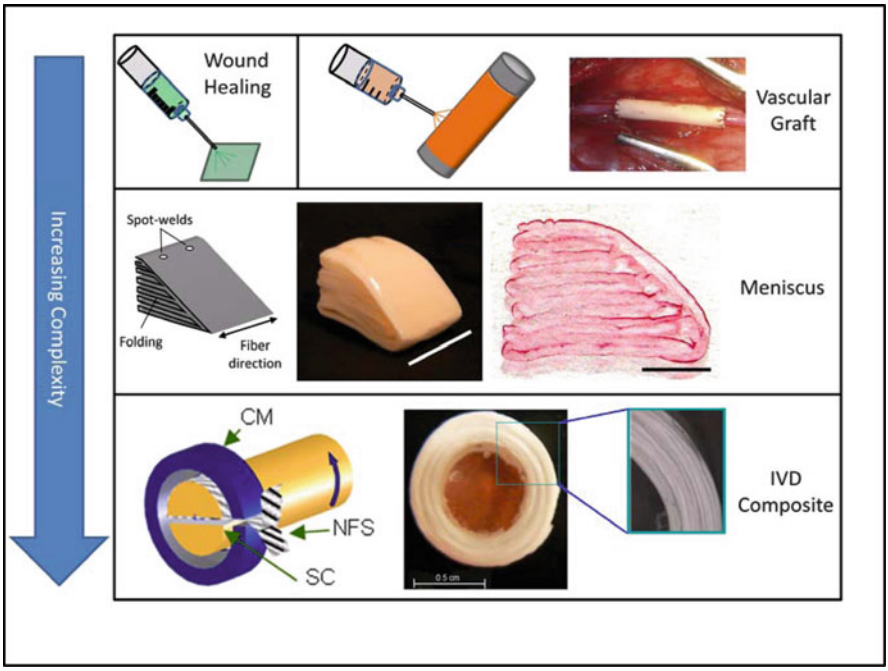

Fig. 5 Fabrication of anatomical constructs. Most collagen-based fiber-reinforced tissues have specialized anatomic form, with multiple levels of organized hierarchy. For potential skin or wound care applications (*top left*), planar structures may be directly implantable and fabrication simply requires electrospinning onto a flat collection target. Likewise, for vascular or nerve applications (*top right*), electrospinning onto a small-diameter mandrel is relatively simple and fabrication is a one-step process. Reprinted from Wise et al. [176] with permission. For complex structures, such as the knee meniscus (*center*) and the intervertebral disc (IVD) (*bottom*), construction algorithms must be developed for in vivo applications, as described in [168]. Custom wrapping can produce cell-laden wedge-shaped structures for meniscus applications that can be colonized by seeded cells. Scale bar = 1 cm. For IVD, annular composites with multiple lamellae can be assembled by using a mandrel with a slotted core (SC) to wrap multiple layers of nanofibrous scaffolds (NFS) within a custom mold (CM). The central mandrel used for wrapping is then removed and eventually replaced by an agarose or other degradable hydrogel core

composite designs to meet the needs of most clinically relevant applications will be reliant on similar creative assembly techniques and material optimization steps. Furthermore, we envision that the techniques described herein will be combined (i.e., coaxial and concurrent multifiber spinning) to further enhance functionality for all applications pursued. This unique combination of nanoscale topography with tunable and biomimetic synthetic/biological materials in dynamic nanofibrous scaffolds will have a profound impact on the field of regenerative medicine and human health.

References

1. Baker BM et al (2009) New directions in nanofibrous scaffolds for soft tissue engineering and regeneration. Expert Rev Med Devices 6(5):515–532
2. Baumgarten PK (1971) Electrostatic spinning of acrylic microfibers. J Colloid Interface Sci 36(1):71–79
3. Seal BL, Otero TC, Panitch A (2001) Polymeric biomaterials for tissue and organ regeneration. Mater Sci Eng R Rep 34(4–5):147–230
4. Li WJ et al (2007) Engineering controllable anisotropy in electrospun biodegradable nanofibrous scaffolds for musculoskeletal tissue engineering. J Biomech 40(8): 1686–1693
5. Huang ZM et al (2003) A review on polymer nanofibers by electrospinning and their applications in nanocomposites. Compos Sci Technol 63(15):2223–2253
6. Li WJ et al (2006) Fabrication and characterization of six electrospun poly(alpha-hydroxy ester)-based fibrous scaffolds for tissue engineering applications. Acta Biomater 2(4): 377–385
7. Jin HJ et al (2002) Electrospinning Bombyx mori silk with poly(ethylene oxide). Biomacromolecules 3(6):1233–1239
8. Zeng J et al (2005) Poly(vinyl alcohol) nanofibers by electrospinning as a protein delivery system and the retardation of enzyme release by additional polymer coatings. Biomacromolecules 6(3):1484–1488
9. Khil MS et al (2003) Electrospun nanofibrous polyurethane membrane as wound dressing. J Biomed Mater Res B Appl Biomater 67(2):675–679
10. Su Q et al (2010) Preparation and characterization of biodegradable electrospun polyanhydride nano/microfibers. J Nanosci Nanotechnol 10(10):6369–6375
11. Costache AD et al (2010) Computational methods for the development of polymeric biomaterials. Adv Eng Mater 12(1–2):B3–B17
12. Metter RB et al (2010) Biodegradable fibrous scaffolds with diverse properties by electrospinning candidates from a combinatorial macromer library. Acta Biomater 6(4): 1219–1226
13. Tan AR et al (2008) Electrospinning of photocrosslinked and degradable fibrous scaffolds. J Biomed Mater Res A 87(4):1034–1043
14. Ratner BD et al (2004) Biomaterials science: an introduction to materials in medicine, 2nd edn. Elsevier Academic, Amsterdam
15. Vacanti CA et al (1991) Synthetic polymers seeded with chondrocytes provide a template for new cartilage formation. Plast Reconstr Surg 88(5):753–759
16. Freed LE et al (1993) Neocartilage formation in vitro and in vivo using cells cultured on synthetic biodegradable polymers. J Biomed Mater Res 27(1):11–23

17. Boland ED et al (2001) Tailoring tissue engineering scaffolds using electrostatic processing techniques: a study of poly(glycolic acid) electrospinning. J Macromol Sci, Pure Appl Chem 38(12):1231–1243
18. Boland ED et al (2004) Utilizing acid pretreatment and electrospinning to improve biocompatibility of poly(glycolic acid) for tissue engineering. J Biomed Mater Res B Appl Biomater 71B(1):144–152
19. Zong XH et al (2002) Structure and process relationship of electrospun bioabsorbable nanofiber membranes. Polymer 43(16):4403–4412
20. Li M et al (2006) Co-electrospun poly(lactide-co-glycolide), gelatin, and elastin blends for tissue engineering scaffolds. J Biomed Mater Res A 79A(4):963–973
21. Kenawy el R et al (2002) Release of tetracycline hydrochloride from electrospun poly (ethylene-co-vinylacetate), poly(lactic acid), and a blend. J Control Release 81(1–2):57–64
22. Li WJ et al (2002) Electrospun nanofibrous structure: a novel scaffold for tissue engineering. J Biomed Mater Res 60(4):613–621
23. Yoshimoto H et al (2003) A biodegradable nanofiber scaffold by electrospinning and its potential for bone tissue engineering. Biomaterials 24(12):2077–2082
24. Lee KH et al (2003) Characterization of nano-structured poly(epsilon-caprolactone) nonwoven mats via electrospinning. Polymer 44(4):1287–1294
25. Baker BM et al (2009) Fabrication and modeling of dynamic multipolymer nanofibrous scaffolds. J Biomech Eng 131(10):101012
26. Ekaputra AK et al (2009) Composite electrospun scaffolds for engineering tubular bone grafts. Tissue Eng A 15(12):3779–3788
27. Li WJ et al (2003) Biological response of chondrocytes cultured in three-dimensional nanofibrous poly(epsilon-caprolactone) scaffolds. J Biomed Mater Res 67A(4):1105–1114
28. Venugopal J et al (2005) In vitro study of smooth muscle cells on polycaprolactone and collagen nanofibrous matrices. Cell Biol Int 29(10):861–867
29. Kim K et al (2003) Control of degradation rate and hydrophilicity in electrospun non-woven poly (D, L-lactide) nanofiber scaffolds for biomedical applications. Biomaterials 24(27):4977–4985
30. Zong X et al (2003) Structure and morphology changes during in vitro degradation of electrospun poly(glycolide-co-lactide) nanofiber membrane. Biomacromolecules 4(2):416–423
31. Xu C et al (2004) Electrospun nanofiber fabrication as synthetic extracellular matrix and its potential for vascular tissue engineering. Tissue Eng 10(7–8):1160–1168
32. Santerre JP et al (2005) Understanding the biodegradation of polyurethanes: From classical implants to tissue engineering materials. Biomaterials 26(35):7457–7470
33. Demir MM et al (2002) Electrospinning of polyurethane fibers. Polymer 43(11):3303–3309
34. Lee CH et al (2005) Nanofiber alignment and direction of mechanical strain affect the ECM production of human ACL fibroblast. Biomaterials 26(11):1261–1270
35. Han JA et al (2011) Electrospinning and biocompatibility evaluation of biodegradable polyurethanes based on L-lysine diisocyanate and L-lysine chain extender. J Biomed Mater Res A 96(4):705–714
36. Schoenta R (1968) Carcinogenic and chronic effects of 4,4′-diaminodiphenylmethane an epoxyresin hardener. Nature 219(5159):1162–1163
37. Hassan MK et al (2006) Biodegradable aliphatic thermoplastic polyurethane based on poly (epsilon-caprolactone) and L-lysine diisocyanate. J Polym Sci A Polym Chem 44 (9):2990–3000
38. Rockwood DN et al (2007) Characterization of biodegradable polyurethane microfibers for tissue engineering. J Biomater Sci Polym Ed 18(6):743–758
39. Guan JJ et al (2002) Synthesis, characterization, and cytocompatibility of efastomeric, biodegradable poly(ester-urethane)ureas based on poly(caprolactone) and putrescine. J Biomed Mater Res A 61(3):493–503
40. Skarja GA, Woodhouse KA (1998) Synthesis and characterization of degradable polyurethane elastomers containing an amino acid-based chain extender. J Biomater Sci Polym Ed 9 (3):271–295

41. Woo GLY, Mittelman MW, Santerre JP (2000) Synthesis and characterization of a novel biodegradable antimicrobial polymer. Biomaterials 21(12):1235–1246
42. Hong Y et al (2008) Generating elastic, biodegradable polyurethane/poly(lactide-co-glycolide) fibrous sheets with controlled antibiotic release via two-stream electrospinning. Biomacromolecules 9(4):1200–1207
43. Parrag IC, Woodhouse KA (2010) Development of biodegradable polyurethane scaffolds using amino acid and dipeptide-based chain extenders for soft tissue engineering. J Biomater Sci Polym Ed 21(6–7):843–862
44. Guan JJ et al (2004) Biodegradable poly(ether ester urethane)urea elastomers based on poly(ether ester) triblock copolymers and putrescine: synthesis, characterization and cytocompatibility. Biomaterials 25(1):85–96
45. Stankus JJ et al (2008) Hybrid nanofibrous scaffolds from electrospinning of a synthetic biodegradable elastomer and urinary bladder matrix. J Biomater Sci Polym Ed 19(5):635–652
46. Stankus JJ, Guan JJ, Wagner WR (2004) Fabrication of biodegradable elastomeric scaffolds with sub-micron morphologies. J Biomed Mater Res A 70A(4):603–614
47. Rockwood DN et al (2008) Culture on electrospun polyurethane scaffolds decreases atrial natriuretic peptide expression by cardiomyocytes in vitro. Biomaterials 29(36):4783–4791
48. Skarja GA, Woodhouse KA (2000) Structure-property relationships of degradable polyurethane elastomers containing an amino acid-based chain extender. J Appl Polym Sci 75 (12):1522–1534
49. Doshi J, Reneker DH (1995) Electrospinning process and applications of electrospun fibers. J Electrostat 35(2–3):151–160
50. Jaeger R, Schonherr H, Vancso GJ (1996) Chain packing in electro-spun poly(ethylene oxide) visualized by atomic force microscopy. Macromolecules 29(23):7634–7636
51. Reneker DH et al (2000) Bending instability of electrically charged liquid jets of polymer solutions in electrospinning. J Appl Phys 87(9):4531–4547
52. Fong H, Chun I, Reneker DH (1999) Beaded nanofibers formed during electrospinning. Polymer 40(16):4585–4592
53. Norris ID et al (2000) Electrostatic fabrication of ultrafine conducting fibers: polyaniline/polyethylene oxide blends. Synth Met 114(2):109–114
54. Jiang HL et al (2005) A facile technique to prepare biodegradable coaxial electrospun nanofibers for controlled release of bioactive agents. J Control Release 108(2–3):237–243
55. Hodge RM, Edward GH, Simon GP (1996) Water absorption and states of water in semi-crystalline poly(vinyl alcohol) films. Polymer 37(8):1371–1376
56. Ding B et al (2002) Preparation and characterization of a nanoscale poly(vinyl alcohol) fiber aggregate produced by an electrospinning method. J Polym Sci B Polym Phys 40(13): 1261–1268
57. Ding B et al (2004) Fabrication of blend biodegradable nanofibrous nonwoven mats via multi-jet electrospinning. Polymer 45(6):1895–1902
58. Herold DA, Keil K, Bruns DE (1989) Oxidation of polyethylene glycols by alcohol-dehydrogenase. Biochem Pharmacol 38(1):73–76
59. Spasova M et al (2007) Preparation of PLIA/PEG nanofibers by electrospinning and potential applications. J Bioact Compat Polym 22(1):62–76
60. Yang DJ et al (2007) Fabrication and characterization of hydrophilic electrospun membranes made from the block copolymer of poly(ethylene glycol-co-lactide). J Biomed Mater Res A 82(3):680–688
61. Sell SA et al (2009) Electrospinning of collagen/biopolymers for regenerative medicine and cardiovascular tissue engineering. Adv Drug Deliv Rev 61(12):1007–1019
62. Lee KY et al (2009) Electrospinning of polysaccharides for regenerative medicine. Adv Drug Deliv Rev 61(12):1020–1032
63. Wolfe PS, Sell SA, Bowlin GL (2011) Regenerative potential of electrospun scaffolds incorporated with platelet rich plasma. In: Proceedings 15th Annual Hilton Head Workshop on regenerative medicine, Hilton Head Island

64. Zeugolis DI et al (2008) Electro-spinning of pure collagen nano-fibres – Just an expensive way to make gelatin? Biomaterials 29(15):2293–2305
65. Huang L, Apkarian RP, Chaikof EL (2001) High-resolution analysis of engineered type I collagen nanofibers by electron microscopy. Scanning 23(6):372–375
66. Matthews JA et al (2002) Electrospinning of collagen nanofibers. Biomacromolecules 3(2): 232–238
67. Song JH, Kim HE, Kim HW (2008) Production of electrospun gelatin nanofiber by water-based co-solvent approach. J Mater Sci Mater Med 19(1):95–102
68. Yang L et al (2008) Mechanical properties of single electrospun collagen type I fibers. Biomaterials 29(8):955–962
69. Telemeco TA et al (2005) Regulation of cellular infiltration into tissue engineering scaffolds composed of submicron diameter fibrils produced by electrospinning. Acta Biomater 1(4): 377–385
70. Dong B et al (2009) Electrospinning of collagen nanofiber scaffolds from benign solvents. Macromol Rapid Commun 30(7):539–542
71. Li M et al (2005) Electrospun protein fibers as matrices for tissue engineering. Biomaterials 26(30):5999–6008
72. Gee AO, Baker BM, Mauck RL (2008) Mechanics and cytocompatibility of genipin crosslinked type I collagen nanofibrous scaffolds. In: Proceedings ASME 2008 Summer Bioengineering Conference, Marco Island. ASME, New York
73. Zhu J, Shao H, Hu X (2007) Morphology and structure of electrospun mats from regenerated silk fibroin aqueous solutions with adjusting pH. Int J Biol Macromol 41(4):469–474
74. Foo CWP et al (2006) Role of pH and charge on silk protein assembly in insects and spiders. Appl Phys A 82(2):223–233
75. Kluge JA et al (2008) Spider silks and their applications. Trends Biotechnol 26(5):244–251
76. Altman GH et al (2003) Silk-based biomaterials. Biomaterials 24(3):401–416
77. Zhang X, Reagan MR, Kaplan DL (2009) Electrospun silk biomaterial scaffolds for regenerative medicine. Adv Drug Deliv Rev 61(12):988–1006
78. Jin HJ, Kaplan DL (2003) Mechanism of silk processing in insects and spiders. Nature 424 (6952):1057–1061
79. Hu X et al (2011) Regulation of silk material structure by temperature-controlled water vapor annealing. Biomacromolecules 12(5):1686–1696
80. Lu Q et al (2010) Water-insoluble silk films with silk I structure. Acta Biomater 6(4):1380–1387
81. Horan RL et al (2005) In vitro degradation of silk fibroin. Biomaterials 26(17):3385–3393
82. Zarkoob S et al (1998) Structure and morphology of nano electrospun silk fibers. American Chemical Society, Polymer Preprints, Division of Polymer Chemistry, 39(2): 244–245
83. Eby RK et al. Production of nonwoven network of synthetically spun silk nanofibers, by electrospinning a solution containing dissolved silk fibers and hexafluoroisopropanol. University of Akron, OH
84. Ohgo K et al (2003) Preparation of non-woven nanofibers of Bombyx mori silk, Samia cynthia ricini silk and recombinant hybrid silk with electrospinning method. Polymer 44(3):841–846
85. Sukigara S et al (2003) Regeneration of Bombyx mori silk by electrospinning – part 1: processing parameters and geometric properties. Polymer 44(19):5721–5727
86. Sukigara S et al (2004) Regeneration of Bombyx mori silk by electrospinning. Part 2. Process optimization and empirical modeling using response surface methodology. Polymer 45(11): 3701–3708
87. Min BM et al (2006) Regenerated silk fibroin nanofibers: water vapor-induced structural changes and their effects on the behavior of normal human cells. Macromol Biosci 6(4):285–292
88. Wang H, Shao HL, Hu XC (2006) Structure of silk fibroin fibers made by an electrospinning process from a silk fibroin aqueous solution. J Appl Polym Sci 101(2):961–968
89. Zhang X, Baughman CB, Kaplan DL (2008) In vitro evaluation of electrospun silk fibroin scaffolds for vascular cell growth. Biomaterials 29(14):2217–2227

90. Meinel AJ et al (2009) Optimization strategies for electrospun silk fibroin tissue engineering scaffolds. Biomaterials 30(17):3058–3067
91. Zhang X et al (2009) Dynamic culture conditions to generate silk-based tissue-engineered vascular grafts. Biomaterials 30(19):3213–3223
92. Xie F et al (2006) Effect of shearing on formation of silk fibers from regenerated Bombyx mori silk fibroin aqueous solution. Int J Biol Macromol 38(3–5):284–288
93. Li C et al (2006) Electrospun silk-BMP-2 scaffolds for bone tissue engineering. Biomaterials 27(16):3115–3124
94. Jin HJ et al (2004) Human bone marrow stromal cell responses on electrospun silk fibroin mats. Biomaterials 25(6):1039–1047
95. Jeong L et al (2006) Time-resolved structural investigation of regenerated silk fibroin nanofibers treated with solvent vapor. Int J Biol Macromol 38(2):140–144
96. Kluge JA et al (2011) Versatile nanofibrous composites for soft tissue repair via silk protein incorporation. In: Proceedings 2011 Orthopaedic Research Society annual meeting, Long Beach. ORS, Rosemont
97. Schneider A et al (2009) Biofunctionalized electrospun silk mats as a topical bioactive dressing for accelerated wound healing. Acta Biomater 5(7):2570–2578
98. Waterhouse A et al (2011) Elastin as a nonthrombogenic biomaterial. Tissue Eng B Rev 17(2): 93–99
99. Kagan HM, Sullivan KA (1982) Lysyl oxidase: preparation and role in elastin biosynthesis. Methods Enzymol 82 Pt A:637–650
100. Boland ED et al (2004) Electrospinning collagen and elastin: preliminary vascular tissue engineering. Front Biosci 9:1422–1432
101. Garrett R, Grisham CM (2002) Principles of biochemistry: with a human focus. Harcourt College Publishers, Fort Worth
102. Ji Y et al (2006) Electrospun three-dimensional hyaluronic acid nanofibrous scaffolds. Biomaterials 27(20):3782–3792
103. Li JX et al (2006) Gelatin and gelatin-hyaluronic acid nanofibrous membranes produced by electrospinning of their aqueous solutions. Biomacromolecules 7(7):2243–2247
104. Um IC et al (2004) Electro-spinning and electro-blowing of hyaluronic acid. Biomacromolecules 5(4):1428–1436
105. Yao C, Li XS, Song TY (2007) Fabrication of zein/hyaluronic acid fibrous membranes by electrospinning. J Biomater Sci Polym Ed 18(6):731–742
106. Hsu FY et al (2010) Electrospun hyaluronate-collagen nanofibrous matrix and the effects of varying the concentration of hyaluronate on the characteristics of foreskin fibroblast cells. Acta Biomater 6(6):2140–2147
107. Li JX et al (2006) Electrospinning of hyaluronic acid (HA) and HA/gelatin blends. Macromol Rapid Commun 27(2):114–120
108. Burdick JA, Prestwich GD (2011) Hyaluronic acid hydrogels for biomedical applications. Adv Mater 23(12):H41–H56
109. Sundararaghavan HG, Metter RB, Burdick JA (2010) Electrospun fibrous scaffolds with multiscale and photopatterned porosity. Macromol Biosci 10(3):265–270
110. Vanderhooft JL et al (2009) Rheological properties of cross-linked hyaluronan-gelatin hydrogels for tissue engineering. Macromol Biosci 9(1):20–28
111. Sahoo S et al (2008) Hydrolytically degradable hyaluronic acid hydrogels with controlled temporal structures. Biomacromolecules 9(4):1088–1092
112. Bhattarai N et al (2006) Alginate-based nanofibrous scaffolds: structural, mechanical, and biological properties. Adv Mater 18(11):1463−+
113. Nie HR et al (2008) Effects of chain conformation and entanglement on the electrospinning of pure alginate. Biomacromolecules 9(5):1362–1365
114. Nie HR et al (2009) Effect of poly(ethylene oxide) with different molecular weights on the electrospinnability of sodium alginate. Polymer 50(20):4926–4934

115. Safi S et al (2007) Study of electrospinning of sodium alginate, blended solutions of sodium alginate/poly(vinyl alcohol) and sodium alginate/poly(ethylene oxide). J Appl Polym Sci 104 (5):3245–3255
116. Duan B et al (2004) Electrospinning of chitosan solutions in acetic acid with poly(ethylene oxide). J Biomater Sci Polym Ed 15(6):797–811
117. Ohkawa K et al (2004) Electrospinning of chitosan. Macromol Rapid Commun 25 (18):1600–1605
118. Sangsanoh P, Supaphol P (2006) Stability improvement of electrospun chitosan nanofibrous membranes in neutral or weak basic aqueous solutions. Biomacromolecules 7(10): 2710–2714
119. Duan B et al (2007) Degradation of electrospun PLGA-chitosan/PVA membranes and their cytocompatibility in vitro. J Biomater Sci Polym Ed 18(1):95–115
120. Schiffman JD, Schauer CL (2007) Cross-linking chitosan nanofibers. Biomacromolecules 8 (2):594–601
121. Duan B et al (2006) A nanofibrous composite membrane of PLGA-chitosan/PVA prepared by electrospinning. Eur Polym J 42(9):2013–2022
122. Duan B et al (2007) Hybrid nanofibrous membranes of PLGA/chitosan fabricated via an electrospinning array. J Biomed Mater Res A 83A(3):868–878
123. Zhang YY et al (2007) Preparation of electrospun chitosan/poly(vinyl alcohol) membranes. Colloid Polym Sci 285(8):855–863
124. Vondran JL, Sun W, Schauer CL (2008) Crosslinked, electrospun chitosan-poly(ethylene oxide) nanofiber mats. J Appl Polym Sci 109(2):968–975
125. Tomihata K, Ikada Y (1997) In vitro and in vivo degradation of films of chitin and its deacetylated derivatives. Biomaterials 18(7):567–575
126. Noh HK et al (2006) Electrospinning of chitin nanofibers: degradation behavior and cellular response to normal human keratinocytes and fibroblasts. Biomaterials 27(21):3934–3944
127. Lee KY, Ha WS, Park WH (1995) Blood compatibility and biodegradability of partially N-acylated chitosan derivatives. Biomaterials 16(16):1211–1216
128. Yusof NL, Lim LY, Khor E (2004) Flexible chitin films: structural studies. Carbohydr Res 339(16):2701–2711
129. Yusof NL et al (2003) Flexible chitin films as potential wound-dressing materials: wound model studies. J Biomed Mater Res A 66(2):224–232
130. Ignatova M et al (2006) Electrospun nano-fibre mats with antibacterial properties from quaternised chitosan and poly(vinyl alcohol). Carbohydr Res 341(12):2098–2107
131. Kang YO et al (2010) Chitosan-coated poly(vinyl alcohol) nanofibers for wound dressings. J Biomed Mater Res B Appl Biomater 92(2):568–576
132. Sun ZC et al (2003) Compound core-shell polymer nanofibers by co-electrospinning. Adv Mater 15(22):1929−1932
133. Huang L et al (2001) Engineered collagen – PEO nanofibers and fabrics. J Biomater Sci Polym Ed 12(9):979–993
134. Ji Y et al (2006) Dual-syringe reactive electrospinning of cross-linked hyaluronic acid hydrogel nanofibers for tissue engineering applications. Macromol Biosci 6(10):811–817
135. Lu JW et al (2006) Electrospinning of sodium alginate with poly(ethylene oxide). Polymer 47(23):8026–8031
136. Frenot A, Henriksson MW, Walkenstrom P (2007) Electrospinning of cellulose-based nanofibers. J Appl Polym Sci 103(3):1473–1482
137. Casper CL et al (2005) Functionalizing electrospun fibers with biologically relevant macromolecules. Biomacromolecules 6(4):1998–2007
138. Shih YRV et al (2006) Growth of mesenchymal stem cells on electrospun type I collagen nanofibers. Stem Cells 24(11):2391–2397
139. McCullen SD et al (2009) Nanofibrous composites for tissue engineering applications. Wiley Interdiscip Rev Nanomed Nanobiotechnol 1(4):369–390

140. Ramdhanie LI et al (2006) Thermal and mechanical characterization of electrospun blends of poly(lactic acid) and poly(glycolic acid). Polym J 38(11):1137–1145
141. Barnes CP et al (2007) Nanofiber technology: designing the next generation of tissue engineering scaffolds. Adv Drug Deliv Rev 59(14):1413–1433
142. Bashur CA et al (2009) Effect of fiber diameter and alignment of electrospun polyurethane meshes on mesenchymal progenitor cells. Tissue Eng A 15(9):2435–2445
143. Lee SJ et al (2007) In vitro evaluation of electrospun nanofiber scaffolds for vascular graft application. J Biomed Mater Res A 83(4):999–1008
144. Caruso AB, Dunn MG (2004) Functional evaluation of collagen fiber scaffolds for ACL reconstruction: cyclic loading in proteolytic enzyme solutions. J Biomed Mater Res A 69(1): 164–171
145. Zhang Y et al (2005) Electrospinning of gelatin fibers and gelatin/PCL composite fibrous scaffolds. J Biomed Mater Res B Appl Biomater 72(1):156–165
146. Sisson K et al (2009) Evaluation of cross-linking methods for electrospun gelatin on cell growth and viability. Biomacromolecules 10(7):1675–1680
147. Ayutsede J et al (2005) Regeneration of Bombyx mori silk by electrospinning. Part 3: characterization of electrospun nonwoven mat. Polymer 46(5):1625–1634
148. Kwon IK, Matsuda T (2005) Co-electrospun nanofiber fabrics of poly(L-lactide-co-epsilon-caprolactone) with type I collagen or heparin. Biomacromolecules 6(4):2096–2105
149. Powell HM, Boyce ST (2009) Engineered human skin fabricated using electrospun collagen-PCL blends: morphogenesis and mechanical properties. Tissue Eng A 15(8):2177–2187
150. Sell SA et al (2006) Electrospun polydioxanone-elastin blends: potential for bioresorbable vascular grafts. Biomed Mater 1(2):72–80
151. Chen F et al (2009) Biocompatibility, alignment degree and mechanical properties of an electrospun chitosan-P(LLA-CL) fibrous scaffold. J Biomater Sci Polym Ed 20(14):2117–2128
152. Chen F et al (2008) Electrospun chitosan-P(LLA-CL) nanofibers for biomimetic extracellular matrix. J Biomater Sci Polym Ed 19(5):677–691
153. Jiang HL et al (2004) Preparation and characterization of ibuprofen-loaded poly(lactide-co-glycolide)/poly(ethylene glycol)-g-chitosan electrospun membranes. J Biomater Sci Polym Ed 15(3):279–296
154. Liang D, Hsiao BS, Chu B (2007) Functional electrospun nanofibrous scaffolds for biomedical applications. Adv Drug Deliv Rev 59(14):1392–1412
155. Huang ZM, Zhang YZ (2005) Micro-structures and mechanical performance of co-axial nanofibers with drug and protein cores and polycaprolactone shells. Chem J Chin Univ Chin 26(5):968–972
156. Yu JH, Fridrikh SV, Rutledge GC (2004) Production of submicrometer diameter fibers by two-fluid electrospinning. Adv Mater 16(17):1562−1566
157. Zhang YZ et al (2004) Preparation of core-shell structured PCL-r-gelatin Bi-component nanofibers by coaxial electrospinning. Chem Mater 16(18):3406–3409
158. Zhang YZ et al (2005) Characterization of the surface biocompatibility of the electrospun PCL-collagen nanofibers using fibroblasts. Biomacromolecules 6(5):2583–2589
159. Li D, Xia YN (2004) Direct fabrication of composite and ceramic hollow nanofibers by electrospinning. Nano Lett 4(5):933–938
160. Wang M et al (2006) Production of submicron diameter silk fibers under benign processing conditions by two-fluid electrospinning. Macromolecules 39(3):1102–1107
161. Huang ZM, Zhang YZ, Ramakrishna S (2005) Double-layered composite nanofibers and their mechanical performance. J Polym Sci B Polym Phys 43(20):2852–2861
162. Jiang HL et al (2006) Modulation of protein release from biodegradable core-shell structured fibers prepared by coaxial electrospinning. J Biomed Mater Res B Appl Biomater 79B(1): 50–57
163. Dror Y et al (2008) Encapsulation of enzymes in biodegradable tubular structures. Macromolecules 41(12):4187–4192

164. Su Y et al (2009) Poly(L-lactide-co-epsilon-caprolactone) electrospun nanofibers for encapsulating and sustained releasing proteins. Polymer 50(17):4212–4219
165. Liu JJ et al (2010) Peripheral nerve regeneration using composite poly(lactic acid-caprolactone)/nerve growth factor conduits prepared by coaxial electrospinning. J Biomed Mater Res A 96(1):13–20
166. Wang C et al (2010) Biodegradable core/shell fibers by coaxial electrospinning: processing, fiber characterization, and its application in sustained drug release. Macromolecules 43(15): 6389–6397
167. Ojha SS et al (2008) Fabrication and characterization of electrospun chitosan nanofibers formed via templating with polyethylene oxide. Biomacromolecules 9(9): 2523–2529
168. Mauck RL et al (2009) Engineering on the straight and narrow: the mechanics of nanofibrous assemblies for fiber-reinforced tissue regeneration. Tissue Eng B Rev 15(2): 171–193
169. Baker BM et al (2008) The potential to improve cell infiltration in composite fiber-aligned electrospun scaffolds by the selective removal of sacrificial fibers. Biomaterials 29(15): 2348–2358
170. Bonani W et al (2011) Biohybrid nanofiber constructs with anisotropic biomechanical properties. J Biomed Mater Res B Appl Biomater 96(2):276–286
171. Guimaraes A et al (2010) Solving cell infiltration limitations of electrospun nanofiber meshes for tissue engineering applications. Nanomedicine 5(4):539–554
172. Gupta P, Wilkes GL (2003) Some investigations on the fiber formation by utilizing a side-by-side bicomponent electrospinning approach. Polymer 44(20):6353–6359
173. Gee AO et al (2010) "Fabrication and Evaluation of Biomimetic-Biosynthetic Nanofibrous Composites". Transactions of the 56th Annual Meeting of the Orthopaedic Research Society, New Orleans. LA
174. Kluge JA et al (2011) Delivery of active FGF-2 from mechanically-stable biological nanofibers accelerates cell ingress into multifiber composites. In: Proceedings American Society of Mechanical Engineers summer bioengineering conference, 22–25 June, Farmington, PA. ASME, New York
175. Ionescu LC et al (2010) An anisotropic nanofiber/microsphere composite with controlled release of biomolecules for fibrous tissue engineering. Biomaterials 31(14):4113–4120
176. Wise SG et al (2011) A multilayered synthetic human elastin/polycaprolactone hybrid vascular graft with tailored mechanical properties. Acta Biomater 7(1):295–303

Adv Polym Sci (2012) 246: 131–170
DOI: 10.1007/12_2011_122

Published online: 6 July 2011

Electrospun Fibers as Substrates for Peripheral Nerve Regeneration

Jörg Mey, Gary Brook, Dorothée Hodde, and Andreas Kriebel

Abstract Since axonal regeneration is possible in the peripheral nervous system, lesions can be treated by suturing disconnected nerve stumps or, when a lesion-induced gap must be bridged, by grafting an autologous nerve. However, nerve transplantations require multiple operations and cause a sensory deficit at the donor site. It is therefore desirable to develop artificial conduits for nerve regeneration as alternatives to the autograft. A core concept for the design of such implants is the incorporation of orientated nanofibers.

Artificial implants have to promote and guide axonal growth, the migration of Schwann cells, and they must not cause excessive inflammatory reactions. With hollow tubes, which are already used as nerve bridges in clinical studies, it is not possible to achieve regeneration over distances much larger than 30 mm. For this purpose, biocompatible tubes are being developed that contain orientated electrospun fibers consisting of a range of natural or synthetic materials. More recently, artificial guidance materials have been endowed with biologically active molecules. Extracellular matrix proteins or synthetic peptides that activate integrin receptors have been coupled to electrospun fibers. Other approaches adopted gradients of neurotrophins or incorporate living cells. One of the long-term goals of this research is to develop cell-free artificial implants that become integrated at the lesion site to the extent that they become populated by migrating host glia and allow a similar degree of regeneration that is supported by the autologous nerve.

J. Mey (✉)
Hospital Nacional de Parapléjicos, SESCAM, C/Finca la Peraleda s/n, 45071 Toledo, Spain

Institut für Biologie II, RWTH Aachen University, Aachen, Germany
e-mail: jmey@sescam.jccm.es

G. Brook and D. Hodde
Institut für Neuropathologie, RWTH Aachen University, Aachen, Germany

A. Kriebel
Institut für Biologie II, RWTH Aachen University, Aachen, Germany

Keywords Artificial implants · Biomaterials · Electrospinning · Extracellular matrix · Growth factors · Peripheral nerve · Regeneration

Contents

Abbreviations

BDNF	Brain-derived neurotrophic factor
CAM	Cell adhesion molecule
CNS	Central nervous system
CNTF	Ciliary neurotrophic factor
DRG	Dorsal root ganglion
ECM	Extracellular matrix
ePTFE	Extended poly(tetrafluoroethylene)
ErbB	Erythroblastic leukemia viral oncogen (epidermal growth factor receptor family)
FGF	Fibroblast growth factor
GDNF	Glial-derived neurotrophic factor
GFR	Receptor of GDNF-family ligands
GGF	Glial growth factor
IGF	Insulin-like growth factor
IL	Interleukin
LIF	Leukemia inhibitory factor

NGF	Nerve growth factor
NT	Neurotrophin
PAN-MA	Poly(acrylonitrile-*co*-methacrylate)
PCL	Poly(ε-caprolactone)
PCLEEP	Poly(caprolactone-*co*-ethyl ethylene phosphate)
PGA	Poly(glycolic acid)
PHB	Poly(hydroxybutyric acid)
pHEMA	Poly(2-hydroxyethyl methacrylate)
pHEMA-MMA	Poly(2-hydroxyethyl methacrylate-*co*-methyl methacrylate)
PLA	Poly(lactic acid); the D- and L-isomers are often referred to as PDLA, PLLA, respectively
PLGA	Poly(lactic-*co*-glycolic acid)
PN	Peripheral nerve
PNS	Peripheral nervous system
PPE	Polyphosphoester
PPy	Poly(pyrrole)
sPEG	Star-shaped poly(ethylene glycol)
STAT	Signal transducer and activator of transcription
TGF	Transforming growth factor
trk	Tyrosine kinase/tropomyosin receptor kinase (neurotrophin receptor)
VEGF	Vascular endothelial growth factor

1 Introduction

Peripheral nerves transmit motor, sensory and autonomic information between the central nervous system (CNS) and the rest of the body. If a peripheral nerve is severed, e.g., by an injury to the face or limbs, these functions are lost. However, in contrast to the mostly non-regenerative processes after spinal cord lesions, axons in the peripheral nervous system (PNS) are able to regenerate, and the long-term functional outcome of peripheral nerve injury depends on the severity of the trauma [1]. The cell somata of PNS neurons are localized in the ventral horn of the spinal cord (motor neurons), the dorsal root ganglia (DRG; sensory neurons), or in the sympathetic chain ganglia close to the spinal column (neurons of the autonomic nervous system). Damage to mammalian peripheral nerve fibers activates a growth program in the axotomized neuronal cell bodies such that their axons regenerate, provided they find a growth-permissive substrate. The ideal growth-promoting substrate is provided by the distal segment of a lesioned peripheral nerve.

For this reason, peripheral nerves can be surgically repaired after simple transection injuries by reconnecting the individual proximal and distal nerve fascicles. However, when the gap between disrupted nerve stumps is too large, the surgeon is required to transplant a segment of an autologous nerve that is taken from elsewhere in the patient [2]. Since sensory nerves such as the sural or peroneal nerve are often

used for such procedures, the inevitable consequence is the loss of sensory function. Although sensory nerves are routinely transplanted even for the repair of motor fibers, experimental data indicate that sensory grafts are less suitable than motor nerves [3]. The limitation of available donor material for autografting and the additional risk of donor site morbidity prompted the need for alternatives to the autologous nerve transplantation.

Although several alternative tissues have been investigated for their potential to support PNS repair, such as muscles or veins [4], a major research focus has been the development of a bioengineering approach to design artificial nerve conduits. Recent advances include internal topographical features that assist in the guidance of axonal regeneration. Among these developments, the use of polymeric nanofibers has provided one of the most promising templates for the purpose of peripheral nerve repair [5, 6]

2 Physiological Requirements of Artificial Nerve Bridges

2.1 Peripheral Nerve Regeneration

To identify the requirements that artificial nerve constructs must meet in order to substitute autologous transplants, a good understanding of peripheral nerve regeneration is important. Peripheral nerve injury invariably causes degeneration of the distal nerve stump. Since axons are disconnected from their cell somata they are eventually degraded. Cytoskeleton and cell membranes are broken up into their molecular constituents. The PNS glia, the Schwann cells, shed their myelin. This anterograde degeneration of the distal nerve segments is referred to as Wallerian degeneration. It coincides with the infiltration of hematogenous macrophages, which clear myelin fragments and neuronal debris. When Schwann cells lose contact with living axons they dedifferentiate and proliferate within endoneurial tubes of the nerve. In the process, the aligned Schwann cells form the so-called bands of Büngner, which provide an excellent growth substrate for axonal regeneration. At the same time, retrograde signals activate a physiological program of regeneration in the neurons. Thus, growth cones are formed by severed axons in the proximal nerve stump (Fig. 1a, b).

The success of this regenerative response depends on the extent of the injury, especially on the maintenance of connections between the proximal fiber fascicles and the endoneurium of the severed, distal segments. This kind of injury (called axonotmesis) can be treated conservatively because many injured neurons survive, and regenerating axons elongate in contact with the bands of Büngner [7]. Injured peripheral nerves, especially the basement membranes, provide an excellent growth substrate for axonal regeneration, where neurite extension reaches velocities of several millimeters per day. Subsequently, the Schwann cells re-myelinate regenerated axons [8]. If axons reach their peripheral targets they may form new

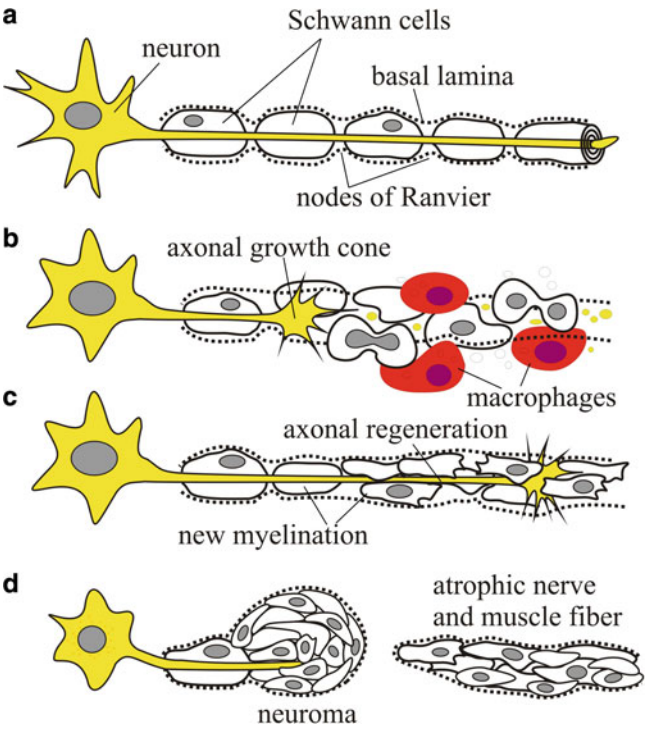

Fig. 1 Peripheral nerve degeneration and regeneration. (**a**) Neurons of the PNS are located in the ventral horns of the spinal cord (motor neurons), the dorsal root ganglia (sensory neurons), or the sympathetic chain ganglia (autonomic nervous system). Axons are myelinated by Schwann cells. (**b**) After nerve injury myelin sheaths and axons degenerate distal to the lesion site. Schwann cells proliferate, and macrophages remove the debris of degenerating fibers. At the lesion site, neurons form axonal growth cones. (**c**) Axons are able to regenerate along longitudinal bands of glia and ECM. Subsequently, Schwann cells remyelinate the new axons. (**d**) After complete transaction proximal and distal nerve stumps retract. Frequently, when axon sprouts fail to cross the site of injury, a neuroma forms. The distal part of the nerve and muscle fibers that are no longer innervated become atrophic

synapses or end organs, and physiological function can be restored (Fig. 1c, d). When the continuity of the endoneurial sheaths is disrupted, if fiber fascicles still remain connected via the perioneurium or epineurium (neurotmesis) recovery is also possible without surgical intervention. After complete transaction, the stumps of the elastic nerves retract, and fiber fascicles must be re-aligned and sutured (end-to-end neurorrhaphy) [1]. Larger nerves are supported by endogenous and exogenous blood vessels, and these, too, are surgically restored.

The problems described above may represent a microsurgical challenge, but do not call for a tissue engineering approach. This is the case, however, when the injury causes larger gaps in the nerve, where end-to-end suturing would lead to excessive tension, impair microvascular blood flow, and result in scarring [2]. Any

larger lesions are repaired with autologous nerve grafts [5] because no better substrate for nerve regeneration is known than the injured peripheral nerve itself.

Consequently, natural peripheral nerves provide the ideal template for biomimetic designs of artificial nerve conduits. Ideally, such constructs would also include molecular signals that guide and support regeneration in the natural environment. Since research on molecular processes associated with peripheral nerve regeneration has accumulated an immense corpus of data over the last half century, we can only mention those pertinent signal transduction pathways that have been considered in the functionalization of nerve constructs.

2.2 Secreted Signals in Peripheral Nerve Regeneration

Axonal injury causes depolarization and action potentials, resulting in an influx of Ca^{2+} ions and the activation of an intracellular signal transduction machinery, which regulates formation of the growth cone [9]. Once axonal growth is initiated, cell survival and continued axonal regeneration depend on the supply of trophic physiological growth factors. Most of these are synthesized by Schwann cells and, to a lesser extent, by macrophages and possibly fibroblasts. Provided that the different subpopulations of peripheral neurons are maintained, interactions with the extracellular matrix (ECM) and with other cells guide elongation of the nerve fibers. Attempts have been made to incorporate molecular signals that mediate these processes in tissue engineered nerve grafts [6].

2.2.1 Regeneration Signals That Activate Axonal Growth

Following the immediate consequences of injury-induced depolarization, the effect of growth factors sets in. Perhaps the single most important signaling molecules in this category are ciliary neurotrophic factor (CNTF) and nerve growth factor (NGF). The neurocytokine CNTF is strongly expressed by myelinating Schwann cells. Although expression of this factor declines after the injury, it seems to be released from the damaged cells and triggers neuronal regeneration [10]. Another important signal is NGF, a member of the neurotrophin family, the expression of which is strongly reduced immediately after the lesion [11], and the absence of which may be important for the initiation of the regenerative response [12]. Similar observations were made for insulin-like growth factor-I (IGF-I) [13]. These and related factors at later stages support survival and regeneration of injured neurons.

2.2.2 Survival Factors for the Damaged Nerve Cells

Even in the PNS, with its high regenerative potential, a large percentage of neuronal cell death can occur after injury, especially if the lesion occurs close to the cell

soma [5]. A number of growth factors were found to be upregulated in regenerating peripheral nerves and, as shown by blocking their activity in vivo, to be physiologically neuroprotective. Thus, NGF, secreted by Schwann cells, is a neurotrophic factor for sensory and autonomic neurons. Leukemia inhibitory factor (LIF), CNTF and glial-derived neurotrophic factor (GDNF) support motoneurons. Related molecules, especially the neurotrophins brain-derived neurotrophic factor (BDNF), neurotrophin-3 (NT-3), NT-4/5, the neuropoietic cytokines, e.g. interleukin-6 (IL-6), and fibroblast growth factors (FGF-1, FGF-2) have also been found to enhance survival of PNS neurons [11, 14, 15]. Most of these molecules have been employed in attempts to support regeneration of peripheral nerve (PN) injury. A complementary strategy to the supply of survival factors would be to interfere with apoptotic pathways that are also initiated by nerve injury. To our knowledge this has not been tested so far in the context of repair strategies with artificial nerve constructs.

2.2.3 Promoters of Axonal Regeneration

Many investigations have been conducted in search of regeneration-promoting molecules in vitro and in vivo. Important candidates that were found to be involved in the physiological context are IGF-I and IGF-II [16, 17], both of which are also beneficial when given exogenously. BDNF and GDNF are important growth-promoting factors for motor neurons, especially in the case of chronic deafferentiation [8, 10, 15]. Although a sufficient supply of these factors in vivo renders additional pharmacological application useless to the injured nerve [18], they may be important tools for artificial nerve grafts. NGF is a powerful neuritogenic factor for sympathetic neurons [19]. It must be noted that neurotrophins can also have neurotoxic effects when they act via the common low affinity NGF (p75) receptor instead of the specific receptor tyrosine kinases (trkA, trkB, trkC) [8]. Receptors for several GDNF family members (c-ret and co-receptors GFRα2, GFRα3) are expressed in small unmyelinated sensory neurons in the DRG and in sympathetic ganglia. Their signals enhance regeneration of sympathetic and nociceptive neurons [20, 21].

2.2.4 Modulators of the Schwann Cell Response

Although the effect of neurons on Schwann cells and other non-neuronal cells in the nerve are mediated to a large extent by cell surface contacts, soluble factors play a major part. The most important inducer of Schwann cell differentiation and myelination is neuregulin-1 of the glial growth factor (GGF) family. GGFs are expressed by neurons and have various glia and muscle cells as recipients. In the PNS, neuregulin-1 can drive the entire pathway of Schwann cell differentiation including axonal myelination [22]. Neuregulin receptors on the Schwann cell are ErbB2/ErbB3 heterodimers, where the ErbB3 subunit binds the ligand while ErbB2

has a kinase activity, which initiates the intracellular signaling cascade [23]. Peripheal nerve injury induces expression of neuregulins and their receptors [24].

Other soluble signals include nuclear receptor ligands such as thyroid hormone, estrogen, and retinoic acid. Triiodothyronine, estrogen, and progesteron enhance axonal regeneration after peripheral nerve injury, though it is questionable whether these hormones are endogenous signals in the process [25]. Retinoic acid signaling, which is activated by sciatic nerve crush [26, 27] promotes peripheral nerve regeneration [28] and seems to be a crucial downstream effect of the action of neurotrophins [29], especially for NGF- and NT-3-dependent sensory neurons [30]. However, retinoid receptor expression is most prominent in Schwann cells and macrophages. The transcription factor Krox20, which is an important regulator of peripheral myelination, is activated by neuregulin and retinoic acid via a retinoid X receptor [31].

2.2.5 Signals for Vascularization

Members of the large, heparin-binding fibroblast growth factor family, especially FGF-1 and FGF-2 are strong promoters of angiogenesis. Another important paracrine factor in angiogenesis is vascular endothelial growth factor (VEGF), which acts downstream of the FGFs, but also has parallel, independent effect [32, 33]. In addition to these primary regulators, synergistic interaction with other factors, including granulocyte colony stimulating factor and platelet-derived growth factor, influence blood vessel formation in regenerating peripheral nerves [34].

2.3 Surface-Bound Signals

If artificial nerve implants are to mimic the physiological stimuli that initiate and maintain regeneration in vivo, the most promising molecular candidates would be extracted from this list of secreted molecules for intercellular communication. In addition, since axonal growth cones advance only in contact with surfaces, regeneration and the infiltration of growth-promoting cells depend on the presence of permissive substrates, which interact via surface-bound signals with cell membrane receptors. Such substrates are (1) the ECM and (2) the plasmalemma of other cells.

2.3.1 Extracellular Matrix

The predominant growth-permissive surface that renders peripheral nerves such an ideal growth substrate is the basal lamina laid down by the Schwann cells.

It consists largely of laminin and collagen IV [35]. Laminin and collagen are therefore the most frequently used ECM proteins in cell culture and three-dimensional constructs (see below). Nerve fibers are grouped in distinct fiber fascicles, which are enclosed by a perineurial matrix (endo-, peri- and epineurium). This matrix consists of fibrillar collagens type I, III, and V, and of fibronectin, which serves as a connecter between cell surface receptors and collagen. The cellular receptors for ECM molecules are heterodimeric transmembrane proteins called integrins [36]. Axonal growth cones express integrins that are activated by specific epitopes of these ECM molecules.

Functional integrin receptors consist of one α- and one β-subunit. On one hand, they interact with the actin cytoskeleton and, on the other hand, they can activate numerous intracellular signaling pathways. Among the two dozen integrins known today the β1-, αv- and α4-containing integrins are particularly important as receptors of peripheral nerve ECM. They have multiple functions, including the regulation of cell adhesion, cell motility, and differentiation [36, 37]. A synergism of neuregulin-1, expressed by axons, and the laminins in the basal lamina surrounding the Schwann cells is crucial for regulation of Schwann cell differentiation and myelination [22].

2.3.2 Surface-Mediated Cell–Cell Interactions

Several classes of molecules mediate communication between axons, Schwann cells, and other cells in the PNS. Since the late 1970s the IgG-domain containing cell adhesion molecules (CAM) are known, especially for their role in axonal growth. Important representatives are L1/Ng-CAM, N-CAM and transient axonal glycoprotein-1, which appear to support axon fasciculation and axonal growth on the surface of non-neuronal cells, including Schwann cells and fibroblasts [38–41]. Related myelin-associated glycoprotein and protein zero are present in myelin membranes and are important during myelination.

Cadherins are Ca^{2+}-binding adhesion molecules that mediate homophilic interaction between cells. Cadherins are particularly important for selective fasciculation of regenerating axons. For instance, E-cadherin mediates attachment of unmyelinated sensory fibers and stabilizes glial network [42], and N-cadherin mediates axon–Schwann cell interactions during regeneration [39, 43].

A lot of research has been done on transcriptional changes and intracellular pathways that correlate with axonal regeneration. The intricacies of lesion-induced intracellular signaling can only concern us here in so far as these pathways have been considered as targets for pharmacological intervention. Suffice it to say that Ras/ERK and PI3K cascades are primarily involved, and that Rho–type GTPases (RhoA, Rac, Cdc42) and a panel of phosphorylation-dependent transcription factors (most importantly STAT-3, ERK), determine neuronal survival, the regenerative response of the growth cones, and also are involved in the glial responses [9]. A considerable overlap and cross-talk between the intracellular signaling pathways

of all soluble and surface-bound signals has been observed – and is far from understood.

2.4 Desired Properties of the Scaffold

From the description above we can deduce some functions that artificial implants must fulfill if they are to promote nerve regeneration in vivo. A general requirement of biocompatibility, which applies to materials implanted anywhere in the body, demands that the implanted construct must not induce inflammatory reactions or tumor formation and is not rejected or encapsulated by scar tissue.

2.4.1 Mechanical Properties

In addition to biochemical signals, mechanical properties are very important because irritation of the tissue, e.g., due to stiffness of the material, may cause inflammation or fibrosis. The basic design of virtually all artificial nerve guides is a flexible tube, either hollow or filled with interior structures for nerve guidance. The choice of the material for the tube, the dimensions of its wall and lumen, as well as the filling determine its biomechanical properties. Implanted devices should have a similar degree of flexibility as the natural peripheral nerve, while at the same time they must be stable enough not to collapse. The Young's modulus of various mammalian nerves has been determined, so present day scaffolds for implantation are mechanically compatible with the surrounding tissue [5, 6].

2.4.2 Biodegradability

It is desirable that the bridge between nerve stumps remains in the body until axonal regeneration is completed. Studies with earlier implants, which were made of non-degradable materials such as silicone, showed some success, but also revealed disadvantages. The long-term presence of the material can elicit an inflammatory foreign body reaction. In several human patients, complications with silicon tube implants required follow-up surgery to remove the implants [44]. Thus, recent research studies and most clinical applications concentrate on nerve scaffolds that are gradually degraded without the release of toxic products [45, 46].

2.4.3 Permeability for Growth Factors and Gas Exchange

Since regeneration and physiological function of the restored nerve need the exchange of gases, water, and biological signals such as hormones or neurotrophins the artificial implant must be sufficiently permeable. On the other hand, osmotic

influx and swelling might reduce its lumen, thereby exerting pressure against the regenerating fibers [47]. This must be avoided.

2.4.4 Guidance of Axon Growth and Schwann Cell Migration

The central function of the implant, remains, of course, the guidance of regenerating axons from the proximal to the distal nerve segment [48]. Consequently, the growth cones have to recognize physical guidance structures, which promote axonal elongation by activating specific receptors on the cell membrane. While biochemical signaling between cells and the scaffold surface is crucial for any interaction to take place, the physical structure of the implant must not only allow infiltration of cells and growth cones but should guide regeneration in the longitudinal direction toward the distal end of the implant. Polymeric nanofibers oriented in parallel can provide ideal scaffolds in this regard. Finally, axons have to enter into the distal fascicles of the existing nerve, which have undergone Wallerian degeneration but still lead to the peripheral targets that are to be innervated again. Thus, an additional requirement is that the growing axons are not trapped inside the implant.

As mentioned above, Schwann cells are indispensable not only for the process of axonal regeneration but also for the subsequent myelination and maintenance of physiological function. Similar molecular interactions as with neurons should therefore allow migration of Schwann cells from the host into the nerve bridge.

3 Design Strategies for Artificial Nerve Bridges

With respect to the properties of the implant that will determine its success, two aspects can be distinguished: first, the physical structure of the scaffold (see Sect. 3), and second, the biochemical functions of its materials (see Sect. 4). The basic structure of all artificial nerve bridges is a tubular graft to connect the proximal with the distal peripheral nerve stump (Fig. 2).

3.1 Hollow Tubes and Multichannel Nerve Conduits

In the simplest case, a hollow cylindrical tube with a single lumen is used. The original purpose of this design was not to replace an entire nerve segment, but only to a bridge a short gap between the proximal and distal nerve stumps, when direct ligature of the respective fiber fascicles might cause a strain that would interfere with the natural process of regeneration. Different techniques have been employed for fabrication of the tube, such as melt extrusion [61], particle leaching

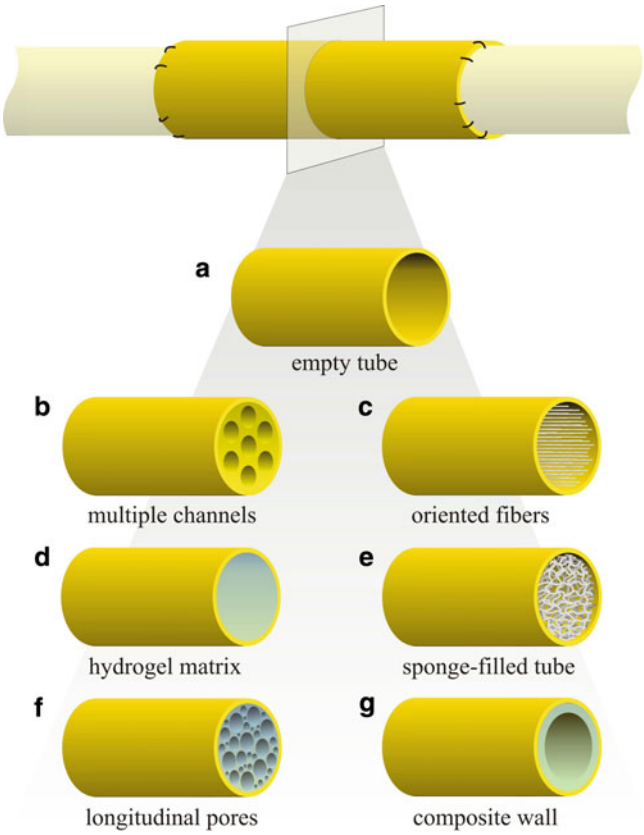

Fig. 2 Design strategies for artificial nerve bridges. (**a**) Empty tube used for bridging gaps between proximal and distal nerve stumps; (**b**) tubular implant with multiple intraluminal channels (e.g., [49–51]); (**c**) aligned microfibers as longitudinal guidance structures (e.g., [52, 53]); (**d**) hydrogel filling of the conduit (e.g., [54, 55]); (**e**) sponge filled tube (e.g., [55, 56]); (**f**) longitudinally oriented pores within the scaffold (e.g., [57, 58]); (**g**) modification of the inner side of the tube with bioactive coating (e.g., [59, 60])

[62], injection molding, and electrospinning: a variety of materials were also tested [6, 46].

Since a hollow tube is the simplest device conceivable as a nerve bridge, this type of implant was soon also tried as a long-distance connector when pieces of nerve had to be replaced. Of all designs, the empty tube has been tested by far most often in vivo (Figs. 2a and 3a, b). The tube may consist of natural (Sect. 4.1) or synthetic materials (Sect. 4.2) or composites. Although case studies with a few patients have been undertaken using more sophisticated designs [66, 67], hollow tubes constitute the only nerve guide design that has been used in larger clinical

trials so far [6, 46]. The many cell culture and animal experiments that led to the clinical studies will not be reviewed here.

3.1.1 Empty Nerve Conduits

The non-degradable tubes that were first implanted in patients, consisted of silicon [68, 69] or polytetrafluoroethylene [70, 71]. In one large study, 26 patients had suffered injuries to the median or ulnar nerves or both and received tubular silicone implants as nerve bridges. Based on sensory and motor function and pain, in 19 cases the outcome of the operation was rated very good or good; however, the implant had to be removed in seven cases because of discomfort caused by the silicone tube [72]. There are divided opinions about whether non-degradable implants are advisable because they may cause a foreign body reaction, and whether the need to remove them in a subsequent operation after regeneration is risky [68]. However, even Lundborg and colleagues who have conducted successful clinical trials with silicon tubes state a preference for biodegradable materials, provided their degradation does not cause further complications [44]. Thus, to date, biodegradable materials are the preferred solution. Three types of such tubes have been approved for implantation in humans and are commercially available. They have been tested in several hundreds of patients.

NeuraGen, consisting of type I collagen, is produced by Integra Neuroscience (www.integra-ls.com). In the largest study so far, NeuraGen implants were used mostly for bridging sensory nerves of the arm. Twenty-six patients were evaluated quantitatively to assess functional recovery of nerve transmission. In 45% of the patients an improvement of sensory functions was seen [73]. In a number of small clinical trials and case studies, the collagen implant has demonstrated its usefulness [74–77], though occasional failures were also reported [78]. In this latter report, another nerve conduit, Neurotube, was also tested, though without better outcome.

Neurotube is a poly(glycolic acid) (PGA) implant, produced by Synovis Life Technologies (www.synovismicro.com). It has been tested in several clinical studies. In one of these, a group of 46 patients received Neurotube implants for lesions of nerves innervating the hand. The results showed good to excellent outcome in 74% of the cases, which was not statistically different from a control group who received autologous nerve transplantations [79]. Other successful studies with the PGA tubes have been published, with repair of median, ulnar, and facial nerves being reported [80–82].

The third commercially available nerve scaffold is Neurolac, produced by Polyganics (www.polyganics.com). It consists of a poly(lactic acid)/poly (ε-caprolactone) blend (PLA/PCL). So far, two clinical studies and case reports have been published, with a total of 36 patients. Although in the first report from 2003 no nerve regeneration was found, the second study reported functional regeneration similar to results with autologous nerve transplants [83]. Again, failures to achieve recovery of sensory functions were reported, e.g., with digital nerve reconstruction in the foot [84].

3.1.2 Multichannel Devices

Without changing the basic design, tubular implants have been constructed to incorporate several intraluminal channels that can accommodate different fiber fascicles within a peripheral nerve (Figs. 2b and 3c, d). Multichannel implants with up to seven compartments were produced using a similar injection-molding technique as for the implant with a single lumen [49, 50]. On the level of fiber fascicles, the multichannel devices appeared to reduce mixing of regenerating axons. Necessarily, these constructs reduced the available space within the implant; and when numbers of regenerated fibers and behavioral improvement were evaluated, the multichannel constructs were no better than hollow tubes [50]. An alternative construction design achieved the similar effect of longitudinal divisions of the otherwise empty tube by integrating one or a few films into the construct. When tested in rat tibial nerves, tubes with one film, i.e., just two compartments, were better than implants with none or three films [85].

In animal experiments, many studies were performed with hollow tubular implants to assess the biocompatibility of the material. Most often, grafts were tested as bridges of the sciatic nerve, and by far most experiments were done with rats where nerve lesions rarely exceeded 20 mm. When short nerve gaps are bridged

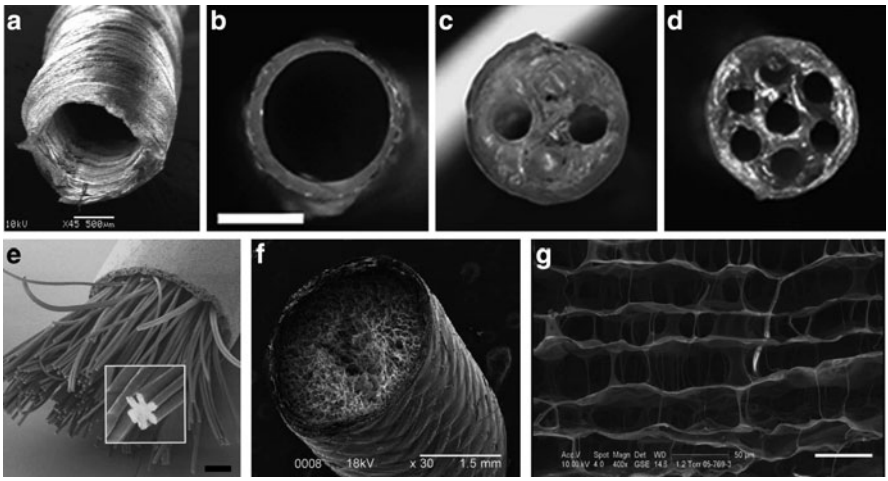

Fig. 3 Examples of artificial nerve guides that were successfully tested in animal experiments. (**a**) SEM images of a nerve tube consisting of electrospun PLGA/PCL microfibers; *scale bar* 500 μm [63]. (**b**–**d**) Collagen conduits with one or multiple interior channels were fabricated from molds with insertion of stainless wires; *scale bar* 1 mm [50]. (**e**) Composite nerve conduit of several hundred PCL filaments each having six leaflets in cross-section (*insert*); *scale bar* 150 μm [64]. (**f**) Poly(glycolic acid) tubes filled with collagen sponge were successfully used to bridge 80 mm gaps of canine peroneal nerves [65]. (**g**) Collagen scaffold produced with directional freezing; longitudinal sections demonstrate oriented channels; extensive fenestration between adjacent channels can also be seen; *scale bars* 50 μm [58]. Figures are reprinted with permission from Elsevier

with tubular implants, a fibrin matrix will fill this distance and allow infiltration of Schwann cells from the nerve stumps. These cells can then form orientated bands of Büngner, which may guide regenerating axons. Experiments with rabbits, cats, dogs, and monkeys indicate that internal guidance structures are needed for larger cell-free implants [86–88]. An extensive list of animal studies with further references is given in a recent review [89]. The construction of three-dimensional guidance structures remains a technical challenge, where polymeric nano- and microfibers take center stage.

3.2 Structured Implants with Polymeric Fibers

One successful strategy to provide such guidance structures in the longitudinal direction of the implant is the use of polymer fibers (Figs. 2c and 3e). These can be produced by a number of different techniques such as drawing, template synthesis, phase separation, self assembly, and electrospinning. Historically, large diameter fibers were tested first. Lundberg and coworkers filled silicone tubes with eight longitudinally oriented polyamide filaments of 250 μm diameter as implants. Across a 15 mm gap in the rat sciatic nerve, this device was a substantial improvement compared with hollow implants [90]. To mimic the natural situation, many more and thinner fibers would provide topological cues and induce the formation of many longitudinal strands of Schwann cells. Cell culture experiments demonstrated that small caliber fibers (5–30 μm) had a stronger effect on the orientation of growing neurites than thicker fibers (500 μm) [91]. In the context of peripheral nerve regeneration, the technique that has been used most frequently for the manufacturing of small diameter fibers is electrospinning.

3.2.1 Electrospinning of Nanofibers

As a process to produce continuous fibers with very small diameters, electrospinning has been known for more than a century. During the last two decades, the method has become increasingly popular in the field of bioengineering because the method is easy to use, very flexible with respect to fiber configuration in situ, and a great range of different materials can be used [92]. Biodegradable polymers that have been spun to nanofibers, tested in vitro, and implanted in the nervous system will be discussed below. The typical electrospinning set-up in a research laboratory consists of a high-voltage power supply (up to 30 kV), the spinneret (a syringe with a flat tip needle), and collector electrodes (Fig. 4). To induce formation of fibers, a high voltage is applied via the spinneret to the polymer solution. This causes electrostatic repulsion within the charged solution, which is stronger than its surface tension, such that a jet erupts from the spinneret. At some distance, the jet enters a stage of bending instability, is stretched under electrostatic forces toward the grounded target electrode, and the solvent evaporates. With a low

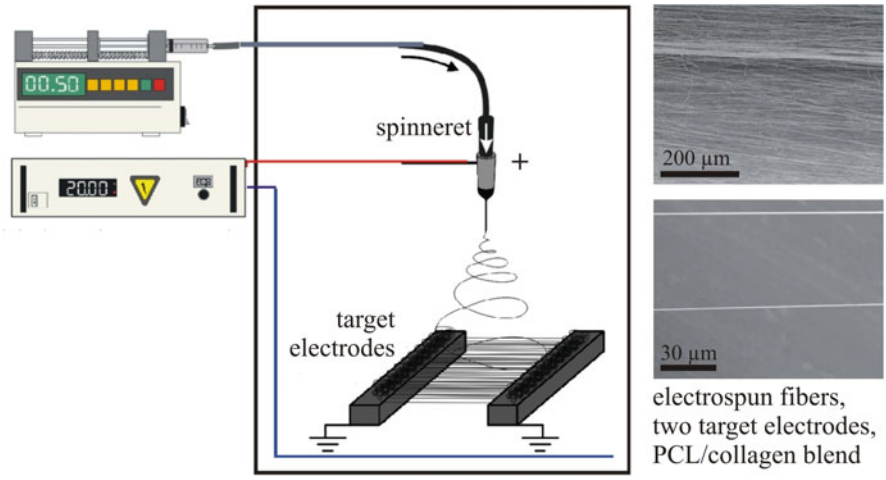

Fig. 4 Electrospinning of aligned nanofibers. The electrospinning set-up used by the authors consists of a high voltage power supply (e.g., 20 kV), the spinneret (a syringe with a flat tip needle) connected to a pump (flow rate e.g., 1 mL/h) and parallel bars as target electrodes to collect parallel fibers [93, 94]. Another frequently used device to assemble aligned fibers is the rotating drum [52, 95, 96]. Scanning electron microscopy images show PCL/collagen fibers collected between parallel bars [97]

flow rate, polymer solution is pumped through the spinneret to ensure continuous formation of fibers, which accumulate on the target. On a single plate electrode, used as a target, mats of randomly coiled fibers accumulate. Several electrospinning devices were tested in order to assemble nanofibers that are aligned in a parallel orientation. Rotating drums in different configurations were devised by several groups [52, 95, 96]. Alternatively, two parallel bars can be used as target electrodes, such that parallel fibers accumulate between them [93, 94]. Using such devices, parallel fibers of diameter from less than 100 nm to more than 5 µm can be produced from various synthetic polymers. A good review with drawings of various devices has been written by Teo and Ramakrishna [92].

Electrospun micro- and nanofibers have high surface-to-volume ratios and provide growth substrates for many neural cell types [97, 98]. Films of electrospun fibers have been used to produce tubular implants and to subdivide nerve conduits into longitudinal compartments [85]. The specific advantage of nanofibers is, of course, their property as individual guidance structures [52, 99]. In one study, PGA microfibers were incorporated in a chitosan tube as implants to bridge 30 mm gaps in the sciatic nerve of beagles. The dogs, which were investigated after 6 months, recovered function of the operated nerves. Skeletal muscles were re-innervated, and the artificial constructs were completely degraded within the half year time-frame of the study [100]. A different research team stacked films of parallel fibers consisting of poly(acrylonitrile-*co*-methylacrylate) (PAN-MA) inside a polysulfone tube. These constructs were implanted in rats to bridge sciatic nerve gaps of 17 mm. Sixteen weeks after surgery, target muscles were found to be innervated again, and

regeneration of sensory and motor nerve fibers could be demonstrated [52]. This represented a significant progress because the scientists incorporated oriented nanofibers in a three-dimensional design. The largest distance of nerve repair has been reported by Matsumoto, Toba and coworkers, who were able to bridge an 80 mm gap of the peroneal nerve in dogs [87]. Their conduits consisted of tubes of PGA/collagen blend, filled with laminin-coated collagen fibers. Regeneration was assessed histologically, electrophysiologically, and with behavioral testing. Very sophisticated guidance structures have been developed by Schlosshauer's group, who also tested functionalization with NGF, transforming growth factor-β1 (TGFβ) and laminin in their experiments. Oriented PCL filaments were made by melt extrusion using nozzles with six-leaf cross-sections. This resulted in yarns of several hundred filaments, each with six longitudinal grooves (Fig. 3e), which caused the alignment of Schwann cells, "artificial bands of Büngner" [53]. As also observed by others [93], the topographic effect of the substrate on glia cells indirectly affected the orientation of growing axons that need not have any contact with the fibers themselves.

3.2.2 Self-Assembling Peptide Scaffolds

The manufacture of self-assembling nanofibrous scaffolds is based on repetitive peptides that consist of alternating hydrophilic and hydrophobic amino acids and spontaneously form stable β-sheet structures. The self-assembling process takes place when the aequeous peptide solution is introduced to a physiological salt-containing solution (i.e., saline, tissue culture media, physiological solutions, or body fluids such as cerebrospinal fluid) and is mediated by non-covalent bonds, such as van der Waals forces, hydrogen bonds, and electrostatic forces. As a result of hydrophobic interactions, different β-sheets pack together and form double-layered β -sheet nanofibers with diameters of about 10 nm, much smaller than typical electrospun nanofibers [101, 102]. Scaffolds based on self-assembled peptides provide several advantages over other biomaterials for their potential use as bridging materials for the nervous system:

1. Their three-dimensional environment has dimensions that are similar to the native ECM in peripheral nerves.
2. The peptides can be degraded into natural L-amino acids that are nontoxic and may be recycled by surrounding cells.
3. They elicit only a minor, if any, inflammatory or immune response.
4. Modifications at the single amino acid level are possible, and various functional motifs can be added to promote neurite outgrowth.
5. The self-assembly process takes place under physiological conditions without the need of temperature changes [102, 103].

Several cell culture studies demonstrated that scaffolds made via self-assembling peptides provide permissive substrates for cell attachment and growth as well as support for extensive neurite outgrowth and synapse formation [104–106],

including the migration of Schwann cells and axonal regeneration from DRG neurites (DRG) [107]. Fewer reports have been published where such scaffolds were used in the nervous system in vivo. In one study of CNS repair, a knife wound in the visual system of 2-day-old hamsters was successfully treated by injection of peptide solution into the lesion site. Here self-assembling nanofiber scaffolds provided a permissive substrate for axonal regrowth, and visual function could be restored [106]. Peptide scaffolds implanted after spinal cord dorsal column transection injuries of rats integrated very well with the host tissue and supported the infiltration by blood vessels and axons [108]. To our knowledge, only one in vivo study focused on the potential of self-assembly nanofibers to repair a peripheral nerve [107]. In this report, a 10 mm gap of the rat sciatic nerve was successfully bridged with a tubular conduit filled with a self-assembling peptide nanofiber scaffold. The distance of axonal regrowth 3 weeks after implantation was significantly enhanced by these conduits when compared to control implants filled with alginate/fibronectin hydrogels, and recovery of gastrocnemius muscle function was also better. However, grafted Schwann cells improved the efficacy of the implants, and autologous nerve grafts still yielded the best outcome [107]. Although these investigations demonstrated that self-assembling peptide scaffolds can serve as permissive substrate in regenerative medicine, the nanofibers of these constructs lack orientation. This is a desired property for long distance guidance within an artificial nerve bridge, which is more easily achieved with the electrospinning method.

3.3 Structured Implants with Gels and Scaffolds

A completely different approach for the internal structure of implants consists in gel scaffolds with a narrow mesh of longitudinal pores or channels. Several laboratories used collagen hydrogels to fill the lumen of different nerve guides, which themselves were made from a range of biocompatible materials (Fig. 2d). Based on histology and measurements of functional recovery, such hydrogel fillings of collagen or laminin proved superior in comparison with saline-filled implants. It is interesting to note that lower concentrations of collagen- or laminin-containing gels (e.g., 1.28 mg/mL collagen, 4 mg/mL laminin) supported better functional recovery than high gel concentrations (e.g., 1.92 mg/mL collagen and 12 mg/mL laminin) [54, 109].

Scientists from the University of Kyoto constructed a sophisticated nerve conduit that consists of a polyglycolic acid tube, filled with a sponge of porcine collagen soaked with laminin (Figs. 2e and 3f) [55, 56]. Tubes of 3–4 mm inner diameter were implanted as bridges into the peroneal nerves of beagle dogs. On the basis of histological and electrophysiological evaluation, these implants were even superior to nerve autografts, although some cases of neuromas occurred [55]. Consequently, similar tubes were implanted for repair in human patients. In two women, the frontal branch of the facial nerve was restored with the construct. Five

months after surgery both were able to lift their eyebrows symmetrically. Electrophysiolgical tests showed recovery of compound muscle action potentials with normal latency [67]. This success was possible with the repair of small caliber nerves, which also showed the best prognosis using hollow tubular implants. Nevertheless, the outcome and the previous animal experiments, where bridges of up to 80 mm were implanted in dogs [56, 89], demonstrated that the inclusion of a collagen matrix was a substantial advancement.

While these results are already very impressive, additional improvement is expected with the design of gels with a fibrillar network that is oriented in the longitudinal direction of the nerve guide (Fig. 2f). One idea to achieve this is the application of strong magnetic fields that can orient collagen or fibrin matrices. Such scaffolds promoted neurite elongation from chick DRG in the desired direction [110]. In mice sciatic nerves, magnetically aligned collagen gels supported regeneration and remyelination of axons over a 6 mm gaps better than control tubes [57].

Another, very promising technique is controlled freeze drying of collagen suspensions (Fig. 3g). When solvent is caused to freeze from one side of the solutions, collagen is displaced to the side, thus resulting in walls of orientated guidance channels. The diameter of these longitudinal pores can be controlled in the range of 20–120 μm. In vitro studies have already demonstrated that such scaffolds can be easily infiltrated by Schwann cells, fibroblasts and regenerating axons, which follow the desired orientation of the scaffold [58, 111, 112]. Three-dimensional constructs produced with this method are commercially available (Matricel www.matricel.net) and have been tested successfully in animal experiments (Bozkurt et al., unpublished data).

3.4 Implantation of Cells with Artificial Nerve Bridges

The closest thing to real nerve transplants are artificial constructs that are pre-seeded with growth promoting cells, and many researcher believe that gaps longer than 30 mm will not be successfully repaired unless supporting cells are included in the scaffold [5, 113]. These cells may derive from the host organism itself or from cultures. They are intended to release physiological signals, many of which may be unknown and thus cannot be mimicked with chemical modification of the implant material. Best suited for this purpose are Schwann cells because they naturally populate the PNS, where they serve a number of important functions during regeneration. As discussed above, Schwann cells secrete the basal lamina that serves as axon guidance substrate, synthesize a host of necessary growth factors, and even participate in the phagocytotic clearance of myelin debris. Later, they are required for myelination of the regenerated fibers [8]. Unfortunately, isolation of Schwann cells from a peripheral nerve and expansion in culture are time-consuming and also carry the risk that culture conditions alter the cellular phenotype.

Other cell sources have therefore been explored as alternatives. They include olfactory ensheathing cells, embryonic stem cells, mesenchymal stem cells [6, 114], and even cell lines such as the immortalized SCTM41 Schwann cells [115]. Genetic modification has been considered for implanting cells as a constant source of growth factors. Most often, fibroblasts have been engineered with this intention, e.g., to produce neurotrophins, CNTF and FGF-2 [116, 117].

The majority of studies on PN regeneration, however, used Schwann cell primary cultures [86, 117–123]. Unfortunately, the implantation of any type of living cells is not without complications. First, the purity of the primary culture is essential because the cells must not be contaminated, e.g., by fibroblasts in a Schwann cell culture. Second, immune rejection of the cells is an issue. Heterologous transplantation poses less of a problem between inbred strains of mice and rats, but it would require immune suppression in humans. Ideally therefore, the cells would have to be taken from the same patient who requires the PN implant. For a potential therapy of CNS lesions, an interesting strategy is the preparation of olfactory ensheathing cells from the human olfactory epithelium. In many physiological respects these glial cells are similar to Schwann cells [124], and the cells could be prepared for autologous implantation. Olfactory ensheathing cells are therefore being explored as a possibility to produce better implants also for peripheral nerves [114]. Nonetheless, because of the fundamental difficulties of immune rejection when foreign tissues are implanted, we consider the development of cell-free artificial nerve bridges as an important goal. Ideally, scaffolds of different lengths and diameters could be produced in advance and stored to be implanted on demand.

4 Materials for Artificial Nerve Conduits

Biocompatible materials are needed for the two essential components of the artificial nerve bridge, i.e., the surrounding tube and its interior structure, the latter being either linear filaments or a scaffold with longitudinal pores. The selected material will determine not only the biochemical interaction between cells and graft but also the physical properties of the implant.

4.1 Natural Materials

Many natural materials are hydrophilic and show excellent biocompatibility. Proteins and carbohydrates of high molecular weight are extracted rather than synthesized chemically. On the down side, when the material is derived from mammalian tissue there is a certain risk of disease transmission and/or allergic reactions. Nevertheless, many biologically derived materials have just the desired properties for applications in nerve repair.

4.1.1 Extracellular Matrix Proteins

The most straight forward approach is to use ECM material that gives structure to the peripheral nerves in situ. Epineurium, perineurium and endoneurium consist largely of one family of ECM proteins: collagen.

Collagen

Of all biologically derived material used in bioengineering, collagen is the most popular, not only for PN conduits but for tissue reconstruction in many other applications. Collagens, which account for more than a quarter of total body protein, are extracellular proteins with a characteristic triple helix structure of three either identical or heteromeric α-chains [35]. Of at least 29 different forms, collagen I, III, and V form fibrils in the ECM of the PNS. The non-fibrillar collagen IV is present in the basement membranes secreted by Schwann cells. In vitro, collagen IV has superior qualities as a substrate for axonal growth, but the fibrillar collagen I is more often used in scaffold production. As reviewed above, collagen has been used to form tubular implants, e.g., NeuraGen [73–76]. It is also one of the materials frequently used for interior guidance structures (Fig. 3b–d, f, g): During matrix formation, collagen hydrogels can be oriented with strong magnetic fields [57], and collagen sponges combined with laminin [55, 56] or chondroitin-6-sulfate [125] were very successful as nerve guides in animal experiments. Using the directional freezing technique, scaffolds with longitudinally oriented pores were created and tested for implantation in PNS and CNS [58, 111, 112]. It is also possible to produce collagen nanofibers by electrospinning [95]. Even blends with other polymers (e.g., 25% collagen, 75% PCL) were significantly better for axon guidance and Schwann cell migration than control fibers without collagen [93].

Fibronectin

Axons and glia cells interact with the ECM via their integrin receptors. Although integrins can directly bind to some epitopes on collagen, an important intermediate molecule between collagen and the cells is the 440 kDa glycoprotein fibronectin, which is also part of the basement membrane. It is primarily produced by fibroblasts. In addition, there is a soluble dimeric form of fibronectin in the plasma, which together with fibrin has an important function in wound healing [126]. The biological activity of fibronectin has been shown to be strongly influenced by the conformation of underlying surfaces [48]. Fibronectin conduits have performed well in PN repair. For instance, tubular implants filled with a solution of fibronectin, laminin, and fibronectin/laminin mixture permitted regeneration across an 18 mm gap in rat sciatic nerves, and all of these ECM molecules promoted migration of Schwann cells into the conduit [127].

Laminin

This is the most important component of the basal lamina. Different laminins exist, all of which are large glycoproteins (500–1,000 kDa) that consist of three polypeptide chains (α, β, and γ). Applied in gels or solution together with collagen and other proteins, laminin enhanced nerve regeneration in vivo and in vitro. In addition to the whole protein, integrin-activating peptide sequences from laminin were identified that also mediate cell adhesion and growth. Well-characterized sequences are those containing Arg-Gly-Asp (RGD, in one letter code) in laminin α-chains [128]; YIGSR, located on the β1-chain; and IKVAV, which is present near the C-terminal end of the α1-chain, close to a heparin-binding domain [48]. When synthetic polymer fibers were functionalized with GRGDS, adhesion and speed of axonal growth cones and of migrating cells were significantly enhanced [98]. Laminins have already been used for a long time as substrates in cell culture experiments. The commercially available Matrigel is a non-defined ECM solution derived from a mouse sarcoma cell line. Its main component is laminin, but Matrigel also contains collagen IV, heparan sulfate proteoglycans, and several growth factors. Used as a thermoreversible gel it is liquid at low temperatures and solidifies at body temperature. As a filling in fiber containing implants, Matrigel supported regeneration in the mouse sciatic nerve. Electromagentic alignment of the material further improved the outcome [109, 121].

4.1.2 Other Natural Proteins

Fibroin (Silk)

Silk is not immunogenic and has high tensile strength, toughness, and elasticity [5]. Its core structural protein is fibroin, extracted from the cocoons of *Bombyx mori* caterpillars (silkworm). The protein exhibited good biocompatibility with Schwann cells and DRG [129]. Fibroin was used for electrospinning of nanofibers [130]. A tubular fibroin construct, filled with about 20 longitudinally aligned fibroin fibers was implanted as a 10 mm nerve bridge in rats and evaluated after 6 months. The detailed anatomical evaluation demonstrated excellent results, though autologous nerve grafts were still superior [131].

4.1.3 Polysaccharides

One risk with the implantation of foreign ECM proteins is development of scar tissue within the regenerating area. This acts as a physical barrier to axonal elongation between the nerve stumps. It appears that this problem is less likely with biocompatible polysaccharides.

Chitin and Chitosan

The exoskeleton of arthropods consists largely of chitin, which is also present in the cell walls of fungi. Second only to cellulose, chitin is the most abundant polysaccharide found in nature. The monomeric building blocks of chitin are *N*-acetyl-D-glucosamine. Chitosan, a linear copolymer of *N*-glucosamine and *N*-acetyl-D-glucosamine, is prepared via partial deacetylation of chitin. Due to similarities with glucosaminoglycans side chains of ECM glycoproteins (e.g., chondroitin sulfate, heparin sulfate, keratan sulfate), chitosan can interact with fibronectin, laminin, and collagen. It has been used extensively in biomedical applications including nerve conduits [6, 100]. In one construct, a double-layered tube was devised comprising an outer chitosan film for mechanical strength and an inner layer of electrospun chitosan fibers (Fig. 2g). In addition, extended YIGSR peptides were covalently bound to the chitosan fibers to enhance interaction with cells. As 10 mm peripheral nerve guides in rats, these constructs were successful as autografts [132, 133]. When chitosan/PLGA implants were complemented with bone marrow-derived stem cells, even 50 mm sciatic gaps in dogs could be repaired almost as well as with autologous nerve transplants [88]. Chitosan scaffolds were also prepared with longitudinal pores, which improved regeneration and functional recovery [134]. In other experiments, chitin/chitosan implants caused infiltration of many inflammatory macrophages, and modification of the material was therefore considered [135].

Alginate and Agarose

Alginate, extracted from brown seaweed, consists of repeat units of mannuronic acid and glucuronic acid. Having free carboxyl groups it can be cross-linked in the presence of calcium. Most often, alginate is used as a gel inside implanted nerve tubes [136, 137]; however, alginate gel has been used as glue to connect nerve stumps 7 mm apart [138], and hollow tubes were made of freeze-dried alginate/chitosan blend. For the delivery of a growth factor, nerve tubes were filled with alginate and implanted in a rat sciatic nerve model. This study showed that regeneration was better in empty conduits, suggesting that the presence of alginate actually impeded regeneration [139]. Agarose is also extracted from seaweed and has been used extensively for cell cultures [48]. In the context of artificial nerve implants, an interesting application has been the use of agarose as a material for creating concentration gradients of growth factors [139, 140].

Hyaluronic Acid

Another important glucosaminoglycan of the ECM in connective tissues, especially cartilage and skin, is hyaluronic acid. It consists of repeating disaccharide units of D-glucoronic acid and D-*N*-acetyl-glucosamine. For biomedical applications,

hyaluronic acid gels proved to be useful because the molecule is involved in many aspects of wound repair, including angiogenesis, reduction of scar formation, and moderation of the inflammatory reaction. A positive effect on PN regeneration was achieved with local application [141]. Hydrogels consisting of hyaluronic acid and ECM proteins were used as carrier matrix in cell-based repair strategies for the PNS [142].

4.1.4 Self-Assembling Peptide Scaffolds

As a new strategy in the design of scaffolds for nerve repair, self-assembling peptide nanofibers have already been mentioned above. They consist of natural amino acids and form a three-dimensional network of nanofibers through spontaneous self-assembly. The ability of EAK16-II (AEAEAKAKAEAEAKAK; one-letter amino acid code for Glu, Ala, Lys), a 16 amino acid peptide derived from the yeast protein zuotin, to self-assemble into a nanofibrous scaffold was observed serendipitously when the peptide was tested for its cytotoxicity in cell culture [143]. This finding has inspired the development of a number of additional self-assembling peptides including RADA16-I (AcN-RADARADARADARADA-CNH_2) and RADA16-II (AcN-RARADADARARADADA-CNH_2), in which Arg (R) and Asp (D) residues substitute Lys and Glu [104]. Studies which demonstrated the compatibility of self assembling peptides with neural tissue were cited above. In a few experiments, these were tested for nerve repair [105–107, 144]. The RADA16 self-assembling peptide solution has been developed into a commercial product intended for wound repair and three-dimensional cell cultures (3DM, www.PuraMatrix.com).

4.2 Synthetic Polymers

In comparison with biologically derived materials, synthetic polymers have several advantages and disadvantages. Since they do not need to be extracted from animal tissue they pose a lower risk of contamination and immunological reaction. Their physical and chemical properties can be better controlled and manipulated. On the other hand, synthetic materials usually do not activate specific cellular receptors and therefore do not by themselves elicit the desired cellular responses such as axonal growth or cell migration. Some materials may even be rejected or encapsulated in scar tissue.

4.2.1 Non-Degradable Materials

The first generation of tubular implants for PN repair were made of silicone rubber, which showed some success [68, 69, 72, 145]. Another non-degradable material is poly(acrylonitrile-*co*-methylacrylate) (PAN-MA). Recently, a peripheral nerve

conduit was designed by stacking oriented, electrospun PAN-MA fibers in the two halves of a longitudinally split polysulfone tube, which were resealed and implanted as a sciatic nerve bridge in rats. In the absence of additional cells or growth factors this construct supported excellent regeneration, which was monitored with histological, physiological, and behavioral methods [52]. This and other studies [85] demonstrated the advantage of three-dimensional arrays of nanofibers as guidance structures in vivo (Fig. 5). Other non-degradable materials used for nerve implants are extended poly(tetrafluoroethylene) (ePTFE, Goretex) and poly (urethane) [71]. Since non-degradable materials may cause a chronic foreign body reaction and therefore need to be removed in a second operation, they are no longer a preferred strategy for artificial nerve implants [6].

4.2.2 Aliphatic Polyesters

Perhaps the most important category of biodegradable synthetic polymers with favorable characteristics for nerve repair is that of aliphatic polyesters. The most important examples are poly(α-hydroxy acids), i.e., poly(lactic acid) (PLA, with stereoisomers PLLA, PDLA), poly(glycolic acid) (PGA), poly(lactic-*co*-glycolic acid) (PLGA), poly(ε-caprolactone) (PCL), and poly(hydroxybutyric acid) (PHB). The compounds are completely biodegradable via hydrolytic digestion, and many cell culture experiments demonstrated excellent biocompatibility with nerve tissue of PLA [147, 148], PGA [149], PLGA [88, 150, 151], PCL [93, 94, 152], and PHB [139, 140, 153]. However, they are not soluble in water, do not directly activate biological signals, so possibilities for conjugation with functional peptides are limited. For nerve bioengineering purposes, poly(α-hydroxy acids) are dissolved in non-aqueous solvents and spun to fibers that can be used as material for the nerve tube or as oriented guidance structures for growing axons and cells. Fibers can also be spun directly from the polymer melts. Often blends of different polymers or blends with biologically derived materials have been used successfully. A few important examples are given below, but, as many other studies could be cited, this selection is somewhat arbitrary.

Poly(L-lactic acid)

Cai and coworkers produced porous tubular PLA conduits, which had an internal structure of aligned PLA filaments. Ten weeks after implantation in a rat sciatic nerve lesion model, this implant supported axon regeneration and remyelination much better than silicone conduits in comparison [154]. Tubes consisting of collagen-coated PGA and braided PLA/PGA were compared in dogs for 40 mm repair of the peroneal nerve. Regeneration, including recovery of muscular function after 12 months, was best in PLA/PGA-collagen tubes, where it reached 80% of the positive control [149].

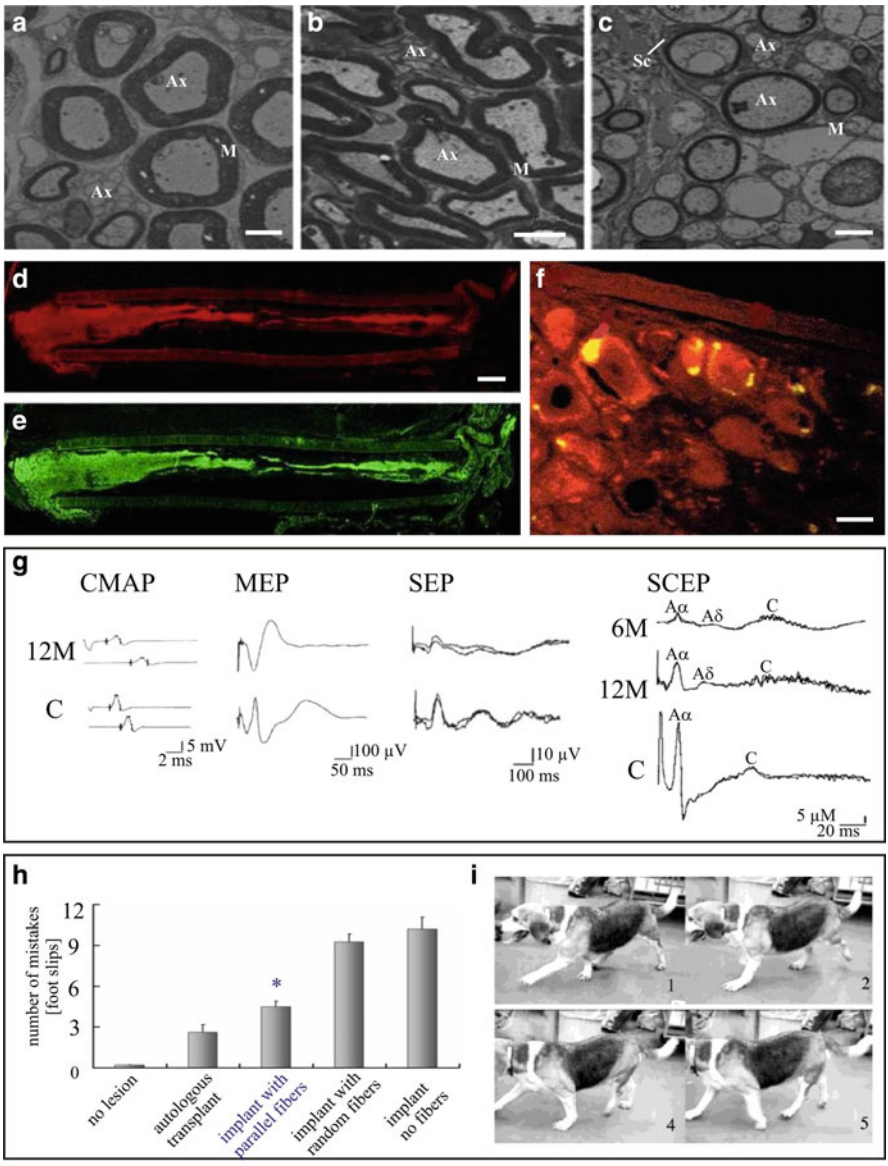

Fig. 5 Evaluation of artificial nerve implants in animal experiments. (**a**–**c**) Electron microscopy of transverse sections: (**a**) non-lesioned sciatic nerve of the rat; (**b**) regeneration in an autologous nerve transplant; (**c**) regeneration in an implant with gradients of NGF and laminin after 4 months; distance 10 mm from the transection site; *Ax* axons, *M* myelin sheaths, *Sc* Schwann cell, *scale bar* 2 µm [146]. (**d**, **e**) Immunohistochemical staining of longitudinal sections of regenerated axons in an implant with electrospun microfibers in rat sciatic nerve after 4 months: *above* neurofilament, axons; *below* S100, Schwann cells [52]. (**f**) Retrograde tracing with FluoroGold from the distal end of a chitosan/PGA implant showing axonal regeneration of sensory neurons from the dorsal root ganglion in dogs at 6 months after implantation [100]. (**g**) Electrophysiological recordings to

Poly(lactic-*co*-glycolic acid)

With electrospinning, PLGA fibers were collected on a rotating mandrel, and tubular nerve conduits from this material were tested as 10 mm bridges in the rat PNS. One month after implantation, no inflammatory response was recorded but successful regeneration was observed only in 5 of 11 rats [150]. Substantial improvements were possible with combinations of PLGA and chitosan, coated with CNTF. Histological evaluations showed that such an implant was able to induce regeneration across a 25 mm tibial nerve gap. In a canine model, the conduit was as good as the autologous nerve transplant [59].

Poly(ε-caprolactone)

Electrospun PCL fibers alone are good substrates for axonal regeneration and the migration of various glial cells [97]. These properties are significantly improved via blending with collagen [93] or covalent binding with ECM-derived peptides ([98], see below). Oliveira and coworkers seeded PCL conduits with mesenchymal stem cells and tested them for repair of median nerves in mice. Motor function after 8 weeks was assessed with a grasping test in addition to histological examination. The study demonstrated good regeneration and a positive effect of the implanted cells [155].

Poly(hydroxybutyric acid)

In experiments with a PHB conduit, excellent results were achieved when the tube was filled with a GGF-containing gel [139, 140]. In a spinal cord implantation experiment, PHB constructs showed good integration and axonal regeneration within the graft [156]. These descriptions make clear that the best results were always obtained when polymer fibers were functionalized or combined with ECM proteins (Sect. 4.3).

Fig. 5 (continued) assess functional regeneration across a gap of 80 mm in dogs after 12 months. Collagen tubes with laminin-coated fibers were implanted into the peroneal nerve. Traces are shown for compound muscle action potential (*CMAP*) of the anterior tibialis muscle after stimulation of the sciatic nerve; motor evoked potentials (*MEP*) in the tibialis muscle after electrical stimulation of the motor cortex; somatosensory evoked potentials (*SEP*) recorded from the cerebral cortex after muscle stimulation; and spinal cord evoked potentials (*SCEP*) with stimulation of the nerve stump distal to the graft [87]. (**h**) Functional demonstration of regeneration (through the implants shown in **d** and **e**) in rats. In the grid walking test the number of mistakes are counted while the rat walks across a grid. Implants with fibers orientated in parallel (*asterisk*) achieved better results than implants without or with non-orientated fibers, yet autologous nerve transplants were still better [52]. (**i**) The largest nerve gaps repaired with artificial implants, which showed recovery of motor functions, were found with dogs. Note movement of the left hind limb [56]

4.2.3 Polyphosphoesters

In addition to various aspects of biocompatibility, which they share with poly (α-hydroxy carboxylic acids), fibers of polyphosphoesters (PPE) offer the potential for coupling of bioactive molecules. PPE were therefore developed as matrices for PN implants [157]. Films of electrospun fibers of poly(caprolactone-*co*-ethyl ethylene phosphate) (PCLEEP) served also as a delivery device for NGF [96] or GDNF [60]. While it was possible to spin parallel aligned fibers of the PCL/PPE copolymer on a rotating drum, incorporation of the growth factor in the spinning solution made this difficult. When rolled films of fibers were tested as a 15 mm nerve bridge in rats, nerve regeneration was observed in all animals after 3 months, even without the growth factor. Electrophysiological examination showed a beneficial effect of the encapsulated growth factor [60].

4.2.4 Poly(ethylene glycol)

This polymer, which is non-adhesive to cells, is used to produce gels and matrices or serves as a linker for proteins. From poly(ethylene glycol), the star-shaped NCO-poly(ethylene glycol)-stat-poly(propylene glycol) (sPEG) with a backbone of 80% ethylene oxide and 20% propylene oxide has been synthesized. A range of biochemical functionalities such as isocyanate, acrylate, and vinyl sulfone can be introduced to provide the basis for covalent modification. Using sPEG with reactive isocyanate endgroups, blends of PCL and PCLdiol were functionalized with ECM-derived peptides, which improved their properties as guidance substrates for axons and Schwann cells from DRG [98, 158]. Recently, an easy method for peptide functionalization of polyester fibers via sPEG has been published, which is promising for in vivo applications [159].

4.2.5 Poly(2-hydroxyethyl methacrylate) and Related Hydrogels

Synthetic hydrogels, a prime example being poly(2-hydroxyethyl methacrylate) (pHEMA), have a very high water content after polymerization. Gels consisting of poly(HEMA-*co*-methyl methacrylate) (pHEMA-MMA) implanted in the spinal cord of adult rats integrated well. Axonal regeneration into the implant was found by 8 weeks [160]. Hydrogels can be used to make scaffolds with structured channels or to encapsulate functional molecules when growth factors are added to pHEMA sheets during polymerization in aqueous solution. A nerve tube consisting of porous pHEMA-MMA was tested in 10 mm rat sciatic nerve gaps. After 8 weeks, the outcome was similar to autografts, and after 16 weeks 60% of the artificial tubes were still comparable to this positive control [161]. In an experimental medical application, pHEMA-MMA tubes filled with collagen resulting in a gel-like outer

and porous inner structure. As implants in the adult rat sciatic nerve, such conduits were very successful over a period of 8 weeks. In long-term survival studies, however, some of these implants tended to collapse and also evoked inflammatory reactions as suggested by the presence of macrophages and giant cells in the implants after 16 weeks [162]. Copolymerization of HEMA with 2-aminoethyl methacrylate provided primary amine groups for covalent binding of laminin-derived oligopeptides. This approach was combined with physical modification of the gel, which contained multiple longitudinal channels [163].

4.2.6 Oxidized Polypyrrole

The electrically conducting polymer poly(pyrrole) (PPy) is interesting for neural applications because electrical stimulation can influence axonal growth. In one study, electrospun PLGA fibers were coated with PPy, and electrical stimulation of the conducting nanofibers enhanced neurite outgrowth [164]. This work and related pioneering studies [165] were done with a PC12 cell line, however, this has only limited predictive value for neurons in vivo. While the material properties of PPy, which was discovered in the 1960s, have been thoroughly characterized, there is still limited experience with PPy as implant material in vivo [166–168]. In a tube of combined PPy and silicone implanted to bridge a 10 mm gap in the rat, regeneration of nerve tissue was only marginally better than that in the plain silicone tube [168]. Future studies will show whether the electrical conductance of PPy and other conducting polymers (polyaniline, polythiophene) is a real advantage in PN implants in vivo.

4.3 Functionalization with ECM Proteins and Peptides

As noted above (Sect. 3.3), tubular implants and scaffolds with longitudinal pores have been made of collagen with very promising results. Similar success was obtained with artificial polymers that were blended or coated with collagen and laminin [55, 67, 149]. On the other hand, synthetic polymers proved very useful in the construction of nerve guides, not least because of their superior physical properties. For instance, many hydrophobic polymers can be spun much more easily than ECM proteins [94]. Unfortunately, they lack the specific biochemical functions involved in nerve regeneration (Sects. 2.2 and 2.3). The purpose of functionalization is therefore to endow synthetic polymers with molecular moieties that activate endogenous cells (neurons, Schwann cells, endothelial cells) in a way that promotes axonal growth. Corresponding to the distinction between secreted and surface-bound signals, two fundamental approaches have been employed: binding of ECM molecules and controlled release of soluble growth factors.

4.3.1 Blends of Synthetic Polymers with Proteins

The use of ECM molecules from the PNS is suggested because axons regenerate naturally along the basal lamina. Thus, ECM proteins or peptides are coupled to synthetic polymers either by blending, adsorption, or covalent binding [169] (Fig. 6). This should promote cells to migrate into the artificial implant and close the gap between the nerve stumps. As discussed above, the main components of the basement membrane are the trimeric laminins plus collagen IV. Fibrous collagens

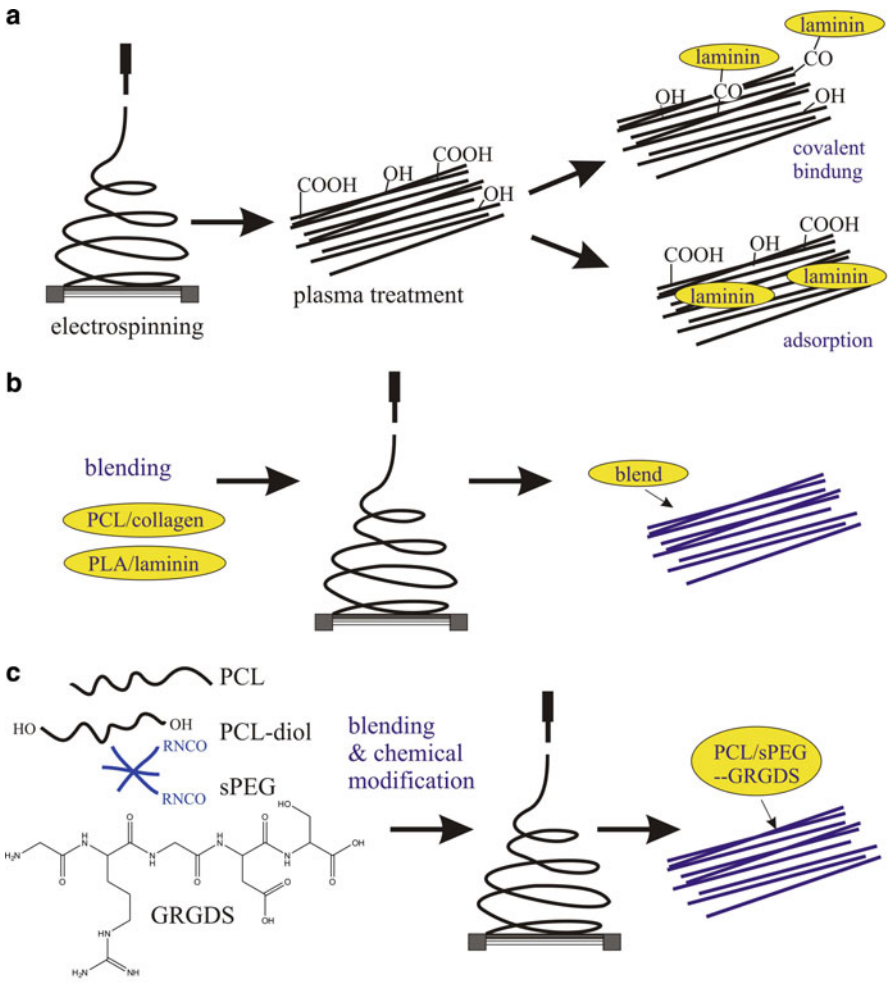

Fig. 6 Functionalization of polymer fibers for nerve regeneration. (**a**) Functionalization with adsorption or covalent binding of ECM molecules to electrospun polymer fibers [169]. (**b**) Functionalization by blending of ECM molecules with synthetic polymers before electrospinning [93]. (**c**) Functionalization by chemical bulk modification of the electrospinning solution [158]

(I, III, V) are major components of the ECM [35]. Thus, a logical strategy was to blend synthetic polymers (e.g., of PLA with laminin [169] or PCL with collagen [93, 170]) and spin this material to fibers, which could then be used for the fabrication of tubular implants or guidance structures. PLA/laminin blends and PCL/collagen blends significantly improved the surface characteristics of electrospun nanofibers in comparison with the pure synthetic polymers. Some groups were able to spin fibers of pure ECM proteins [96, 171]; however, we found it difficult to produce aligned fiber substrates of good quality with this method [94].

4.3.2 Covalent Functionalization of Polymer Fibers

Instead of whole ECM proteins, which are extracted from biological sources, specific peptide sequences from laminin, fibronectin, or collagen can be synthesized [48, 133]. Their design was made possible by the knowledge of specific amino acid sequences in the ECM that bind to integrin receptors of Schwann cells and neurons. These peptides are adhesive because of the intracellular connection of integrins to the cytoskeleton. In addition, they activate a number of signal transduction cascades within the cells [36]. So far, peptides with the amino acid sequences RGD, YIGSR, IKVAV, and longer versions of those have been successfully applied. We showed, for instance, that covalent binding of GRGDS to electrospun nanofibers of PCL improved their ability to guide axonal growth [98]. Several functionalization strategies with ECM molecules are also being tested in vivo: The interior surface of a chitosan tube was modified with various laminin peptides. As an artificial bridge of the rat sciatic nerve, the tube with one of these sequences promoted regeneration to a similar degree as a transplanted nerve, although not as well as autologous implants [133]. In addition to ECM proteins, the cell adhesion molecules (CAMs, important examples for nerve regeneration are L1, N-CAM) constitute another group of surface-bound signals that can induce axonal growth. These transmembrane proteins, which are exposed on cell membranes and are not part of the ECM, are also being considered for functionalization [172].

In conclusion, the chemical functionalization of synthetic materials with ECM molecules was an important step in the development of artificial implants with biological activities. Apart from these signals, which are always fixed to surfaces, peripheral nerve regeneration in vivo depends on a number of signals that are secreted from Schwann cells or the neurons themselves (Sect. 2.2).

4.4 Controlled Release of Growth Factors

To apply soluble factors in vivo, the first ideas were to fill implanted devices with a solution of the growth factor or with growth-factor-secreting cells. In a more sophisticated manner, carriers are incorporated that gradually release the active

molecules over longer periods. Several problems have yet to be solved [47]. For instance, the biological activity should be present for several weeks to months, especially in the case of longer nerve lesions. Also, sterilization should be possible without compromising the function of the signals. As these issues have been studied in several experiments, examples for the major paths of delivery are given below. The reader can find additional references in [89].

4.4.1 Immobilization in the Tubular Wall

A common feature of artificial nerve conduits is an outer wall in the form of a tube. Different techniques have been developed to immobilize growth factors such that they are released over time from the scaffold wall to the inside. In one study, tubes were fabricated by dip-molding from a solution of ethylene-vinyl acetate, bovine serum albumin, and FGF-2. In vitro assays revealed a burst phase of FGF release for the first 3 days (50% of total protein), which then declined to a rate of 0.1–0.5% per day. In vivo, after 4 weeks these tubes were clearly superior in bridging a 15 mm sciatic nerve gap compared to tubes without the growth factor [173]. Madduri and coworkers incorporated NGF and GDNF in conduits consisting of collagen [174] or fibroin (silk) fibers [130]. During biological degradation of the scaffold, the neurotophic factors were gradually released.

4.4.2 Growth Factors Released from Gels

Advanced conduit designs involve internal scaffolds for stabilization and guidance of the regenerating tissue. Hence, an obvious approach is to incorporate the growth factor into this polymer by mixing before gelling. This was done with NGF and NT-3 in pHEMA [175]. The growth factor can be equally distributed over the conduit or in the form a gradient to attract continued regeneration in the distal direction of the implant. In some cases, it could become a problem that axons are trapped within the chemoattractive environment of the conduit ("candy store phenomenon"). In a successful example of the gradient strategy, 40 mm gaps in the peroneal nerve of rabbits were bridged within little more than 6 weeks. This was achieved using PHB conduits filled with GGF (pro-neuregulin-1), which was suspended in alginate [140]. Neither empty nor alginate-filled tubes without GGF were able to support growth of Schwann cells or axons across the complete gap, even after 9 weeks [139]. Integration of polysaccharides into the polymer can enhance growth factor retention due to hydrophobic, electrostatic, or ionic interaction. This is a specific activation effect with heparan sulfate proteoglycans and growth factors FGF-2, VEGF, and GDNF [176, 177]. This synergistic interaction was exploited by using alginate/heparin gels as a matrix for FGF-2, which increased vascularization and faster axonal growth through the artificial implants [137]. Combining growth factors with ECM proteins was also promising. Dodla and

colleagues devised an agarose gel to apply gradients of NGF and laminin. Both gradients had a positive effect on nerve regeneration [146].

4.4.3 Microspheres as Delivery Vectors

Instead of inducing growth factors into the conduit wall or the inner matrix, they can be encapsulated in microspheres before incorporation. With this approach, the release kinetics can be tested and tuned beforehand in vitro. Microspheres of PLGA and PLA with GDNF were embedded into the inner half of a PCL-tube fabricated by dip-coating. The microspheres were formed by adding an oil-in-oil emulsion of PLA and PLGA (the latter containing GDNF) drop-wise to an aqueous solution, followed by centrifugation and lyophilization. The GDNF release kinetics observed in vitro showed a strong release of 4.6 ng GDNF per mg microsphere during the first day. The subsequent release approached zero-order kinetics and reached a cumulative release of 6.4 ng/mg microsphere at day 64. The bridging of a 15 mm rat sciatic nerve gap with this nerve conduit was much better than without the GDNF, similar to results obtained with nerve autografts [178]. In another study, nerve conduits containing PPE microspheres with NGF were successfully used to bridge a 10 mm rat sciatic nerve gap. Three months after implantation, rats with NGF-microsphere conduits showed a higher percentage of positive reflex response than controls after pinching distal nerve trunks [179].

4.4.4 Release from Electrospun Fibers

Aligned electrospun fibers, which are perhaps the most promising topological cues for axon guidance, were also used to deliver growth factors. For example, PCLEEP-fibers containing GDNF have been obtained by mixing GDNF into the polymer solution followed by electrospinning. The fibers were spun into a PCLEEP film, which was later rolled to form a tube on the inner surface of a nerve guide (Fig. 2g). Release kinetics were characterized by an initial burst of about 30% of protein followed by relatively stable release until leveling off after almost 2 months. In vivo investigations with 15 mm rat PN lesions revealed a significantly higher number of myelinated axons inside the GDNF-implant compared to the controls [60]. Recently, a conduit was designed that consisted of a PLA-*co*-PCL shell made of electrospun nanofibers filled with an NGF-containing core of bovine serum albumin. Again, when tested as a sciatic nerve bridge of 10 mm in rats, results after 12 weeks were similar to those obtained with autografts [148].

In summary many different and equally promising strategies of functionalization have been followed during the last decade (Figs. 5 and 6). Unfortunately, since there are hardly any studies that compare different strategies of functionalization, at this moment it is difficult to decide which molecules should be preferred in the future and which delivery strategy is most suitable.

5 Conclusion

In contrast to long-distance connections within the CNS such as the optic nerve or the white matter tracts of the spinal cord, lesioned peripheral nerves contain the inherent cellular and molecular components that are required to support successful axonal regeneration. The development of axon growth-promoting devices that incorporate a number of these components has become an expanding area of research. Although a number of biocompatible materials have been developed, which offer great potential for therapies of peripheral nerve injury, several technical or scientific challenges need to be addressed.

5.1 Standardized Control of Efficiency

Many experiments carried out using different biomaterials are not comparable with each other because different cell cultures, animal models, or criteria of success were used. In general, we have observed that a considerable number of publications reporting innovative materials failed to use appropriate biological tests. Papers falling into this category have not been discussed in the present review. Even in many animal studies, the inflammatory reactions, effects on gene expression, and long-term results are rarely investigated. Clearly, a systematic approach with internationally agreed standards would be desirable for such investigations to allow a better degree of comparison.

5.2 Structured Three-Dimensional Implants

So far, most studies of PN regeneration in vivo have only implanted hollow tubes, where axons start to grow on the inner surface of the implant. Thus a major technical challenge is the construction of three-dimensional nerve bridges with an internal architecture that is capable of guiding axonal growth and migration of the endogenous Schwann cells. In our opinion, the most promising approaches are the three-dimensional integration of microfibers in parallel orientation and the production of orientated channels in gels or matrices of ECM proteins.

5.3 Biomimetic Functionalization of Implants

With the use of proteins and peptides derived from ECM, artificial implants can already mimic the signals that regenerating axons encounter in the environment of the lesioned PNS. However, the concept of targeted use of factors that specifically

activate Schwann cells, sensory neurons, or motor neurons is still in its infancy. In addition to the selection of the appropriate combination of molecular signals, the ideal temporal and spatial presentation of such molecules for the efficient support of axon regeneration and tissue repair remains unknown. In this context, it is possible that neurotrophic signals might be required for several months and with increasing gradients towards the distal end of the implant.

5.4 The Thirty Millimeter Mark

Studies have demonstrated that peripheral nerve regeneration through artificial implants can cover distances of up to 30 mm but rarely beyond. Successful motor fiber regeneration appears to be more difficult than that of sensory axons, and thin fascicles regenerate more easily than large caliber nerves. Since larger gaps must occasionally be bridged in cases of human nerve injury, the usefulness of future constructs will be judged by their ability to support motor and sensory axon regeneration over long distances. For this, it is likely that experiments with animals larger than the rat will be required. We are convinced that results from basic research on mechanisms of axonal growth in combination with engineering methods (such as electrospinning, freeze-drying, and chemical functionalization) will result in further progress, with the development of artificial nerve implants that approach or even exceed the efficiency of the autograft. Some very substantial advances have already been made in the last few years. Thus, there is great hope and expectation that such strategies will provide the neurosurgeon with a range of cell-free scaffolds that can be used on demand.

Acknowledgment A research project to develop an artificial nerve implant, conducted by JM and GB, is supported by the Deutsche Forschungsgemeinschaft (ME 1261/11-1).

References

1. Sunderland S (1951) Brain 74:491
2. Pabari A, Yang SY, Seifalian AM, Mosahebi A (2010) J Plast Reconstr Aesthet Surg 63:1941
3. Brenner MJ, Hess JR, Myckatyn TM, Hayashi A, Hunter DA, Mackinnon SE (2006) Laryngoscope 116:1685
4. Meek MF, Varejao AS, Geuna S (2004) Tissue Eng 10:1027
5. Deumens R, Bozkurt A, Meek MF, Marcus MAE, Joosten EAJ, Weis J, Brook GA (2010) Prog Neurobiol 92:245
6. Gu X, Ding F, Yang Y, Liu J (2011) Prog Neurobiol 93:204
7. Sulaiman OAR, Boyd JG, Gordon T (2005) Axonal regeneration in the peripheral nervous system of mammals. In: Kettenmann H, Ransom BR (eds) Neuroglia. Oxford University Press, Oxford, pp 454–466
8. Boyd JG, Gordon T (2003) Mol Neurobiol 27:277
9. Makwana M, Raivich G (2005) FEBS J 272:2628

10. Sendtner M, Stöckli KA, Thoenen H (1992) J Cell Biol 118:139
11. Heumann R, Korsching S, Bandtlow C, Thoenen H (1987) J Cell Biol 104:1623
12. Shadiack AM, Sun Y, Zigmond RE (2001) J Neurosci 21:363
13. Kanje M, Skottner A, Lundborg G, Sjoberg J (1991) Brain Res 563:285
14. Huang EJ, Reichardt LF (2001) Annu Rev Neurosci 24:677
15. Sendtner M, Kreutzberg GW, Thoenen H (1990) Nature 345:440
16. Glazner GW, Lupien S, Miller JA, Ishii DN (1993) Neuroscience 54:791
17. Emel E, Ergun SS, Kotan D, Gursoy EB, Parman Y, Zengin A, Nurten A (2011) J Neurosurg 114:522
18. Gordon T (2010) J Commun Disord 43:265
19. Hoyle GW, Mercer EH, Palmiter RD, Brinster RL (1993) Neuron 10:1019
20. Trupp M, Rydén M, Jörnvall H, Funakoshi H, Timmusk T, Arenas E, Ibánez CF (1995) J Cell Biol 130:137
21. Keast JR, Forrest SL, Osborne PB (2010) J Comp Neurol 518:3024
22. Nave KA, Salzer JL (2006) Curr Opin Neurobiol 16:492
23. Citri A, Skaria KB, Yarden Y (2003) Exp Cell Res 284:54
24. Carroll SL, Miller ML, Frohnert PW, Kim SS, Corbett JA (1997) J Neurosci 17:1642
25. Panaite PA, Barakat-Walter I (2010) J Neurosci Res 88:1751
26. Zhelyaznik N, Schrage K, McCaffery P, Mey J (2003) Eur J Neurosci 18:1033
27. Zhelyaznik N, Mey J (2006) Neuroscience 141:1761
28. Taha MO, Rosseto M, Fraga MM, Mueller SF, Fagundes DJ, Novo NF, Caricati-Neto A (2004) Transpl Proc 36:404
29. Corcoran J, Maden M (1999) Nat Neurosci 2:307
30. Corcoran J, Shroot B, Pizzey J, Maden M (2000) J Cell Sci 113:2567
31. Latasa J-J, Ituero M, Moran-González A, Aranda A, Cosgaya JM (2010) Glia 58:1451
32. Murakami M, Simons M (2008) Curr Opin Hematol 15:215
33. Pola R, Aprahamian TR, Bosch-Marce M, Curry C, Gaetani E, Flex A, Smith RC, Isner JM, Losordo DW (2004) Neurobiol Aging 25:1361
34. Pan HC, Wu HT, Cheng FC, Chen CH, Sheu ML, Chen CJ (2009) Biochem Biophys Res Commun 382:177
35. Koopmans G, Hasse B, Sinis N (2009) Int Rev Neurobiol 87:363
36. Geiger B, Bershadsky A, Pankov R, Yamada KM (2001) Nat Rev Mol Cell Biol 2:794
37. Hynes RO (1992) Cell 69:11
38. Martini R, Schachner M (1988) J Cell Biol 106:1735
39. Bixby JL, Lilien J, Reichardt LF (1988) J Cell Biol 107:353
40. Martini R (1994) J Neurocytol 23:1
41. Soares S, Traka M, von Boxberg Y, Bouquet C, Karagogeos D, Nothias F (2005) Eur J Neurosci 21:1169
42. Hasegawa M, Seto A, Uchiyama N, Kida S, Yamashima T, Yamashita J (1996) J Neuropathol Exp Neurol 55:424
43. Thornton MR, Mantovani C, Birchall MA, Terenghi G (2005) J Anat 206:69
44. Dahlin L, Lundborg G (2001) J Hand Surg Br 26:393
45. Meek MF, Jansen K (2009) J Biomed Mater Res A 89:734
46. Meek MF, Coert JH (2008) Ann Plast Surg 60:466
47. de Ruiter GC, Malessy MJ, Yaszemski MJ, Windebank AJ, Spinner RJ (2009) Neurosurg Focus 26:E5
48. Dalton PD, Mey J (2009) Front Biosci 14:769
49. de Ruiter GC, Spinner RJ, Malessy MJ, Moore MJ, Sorenson EJ, Currier BL, Yaszemski MJ, Windebank AJ (2008) Neurosurgery 63:144
50. Yao L, de Ruiter GC, Wang H, Knight AM, Spinner RJ, Yaszemski MJ, Windebank AJ, Pandit A (2010) Biomaterials 31:5789
51. Yao L, Windebank AJ, Pandit A (2010) J Biomater Sci Polym Ed 21:1081
52. Kim YT, Haftel VK, Kumar S, Bellamkonda RV (2008) Biomaterials 29:3117

53. Ribeiro-Resende VT, Koenig B, Nichterwitz S, Oberhoffner S, Schlosshauer B (2009) Biomaterials 30:5251
54. Labrador RO, Buti M, Navarro X (1998) Exp Neurol 149:243
55. Inada Y, Morimoto S, Takakura Y, Nakamura T (2004) Neurosurgery 55:640
56. Toba T, Nakamura T, Shimizu Y, Matsumoto K, Ohnishi K, Fukuda S, Yoshitani M, Ueda H, Hori Y, Endo K (2001) J Biomed Mater Res 58:622
57. Ceballos D, Navarro X, Dubey N, Wendelschafer-Crabb G, Kennedy WR, Tranquillo RT (1999) Exp Neurol 158:290
58. Möllers S, Heschel I, Damink LH, Schugner F, Deumens R, Muller B, Bozkurt A, Nava JG, Noth J, Brook GA (2009) Tissue Eng A 15:461
59. Shen H, Shen ZL, Zhang PH, Chen NL, Wang YC, Zhang ZF, Jin YQ (2010) J Biomed Mater Res B Appl Biomater 95:161
60. Chew SY, Mi R, Hoke A, Leong KW (2007) Adv Funct Mat 17:1288
61. Chiono V, Vozzi G, Vozzi F, Salvadori C, Dini F, Carlucci F, Arispici M, Burchielli S, Di SF, Geuna S, Fornaro M, Tos P, Nicolino S, Audisio C, Perroteau I, Chiaravalloti A, Domenici C, Giusti P, Ciardelli G (2009) Biomed Microdevices 11:1037
62. Bian YZ, Wang Y, Aibaidoula G, Chen GQ, Wu Q (2009) Biomaterials 30:217
63. Panseri S, Cunha C, Lowery J, Del Carro U, Taraballi F, Amadio S, Vescovi A, Gelain F (2008) BMC Biotechnol 8:39
64. Whitlock EL, Tuffaha SH, Luciano JP, Yan Y, Hunter DA, Magill CK, Moore AM, Tong AY, Mackinnon SE, Borschel GH (2009) Muscle Nerve 39:787
65. Nakamura T, Inada Y, Fukuda S, Yoshitani M, Nakada A, Itoi S, Kanemaru S, Endo K, Shimizu Y (2004) Brain Res 1027:18
66. Fan W, Gu J, Hu W, Deng A, Ma Y, Liu J, Ding F, Gu X (2008) Microsurgery 28:238
67. Inada Y, Hosoi H, Yamashita A, Morimoto S, Tatsumi H, Notazawa S, Kanemaru S, Nakamura T (2007) Neurosurgery 61:E1105–E1107
68. Lundborg G, Rosen B, Dahlin L, Danielsen N, Holmberg J (1997) J Hand Surg Am 22:99
69. Lundborg G, Rosen B, Dahlin L, Holmberg J, Rosen I (2004) J Hand Surg Br 29:100
70. Pitta MC, Wolford LM, Mehra P, Hopkin J (2001) J Oral Maxillofac Surg 59:493
71. Stanec S, Stanec Z (1998) Br J Plast Surg 51:637
72. Braga-Silva J (1999) J Hand Surg Br 24:703
73. Wangensteen KJ, Kalliainen LK (2009) J Hand NY 5:273
74. Ashley WW Jr, Weatherly T, Park TS (2006) J Neurosurg 105:452
75. Farole A, Jamal BT (2008) J Oral Maxillofac Surg 66:2058
76. Taras JS, Jacoby SM (2008) Tech Hand Up Extrem Surg 12:100
77. Lohmeyer J, Zimmermann S, Sommer B, Machens HG, Lange T, Mailänder P (2007) Chirurg 78:142
78. Moore AM, Kasukurthi R, Magill CK, Farhadi HF, Borschel GH, Mackinnon SE (2009) Hand NY 4:180
79. Weber RA, Breidenbach WC, Brown RE, Jabaley ME, Mass DP (2000) Plast Reconstr Surg 106:1036
80. Agnew SP, Dumanian GA (2010) J Hand Surg Am 35:838
81. Donoghoe N, Rosson GD, Dellon AL (2007) Microsurgery 27:595
82. Navissano M, Malan F, Carnino R, Battiston B (2005) Microsurgery 25:268
83. Bertleff MJ, Meek MF, Nicolai JP (2005) J Hand Surg Am 30:513
84. Meek MF, Nicolai JP, Robinson PH (2006) J Reconstr Microsurg 22:149
85. Clements IP, Kim Y-T, English AW, Lu X, Chung A, Bellamkonda RV (2009) Biomaterials 30:3834
86. Brown RE, Erdmann D, Lyons SF, Suchy H (1996) J Reconstr Microsurg 12:149
87. Matsumoto K, Ohnishi K, Kiyotani T, Sekine T, Eng HUM, Nakamura T, Endo K, Shimizu Y (2000) Brain Res 868:315
88. Ding F, Wu J, Yang Y, Hu W, Zhu Q, Tang X, Liu J, Gu X (2010) Tissue Eng A 16:3779
89. Siemionow M, Bozkurt M, Zor F (2010) Microsurgery 30:574

90. Lundborg G, Dahlin L, Dohi D, Kanje M, Terada N (1997) J Hand Surg Br 22:299
91. Smeal RM, Rabbitt R, Biran R, Tresco PA (2005) Ann Biomed Eng 33:376
92. Teo WE, Ramakrishna S (2006) Nanotechnology 17:R89–R106
93. Schnell E, Klinkhammer K, Balzer S, Brook GA, Klee D, Dalton PD, Mey J (2007) Biomaterials 28:3012
94. Klinkhammer K, Seiler N, Grafahrend D, Mey J, Brook GA, Möller M, Dalton PD, Klee D (2009) Tissue Eng 15:77
95. Matthews JA, Wnek GE, Simpson DG, Bowlin GL (2002) Biomacromolecules 3:232
96. Chew SY, Wen J, Yim EK, Leong KW (2005) Biomacromolecules 6:2017
97. Gerardo-Nava J, Führmann T, Klinkhammer K, Seiler N, Mey J, Klee D, Möller M, Dalton PD, Brook GA (2008) Nanomedicine 4:11
98. Bockelmann J, Klinkhammer K, von Holst A, Seiler N, Faissner A, Brook GA, Klee D, Mey J (2011) Tissue Eng A 17:475
99. Lietz M, Dreesmann L, Hoss M, Oberhoffner S, Schlosshauer B (2006) Biomaterials 27:1425
100. Wang X, Hu W, Cao Y, Yao J, Hu J, Gu X (2005) Brain 128:1897
101. Cao H, Liu T, Chew SY (2009) Adv Drug Deliv Rev 61:1055
102. Gelain F, Horii A, Zhang S (2007) Macromol Biosci 7:544
103. Gelain F, Unsworth LD, Zhang S (2010) J Control Release 145:231
104. Holmes TC, de Lacalle S, Su X, Liu G, Rich A, Zhang S (2000) Proc Natl Acad Sci USA 97:6728
105. Silva GA, Czeisler C, Niece KL, Beniash E, Harrington DA, Kessler JA, Stupp SI (2004) Science 203:1352
106. Ellis-Behnke RG, Liang YX, You SW, Tay DK, Zhang S, So KF, Schneider GE (2006) Proc Natl Acad Sci USA 103:5054
107. McGrath AM, Novikova LN, Novikov LN, Wiberg M (2010) Brain Res Bull 83:207
108. Guo J, Su H, Zeng Y, Liang YX, Wong WM, Ellis-Behnke RG, So KF, Wu W (2007) Nanomedicine 3:311
109. Verdu E, Labrador RO, Rodriguez FJ, Ceballos D, Fores J, Navarro X (2002) Restor Neurol Neurosci 20:169
110. Dubey N, Letourneau PC, Tranquillo RT (1999) Exp Neurol 158:338
111. Bozkurt A, Brook GA, Moellers S, Lassner F, Sellhaus B, Weis J, Woeltje M, Tank J, Beckmann C, Fuchs P, Damink LO, Schugner F, Heschel I, Pallua N (2007) Tissue Eng 13:2971
112. Bozkurt A, Deumens R, Beckmann C, Olde Damink L, Schugner F, Heschel I, Sellhaus B, Weis J, Jahnen-Dechent W, Brook GA, Pallua N (2009) Biomaterials 30:169
113. Hood B, Levene HB, Levi AD (2009) Neurosurg Focus 26:E4
114. Radtke C, Wewetzer K, Reimers K, Vogt PM (2011) Cell Transplant 20:145–152
115. Lago N, Casas C, Muir EM, Rogers J, Navarro X (2009) Restor Neurol Neurosci 27:67
116. Schmidt CE, Baier Leach J (2003) Annu Rev Biomed Eng 5:293
117. Sørensen J, Haase G, Krarup C, Gilgenkrantz H, Kahn A, Schmalbruch H (1998) Ann Neurol 43:205
118. Radtke C, Akiyama Y, Lankford KL, Vogt PM, Krause DS, Kocsis JD (2005) Neurosci Lett 387:85
119. Guenard V, Kleitman N, Morrissey TK, Bunge RP, Aebischer P (1992) J Neurosci 12:3310
120. Kim DH, Connolly SE, Kline DG, Voorhies RM, Smith A, Posell M, Yoes T, Daniloff JK (1994) J Neurosurg 80:254
121. Lohmeyer JA, Shen ZL, Walter GF, Berger A (2007) Int J Artif Organs 30:64
122. Sinis N, Schaller HE, Becker ST, Schlosshauer B, Doser M, Roesner H, Oberhoffner S, Muller HW, Haerle M (2007) Restor Neurol Neurosci 25:131
123. May F, Weidner N, Matiasek K, Caspers C, Mrva T, Vroemen M, Henke J, Lehmer A, Schwaibold H, Erhardt W, Gänsbacher B, Hartung R (2004) J Urol 172:374
124. Kawaja MD, Boyd JG, Smithson LJ, Jahed A, Doucette R (2009) J Neurotrauma 26:155
125. Chamberlain LJ, Yannas IV, Hsu HP, Strichartz G, Spector M (1998) Exp Neurol 154:315

126. Pankov R, Yamada KM (2002) J Cell Sci 115:3861
127. Bailey SB, Eichler ME, Villadiego A, Rich KM (1993) J Neurocytol 22:176
128. Hersel U, Dahmen C, Kessler H (2003) Biomaterials 24:4385
129. Yang Y, Chen X, Ding F, Zhang P, Liu J, Gu X (2007) Biomaterials 28:1643
130. Madduri S, Papaloizos M, Gander B (2010) Biomaterials 31:2323
131. Yang Y, Ding F, Wu J, Hu W, Liu W, Liu J, Gu X (2007) Biomaterials 28:5526
132. Itoh S, Matsuda A, Kobayashi H, Ichinose S, Shinomiya K, Tanaka J (2005) J Biomed Mater Res B Appl Biomater 73:375
133. Wang W, Itoh S, Matsuda A, Aizawa T, Demura M, Ichinose S, Shinomiya K, Tanaka J (2008) J Biomed Mater Res A 85:919
134. Huang J, Lu L, Hu X, Ye Z, Peng Y, Yan X, Geng D, Luo Z (2010) Neurorehabil Neural Repair 24:736
135. Yang Y, Gu X, Tan R, Hu W, Wang X, Zhang P, Zhang T (2004) Biotechnol Lett 26:1793
136. Suzuki K, Suzuki Y, Ohnishi K, Endo K, Tanihara M, Nishimura Y (1999) Neuroreport 10:2891
137. Ohta M, Suzuki Y, Chou H, Ishikawa N, Suzuki S, Tanihara M, Suzuki Y, Mizushima Y, Dezawa M, Ide C (2004) J Biomed Mater Res A 71:661
138. Suzuki K, Suzuki Y, Tanihara M, Ohnishi K, Hashimoto T, Endo K, Nishimura Y (2000) J Biomed Mater Res 49:528
139. Mohanna PN, Young RC, Wiberg M, Terenghi G (2003) J Anat 203:553
140. Mohanna PN, Terenghi G, Wiberg M (2005) Scand J Plast Reconstr Surg Hand Surg 39:129
141. Ozgenel GY (2003) Microsurgery 23:575
142. Suri S, Schmidt CE (2010) Tissue Eng A 16:1703
143. Zhang S, Holmes T, Lockshin C, Rich A (1993) Proc Natl Acad Sci USA 90:3334
144. Rafiuddin AM, Jayakumar R (2003) Brain Res 993:208
145. Lundborg G, Dahlin LB, Danielsen N, Gelberman RH, Longo FM, Powell HC, Varon S (1982) Exp Neurol 76:361
146. Dodla MC, Bellamkonda RV (2008) Biomaterials 29:33
147. Yang F, Murugan R, Wang S, Ramakrishna S (2005) Biomaterials 26:2603
148. Liu JJ, Wang CY, Wang JG, Ruan HJ, Fan CY (2011) J Biomed Mater Res A 96:13
149. Ichihara S, Inada Y, Nakada A, Endo K, Azuma T, Nakai R, Tsutsumi S, Kurosawa H, Nakamura T (2009) Tissue Eng C Meth 15:387
150. Bini TB, Gao S, Tan TC, Wang S, Lim A, Hai LB, Ramakrishna S (2004) Nanotechnology 15:1459
151. Yucel D, Kose GT, Hasirci V (2010) Biomaterials 31:1596
152. Wang S, Yaszemski MJ, Knight AM, Gruetzmacher JA, Windebank AJ, Lu L (2009) Acta Biomater 5:1531
153. Aberg M, Ljungberg C, Edin E, Millqvist H, Nordh E, Theorin A, Terenghi G, Wiberg M (2009) J Plast Reconstr Aesthet Surg 62:1503
154. Cai J, Peng X, Nelson KD, Eberhart R, Smith GM (2005) J Biomed Mater Res A 75:374
155. Oliveira JT, Almeida FM, Biancalana A, Baptista AF, Tomaz MA, Melo PA, Martinez AM (2010) Neuroscience 170:1295
156. Novikova LN, Pettersson J, Brohlin M, Wiberg M, Novikov LN (2008) Biomaterials 29:1198
157. Wang S, Wan AC, Xu X, Gao S, Mao HQ, Leong KW, Yu H (2001) Biomaterials 22:1157
158. Klinkhammer K, Bockelmann J, Simitzis C, Brook GA, Grafahrend D, Groll J, Möller M, Mey J, Klee D (2010) J Mater Sci Mater Med 21:2637
159. Grafahrend D, Heffels KH, Beer MV, Gasteier P, Moller M, Boehm G, Dalton PD, Groll J (2011) Nat Mater 10:67
160. Tsai EC, Dalton PD, Shoichet MS, Tator CH (2004) J Neurotrauma 21:789
161. Belkas JS, Munro CA, Shoichet MS, Midha R (2005) Restor Neurol Neurosci 23:19
162. Belkas JS, Munro CA, Shoichet MS, Johnston M, Midha R (2005) Biomaterials 26:1741
163. Yu TT, Shoichet MS (2005) Biomaterials 26:1507
164. Lee JY, Bashur CA, Goldstein AS, Schmidt CE (2009) Biomaterials 30:4325

165. Gomez N, Schmidt CE (2007) J Biomed Mater Res A 81:135
166. Schmidt CE, Shastri VR, Vacanti JP, Langer R (1997) Proc Natl Acad Sci USA 94:8948
167. George PM, Saigal R, Lawlor MW, Moore MJ, LaVan DA, Marini RP, Selig M, Makhni M, Burdick JA, Langer R, Kohane DS (2009) J Biomed Mater Res A 91:519
168. Wang X, Gu X, Yuan C, Chen S, Zhang P, Zhang T, Yao J, Chen F, Chen G (2004) J Biomed Mater Res A 68:411
169. Koh HS, Yong T, Chan CK, Ramakrishna S (2008) Biomaterials 29:3574
170. Zhang YZ, Venugopal J, Huang ZM, Lim CT, Ramakrishna S (2005) Biomacromolecules 6:2583
171. Heydarkhan-Hagvall S, Schenke-Layland K, Dhanasopon AP, Rofail F, Smith H, Wu BM, Shemin R, Beygui RE, Maclellan WR (2008) Biomaterials 29:2907
172. Webb K, Budko E, Neuberger TJ, Chen S, Schachner M, Tresco PA (2001) Biomaterials 22:1017
173. Aebischer P, Salessiotis AN, Winn SR (1989) J Neurosci Res 23:282
174. Madduri S, Feldman K, Tervoort T, Papaloizos M, Gander B (2010) J Control Release 143:168
175. Moore K, MacSween M, Shoichet M (2006) Tissue Eng 12:267
176. Forsten-Williams K, Chu CL, Fannon M, Buczek-Thomas JA, Nugent MA (2008) Ann Biomed Eng 36:2134
177. Barnett MW, Fisher CE, Perona-Wright G, Davies JA (2002) J Cell Sci 115:4495
178. Kokai LE, Bourbeau D, Weber DJ, McAtee J, Marra K (2011) Tissue Eng Part A 17:1263–1275
179. Xu X, Yee WC, Hwang PY, Yu H, Wan AC, Gao S, Boon KL, Mao HQ, Leong KW, Wang S (2003) Biomaterials 24:2405

Adv Polym Sci (2012) 246: 171–212
DOI: 10.1007/12_2011_141

Published online: 14 September 2011

Highly Aligned Polymer Nanofiber Structures: Fabrication and Applications in Tissue Engineering

Vince Beachley, Eleni Katsanevakis, Ning Zhang, and Xuejun Wen

Abstract Many types of tissue in the body, such as nerve, muscle, tendon, ligament, bone, and blood vessels, rely on a highly organized microstructure in order to impart their desired functionality. Cell and extracellular matrix (ECM) alignment in these tissues allows for increased mechanical strength and cell communication. In tissue engineering, aligned polymer nanofibers can be used to take on the role of natural ECM fibers in order to provide mechanical strength, sites for cell attachment, and modulation of cell behavior via morphological cues. A wide variety of physical and electrostatic techniques are available for assembly of aligned

V. Beachley and E. Katsanevakis
Clemson-MUSC Bioengineering Program, Department of Bioengineering, Clemson University, Charleston, SC 29425, USA

N. Zhang
Clemson-MUSC Bioengineering Program, Department of Bioengineering, Clemson University, Charleston, SC 29425, USA

Department of Microbiology and Immunology, Medical University of South Carolina, Charleston, SC 29425, USA

X. Wen (✉)
Clemson-MUSC Bioengineering Program, Department of Bioengineering, Clemson University, Charleston, SC 29425, USA

Department of Regenerative Medicine and Cell Biology, Medical University of South Carolina, Charleston, SC 29425, USA

Department of Orthopedic Surgery, Medical University of South Carolina, Charleston, SC 29425, USA

The Institute for Advanced Materials and Nano Biomedicine (iNANO), Tongji University, Shanghai 200072, People's Republic of China
e-mail: xjwen@clmson.edu

nanofiber structures, and many of these structures have been evaluated as tissue engineering scaffolds. It is widely understood that aligned microstructure induces an aligned morphology in most cell types, but aligned nanofibrous topography also influences other cell behaviors such as differentiation, gene expression, and ECM deposition. With a greater understanding of aligned nanofiber scaffold fabrication techniques, and cell interactions with these scaffolds, researchers may be able to overcome current challenges and develop better strategies for regenerating aligned tissues.

Keywords Characterization · Contact guidance · Fabrication · Nanofibers · Regeneration · Scaffold · Tissue engineering

Contents

1 Introduction

Natural tissues have a fibrous extracellular matrix (ECM) component made up of collagen, elastin, keratin, or other similar types of natural nanofibers. This nanofibrous ECM provides mechanical strength, storage locations for biomolecules, and structural support for cell attachment and organization. It also serves as a template for tissue formation during development, regeneration, and remodeling. For example, ECM deposition precedes cell migration in embryonic branching morphogenesis; nerve cells grow along aligned ECM tubes in peripheral nerve regeneration; and hydroxyapatite calcifies on collagen nanofibers to form bone during remodeling [1–3]. Polymeric nanofibers have received a great amount of attention in recent years due to their potential to fill some of the roles of ECM nanofibers in tissue engineering. Polymeric nanofibers have proven to be excellent substrates for cell attachment and growth, and the microstructure of polymeric nanofiber grafts can predictably modulate cell behaviors such as morphology, differentiation, ECM deposition, and migration [4]. In addition, the bioactivity of polymer nanofibers can easily be optimized due to a wide variety of available molecular compositions, methods of biomolecule incorporation, and surface modification techniques.

Many types of tissue, such as muscle, nerve, blood vessel, and connective tissue, require a well-aligned cellular and ECM organization for proper tissue function. Nerves are able to transmit signals throughout the body quickly through long well-aligned axons, and muscles, blood vessels, bone, tendons, and ligaments are able to apply and resist loads efficiently due to the aligned organization of cells and ECM fibers. Cells that are cultured in vitro on aligned nanofibrous scaffolds adopt an aligned elongated morphology that mimics the natural morphology of cell in aligned tissues in vivo. In addition to cell shape and organization, aligned nanofiber substrates have shown the ability to modulate cell behaviors such as differentiation, migration, and ECM assembly. It is of the highest importance that a tissue engineering scaffold used to mimic aligned tissues is able to impart uniaxial alignment in its resident cells in order to induce biomimetic organization and desired cellular responses. Challenges in tissue engineering applications of aligned nanofiber scaffolds include optimizing substrate topographical cues to promote desired cell responses and designing scaffolds with architecture conductive to the formation of tissue-like structures in vitro and in vivo.

Methods associated with many different fiber fabrication techniques are available for production of aligned nanofibers. However, the vast majority of research in this field is focused on aligned nanofiber fabrication using electrospinning. An overview of current aligned fiber fabrication technologies is presented, as well as a more detailed review of aligned fiber fabrication using the electrospinning technique. Cell interactions with aligned as compared to randomly oriented nanofibrous topographies are presented as well as specific tissue engineering applications of aligned nanofibrous scaffolds.

2 Methods of Fabricating Aligned Polymer Nanofibrous Structures

There are many techniques that utilize mechanical, electrical, or magnetic forces to align polymer nanofibers. Most aligning procedures are coupled with polymer nanofiber fabrication in a single step, while other are used to impart alignment to collections of nonaligned fibers post-fabrication. In the field of tissue engineering, the most common method of aligned nanofiber fabrication is electrospinning, but several other promising methods have also been explored for assembly of aligned nanofiber arrays. A brief overview of different methods of aligned nanofiber array fabrication is presented below.

2.1 Electrospinning

Electrospinning is an electrostatic method of fabricating polymer nanofibers that has generated widespread interest in the tissue engineering field due to its simplicity, immense versatility, and readiness for industrial scale-up. Electrospinning utilizes an electric field to eject a polymer solution or melt from a needle or small orifice as a thin liquid jet [5]. The electric field generates forces on the polymer solution that overcome surface tension forces in the needle, resulting in the ejection of a jet that is accelerated toward a grounded target. Violent whipping motions thin the jet as it travels toward the target and thus increase its surface area. A very high surface area to volume ratio promotes evaporation of the solvent, or cooling of a melt, resulting in the formation of polymer fibers at the target. When a flat target is used as the collecting area, a random fibrous mesh is formed, but many different variations of the electrospinning setup have been employed to allow fabrication of nanofibers with uniaxial alignment. There are two basic methods that are most commonly used to fabricate aligned nanofiber structures: (1) mechanical alignment using a high speed target, and (2) electrostatic alignment using a manipulated electric field. The preferred method of high speed target collection is the rotating mandrel technique and the preferred method of electric field manipulation is the parallel plate technique. The electrospinning technique will be discussed in further detail in Sect. 3.

2.2 Drawing

Polymer nanofibers can be directly drawn from a viscous polymer solution or melt when a droplet of polymer solution is mechanically stretched [6]. For example, the tip of a rod was dipped in a polymer melt and simply pulled out to form nanofibers with diameters as low as 60 nm and lengths up to 500 mm [7]. Resulting nanofibers can be manually oriented into aligned arrays or formed into arrays by automated

procedures [8]. A rotating collecting system was developed that can continuously draw a nanofiber from a nozzle and simultaneously arrange it into an aligned nanofiber array [9]. Polymer nanofibers with diameters ranging from 50 to 500 nm were formed into arrays with well-controlled diameter, alignment, and spacing using this system.

2.3 Extrusion

Continuous polymer fibers are formed when a polymer solution or melt is mechanically pushed with a ram through a die of desired cross-section. This method of fabrication is most commonly used in the textile industry, but conventional methods of fiber extrusion in the textile industry are not suitable for producing uniform polymer fibers in the nanometer diameter range. However, modified extrusion methods have been developed to successfully fabricate polymer fibers in the nanometer diameter range. Polymer nanofibers 100–200 nm in diameter and several micrometers in length were fabricated with a system utilizing air pressure to force 1–2 μm microsphere droplets though a steel mesh die [10]. In addition, continuous well-aligned polymer nanofibers with an average diameter as low as 424 nm were fabricated with a rotary system that utilized centrifugal force to push a polymer solution through a die [11]. The diameter of nanofibers produced by this method decreased as the rotational speed was increased.

2.4 Templating

Templating is a method used to fabricate arrays of uniaxially aligned nanofibers. Polymer solutions and melts are injected into alumina network templates by wetting, capillary forces, gravity, or extrusion [12]. Alumina network molds have been fabricated with pore diameters such as 25–400 nm and with pore depths ranging from 100 nm to several hundred micrometers [13]. Solid polymer nanofiber arrays are released from the molds after mold destruction or mechanical detachment [13, 14]. Nanofiber arrays produced by templating contain large areas of vertically aligned fibers of limited length that share a molded end base. Parameters such as fiber diameter, fiber height, and fiber spacing can be controlled by changing template dimensions and fabrication parameters such as melt time and temperature [15, 16]. The templating method can be used to fabricate surfaces with well-controlled properties, such as roughness, and wettability [15, 17]; however, nanofiber arrays fabricated by the templating method are not well suited for contact-guided cell alignment because of the limits in maximum fiber length. Templated fiber arrays are best suited for tissue engineering applications associated with surface chemistry, such as cell–substrate interaction studies and implant coatings [14, 16].

2.5 Micropatterning

Solution phase self-assembling nanofibers such as peptide amphiphiles (PA) have been observed to orient in aligned arrays when formed on micropattered surfaces. Aligned nanofiber assemblies have been observed on freshly cleaved mica surfaces [18], and the growth rate of PA fibers was quantified [19]. Large bundles of aligned PA nanofibers were assembled in an orientation parallel to patterned microchannels using a technique that incorporated sonication [20, 21]. Nanofibers fabricated by self-assembly are generally small compared to those fabricated by other techniques. Individual fiber diameters are several to tens of nanometers, and fiber lengths can reach several micrometers [4].

2.6 Fluid Flow

Fluid flow can be used to align polymer chains or precursors in solution, which become aligned nanofibers after subsequent solvent evaporation or polymerization. The mechanism of alignment is shear forces present in flowing fluids. Gravitational forces are easily utilized to generate fluid flow through dipping procedures that result in fiber alignment [22, 23]. Pressure driven fluid flow through pipettes and within microchannels has also been explored as a mechanism for forming aligned nanofibers [24–26]. Collagen fibers polymerized in 10–100 μm channels showed statistically significant alignment compared to controls when introduced to the channels under flow conditions, but not when introduced under static conditions [27]. Microchannel fluid flow was also combined with a drawing technique to produce aligned lipid nanotubes [28].

2.7 Magnetic Field-Assisted Alignment of Nanofiber Strands

High powered magnetic fields can be used to produce aligned nanofiber arrays from some materials. Magnetic alignment exploits anisotropy of the diamagnetic susceptibility of molecules. Several research teams have used strong magnetic fields to induce the alignment of cellulose [29, 30], collagen [31], and PA [32] nanofibers assembled under a strong magnetic field. The addition of magnetic beads allowed the fabrication of thin gels of aligned collagen using a small magnet [33]. This technique was used to induce collagen fiber alignment in plain and cell-containing gels several millimeters thick. It was hypothesized that the magnetic beads pulled fibers along the field lines formed by the magnet, resulting in a mechanism that might be similar to fluid flow alignment.

2.8 Surface-Induced Polymerization

Aligned nanofiber arrays can be directly produced during polymer synthesis with surface-induced polymerization reactions. Several types of polymers have been fabricated into nanofiber arrays on different substrates using surface-induced polymerization reactions [34–36]. Nanofibers were observed with lengths from a few hundred nanometers to several micrometerss and with diameters from 35 to 200 nm. Aligned nanofiber arrays formed by this method are vertically aligned and share a common base similar to those fabricated by the templating method.

2.9 Bacterial Cellulose

Cellulose nanofibers produced by bacterial cultures in vitro have found use in a variety of applications, including biomedical applications [37]. Potential advantages of bacterial cellulose nanofiber production include high yield and low cost. Cellulose nanofibers are synthesized by Acetobacter bacteria by a process that involves extracellular secretion of chains of polymerized glucose residues. Subsequent assembly of the chains and crystallization into ribbons results in networks of cellulose nanofibers with diameters less than 100 nm. Recently, methods of forming aligned nanofibrous networks with Acetobacter culture have been developed. Several groups found that bacteria cultured with various substrates were able to produced cellulose nanofibers with aligned orientations along the features of those substrates [38–40]. Large networks of aligned cellulose nanofibers were produced by Acetobacter when an electrical field was applied [41]. Aligned orientation was attributed to bacterial motion induced by the applied electric field.

2.10 Post-Fabrication Drawing of Nanofiber Arrays

A simple and intuitive way to impart alignment in randomly oriented nanofiber meshes is uniaxial stretching. When a randomly aligned nanofiber mesh is subject to a large uniaxial strain it can be transformed into an elongated aligned mesh. The mechanism of alignment is a mechanically induced reorientation of the randomly aligned nonwoven fibers in the direction of physical stretching. This technique, sometimes referred to as “post-drawing,” is used to impart or improve alignment in random or aligned nanofiber meshes. This technique is most commonly associated with electrospinning. In addition to reorienting fibers in the mesh, post-drawing can also elongate individual fibers, resulting in decreased fiber diameter [42]. In many cases, post-drawing procedures are conducted under elevated temperatures [42–44]. The post-drawing alignment mechanism has also been utilized in a modified electrospinning system to produce continuous uniaxial fiber bundle yarns [45].

3 Electrospinning of Aligned Nanofibrous Structures

The vast majority of publications related to the fabrication of aligned polymer nanofibrous structures and their application in tissue engineering involve the electrospinning fabrication technique. The two basic approaches used to obtain aligned nanofibers from an electrospinning jet are the rotating mandrel and parallel plate techniques. The rotating mandrel technique utilizes high velocities and mechanical tensile forces to impart alignment, while the parallel plate technique utilizes electrical forces to induce fiber alignment. The arrangement and composition of aligned nanofiber meshes collected by both techniques are influenced by the specific parameters of each electrospinning setup. In addition, a wide variety of modifications to these standard techniques have been explored in an attempt to discover more versatile aligned fiber fabrication methods. These modifications could facilitate the fabrication of better tissue engineering scaffolds by allowing better control over fiber length, alignment, placement, and three-dimensional (3D) organization.

3.1 Rotating Mandrel

The jet formed during electrospinning is ejected at a high rate of speed, reported as being up to several meters per second [46]. The deposition pattern of the high velocity jet can be controlled by using a target that is also moving at a high rate of speed. For this reason, the most common way of collecting aligned electrospun nanofibers, known as the rotating mandrel technique, utilizes a high speed grounded rotating mandrel as the collection target (Fig. 1a). Mandrel diameters are generally a few centimeters or larger and are rotated at speeds from zero to several thousand revolutions per minute (rpm). The tangential velocity is the most informative value to use when comparing different studies because mandrel diameters tend to vary significantly between studies. Relatively thick aligned fiber mats can be collected using this method, but the degree of alignment and the collection rate may decrease with mat thickness due to repulsive residual charges and the insulating effects of previously deposited nanofibers [47].

The speed of a rotating collector has several effects on the microstructure of collected fibers and their spatial arrangement. It is hypothesized that when the tangential velocity at the edge of a rotating mandrel matches the speed of the electrospinning jet, the degree of alignment will be maximized [48]. Fiber orientation resulting from different mandrel velocities can be classified in three stages: (1) mandrel velocity is too low to initiate fiber alignment, (2) mandrel velocity initiates increasing fiber alignment with increasing speed to a maximum, and (3) fiber alignment decreases due to fiber fracture caused by extreme velocities [49]. The threshold speed for fiber alignment is different from system to system. Several groups using various synthetic polymers saw the onset of fiber alignment at around 3 m/s [50–53], whereas others have required speeds approaching 10 m/s [54] for the

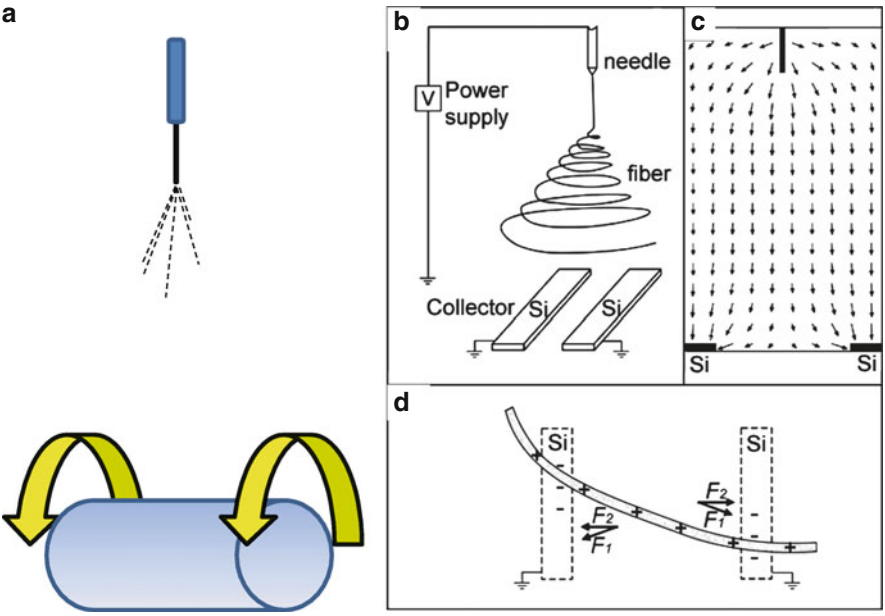

Fig. 1 Setup for electrospinning aligned nanofibers using the (**a**) rotating mandrel, and the (**b**) parallel plate techniques. (**c**) Calculated electric field strength vectors and (**d**) electrostatic force (F) analysis associated with the parallel plate techniques [62]

onset of alignment. The degree of alignment generally increases with increasing tangential velocity after the onset of fiber alignment [50–56]. As mandrel speeds continue to increase, fibers may begin to break due to tensile forces exerted by the mandrel on the fibers [54]. Fiber breakage can result in decreasing fiber alignment and quality [48]. The mandrel speed associated with fiber breakage is dependent on the material properties of the electrospun polymer and it has been shown that nanofibers electrospun from brittle materials are more likely to break at lower mandrel speeds [57].

The tensile force exerted on the electrospinning jet by a rotating mandrel can result in a reduction of fiber diameter for deformable materials. Fiber diameter generally decreases with increasing mandrel speed [50, 54–56, 58, 59], although slight increases in diameter have been observed under certain conditions [49, 60]. Reported fiber diameter reductions of around 15–40% versus static collection have been observed when mandrels were rotated at 5–15 m/s [50, 54–56, 58, 59]. Though the exact tangential velocity must be determined in order to allow maximum alignment, the tensile force exerted by the rotating mandrel also affects the fiber diameter and can even influence fiber molecular orientation [49, 61]. This must be taken into account when deciding on an optimal mandrel speed.

Despite a general agreement for some trends related to mandrel effects on fiber microstructure, it is difficult to precisely predict how a rotating mandrel will affect nanofiber structure for a specific system due to the amount of variables involved.

Fiber jet speed and material elasticity are two of the most important parameters involved in the jet–mandrel interaction and each of these properties are influenced by multiple electrospinning parameters, such as solution conductivity, viscosity, voltage, and feed rate. In addition, material properties cannot be accurately predicted without knowing the exact degree of solvent evaporation at the point when fibers are taken up by the collector.

3.2 Parallel Plate

Another method of collecting aligned nanofibers is by manipulation of the electric field in the collecting area. The highly charged electrospinning jet is sensitive to the surrounding electric field and will align in certain electrical field configurations. The most commonly used method of aligning nanofibers with an electric field is the parallel plate technique. When two grounded parallel plates are set up as the collecting target they create an electric field that causes deposition of nanofibers aligned perpendicular to the plates across the air gap between them. Analysis of the electric field present in a parallel plate electrospinning setup and the resulting forces exerted on the electrospun nanofibers was first conducted by Li et al. [62]. Diagrams of this analysis are displayed in Fig. 1b, c. The electrical properties of the polymer solution become increasingly important when electrospinning nanofibers across parallel plates because electrostatic forces are responsible for aligning the fibers. Many polymer solutions that are easily electrospun into nanofibers on a flat target do not align well on parallel plates because the solution properties do not facilitate good alignment with the electric field.

It can be hypothesized that the electrical properties of a polymer solution must be within a critical range to facilitate effective deposition across parallel plates. If a solution's conductivity is too low, the electrostatic forces may not be sufficient to pull fibers across the gap; but if it is too high, then random whipping instabilities may dominate the motion of the jet. For example, it was hypothesized that fiber collection across parallel plates was ineffective for an electrospun polyelectrolyte solution [poly(phenylene vinylene), PPV] because its high conductivity contributed to a highly unstable jet that could not be effectively stabilized by the aligning forces at the collection site [63]. Addition of a neutral polymer (polyvinyl pyrrolidone, PVP) to this solution allowed the formation of well-aligned nanofibers (Fig. 2a–c). In another study, it was hypothesized that parallel plate fiber collection became ineffective after the addition of NaCl to the polymer solution due to jet instabilities caused by increased solution conductivity [64]. Nanofibers electrospun from a melt were aligned only at gap distances less than 1 cm and collected as randomly oriented meshes at greater gap widths [65]. In this case, the forces exerted by the electric field on the solution may have been too small to result in alignment due to low conductivity.

Electrostatic forces exerted on an electrospun jet can be controlled independently of solution properties by changing the applied voltage. An increase in the

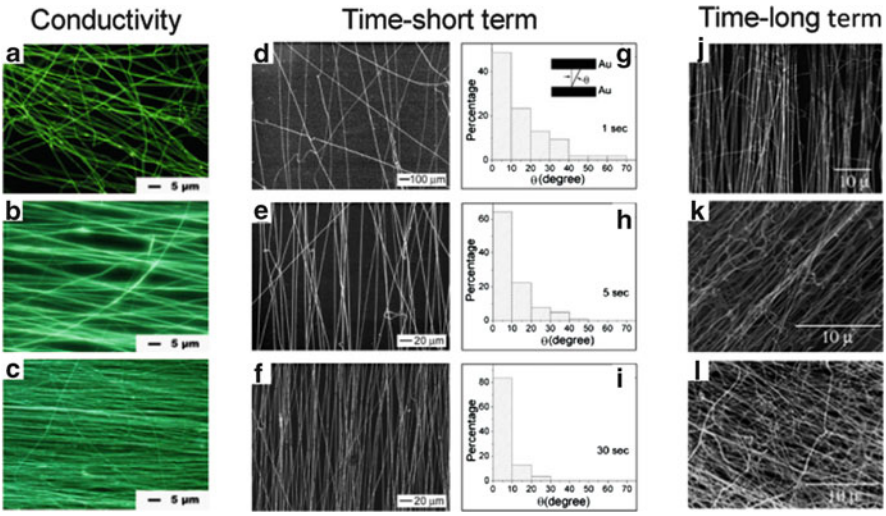

Fig. 2 Fiber alignment increased with decreasing solution conduction for (**a**) pure PPV, (**b**) PPV/PVP 50:50, and (**c**) PPV/PVP 20:80 [63]. Fiber alignment increased with time from (**d**, **g**) 1 s, to (**e**, **h**) 5 s, to (**f**, **i**) 30 s [67]. Fiber alignment decreased with increasing time from (**j**) 5 min, to (**k**) 15 min, to (**l**) 2.5 h [71]

voltage of an electrospinning setup results in an increase in the electric field strength and thus an increase in the forces acting on the fibers. However, increased voltage also increases the jet instability, which may decrease fiber alignment. Therefore, a critical voltage that balances the magnitude of the aligning forces and the resultant jet instabilities must be obtained for optimal fiber deposition and alignment across parallel plates [66].

Another limitation that is specific to the parallel plate electrospinning technique is the collection of extremely thin nanofibers, which have been observed to break because they were unable to sustain the forces of their own weight and of the repulsive charges from other fibers [62]. An electrically resistive substrate inserted into the gap between the plates can provide support to fibers suspended between the plates without influencing fiber quality [62], and may also help to shield any conductive materials below the air gap, which may attract unwanted non-aligned nanofibers. Substrates with bulk resistivity greater than 10^{22} Ω cm, such as quartz and polystyrene, are suitable for placement between parallel electrodes, while materials with bulk resistivity of less than 10^{12} Ω cm, such as glass, may result in random fiber orientations [67, 68].

3.2.1 Charge Retention

Nanofibers collected in full contact with a conductive electrode immediately discharge. However, fibers suspended in air across parallel plates retain charge

throughout the portion of the fiber that does not have contact with the conductive plates [62]. The accumulation of both charge and material in between the gap has a significant effect on the electric field, thus the fiber deposition patterns are constantly changing as fiber density increases. Charge retention can have effects on subsequent fiber alignment and collection rate due the repulsive forces exerted on the electrospinning jet. Residual charge can initially improve alignment in low density arrays because parallel alignment is the lowest energy state of an array of charged fibers [62, 67, 69]. Improved alignment at various time points up to 30 s are shown in Fig. 2d–i [67]. Numerical models are in agreement with the positive effects that residual charge has on alignment at low fiber densities [70]. However, over longer periods of fiber collection, as fiber density increases, the alignment of subsequent fibers can become poor due to build-up of charge and materials (Fig. 2j–l) [71]. As fiber density continues to increase, the charge repulsion and material build-up can resist further fiber deposition between the parallel plates almost entirely. Therefore, thick layers of aligned fibers are difficult to fabricate by this method [72].

3.2.2 Gap Size and Plate Geometry

The electric field and thus the collection dynamics of parallel plate electrospinning setups are affected by the geometry of the parallel plate configuration. The gap size has an especially significant role in fiber alignment and array density. The draw of the aligning electrostatic forces created by parallel plates decreases with increasing gap distance, making it is more difficult to collect aligned nanofibers across a larger distance [73]. Although nanofibers as long as 50 cm have been collected across parallel plates, fiber density and rate of deposition generally decrease with increasing gap distance until no fiber collection is possible [74, 75]. Collection of densely aligned nanofiber arrays becomes infeasible as gap size increases due to decreasing electrostatic forces and charge repulsion. Because of the gap size limitations, fiber length in high-density aligned nanofiber arrays is usually limited to a few centimeters. Nanofibers electrospun across various gap distances from 3 to 6 cm demonstrated a highly reduced fiber array density with increasing gap distance [66, 69].

Gap distance also has an effect on fiber alignment. As the gap size increases, fiber alignment may initially increase and then decrease with a critical value of maximum alignment. The critical values of maximum alignment for two different electrospinning systems were 1 and 3 mm [66, 73]. Reported results on the effect of gap distance on alignment can vary significantly from study to study, which is not surprising due to the many components involved in fiber alignment across parallel plates. For example, alignment was observed to increase with an increase in gap distance from 2 to 6 cm with one electrospinning system [69], and decrease with an increase in gap distance from 0.5 to 2.5 cm with another system [64].

3.2.3 Effects of Electrostatic Forces on Fiber Morphology

The columbic forces that align electrospun nanofibers across two parallel plates exert a mechanical force much like the mechanical tensile forces exerted by a rotating mandrel. Like the rotating mandrel, parallel plate collection sometimes results in nanofibers with reduced diameters compared to those formed using flat plate collection. Whereas the magnitude of the force in a rotating mandrel is set by the speed of the collector, the magnitude of the force in a parallel plate system is set by the strength of the electric field and the electrical properties of the jet. It can be anticipated that electrospinning setups that incorporate large electrostatic forces or more deformable materials may result in a more pronounced decrease in fiber diameter. The diameter of nanofibers collected across a parallel plate decreased with increasing concentrations of carbon nanotubes [76]. This result is anticipated because the forces pulling the fibers across the parallel plates should increase with increasing nanotube concentration due to the increased conductivity of the solution. Fiber diameter decrease for parallel plate collection was also especially pronounced for melt electrospinning, which could be due to the deformability of hot fibers that had not fully cooled before alignment [65].

3.3 Challenges in Electrospinning Aligned Nanofiber Structures

Both the rotating mandrel and parallel plate technique have advantages and disadvantages. The rotating mandrel can be used to collect large-area thick mats of aligned fibers, but highly aligned assemblies may be difficult to fabricate and the fiber arrays may be tightly wound or broken due to high rotation speeds [72]. The parallel plate technique allows easy transfer of fiber arrays to other substrates, but this technique is sensitive to solution properties and there are limitations in array fiber density and thickness and in fiber length [72]. These limitations constrain the specific types of aligned structures that can be fabricated by electrospinning and reduce the applicability of this technique. Many interesting innovations have been developed to address these limitations and allow greater control over fiber array deposition area, fiber alignment, continuous fiber length, fiber mat density, and yield.

3.3.1 Focusing and Steering the Electrospinning Jet

Under normal electrospinning conditions, the deposition area of an electrospinning jet can be undesirably large and difficult to predict. This can lead to difficulties in precise and repeatable fabrication of uniform nanofiber arrays, and materials may be wasted. It is desirable to explore methods to control the deposition of an electrospinning jet in terms of both focused fiber deposition area and controlled placement of the fiber deposition area. The range of fiber deposition is usually decreased as the needle-to-collector distance is decreased; however, this alone may

not provide the desired level of fiber deposition focus and may result in unwanted side effects [77]. Several technologies such as repulsive electric fields, sharp-edged collectors, and attractive oppositely charged electrodes have been applied to focus and control the deposition location of an electrospinning jet.

The area of aligned nanofiber deposition can be focused by confinement and general stabilization of the whipping motions of the electrospinning jet early in its trajectory. Objects with the same charge as an electrospinning jet exert a repulsive force on the jet, and when placed in a proper configuration can produce an electrostatic force that acts as a barrier to confine the jet. Positively charged rings, cylinders, and plates have been placed around an electrospinning jet to electrostatically confine it and reduce the final fiber deposition area at the collection target [78–80]. In one instance, the diameter of randomly deposited nanofiber mesh was reduced from 7 to 1 cm with the addition of positively charged ring electrodes placed around the electrospinning jet path [80].

The deposition area can also be focused using a thin sharp-edged collector. A thin sharp edge confines the actual area for fiber deposition, and focuses the electric field (Fig. 3), promoting a narrow deposition of fibers [81]. Several groups have used thin rotating disks in place of a standard rotating mandrel to collect thin highly aligned nanofiber bundles. A system similar to a sharp-edged disk employed a thin wire wrapped around spokes connected to a rotating mandrel [82]. In a variation of that technique, a wire can be wrapped around an insulating cylinder to allow collection of multiple focused aligned nanofiber arrays simultaneously [83]. Thin sharp edges have also been used in the configuration of a parallel plate

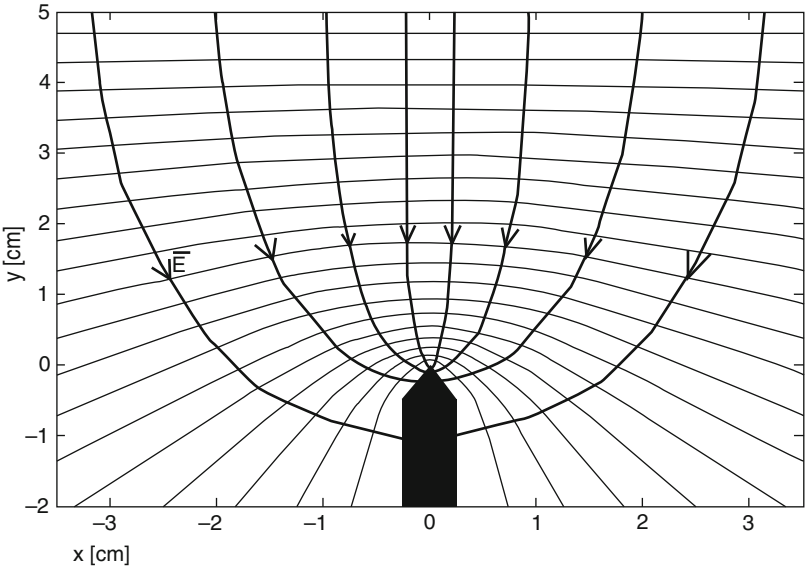

Fig. 3 Electrostatic field simulation for a sharp-edged collector. Equipotential lines of the electric potential and electrostatic field lines are plotted [81]

collector. Two steel blades placed upright in a direction perpendicular to a standard parallel plate setup were used to collect thin aligned nanofiber arrays at gap distances up to several centimeters [75], and sharpened parallel plates were able to attract a greater quantity of fibers than standard parallel plates [84].

Another method of focusing and controlling the deposition of an electrospun nanofiber array is to use an oppositely charged auxiliary electrode to attract the jet. Electrospinning systems using this technology are generally arranged so that a collecting mandrel is placed between the nozzle tip and the oppositely charged electrode (Figs. 4 and 5). Narrow aligned nanofiber arrays were fabricated on the surface of a rotating mandrel when an oppositely charged pin electrode was placed immediately behind or inside of it [85, 86]. It was found that the width of the aligned fiber deposition area on the collector narrowed with decreasing collector to spinneret distance and increasing field strength [77]. Parallel arrays of oppositely charged strip

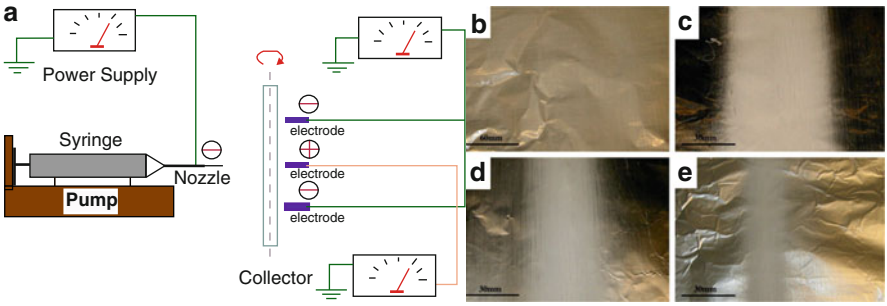

Fig. 4 (**a**) Electrospinning setup with counter electrodes used to focus the area of fiber deposition. (**b**–**e**) Images of resultant nanofiber mats electrospun with (**b**) no auxiliary electrodes, (**c**) one auxiliary counter electrode, and (**d**, **e**) both counter and like electrodes with different separation distances between them [48]

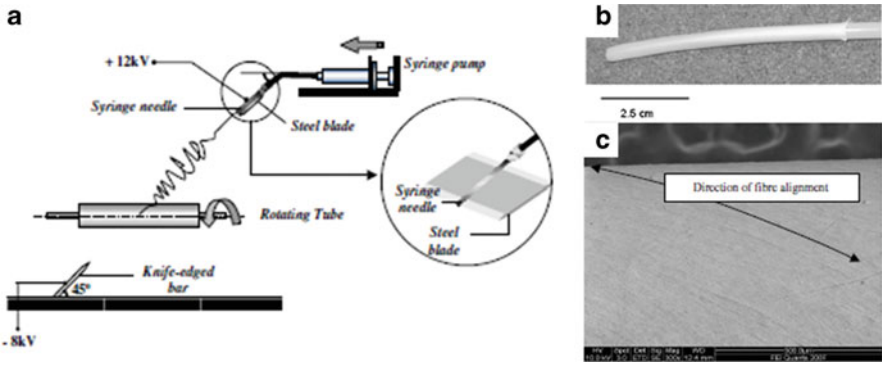

Fig. 5 (**a**) Electrospinning setup using an auxiliary counter electrode to direction the path of an electrospinning jet. (**b**, **c**) A tubular structure with diagonally oriented aligned nanofibers was fabricated when a mandrel was placed in the path of the jet at an angle [87]

and sharp-edged bar electrodes have also been placed below rotating mandrel collectors to confine aligned nanofiber array deposition [87, 88]. Electrode arrays containing both like and opposite charges can be arranged to focus the deposition area even more effectively. The width of a nanofiber array collected on a rotating mandrel was reduced by up to 60% when two like-charged electrodes (same charge as the jet) were placed on each side of an oppositely charged counter electrode (Fig. 4) [48]. Oppositely charged electrodes are also capable of patterning the location and arrangement of aligned nanofiber deposition on a rotating mandrel. The attractive force between an electrospinning jet and an oppositely charged electrode is strong enough to redirect the direction of the jet to the position of the electrode, even if it is not located directly below the nozzle [85]. When the counter electrode is positioned off-center relative to the nozzle, the electrospinning jet can be forced to take a trajectory at an angle to the rotating mandrel and allow collection of aligned fiber arrays with various angular orientations (Fig. 5) [87]. Therefore, precisely oriented aligned nanofibers can be honed to a specific axial location on a rotating mandrel. Lateral translation of either the oppositely charged electrode or the mandrel itself allows dynamic control of fiber deposition over the entire mandrel [86].

3.3.2 Fiber Alignment

Generally, the methods of fiber array confinement described above also result in improved array alignment due to geometrical constraints and the focused electric field. When the nanofiber jet is focused there is less probability for misalignment, and the increased electrostatic forces generated may improve fiber alignment control. Specific examples of improved fiber alignment exist for each of the three general methods described above. A confining electric field generated by two like-charged plates applied around an electrospinning jet was observed to improve deposited fiber alignment across parallel plates [78]. When a thin blade is used as the collecting surface, a greater percentage of aligned fibers may be collected because unaligned fibers might miss the target or only a small portion of the fiber will cross the thin blade. In addition, the increased electrostatic force generated by thin blade collectors can improve fiber alignment independently of geometrical constraints [87]. Improved fiber alignment has also been observed when oppositely charged counter electrodes were added to a conventional rotating mandrel setup. This resulted in aligned nanofiber collection at lower speeds [48].

Other methods have been developed to improve fiber alignment in nanofiber arrays of larger area. One innovative way to increase fiber alignment using the parallel plate technique is to apply an alternating potential to the two collection plates. Initially, the nanofiber jet is more attracted to one plate than to the other. When the field is switched the jet moves to the other plate, and oscillation guides fiber deposition back and forth across the plates (Fig. 6) [89–91]. In one configuration, an AC potential is applied to one plate, while the other remains grounded [89, 90]. A different configuration utilized high voltage reed relays or switches to alternate charge and ground between two parallel plates [91, 92]. This configuration has been

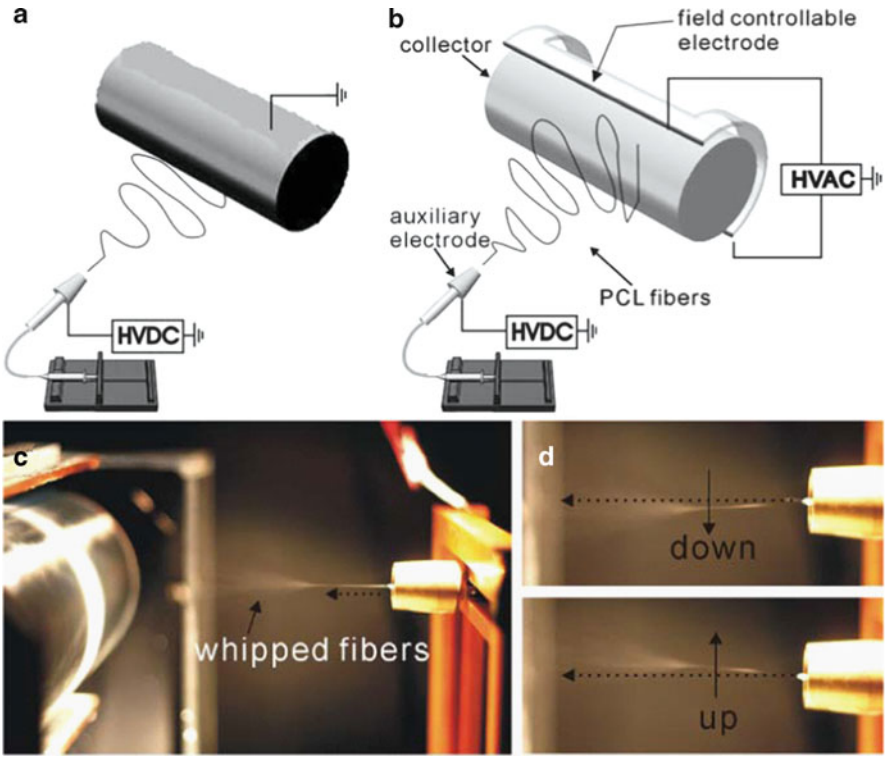

Fig. 6 Electrospinning with (**a**) normal rotating mandrel compared to (**b**) modified system with AC field controllable counter electrode. (**c**, **d**) The effect of the AC electrode on the jet is shown, where (**c**) corresponds to a normal setup and (**d**) is with the AC electrode [89]

used with both repulsive (same charge as jet) voltage/ground and attractive (opposite charge as jet) voltage/ground alternations between plates [91, 92]. Orientation may be affected by the frequency of the applied field, with an optimum frequency for maximum alignment [79, 89].

Interestingly, when an AC potential is applied to the electrospinning nozzle instead of a DC potential, fiber alignment on a rotating mandrel can also be improved. It is hypothesized that this could be due to decreased net charge and thus decreased jet instability [93]. Further investigation into this technique showed that addition of a DC potential biased to an AC potential improved the quality and alignment of nanofibers collected on a rotating mandrel as compared to AC or DC potentials alone [94].

3.3.3 Fiber Length

Verifiable single continuous nanofibers can be fabricated by the parallel plate method. Increasing the maximum length of fibers that can be collected across

parallel plates may increase the applications of this method. Long nanofibers up to 50 cm were collected using a parallel plate setup with very large plates (30.5 × 7.5 × 0.7 cm), and maximum fiber length was observed to increase with increasing plate size [74]. It was hypothesized that even longer fibers could be collected with larger plates. External forces can also be utilized to suspend long nanofibers across a gap. Long suspended nanofibers (25 cm) were formed when a nanofiber jet was shot sideways and adhered to a raised target at one end, while the other end was pulled down by gravity and adhered to a support [95]. Another system utilized gas flow to pull one end of an adhered nanofiber toward an electrode to suspend it across a long gap (>20 cm) [96].

3.3.4 Fiber Density and Thickness (Parallel Plate)

A major limitation of the parallel plate technique is limited fiber density and mat thickness, as explained in Sect. 3.2.1. This problem can be overcome by utilizing other forces that are able to overcome the electrostatic repulsive force between nanofibers. Thick aligned nanofiber mats were fabricated across parallel plates when a magnetic field was used to attract fibers to a mesh across parallel plates [97]. Another technique utilized mechanical forces to assemble low density aligned fiber arrays into thicker constructs [98]. This technique used automated tracks to provide continuous mechanical assembly of fiber arrays, and allows theoretically infinite mat thicknesses.

3.3.5 Yield

In order to be practical for industrial scale-up, aligned fiber fabrication should have a high yield. The simplest method of maximizing yield for both the parallel plate and rotating mandrel techniques is the use of multiple spinnerets to deposit aligned nanofibers over long sections of rotating mandrel or parallel plate simultaneously [99–101]. It is important to consider interference between the jets when multiple spinnerets are used because like-charged jets repel one another and oppositely charged jets attract one another [102]. Another method of increasing yield is to move the collecting surface. Several groups have translated rotating mandrels normal to the electrospinning jet to increase the area of coverage [86, 101, 103]. Multiple parallel plate-type aligned nanofiber arrays can be collected simultaneously when a rotating wire mandrel collector is used [71, 104]. In this case, the wire spokes act as individual parallel plate collectors and, as the wire mandrel rotates, different parallel wire gap locations are present directly beneath the electrospinning nozzle [105]. Similar to the wire frame technique, a rotating mandrel with fins has been used to fabricate many suspended aligned nanofiber arrays simultaneously [42]. Parallel plates have also been put into motion to increase nanofiber yield. When two parallel plates are replaced by two parallel conductive tracks moving normal to an electrospinning nozzle, continuous aligned nanofiber array production across the tracks is possible [98].

4 Cell Interactions with Aligned Nanofibrous Structures

Cell morphology is highly sensitive to nanofibrous topography. Cells adopt different shapes on nanofibrous surfaces than on flat surfaces, and fiber diameter and orientation further modulate cell configuration [4]. Aligned cell morphologies commonly observed on aligned nanofibrous substrates are especially important in designing tissue engineering environments that mimic aligned tissues such as nerve, muscle, ligament, and tendon. In addition to the practical advantages of alignment in such tissues, variations in cell morphology generally correspond to changes in cytoskeletal arrangement that can further modulate other cell behaviors such as elongation, proliferation, migration, ECM production, and differentiation.

4.1 Cell Morphology and Alignment

Cell orientation on nanofibrous substrates is generally described as rounded or polygonal, which corresponds to a lack of organized actin fibers, or as elongated or spindle-shaped, which corresponds to well-organized actin fibers in the direction of elongation [52, 106]. These morphologies are in contrast to the flat well-spread shape seen on flat surfaces [106]. Elongated cell morphology can be quantified by its aspect ratio, which is the ratio of the length of the cell's long axis to its short axis. The dependence of cell morphology on substrate fiber orientation has been quantified as a systematic increase in aspect ratio as fiber orientation progresses from random to aligned [50]. Quantification of cell morphology varies greatly for specific cell types, substrates, and culture times, but in one representative example, cell aspect ratio on highly aligned nanofibers was quantified as twice that seen on randomly oriented nanofibers and three times that seen on a glass control 24 h after seeding [52].

The angular direction of cell elongation corresponds to the direction of the underlying fibrous substrate and, thus, cell populations cultured on well-aligned nanofibrous substrates are well aligned in relation to one another. Most cell types, including neural, muscle, fibroblast, endothelial, and mesenchymal stem cells (MSCs), adopt an aligned morphology when cultured on aligned nanofibrous substrates [56, 103, 107–111]. According to several studies, the quantitative degree of cellular alignment generally corresponds to the degree of underlying fiber alignment [50, 59, 112–114]. Among these studies, quantitative cell alignment values were reported to be slightly higher, lower, or near identical to that of the underlying fiber substrates. A representative distribution of cell and fiber orientation is displayed in Fig. 7 [114]. Cells can organize into an aligned orientation soon after they attach to an aligned nanofibrous substrate. MSCs and fibroblasts were organized in the direction of the underlying fibrous substrate after 24 h in culture, and a more detailed observation of C2C12 cells revealed F-actin organization into parallel stress fibers after just 30 min, with substantial cell elongation after 2 h (Fig. 8) [52, 56].

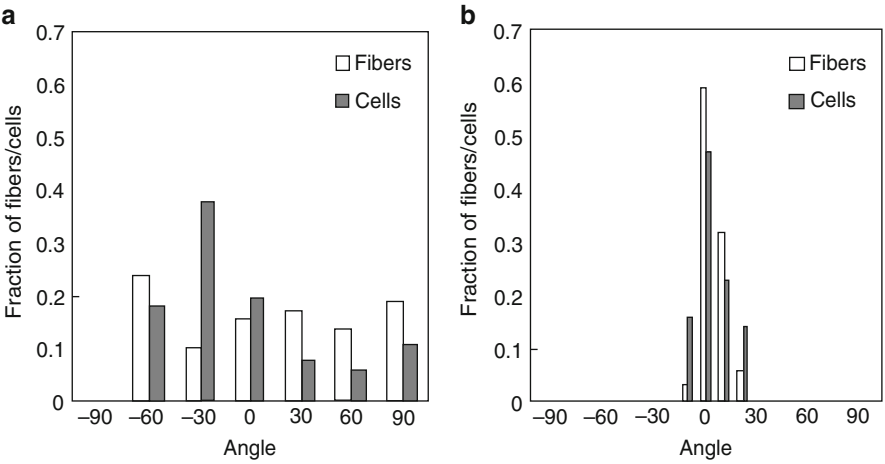

Fig. 7 Angular distribution of nanofiber substrates and the cells cultured on them are shown in normalized histograms. (**a**) Substrate was collected on a solid plate, and (**b**) substrate was collected on a rotating mandrel [114]

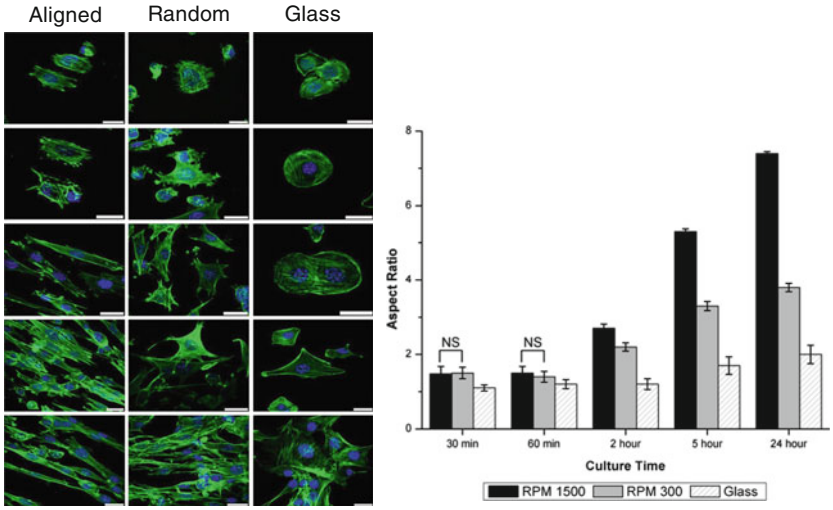

Fig. 8 *Left*: C2C12 cells were seeded on aligned and randomly oriented fibers and on a glass control. Confocal images taken at 30 min, 60 min, 2 h, 5 h, and 24 h after seeding are shown, with increasing time from *top* to *bottom*. Actin is stained *green* and nuclei are stained *blue*. *Scale bar*: 25 μm. *Right*: Quantification of cell aspect ratio is shown for all time points. All data sets are significantly different from each other except those indicated by *NS* [52]

Cell alignment parallel to aligned nanofibrous substrates is consistently observed in many studies, even though different cell types and different types of nanofibrous materials have been employed. However, there are some interesting exceptions.

Table 1 Neural cell elongation on aligned nanofiber substrates

Reference	Cell type	Culture time (days)	Max. length	% Increase[a]
[113]	Rat DRG E15	3	760 μm	20
[118]	Rat DRG P4-P5	6	3.5 mm	300
[119]	Chick DRG E9	5	11 mm	500
[117]	Mouse NSC C17.2	2	95 μm	100
[107]	Mouse NSC C17.2	2	100 μm	25
[120]	Mouse NSC CE3/RW4	14	1.7 μm	40
[121]	Human NSC H9	7	450 μm	300

[a]Increase in elongation of neural cells on aligned nanofibrous substrate as compared to randomly oriented nanofiber substrate

Neurites growing on a nanofibrous scaffold inserted in the brain were observed to preferentially align in the direction perpendicular, not parallel, to the aligned nanofibers [115]. Interestingly, a small but surprisingly significant amount of neurites grown in vitro also oriented perpendicular to the aligned nanofiber direction: 94% parallel, 4% perpendicular, 2% intermediate [107].

4.2 Cell Elongation

Cell elongation is closely related to cell shape, but also accounts for accelerated cell growth or maturation. Elongation is an especially important property in skeletal muscle and neural tissue engineering, where native cell types may reach lengths of several centimeters or more than a meter, respectively. Aligned nanofibrous substrates are consistently reported to promote accelerated elongation in neural cells as compared to randomly aligned substrates, (see Table 1). Myotube length on aligned nanofibers was also observed to be twice that seen on randomly aligned scaffolds, while myotube thickness remained similar [110]. Furthermore, the fiber diameter of aligned nanofiber scaffolds has a significant effect on the rate of elongation. 3T3 fibroblast elongation on single fibers increased systematically as fiber size decreased from 10 μm to 500 nm, with a 50% increase in length when fiber diameter was reduced from 4 μm to 500 nm [116]. Neural stem cells (NSCs) also increased in length with decreasing fiber size. Two similar studies demonstrated a 25% increase in neurite length when fiber diameter was reduced from 1.5 μm to 300 nm [107], and a 70% increase in neurite length when fiber diameter was reduced from 917 to 500 nm [117]. There is evidence that a critical value of optimum fiber diameter may exist because maximum neurite elongation on aligned nanofibers with diameters of 307–917 nm was determined to be around 500 nm [117].

4.3 Cell Proliferation

Cell proliferation is a vital process in tissue regeneration. It is generally desirable to maximize cell proliferation in tissue engineering scaffolds, but in some cases, such

as astrocyte proliferation at a neural tissue–implant interface, minimization of cell proliferation may be desired. In designing tissue engineering scaffolds it is important to be able to understand the effects of scaffold microstructure on cell proliferation.

It is well documented that nanofibrous microstructure can have an effect on cell proliferation; however the effect is quite varied across different studies using different types of scaffolds and cell types. When comparing nanofiber substrates versus flat controls, cell proliferation was higher on nanofibers in several studies [122, 123] and higher on flat control in several others [124, 125]. The specific fiber diameter of nanofiber substrates also has been shown to have varied effects on cell proliferation [126–129]. Similarly, the effect of nanofiber orientation on cell proliferation varied greatly between individual studies. Cell numbers on aligned nanofiber scaffolds have been observed at significantly higher values of up to twice those seen on randomly aligned control scaffolds after 3–70 days of culture [54, 123, 130, 131]. In contrast, no significant difference in cell proliferation for different degrees of fiber orientation was observed in several other studies over 3–21 days [50, 59, 112, 114, 132–134].

Unfortunately it becomes very difficult to quantitatively analyze the effects of nanofiber microstructure and orientation on proliferation because of factors inherent to these types of scaffolds that can interfere with results. Cell proliferation may be induced by substrate signals transduced through the cytoskeleton, or cell numbers may simply be increased because of spatial considerations. Cell morphologies induced by substrates with certain fiber orientations may allow higher monolayer cell packing density, or certain fiber orientations may allow greater cell penetration and expansion into the volume of the scaffolds.

4.4 ECM Production

Although aligned polymer nanofibers have some similarities to natural ECM, it is vital to tissue regeneration that resident cells produce their own natural matrix to compliment or replace the engineered scaffold. Substrate microstructure has pronounced effects on both the amount of ECM produced by resident cells and the architecture of that matrix. Increased ECM production has been observed in cells cultured on nanofibrous substrates compared to those on flat substrates and large (15 μm) microfibers [106, 135]. The specific fiber diameter of nanofibrous substrates may also affect the ECM production of attached cells [129].

The orientation of nanofibrous substrates modulates ECM production by resident cells in both quantity and quality. Increased calcium and collagen production were observed when cells were cultured on aligned nanofibers as opposed to randomly oriented scaffolds [114, 132, 133]. However, in other cases, the magnitude of ECM production was unaffected by nanofiber substrate orientation [59, 130, 132]. In addition to increasing the magnitude of ECM production, nanofibrous substrates may also promote ordered arrangement of synthesized ECM similar to that seen in

natural tissues. Quantitative analysis of the collagen I matrix produced by fibroblasts cultured on nanofiber scaffolds revealed a linear orientation for aligned scaffolds that was not present for randomly aligned substrates [112]. Optimized collagen arrangement may result in improved function in regenerated tissue. A 10-week fibroblast culture on nanofiber scaffolds resulted in an increase in scaffold mechanical strength of 63% for aligned scaffolds compared to 25% for randomly oriented scaffolds, despite similar overall amounts of collagen [130].

It can be hypothesized that cell shape changes induced by the nanofibrous structure lead to stimulation of ECM production. Several mechanisms may promote higher quantities of ECM deposition. There is evidence that cell maturation to a matrix-producing phenotype can be accelerated by aligned architecture. Collagen production of fibroblasts on aligned nanofiber substrate was 300% greater than on randomly oriented fibers at day 3, but was only 50% greater by day 7 [133]. Calcium production by bone marrow mesenchymal stem cells (BMSCs) was 50% higher at day 21, but not at days 4–14 [114]. It is also possible that cells are consistently stimulated to produce a greater amount of ECM, or that deposition increases could be a combination of both processes.

4.5 Cell Infiltration and Migration

Migration and infiltration of cells into tissue engineering scaffolds are crucial factors for their success. Many types of scaffold design require that cells seeded in vitro or recruited in vivo are allowed to infiltrate and populate the scaffolds quickly. Microstructure has a significant effect on cell migration and infiltration, and understanding these effects may lead to better scaffold design.

Random nanofibrous architecture has been observed to restrict cell migration as compared to flat controls [123, 136–138]. However, cell migration on nanofibrous substrates is greatly increased when the fibers are patterned in an aligned orientation. The number of cells migrating to a location 1.5 cm from their original seeding area was two to three times higher when aligned nanofibers guided cell migration as compared to random fibers or control film [123]. Cell migration into an in vitro wound defect model was increased by fivefold on substrates where aligned nanofibers were oriented toward the defect as compared to both randomly aligned fiber substrates or aligned fiber substrates oriented perpendicular to the defect (Fig. 9) [118]. Similarly, glioma cell migration velocity on aligned fibers was five times that seen on randomly oriented fiber substrates [139]. In addition, glioma stem cells containing neurospheres did not show cell detachment on random nanofiber substrates, but detached and migrated out on aligned nanofibers. Several factors could contribute to the migratory behavior of cells on nanofibrous substrates with different orientations: (1) Geometrical constraints may confine the random movement of cells on aligned nanofibers to one dimension, resulting in greater linear travel distances. (2) Cell morphologies and focal adhesion patterns modulated by the different types nanofibrous substrates may promote or hinder

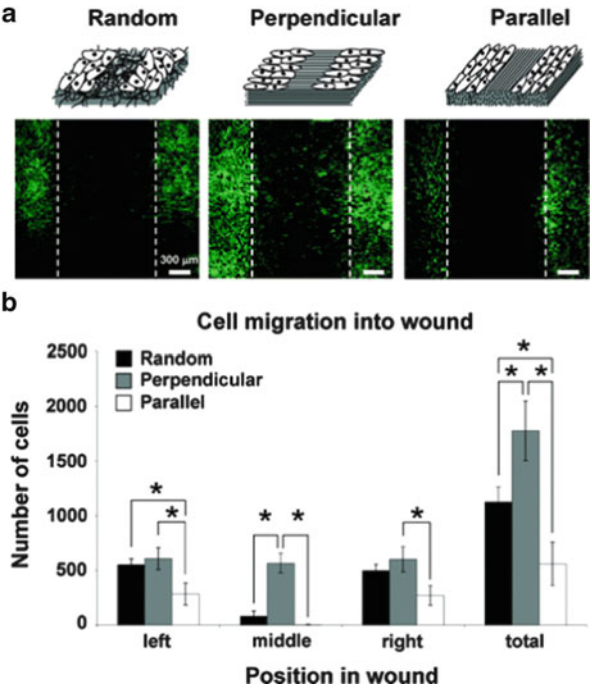

Fig. 9 (**a**) Dermal fibroblast migration into an in vitro wound healing model after 48 h on substrates with fibers aligned randomly, perpendicular to the defect or parallel to the defect. Cells are stained *green* for actin and *blue* for nuclei. *Dotted lines* are drawn at the initial edges of the wound. (**b**) Cell migration is quantified by the number of cells within the wound area divided equally into left, middle, and right zones. Statistically significant differences are marked with an *asterisk* [118]

cell migration [136, 139]. (3) Nanofibrous substrates may transduce cues through the cytoskeleton that encourage migratory or remodeling behaviors [122].

For regeneration of 3D tissue structures it is vital that tissue engineered scaffolds allow cell infiltration throughout their volume. The cell permeability of electrospun scaffolds with random orientation decreases with decreasing fiber size [140, 141], and small diameter scaffolds may completely exclude cell penetration. Fiber orientation can also have a significant effect on cell infiltration into nanofibrous scaffolds. In some cases, aligned orientations resulted in greater cell penetration as compared to randomly oriented scaffolds [142, 143]. In contrast, cell penetration has been observed into randomly aligned scaffolds, but not those with aligned orientations [115]. Similar cell infiltration into nanofibrous scaffolds with random and aligned orientation has also been observed [130]. There could be many factors involved in these discrepancies, such as fiber diameter, fiber mechanical properties, fiber-to-fiber adhesions, structural tensions on the fibers within the scaffold, and cell type preferences. Regardless of fiber orientation, cell penetration in nanofibrous scaffolds is generally limited and methods of addressing this limitation should be explored.

4.6 Differentiation and Gene Expression

In tissue engineering, it is crucial that cells introduced to a repair location differentiate into and/or maintain a desired phenotype. This is especially true when different

types of stem cells are intended to populate regenerating tissues. It is well established that different types of soluble cues can have strong effects on the differentiation of cells, but there is also strong evidence that structural features can be used to guide differentiation.

Although the effects of nanofibrous topography can be quite strong, its effects can be variable depending on cell types and specific experimental conditions. For example, one specific variable that can affect the differentiation induction of fibrous substrates is the diameter of the fibers [107]. Fibrous architecture has been observed to promote, prevent, and have no effect on differentiation as compared to a flat control for various cell types [106, 124, 138, 144]. This inconsistency might be due to the preferences of different cell types. It can be hypothesized that multipotent cells are directed to a phenotype that most closely corresponds to the morphology induced by the substrate that they are attached to. Accordingly, aligned nanofiber substrates have demonstrated the ability to promote differentiation of cells into several lineages that exhibit an elongated phenotype in vivo. BMSCs cultured on aligned nanofibers displayed ligament protein expression that suggested promotion of ligament phenotype maturation [59]. Tendon stem/progenitor cells expressed significantly higher amounts of tendon-specific genes when growing on aligned nanofibers compared to randomly oriented nanofibers in both normal and osteogenic media [145]. Several studies have observed myotube formation by skeletal muscle progenitor cells on aligned nanofiber substrates [146, 147]. The prevalence of nuclei contained in myotubes on aligned fibers has been quantified as up to 60% more than on randomly oriented fibers [52]. Primary cardiac ventricular cells also demonstrated development into a more mature phenotype when cultured on aligned nanofibers than on randomly oriented nanofibers, as confirmed by a threefold decrease in atrial natriuretic peptide expression [108]. Aligned architecture has a pronounced effect on neural differentiation and has been utilized to promote embryonic stem cell differentiation into neurons as opposed to astrocytes without the use of differentiation-inducing agents [148]. In agreement, embryonic stem cell differentiation into astrocytes on aligned nanofiber substrates was quantified as 33% less than on random fiber substrates [120]. Aligned nanofiber substrates also enhanced Schwann cell maturation compared to randomly oriented fibers, as indicated by upregulation of myelin-specific gene expression [109].

Cell differentiation is a complicated process and it is difficult to make a general hypothesis on the effect of surface topography on differentiation due to conflicting results and wide variations in specific experimental conditions. However, there is a significant amount of evidence indicating that aligned fibrous substrates promote differentiation into cellular phenotypes that exhibit an elongated morphology in vivo.

4.7 Mechanisms

Nanofibrous architecture presents a very different set of structural and biochemical cues to attached cells to that presented by flat culture surfaces. These variations

result in modulation of cell behaviors as the result of structural features. It can be theorized that three major mechanisms related to substrate structure are involved: (1) nutrient infiltration, (2) surface molecule presentation, and (3) cell shape-related mechanisms.

The 3D architecture of nanofibrous substrates may allow better nutrient exchange compared to flat surfaces because cells cultured on flat surfaces are limited to nutrient exchange on only one side. Specific nanofibrous orientations, such as aligned, can also offer different nutrient exchange potentials as compared to random orientations.

Nanofibrous substrates are also able to absorb greater amounts of protein and present surface biomolecules to cells very efficiently because of their high surface area-to-volume ratio. Studies have shown that nanofibrous substrates can absorb as much as 16 times more protein than flat surfaces, and increased protein absorption was related to specific changes in cell behavior between the two substrates [149, 150]. When a specific molecule is attached to a substrate to modulate cell behavior, the density of molecule presentation can be much higher in nanofibrous than in flat structures. Thus, biomolecule incorporation in nanofibers can lead to more efficient modulation of cell behaviors than other methods of presentation [151].

Cell shape has been shown to strongly influence cell behavior. The differentiation of MSCs was directed toward an osteoblastic fate when cells were allowed to flatten and spread, and were directed toward an adipogenic fate when constrained to a rounded shape [152]. Cytoskeletal organization, which is related to cell shape, could be the mechanism by which cell shape modulates other cell behaviors. In the previously described study, flattened or spread cells had more prominent stress fibers than rounded cells, and inhibition of myosin-generated cytoskeletal tension in those spread cells lead to adipogenic behaviors without changing cell shape [152]. In a similar study, differentiation of an adipogenic cell line was inhibited by allowing them to adopt a well-spread shape, but this inhibitory effect could be reversed by chemically disrupting the cytoskeleton [153]. The mechanism of transduction of cell shape and cytoskeletal properties into gene expression could be due to the transmission of mechanical forces from the cytoskeleton directly to the nucleus [154]. Nuclear shape has been directly measured and correlated with changes in gene expression and protein synthesis [155, 156]. Because aligned and randomly oriented nanofibrous substrates share similar dimensionality, it can be theorized that mechanisms related to cell shape are the major cause of cell behavior differences observed between the two substrates.

Topography-induced cell morphologies can be explained by cell receptor and membrane interactions with their underlying substrate. The elongated cell morphology commonly observed on aligned nanofiber substrates may be regulated by receptor adhesion characteristics and cell membrane configurations associated with nanofiber structure and orientation. Nanofibrous topography could be a key factor for activation of adhesion proteins and integrin expression, and the specific orientation and diameter of nanofibrous substrates can result in significant effects on overall expression and distribution patterns of integrin receptors [132, 134, 145]. Integrin receptor expression was up to 15 times greater in cells attached to aligned

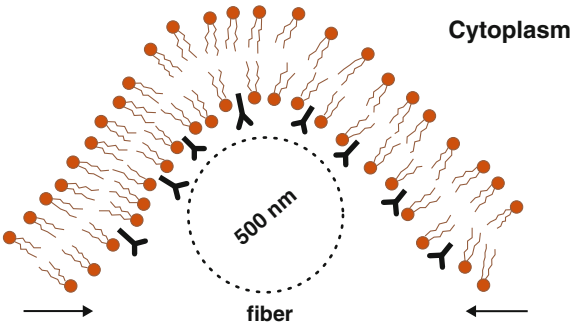

Fig. 10 Cell membrane wrapping around a nanofiber with compatible ligands. *Arrows* indicate membrane wrapping to reduce free energy of the interaction and increase the local curvature of the membrane [116]

nanofiber substrates compared to those with random orientation [145]. In addition, the location and orientation of filament structures protruding out of cells was different on aligned and randomly oriented nanofiber structures [117, 145]. The geometry of nanofibers may also lead to interactions with the cell membrane that result in an elongated structure. When a cell comes in contact with a fiber, its membrane receptors bind to ligands on the fiber surface and the membrane wraps around the fiber to reduce the free energy of the reaction (Fig. 10) [116]. This results in increased elastic energy, associated with increased curvature of the membrane, which is reduced as the cell elongates along the fiber [116].

5 Tissue Engineering Applications

Aligned nanofibrous structures have many applications in the biomedical field, including sutures [46, 157] and drug delivery applications [46]. However, one of the most promising uses for these aligned structures is in tissue engineering constructs applications and tissue regeneration. As previously mentioned, tissues such as nerve, blood vessel, skeletal muscle, and bone contain highly aligned collagen fibrils or other aligned protein nanofibers. This precisely arranged structure is very important in order to provide the necessary properties for these tissues to serve their intended function. When these tissues become injured or degenerated, intervention must take place to restore function. Regeneration of aligned tissue using an aligned nanofiber tissue engineering approach has been investigated in tissue types including, but not limited to, neural [109, 117, 158–163], vascular [87, 131, 164–170], skeletal muscle [52, 110], bone [58, 114, 171–175], cartilage [111, 130, 176–180], ligament [104, 123, 181], and tendon [145, 175]. This research area focuses on fabricating highly aligned natural or synthetic polymer nanofiber structures in order to serve as a matrix for cells to regenerate aligned tissue with structures similar to native tissue. Evidence presented in Sect. 4 leads to the hypothesis that regeneration of aligned tissues will be more effective when the native structure is mimicked as closely as possible. The synthetic scaffold serves as a template for the cells to attach to and align on, and also promotes newly produced

ECM to align. Researchers are now using this approach to attempt to regenerate a wide variety of aligned tissues. Such approaches are summarized below, with a focus on the most advanced, clinically related translational approaches.

5.1 Neural Tissue

Neural tissue regeneration is one of the most commonly investigated applications of aligned nanofiber-based tissue engineering constructs. The most clinically relevant studies are related to peripheral nerve regeneration through the use of nerve conduits after injury or degeneration. The ability of nerves to regenerate and restore function depends on the alignment and elongation of healthy neurites across an injury site to reestablish connections. Though the peripheral nervous system has a natural regenerative capacity, surgical intervention may be necessary to stimulate axonal growth across the damaged nerve gap in order to restore function, especially in more serious injuries. Current methods to accomplish this include the use of allografts or autografts; however, there are many issues associated with these methods, including limited availability. A common tissue engineering approach to stimulate nerve regeneration is the implantation of a semipermeable nerve conduit that connects two nerve stumps. These conduits allow the free exchange of nutrients and growth factors required for nerve regeneration while providing a protected growth environment. Recently, the use of aligned nanofibers in nerve conduits has generated a lot of interest due to their ability to promote alignment and elongation in regenerating axons, and preferential differentiation of neural stem cells into neurons. In natural peripheral nerve regeneration, axon regrowth is guided by aligned ECM proteins [2]. Aligned nanofiber substrates may be able to fill this role in tissue engineering approaches.

Nanofibrous architecture has been incorporated into nerve conduits in several configurations. Electrospinning is the preferred method of nanofiber fabrication for these scaffolds due to its versatility and its capacity to produce long aligned fibers (of several centimeters) that completely span the nerve gap. Nerve conduits may be fabricated entirely from aligned nanofibers or they may be attached to the inner surface of a nerve conduit made from another material. Single material nanofiber conduits can be manufactured by rolling flat aligned nanofiber sheets into a tubular structure (Fig. 11), but modified one-step electrospinning methods have also been

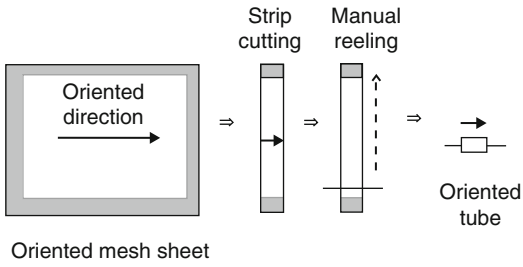

Fig. 11 3D construction of nerve conduit by rolling a sheet of aligned nanofibers [192]

developed to form tubular structures with axial nanofiber alignment [82]. Composite nerve guidance tubes containing axially aligned nanofibers attached to their inner walls can be fabricated when polymer films are coated with aligned nanofibers and rolled into a tubular structure [119, 159].

Nerve conduits have been evaluated in nerve defect models, such as the sciatic nerve, in order to evaluate their capacity to promote nerve tissue regeneration [159]. The results of several such studies have demonstrated significantly enhanced nerve regeneration for conduits containing aligned nanofibers, as compared to controls without fibers. For instance, a 15 mm critical defect gap was effectively bridged in 100% of the rats treated with rolled polymer film conduits coated with aligned nanofibers, whereas controls, without nanofibers, only bridged the gap in 50% of the rats [159]. Both axially and circumferentially aligned nanofibers promoted a significant increase in nerve cross-sectional area compared to controls, but grafts with axial nanofiber alignment promoted more myelinated axons and a higher percentage of electrophysiological recovery than grafts with circumferentially aligned fibers [159]. While these results are promising, aligned nanofibers were only present on the inner walls of these conduits, and thus only neurons regenerating near the walls of the grafts had direct contact with the nanofibrous architecture. Other methods have been developed to distribute aligned nanofibers throughout the volume of a nerve bridging conduit. Flat nanofiber-containing sheets rolled into spiral shapes [115, 158] provide some aligned fiber structure throughout the graft volume. Micrometer diameter nanofiber yarns were also inserted into bridging conduits to distribute nanofibrous structure throughout their full thickness [163]. In some cases, nerve conduits containing aligned nanofiber yarns performed better than nerve autografts in promoting recovery of sensory and motor function after sciatic nerve resection [163]. Growth factor incorporation, such as nerve growth factor and glial cell-derived neurotrophic factor, can further improve the performance of nerve bridging conduits containing aligned nanofibers [159, 163].

Similar neural applications of aligned nanofibers include spinal cord repair and regeneration of aligned neural tracks in the brain. These applications, however, are much more difficult to address due to the increased inflammatory response in CNS tissue, as well as the lack of natural regeneration in CNS tissues.

5.2 Vascular Tissue

Aligned nanofibrous scaffolds are also being investigated as tissue engineering solutions for disease and degeneration in cardiovascular tissues [87, 165, 167, 168]. Aligned nanofibers could have several cardiovascular system applications, such as cardiac patches [43, 108], but the main thrust of research in this area is in the design of a vascular graft. The prevalence of vascular and heart disease is extremely high, with many of these problems arising from occlusions in coronary and peripheral arteries. Autologous grafting procedures are limited by a lack of donor tissue and by patient morbidity associated with harvest surgery. Current prosthetic grafts

suffer from low patency rates due to issues arising from thrombosis, compliance mismatch, and biocompatibility. It is apparent that a better graft is needed, and aligned nanofibers offer several attractive properties for vascular graft design. Aligned nanofibers may be used to direct smooth muscle cell arrangement in a circumferentially aligned orientation similar to natural vessels and could promote ordered ECM assembly in this configuration. In addition, aligned nanofibers can offer excellent mechanical strength. Tensile strength increases with increasing degree of fiber alignment, which is extremely important in resisting the high pressures associated with this application [182].

Similar to nerve conduits, vascular grafts can be fabricated by rolling flat aligned electrospun nanofibrous sheets into tubular constructs [87]. Fiber sheets are rolled in a way that aligns fibers in the circumferential direction in order to provide mechanical strength and circumferential cell guidance specific to vascular tissue. Fully cellularized grafts may be fabricated when cells are grown on aligned nanofiber sheets before rolling into a tubular structure [168]. Such fully cellularized grafts showed promising results after 60 days in vivo [168]. The cellular morphology and orientation of the ECM produced in the grafts were very similar to that of the native ECM, perhaps in part due to the aligned nanofiber microstructure.

One-step fabrication of tubular grafts directly on a rotating mandrel is desirable to improve efficiency, as well as to ensure a uniform structure with adhesion between layers and no line of weakness. Randomly oriented tubular vascular grafts are commonly fabricated in one step using the rotating mandrel electrospinning method. However, this method alone is not sufficient for the fabrication of a small diameter graft with circumferential fiber alignment. Fiber alignment is dependent on matching the electrospinning jet speed with the tangential velocity of the collecting mandrel, and the tangential velocity of the mandrel is dependent on both the rotational velocity and the collection mandrel diameter (tangential velocity = rotational velocity × mandrel diameter × π). Therefore, when a small mandrel of a few millimeters is used, the required rotational velocities become so high that ordered collection is disrupted. However, a small diameter tubular graft with aligned fibers has been fabricated directly on a rotating mandrel using a modified collection method, as described in Sect. 3.3.1 (Fig. 5). In this case, the path of the electrospinning jet was controlled by oppositely charged electrodes, and a nonconductive rotating mandrel was placed between the spinneret and the electrodes to collect nanofibers. This method allowed the fabrication of well-aligned nanofiber tubes with controlled fiber angles, which were collected on mandrels as small as 4 mm at rotational speeds less than 1,000 rpm [87].

5.3 Skeletal Muscle

Skeletal muscle tissue engineering requires a considerably different structure than the two other tissues discussed above. The main concern with skeletal muscle regeneration is the alignment and maturation of large multinucleated muscle fibers.

This is especially important because it affects the ability of the muscle to contract as a whole. For this reason, an aligned nanofibrous tissue engineering approach is being investigated for skeletal muscle regeneration [52, 110, 146]. The focus in regenerating this tissue is to promote the development of full-thickness skeletal muscle grafts that can be implanted in variously shaped skeletal muscle defects caused by congenital conditions, traumatic injury, and tumor excision. Such grafts should promote the in vivo development of a 3D extracellular matrix and fully functional vascularized multinucleated muscle fibers. Current research, however, is still generally focused on 2D nanofiber scaffolds. Progenitor cell lines such as C2C12 myoblasts or explanted skeletal muscle cells are most often seeded onto highly aligned nanofibrous sheets to determine the ability of the aligned scaffolds to guide cellular alignment and myotube formation [52, 110]. Results indicate that cells seeded onto aligned nanofibrous scaffolds exhibit significantly greater alignment, myotube formation, and myotube contractility, as indicated by correctly arranged sarcomeric contractile machinery [52, 110]. Challenges in utilizing aligned nanofibers in skeletal muscle tissue engineering include the design of structures that promote alignment and myotube maturation in 3D, while promoting the vascularization that is required for sustaining cell survival and function within thicker constructs.

5.4 Bone

Bone is another tissue investigated for aligned nanofibrous tissue regeneration strategies. With bone disease and defects being extremely prevalent in today's active and aging population, the need for bone substitutes is very high. Current strategies for treating critically sized defects in bone include allografts and autografts; however, these methods have many issues, including lack of available donors, donor site morbidity [183], and infection [184]. For these reasons, researchers are investigating a regenerative approach when trying to solve this problem. With the structure and composition of bone consisting of hydroxyapatite deposited on highly aligned collagen fibers, it makes sense that aligned nanofibers are now being investigated as scaffolds for the regeneration of bone tissue. Aligned nanofiber scaffolds can provide mechanical strength and promote cellular alignment and ordered ECM production. In addition, hydroxyapatite can be coated onto these aligned nanofibers, or incorporated within, in order to from a bonelike composite structure [185, 186]. From here, strategies could be developed to create numerous different types of 3D structures, incorporating aligned nanofibers, which may allow the regeneration of multiple types and structures of bone.

5.5 Cartilage, Tendons and Ligaments

Aligned nanofiber-based approaches are also being investigated for regeneration of connective tissue such as cartilage, tendons, and ligaments. Aligned collagen fibrils,

found in the superficial zone of articular cartilage, provide crucial tensile strength to the tissue. Degeneration of the collagen in this zone, due to osteoarthritis, aging, and injury, often results in significantly diminished mechanical properties of the cartilage. Tissue engineering approaches are being investigated as methods to regenerate the superficial zone of articular cartilage to restore function [111, 130]. MSCs cultured on aligned nanofiber substrates have demonstrated enhanced chondrogenic differentiation and deposited a well organized ECM that had significantly greater mechanical strength than unorganized ECM deposited on non-aligned nanofiber substrates [111, 130].

Aligned nanofibrous scaffolds are also well suited for the regeneration of ligaments and tendons because they mimic the tightly packed aligned collagen fibrils that are a major component of these tissues. Explanted tendon and ligament cells have been cultured on aligned nanofibers and in aligned nanofiber/hydrogel composite substrates to evaluate their potential as tissue engineering scaffolds [104, 112]. However, similar to bone and skeletal muscle regeneration, research in aligned fiber-based regeneration of cartilage, tendon, and ligament tissue is generally limited to in vitro responses of tissue-specific cells to aligned nanofibrous substrates.

Directly after implantation, tendon and ligament scaffolds would have to withstand the large forces that these tissues experience daily. For this reason, tissue scaffolds must be both mechanically strong and promote tissue regeneration. Aligned nanofibrous scaffolds in yarn-like structures may be suitable for mimicking the natural structure of these tissues and enhancing the mechanical properties. Several techniques have been investigated to fabricate nonwoven and braided yarn-like structures from aligned nanofibers [45, 187, 188].

5.6 Cornea

Other less conventional tissues are also being investigated using an aligned nanofibrous tissue engineering approach, including the cornea. The very distinct structure of the cornea creates a transparent membrane that is minimally disruptive to the passage of light, for enhanced vision. This structure is composed of proteoglycans and highly aligned collagen I and collagen IV fibers, which are of uniform diameter and uniformly spaced apart. These aligned protein nanofibers are formed into lamellae and can be stacked at varying angles [68, 189]. Tissue engineering approaches are now being considered as a potential treatment for corneal blindness. Preliminary data indicate that a tissue engineering scaffold fabricated by electrospinning collagen I is a promising method for cornea tissue regeneration [68, 189].

5.7 Challenges

Nanofiber-based tissue engineering strategies are faced with similar challenges to those encountered throughout the field of tissue engineering. These challenges

include selection and design of materials that are bioactive and possess suitable mechanical properties, as well as optimized degradation rates. In addition, scaffolds must be designed in a way that allows cell infiltration throughout their volume and promotes functional vascular formation to sustain cellular ingrowth.

Great advances are constantly being made in the design of new biomaterials and the identification of functional molecules that produce desirable cell responses. However, it can be difficult to apply these advances to aligned nanofibrous-based tissue engineering strategies due to fabrication constraints, such as specific solubility and electrical property requirements as well as thermal or chemical biomolecule deactivation. The major materials-related challenges in aligned nanofibrous scaffold fabrication are generally related to developing methods to fabricate aligned nanofibers from the most desirable materials and finding ways to incorporate the most desirable functional molecules. In addition, the unique structure of aligned nanofibers can have a pronounced effect on material properties such as mechanical strength and degradation rate, and on cell interactions with surface molecules.

The second major challenge in aligned nanofiber tissue engineering is in assembling the fibers into 3D structures with an architecture that is permeable to cell infiltration and vascular ingrowth. Aligned nanofibers in a 3D bundle or stack tend to be tightly packed together and thus offer little room for cell infiltration. Methods of fabricating 3D aligned nanofiber structures with a loose structure or controlled packing density must be developed to improve the cell penetration properties of these scaffolds. Examples of strategies to address this problem include incorporating a sacrificial fiber component into an aligned nanofiber mat [190], and fabrication of a composite material in which aligned nanofibers are fixed in a cell-permeable substrate at a controlled packing density [191].

6 Concluding Remarks

Many tissues rely on a well-aligned cellular and ECM orientation to perform their required functions. Damage and degeneration of these tissues requires a regenerative response that restores function. It is hypothesized that tissue engineering approaches that restore similar cellular morphology and structural architectures result in better functional recovery. It has been shown in vitro that cell behaviors such as morphology, elongation, proliferation, ECM production, and differentiation can all be modulated by scaffold architecture. Furthermore, aligned substrates, such as aligned polymer nanofibers, promote cell behaviors associated with aligned tissues. Behaviors desirable in aligned tissue engineering include elongation, unidirectional alignment, ordered ECM production, accelerated unidirectional migration, and preferred differentiation of stem cells into phenotypes associated with aligned tissues. Despite the promise of aligned polymer nanofibers, functional in vivo tissue engineering strategies are somewhat limited due to difficulties in assembling aligned nanofiber scaffolds with precisely controlled architecture. This is especially relevant for 3D scaffolds required for regeneration of thick

vascularized tissues. Researchers are currently exploring better and more versatile ways to fabricate electrospun aligned nanofibers and assemble them into structures. Such techniques increased fiber alignment, length, and yield, and allowed more precise control of fiber deposition location, fiber density, and fiber orientation within aligned nanofiber structures. We hypothesize that the potential of aligned polymer nanofibers in the clinical setting will be realized as innovative methods of aligned nanofiber assembly are applied to the design of better, more precisely assembled functional tissue engineering scaffolds.

Acknowledgment This work is supported by the grants from NIH (NS050243), NIH/NCRR (P20RR021949), and American Heart Association.

References

1. Sakai T, Larsen M, Yamada KM (2003) Fibronectin requirement in branching morphogenesis. Nature 423(6942):876–881
2. Fawcett JW, Keynes RJ (1990) Peripheral nerve regeneration. Annu Rev Neurosci 13:43–60
3. Rebustini IT et al (2007) Laminin alpha5 is necessary for submandibular gland epithelial morphogenesis and influences FGFR expression through beta1 integrin signaling. Dev Biol 308(1):15–29
4. Beachley V, Wen X (2010) Polymer nanofibrous structures: fabrication, biofunctionalization, and cell interactions. Prog Polym Sci 35(7):868–892
5. Huang Z-M et al (2003) A review on polymer nanofibers by electrospinning and their applications in nanocomposites. Compos Sci Technol 63(15):2223–2253
6. Jeong HE et al (2006) Stretched polymer nanohairs by nanodrawing. Nano Lett 6 (7):1508–1513
7. Xing X, Wang Y, Li B (2008) Nanofibers drawing and nanodevices assembly in poly (trimethylene terephthalate). Opt Express 16(14):10815–10822
8. Nain A et al (2006) Drawing suspended polyer micro-/nanofibers using glass micropipettes. Appl Phys Lett 89:1831051–1831053
9. Nain AS et al (2009) Dry spinning based spinneret based tunable engineered parameters (STEP) technique for controlled and aligned deposition of polymeric nanofibers. Macromol Rapid Commun 30(16):1406–1412
10. Cheng F et al (2006) Conducting poly(aniline) nanotubes and nanofibers: controlled synthesis and application in lithium/poly(aniline) rechargeable batteries. Chemistry 12(11):3082–3088
11. Badrossamay MR et al (2010) Nanofiber assembly by rotary jet-spinning. Nano Lett 10 (6):2257–2261
12. Li HY, Ke YC, Hu YL (2006) Polymer nanofibers prepared by template melt extrusion. J Appl Polym Sci 99(3):1018–1023
13. Grimm S et al (2008) Nondestructive replication of self-ordered nanoporous alumina membranes via cross-linked polyacrylate nanofiber arrays. Nano Lett 8(7):1954–1959
14. Porter JR, Henson A, Popat KC (2009) Biodegradable poly(epsilon-caprolactone) nanowires for bone tissue engineering applications. Biomaterials 30(5):780–788
15. Lee W et al (2004) Nanostructuring of a polymeric substrate with well-defined nanometer-scale topography and tailored surface wettability. Langmuir 20(18):7665–7669
16. Tao SL, Desai TA (2007) Aligned arrays of biodegradable poly(epsilon-caprolactone) nanowires and nanofibers by template synthesis. Nano Lett 7(6):1463–1468
17. Sheng XL, Zhang JH (2009) Superhydrophobic behaviors of polymeric surfaces with aligned nanofibers. Langmuir 25(12):6916–6922

18. Prasanthkumar S et al (2010) Solution phase epitaxial self-assembly and high charge-carrier mobility nanofibers of semiconducting molecular gelators. J Am Chem Soc 132(26):8866–8867
19. Weronski KJ et al (2010) Time-lapse atomic force microscopy observations of the morphology, growth rate, and spontaneous alignment of nanofibers containing a peptide-amphiphile from the hepatitis G virus (NS3 protein). J Phys Chem B 114(1):620–625
20. Hung AM, Stupp SI (2009) Understanding factors affecting alignment of self-assembling nanofibers patterned by sonication-assisted solution embossing. Langmuir 25(12):7084–7089
21. Hung AM, Stupp SI (2007) Simultaneous self-assembly, orientation, and patterning of peptide-amphiphile nanofibers by soft lithography. Nano Lett 7(5):1165–1171
22. Nogueira GM et al (2010) Layer-by-layer deposited chitosan/silk fibroin thin films with anisotropic nanofiber alignment. Langmuir 26(11):8953–8958
23. Kyotani M et al (2010) Entanglement-free fibrils of aligned polyacetylene films that produce single nanofibers. Nanoscale 2(4):509–514
24. Mata A et al (2009) Micropatterning of bioactive self-assembling gels. Soft Matter 5 (6):1228–1236
25. Everett TA, Higgins DA (2009) Electrostatic self-assembly of ordered perylene-diimide/polyelectrolyte nanofibers in fluidic devices: from nematic domains to macroscopic alignment. Langmuir 25(22):13045–13051
26. Merzlyak A, Indrakanti S, Lee SW (2009) Genetically engineered nanofiber-like viruses for tissue regenerating materials. Nano Lett 9(2):846–852
27. Lee P et al (2006) Microfluidic alignment of collagen fibers for in vitro cell culture. Biomed Microdevices 8(1):35–41
28. Guo Y et al (2006) Alignment of glycolipid nanotubes on a planar glass substrate using a two-step microextrusion technique. J Nanosci Nanotechnol 6(5):1464–1466
29. Kim J et al (2008) Magnetic field effect for cellulose nanofiber alignment. J Appl Phys 104 (9):096104
30. Sugiyama J, Chanzy H, Maret G (1992) Orientation of cellulose microcrystals by strong magnetic fields. Macromolecules 25(16):4232–4234
31. Torbet J, Ronziere MC (1984) Magnetic alignment of collagen during self-assembly. Biochem J 219:1057–1059
32. Lowik D et al (2007) A highly ordered material from magnetically aligned peptide amphiphile nanofiber assemblies. Adv Mater 19(9):1191−+
33. Guo C, Kaufman LJ (2007) Flow and magnetic field induced collagen alignment. Biomaterials 28(6):1105–1114
34. Rollings DA et al (2007) Formation and aqueous surface wettability of polysiloxane nanofibers prepared via surface initiated, vapor-phase polymerization of organotrichlorosilanes. Langmuir 23(10):5275–5278
35. Sun QH et al (2009) Fabrication of aligned polyaniline nanofiber array via a facile wet chemical process. Macromol Rapid Commun 30(12):1027–1032
36. Li M, Wei ZX, Jiang L (2008) Polypyrrole nanofiber arrays synthesized by a biphasic electrochemical strategy. J Mater Chem 18(19):2276–2280
37. Czaja WK et al (2007) The future prospects of microbial cellulose in biomedical applications. Biomacromolecules 8(1):1–12
38. Kondo T et al (2002) Biodirected epitaxial nanodeposition of polymers on oriented macromolecular templates. Proc Natl Acad Sci USA 99(22):14008–14013
39. Putra A et al (2008) Tubular bacterial cellulose gel with oriented fibrils on the curved surface. Polymer 49(7):1885–1891
40. Uraki Y et al (2007) Honeycomb-like architecture produced by living bacteria, gluconacetobacter xylinus. Carbohydr Polym 69(1):1–6
41. Sano MB et al (2010) Electromagnetically controlled biological assembly of aligned bacterial cellulose nanofibers. Ann Biomed Eng 38(8):2475–2484
42. Afifi AM et al (2009) Fabrication of aligned poly(L-lactide) fibers by electrospinning and drawing. Macromol Mater Eng 294(10):658–665

43. Zong X et al (2005) Electrospun fine-textured scaffolds for heart tissue constructs. Biomaterials 26(26):5330–5338
44. Ji JY et al (2009) Significant improvement of mechanical properties observed in highly aligned carbon-nanotube-reinforced nanofibers. J Phys Chem C 113(12):4779–4785
45. Smit E, Buttner U, Sanderson RD (2005) Continuous yarns from electrospun fibers. Polymer 46(8):2419–2423
46. Reneker DH, Chun I (1996) Nanometre diameter fibres of polymer, produced by electrospinning. Nanotechnology 7(3):216–223
47. Yee WA et al (2007) Morphology, polymorphism behavior and molecular orientation of electrospun poly(vinylidene fluoride) fibers. Polymer 48(2):512–521
48. Wu YQ, Carnell LA, Clark RL (2007) Control of electrospun mat width through the use of parallel auxiliary electrodes. Polymer 48(19):5653–5661
49. Edwards MD et al (2010) Development of orientation during electrospinning of fibres of poly (epsilon-caprolactone). Eur Polym J 46(6):1175–1183
50. Bashur CA, Dahlgren LA, Goldstein AS (2006) Effect of fiber diameter and orientation on fibroblast morphology and proliferation on electrospun poly(D, L-lactic-co-glycolic acid) meshes. Biomaterials 27(33):5681–5688
51. Wang HB et al (2009) Creation of highly aligned electrospun poly-L-lactic acid fibers for nerve regeneration applications. J Neural Eng 6(1):016001
52. Aviss KJ, Gough JE, Downes S (2010) Aligned electrospun polymer fibres for skeletal muscle regeneration. Eur Cells Mater 19:193–204
53. Courtney T et al (2006) Design and analysis of tissue engineering scaffolds that mimic soft tissue mechanical anisotropy. Biomaterials 27(19):3631–3638
54. Zhong S et al (2006) An aligned nanofibrous collagen scaffold by electrospinning and its effects on in vitro fibroblast culture. J Biomed Mater Res A 79(3):456–463
55. Lee JY et al (2010) Enhanced polarization of embryonic hippocampal neurons on micron scale electrospun fibers. J Biomed Mater Res A 92A(4):1398–1406
56. Li WJ et al (2007) Engineering controllable anisotropy in electrospun biodegradable nanofibrous scaffolds for musculoskeletal tissue engineering. J Biomech 40(8): 1686–1693
57. Chan KHK et al (2010) Morphologies and electrical properties of electrospun poly (R)-3-hydroxybutyrate-co-(R)-3-hydroxyvalerate/multiwalled carbon nanotubes fibers. J Appl Polym Sci 116(2):1030–1035
58. Thomas V et al (2006) Mechano-morphological studies of aligned nanofibrous scaffolds of polycaprolactone fabricated by electrospinning. J Biomater Sci Polym Ed 17(9):969–984
59. Bashur CA et al (2009) Effect of fiber diameter and alignment of electrospun polyurethane meshes on mesenchymal progenitor cells. Tissue Eng A 15(9):2435–2445
60. McClure MJ et al (2009) Electrospinning-aligned and random polydioxanone-polycaprolactone-silk fibroin-blended scaffolds: geometry for a vascular matrix. Biomed Mater 4(5):055010
61. Jose MV et al (2007) Morphology and mechanical properties of Nylon 6/MWNT nanofibers. Polymer 48(4):1096–1104
62. Li D, Wang YL, Xia YN (2003) Electrospinning of polymeric and ceramic nanofibers as uniaxially aligned arrays. Nano Lett 3(8):1167–1171
63. Xin Y et al (2008) Fabrication of well-aligned PPV/PVP nanofibers by electrospinning. Mater Lett 62(6–7):991–993
64. Kuo CC, Wang CT, Chen WC (2008) Highly-aligned electrospun luminescent nanofibers prepared from polyfluorene/PMMA blends: fabrication, morphology, photophysical properties and sensory applications. Macromol Mater Eng 293(12):999–1008
65. Dalton PD et al (2007) Electrospinning of polymer melts: phenomenological observations. Polymer 48(23):6823–6833
66. Jalili R et al (2006) Fundamental parameters affecting electrospinning of PAN nanofibers as uniaxially aligned fibers. J Appl Polym Sci 101(6):4350–4357

67. Li D, Wang YL, Xia YN (2004) Electrospinning nanofibers as uniaxially aligned arrays and layer-by-layer stacked films. Adv Mater 16(4):361–366
68. Wray LS, Orwin EJ (2009) Recreating the microenvironment of the native cornea for tissue engineering applications. Tissue Eng A 15(7):1463–1472
69. Bazbouz MB, Stylios GK (2008) Alignment and optimization of nylon 6 nanofibers by electrospinning. J Appl Polym Sci 107(5):3023–3032
70. Liu LH, Dzenis YA (2008) Analysis of the effects of the residual charge and gap size on electrospun nanofiber alignment in a gap method. Nanotechnology 19(35):355307
71. Katta P et al (2004) Continuous electrospinning of aligned polymer nanofibers onto a wire drum collector. Nano Lett 4(11):2215–2218
72. Teo WE, Ramakrishna S (2006) A review on electrospinning design and nanofibre assemblies. Nanotechnology 17:R89–R106
73. Pokorny M, Niedoba K, Velebny V (2010) Transversal electrostatic strength of patterned collector affecting alignment of electrospun nanofibers. Appl Phys Lett 96(19):193111
74. Beachley V, Wen X (2009) Effect of electrospinning parameters on the nanofiber diameter and length. Mater Sci Eng C 29:663–668
75. Teo WE, Ramakrishna S (2005) Electrospun fibre bundle made of aligned nanofibres over two fixed points. Nanotechnology 16(9):1878–1884
76. Ayutsede J et al (2006) Carbon nanotube reinforced Bombyx mori silk nanofibers by the electrospinning process. Biomacromolecules 7(1):208–214
77. Carnell LS et al (2009) Electric field effects on fiber alignment using an auxiliary electrode during electrospinning. Scr Mater 60(6):359–361
78. Acharya M, Arumugam GK, Heiden PA (2008) Dual electric field induced alignment of electrospun nanofibers. Macromol Mater Eng 293(8):666–674
79. Kim G, Kim W (2006) Formation of oriented nanofibers using electrospinning. Appl Phys Lett 88:233101
80. Deitzel JM et al (2001) Controlled deposition of electrospun poly(ethylene oxide) fibers. Polymer 42:8163–8170
81. Theron A, Zussman E, Yarin AL (2001) Electrostatic field-assisted alignment of electrospun nanofibres. Nanotechnology 12(3):384–390
82. Yao L et al (2009) Orienting neurite growth in electrospun fibrous neural conduits. J Biomed Mater Res B Appl Biomater 90B(2):483–491
83. Bhattarai N et al (2005) Electrospun chitosan-based nanofibers and their cellular compatibility. Biomaterials 26(31):6176–6184
84. Secasanu VP, Giardina CK, Wang YD (2009) A novel electrospinning target to improve the yield of uniaxially aligned fibers. Biotechnol Prog 25(4):1169–1175
85. Carnell LS et al (2008) Aligned mats from electrospun single fibers. Macromolecules 41 (14):5345–5349
86. Sundaray B et al (2004) Electrospinning of continuous aligned polymer fibers. Appl Phys Lett 84(7):1222–1224
87. Teo WE et al (2005) Porous tubular structures with controlled fibre orientation using a modified electrospinning method. Nanotechnology 16(6):918–924
88. Mo XM, Weber HJ (2004) Electrospinning P(LLA-CL) nanofiber: a tubular scaffold fabrication with circumferential alignment. Macromol Symp 217:413–416
89. Lee H, Yoon H, Kim G (2009) Highly oriented electrospun polycaprolactone micro/nanofibers prepared by a field-controllable electrode and rotating collector. Appl Phys A Mater Sci Process 97(3):559–565
90. Kim GH (2006) Electrospinning process using field-controllable electrodes. J Polym Sci B Polym Phys 44(10):1426–1433
91. Attout A, Yunus S, Bertrand P (2008) Electrospinning and alignment of polyaniline-based nanowires and nanotubes. Polym Eng Sci 48(9):1661–1666
92. Ishii Y, Sakai H, Murata H (2008) A new electrospinning method to control the number and a diameter of uniaxially aligned polymer fibers. Mater Lett 62(19):3370–3372

93. Kessick R, Fenn J, Tepper G (2004) The use of AC potentials in electrospraying and electrospinning processes. Polymer 45(9):2981–2984
94. Sarkar S, Deevi S, Tepper G (2007) Biased AC electrospinning of aligned polymer nanofibers. Macromol Rapid Commun 28(9):1034–1039
95. Rafique J et al (2007) Electrospinning highly aligned long polymer nanofibers on large scale by using a tip collector. Appl Phys Lett 91:063126
96. Zhou W et al (2007) Gas flow-assisted alignment of super long electrospun nanofibers. J Nanosci Nanotechnol 7(8):2667–2673
97. Liu YQ et al (2010) Magnetic-field-assisted electrospinning of aligned straight and wavy polymeric nanofibers. Adv Mater 22(22): 2454−+
98. Beachley V, Wen X (2010) Fabrication of three dimensional aligned nanofiber array, *US-7828539*, Clemson University (Clemson, SC, US) US
99. Madhugiri S et al (2003) Electrospun MEH-PPV/SBA-15 composite nanofibers using a dual syringe method. J Am Chem Soc 125(47):14531–14538
100. Kidoaki S, Kwon IK, Matsuda T (2005) Mesoscopic spatial designs of nano- and microfiber meshes for tissue-engineering matrix and scaffold based on newly devised multilayering and mixing electrospinning techniques. Biomaterials 26(1):37–46
101. Ding B et al (2004) Fabrication of blend biodegradable nanofibrous nonwoven mats via multi-jet electrospinning. Polymer 45(6):1895–1902
102. Theron SA et al (2005) Multiple jets in electrospinning: experiment and modeling. Polymer 46(9):2889–2899
103. Chow WN et al (2007) Evaluating neuronal and glial growth on electrospun polarized matrices: bridging the gap in percussive spinal cord injuries. Neuron Glia Biol 3:119–126
104. Hayami JWS et al (2010) Design and characterization of a biodegradable composite scaffold for ligament tissue engineering. J Biomed Mater Res A 92A(4):1407–1420
105. Yao YF et al (2007) Fiber-oriented liquid crystal polarizers based on anisotropic electrospinning. Adv Mater 19(21): 3707−+
106. Li WJ et al (2003) Biological response of chondrocytes cultured in three-dimensional nanofibrous poly(epsilon-caprolactone) scaffolds. J Biomed Mater Res A 67(4):1105–1114
107. Yang F et al (2005) Electrospinning of nano/micro scale poly(L-lactic acid) aligned fibers and their potential in neural tissue engineering. Biomaterials 26(15):2603–2610
108. Rockwood DN et al (2008) Culture on electrospun polyurethane scaffolds decreases atrial natriuretic peptide expression by cardiomyocytes in vitro. Biomaterials 29(36):4783–4791
109. Chew SY et al (2008) The effect of the alignment of electrospun fibrous scaffolds on Schwann cell maturation. Biomaterials 29(6):653–661
110. Choi JS et al (2008) The influence of electrospun aligned poly(epsilon-caprolactone)/collagen nanofiber meshes on the formation of self-aligned skeletal muscle myotubes. Biomaterials 29(19):2899–2906
111. Wise JK et al (2009) Chondrogenic differentiation of human mesenchymal stem cells on oriented nanofibrous scaffolds: engineering the superficial zone of articular cartilage. Tissue Eng A 15(4):913–921
112. Moffat KL et al (2009) Novel nanofiber-based scaffold for rotator cuff repair and augmentation. Tissue Eng A 15(1):115–126
113. Corey JM et al (2007) Aligned electrospun nanofibers specify the direction of dorsal root ganglia neurite growth. J Biomed Mater Res A 83A(3):636–645
114. Ma J, He X, Jabbari E (2011) Osteogenic differentiation of marrow stromal cells on random and aligned electrospun poly(l-lactide) nanofibers. Ann Biomed Eng 39:14–25
115. Nisbet DR et al (2009) Neurite infiltration and cellular response to electrospun polycaprolactone scaffolds implanted into the brain. Biomaterials 30(27):4573–4580
116. Tian F et al (2008) Quantitative analysis of cell adhesion on aligned micro- and nanofibers. J Biomed Mater Res A 84(2):291–299
117. He LM et al (2010) Synergistic effects of electrospun PLLA fiber dimension and pattern on neonatal mouse cerebellum C17.2 stem cells. Acta Biomater 6(8):2960–2969

118. Patel S et al (2007) Bioactive nanofibers: synergistic effects of nanotopography and chemical signaling on cell guidance. Nano Lett 7(7):2122–2128
119. Madduri S, Papaloizos M, Gander B (2010) Trophically and topographically functionalized silk fibroin nerve conduits for guided peripheral nerve regeneration. Biomaterials 31 (8):2323–2334
120. Xie JW et al (2009) The differentiation of embryonic stem cells seeded on electrospun nanofibers into neural lineages. Biomaterials 30(3):354–362
121. Lam HJ et al (2010) In vitro regulation of neural differentiation and axon growth by growth factors and bioactive nanofibers. Tissue Eng A 16(8):2641–2648
122. Meng J et al (2009) Enhancement of nanofibrous scaffold of multiwalled carbon nanotubes/polyurethane composite to the fibroblasts growth and biosynthesis. J Biomed Mater Res A 88 (1):105–116
123. Shang SH et al (2010) The effect of electrospun fibre alignment on the behaviour of rat periodontal ligament cells. Eur Cells Mater 19:180–192
124. Chua KN et al (2006) Surface-aminated electrospun nanofibers enhance adhesion and expansion of human umbilical cord blood hematopoietic stem/progenitor cells. Biomaterials 27(36):6043–6051
125. Sangsanoh P et al (2007) In vitro biocompatibility of schwann cells on surfaces of biocompatible polymeric electrospun fibrous and solution-cast film scaffolds. Biomacromolecules 8 (5):1587–1594
126. Chen M et al (2007) Role of fiber diameter in adhesion and proliferation of NIH 3T3 fibroblast on electrospun polycaprolactone scaffolds. Tissue Eng 13(3):579–587
127. Rubenstein D et al (2007) Bioassay chamber for angiogenesis with perfused explanted arteries and electrospun scaffolding. Microcirculation 14(7):723–737
128. McKenzie JL et al (2004) Decreased functions of astrocytes on carbon nanofiber materials. Biomaterials 25(7–8):1309–1317
129. Elias KL, Price RL, Webster TJ (2002) Enhanced functions of osteoblasts on nanometer diameter carbon fibers. Biomaterials 23(15):3279–3287
130. Baker BM, Mauck RL (2007) The effect of nanofiber alignment on the maturation of engineered meniscus constructs. Biomaterials 28(11):1967–1977
131. Lu H et al (2009) Growth of outgrowth endothelial cells on aligned PLLA nanofibrous scaffolds. J Mater Sci Mater Med 20(9):1937–1944
132. Meng J et al (2010) Electrospun aligned nanofibrous composite of MWCNT/polyurethane to enhance vascular endothelium cells proliferation and function. J Biomed Mater Res A 95 (1):312–320
133. Lee CH et al (2005) Nanofiber alignment and direction of mechanical strain affect the ECM production of human ACL fibroblast. Biomaterials 26(11):1261–1270
134. Liu Y et al (2009) Effects of fiber orientation and diameter on the behavior of human dermal fibroblasts on electrospun PMMA scaffolds. J Biomed Mater Res A 90A(4):1092–1106
135. Li WJ, Jiang YJ, Tuan RS (2006) Chondrocyte phenotype in engineered fibrous matrix is regulated by fiber size. Tissue Eng 12(7):1775–1785
136. Liu Y et al (2009) Control of cell migration in two and three dimensions using substrate morphology. Exp Cell Res 315(15):2544–2557
137. Chua KN et al (2005) Stable immobilization of rat hepatocyte spheroids on galactosylated nanofiber scaffold. Biomaterials 26(15):2537–2547
138. Shih YR et al (2006) Growth of mesenchymal stem cells on electrospun type I collagen nanofibers. Stem Cells 24(11):2391–2397
139. Johnson J et al (2009) Quantitative analysis of complex glioma cell migration on electrospun polycaprolactone using time-lapse microscopy. Tissue Eng Part C Methods 15(4):531–540
140. Pham QP, Sharma U, Mikos AG (2006) Electrospun poly(epsilon-caprolactone) microfiber and multilayer nanofiber/microfiber scaffolds: characterization of scaffolds and measurement of cellular infiltration. Biomacromolecules 7(10):2796–2805

141. Balguid A et al (2009) Tailoring fiber diameter in electrospun poly(epsilon-caprolactone) scaffolds for optimal cellular infiltration in cardiovascular tissue engineering. Tissue Eng A 15(2):437–444
142. Kurpinski KT et al (2010) The effect of fiber alignment and heparin coating on cell infiltration into nanofibrous PLLA scaffolds. Biomaterials 31(13):3536–3542
143. Cao HQ et al (2010) The topographical effect of electrospun nanofibrous scaffolds on the in vivo and in vitro foreign body reaction. J Biomed Mater Res A 93A(3):1151–1159
144. Nur EKA et al (2006) Three-dimensional nanofibrillar surfaces promote self-renewal in mouse embryonic stem cells. Stem Cells 24(2):426–433
145. Yin Z et al (2010) The regulation of tendon stem cell differentiation by the alignment of nanofibers. Biomaterials 31(8):2163–2175
146. Huber A, Pickett A, Shakesheff KM (2007) Reconstruction of spatially orientated myotubes in vitro using electrospun, parallel microfibre arrays. Eur Cells Mater 14:56–63
147. Dang JM, Leong KW (2007) Myogenic induction of aligned mesenchymal stem cell sheets by culture on thermally responsive electrospun nanofibers. Adv Mater Deerfield 19(19):2775–2779
148. Lee MR et al (2010) Direct differentiation of human embryonic stem cells into selective neurons on nanoscale ridge/groove pattern arrays. Biomaterials 31(15):4360–4366
149. Leong MF et al (2009) Effect of electrospun poly(D, L-lactide) fibrous scaffold with nanoporous surface on attachment of porcine esophageal epithelial cells and protein adsorption. J Biomed Mater Res A 89(4):1040–1048
150. Baker SC, Southgate J (2008) Towards control of smooth muscle cell differentiation in synthetic 3D scaffolds. Biomaterials 29(23):3357–3366
151. Silva GA et al (2004) Selective differentiation of neural progenitor cells by high-epitope density nanofibers. Science 303(5662):1352–1355
152. McBeath R et al (2004) Cell shape, cytoskeletal tension, and RhoA regulate stem cell lineage commitment. Dev Cell 6(4):483–495
153. Spiegelman BM, Ginty CA (1983) Fibronectin modulation of cell shape and lipogenic gene expression in 3T3-adipocytes. Cell 35(3 Pt 2):657–666
154. Maniotis AJ, Chen CS, Ingber DE (1997) Demonstration of mechanical connections between integrins, cytoskeletal filaments, and nucleoplasm that stabilize nuclear structure. Proc Natl Acad Sci USA 94(3):849–854
155. Thomas CH et al (2002) Engineering gene expression and protein synthesis by modulation of nuclear shape. Proc Natl Acad Sci USA 99(4):1972–1977
156. McBride SH, Knothe ML (2008) Tate. Modulation of stem cell shape and fate A: the role of density and seeding protocol on nucleus shape and gene expression. Tissue Eng A 14(9):1561–1572
157. Hu W, Huang ZM (2010) Biocompatibility of braided poly(L-lactic acid) nanofiber wires applied as tissue sutures. Polym Int 59(1):92–99
158. Valmikinathan CM et al (2008) Novel nanofibrous spiral scaffolds for neural tissue engineering. J Neural Eng 5(4):422–432
159. Chew SY et al (2007) Aligned protein-polymer composite fibers enhance nerve regeneration: a potential tissue-engineering platform. Adv Funct Mater 17(8):1288–1296
160. Horne MK et al (2010) Three-dimensional nanofibrous scaffolds incorporating immobilized BDNF promote proliferation and differentiation of cortical neural stem cells. Stem Cells Dev 19(6):843–852
161. Hou XX et al (2008) Stretching-induced orientation to improve mechanical properties of electrospun pan nanocomposites. Int J Mod Phys B 22(31–32):5913–5918
162. Yoon H et al (2010) Fabricating highly aligned electrospun poly(epsilon-caprolactone) micro/nanofibers for nerve tissue regeneration. Polymer-Korea 34(3):185–190
163. Koh HS et al (2010) In vivo study of novel nanofibrous intra-luminal guidance channels to promote nerve regeneration. J Neural Eng 7(4):046003
164. Zhu YB et al (2010) Macro-alignment of electrospun fibers for vascular tissue engineering. J Biomed Mater Res B Appl Biomater 92B(2):508–516

165. Zhang XH et al (2009) Dynamic culture conditions to generate silk-based tissue-engineered vascular grafts. Biomaterials 30(19):3213–3223
166. Xu CY et al (2004) Aligned biodegradable nanotibrous structure: a potential scaffold for blood vessel engineering. Biomaterials 25(5):877–886
167. Uttayarat P et al (2010) Micropatterning of three-dimensional electrospun polyurethane vascular grafts. Acta Biomater 6(11):4229–4237
168. Hashi CK et al (2007) Antithrombogenic property of bone marrow mesenchymal stem cells in nanofibrous vascular grafts. Proc Natl Acad Sci USA 104(29):11915–11920
169. He W et al (2006) Biodegradable polymer nanofiber mesh to maintain functions of endothelial cells. Tissue Eng 12(9):2457–2466
170. Han ZZ et al (2008) Growing behavior of endothelial cells on electrospun aligned nanofibrous film of polyurethane. Chem J Chin Univer-Chin 29(5):1070–1073
171. Jose MV et al (2010) Aligned bioactive multi-component nanofibrous nanocomposite scaffolds for bone tissue engineering. Macromol Biosci 10(4):433–444
172. Chen F et al (2010) Hydroxyapatite nanorods/poly(vinyl pyrolidone) composite nanofibers, arrays and three-dimensional fabrics: electrospun preparation and transformation to hydroxyapatite nanostructures. Acta Biomater 6(8):3013–3020
173. Jose MV et al (2009) Fabrication and characterization of aligned nanofibrous PLGA/Collagen blends as bone tissue scaffolds. Polymer 50(15):3778–3785
174. Jose MV et al (2009) Aligned PLGA/HA nanofibrous nanocomposite scaffolds for bone tissue engineering. Acta Biomater 5(1):305–315
175. Xie JW et al (2010) "Aligned-to-random" nanofiber scaffolds for mimicking the structure of the tendon-to-bone insertion site. Nanoscale 2(6):923–926
176. Subramanian A et al (2004) Synthesis and evaluation of scaffolds prepared from chitosan fibers for potential use in cartilage tissue engineering. Biomed Sci Instrum 40:117–122
177. Subramanian A et al (2005) Preparation and evaluation of the electrospun chitosan/PEO fibers for potential applications in cartilage tissue engineering. J Biomater Sci Polym Ed 16(7):861–873
178. Baker BM et al (2009) Tissue engineering with meniscus cells derived from surgical debris. Osteoarthritis Cartilage 17(3):336–345
179. Nerurkar NL, Elliott DM, Mauck RL (2007) Mechanics of oriented electrospun nanofibrous scaffolds for annulus fibrosus tissue engineering. J Orthop Res 25(8):1018–1028
180. Yeganegi M, Kandel RA, Santerre JP (2010) Characterization of a biodegradable electrospun polyurethane nanofiber scaffold: mechanical properties and cytotoxicity. Acta Biomater 6(10):3847–3855
181. Sell SA, McClure MJ, Ayres CE, Simpson DG, Bowlin GL (2011) Preliminary investigation of airgap electrospun silk-fibroin-based structures for ligament analogue engineering. J Biomater Sci Polym Ed 22:1253–1273
182. Wu H et al (2010) Electrospinning of small diameter 3-D nanofibrous tubular scaffolds with controllable nanofiber orientations for vascular grafts. J Mater Sci Mater Med 21(12): 3207–3215
183. Silber JS et al (2003) Donor site morbidity after anterior iliac crest bone harvest for single-level anterior cervical discectomy and fusion. Spine (Phila Pa 1976) 28(2):134–139
184. Mankin HJ, Hornicek FJ, Raskin KA (2005) Infection in massive bone allografts. Clin Orthop Relat Res 432:210–216
185. Li X et al (2008) Coating electrospun poly(epsilon-caprolactone) fibers with gelatin and calcium phosphate and their use as biomimetic scaffolds for bone tissue engineering. Langmuir 24(24):14145–14150
186. Ngiam M et al (2009) The fabrication of nano-hydroxyapatite on PLGA and PLGA/collagen nanofibrous composite scaffolds and their effects in osteoblastic behavior for bone tissue engineering. Bone 45(1):4–16
187. Teo W-E et al (2007) A dynamic liquid support system for continuous electrospun yarn fabrication. Polymer 48(12):3400–3405

188. Hu W, Huang ZM, Liu XY (2010) Development of braided drug-loaded nanofiber sutures. Nanotechnology 21(31):315104
189. Meek KM, Boote C (2004) The organization of collagen in the corneal stroma. Exp Eye Res 78(3):503–512
190. Baker BM et al (2008) The potential to improve cell infiltration in composite fiber-aligned electrospun scaffolds by the selective removal of sacrificial fibers. Biomaterials 29(15):2348–2358
191. Beachley V, Wen XJ (2009) Fabrication of nanofiber reinforced protein structures for tissue engineering. Mater Sci Eng C 29(8):2448–2453
192. Wang W et al (2009) Effects of Schwann cell alignment along the oriented electrospun chitosan nanofibers on nerve regeneration. J Biomed Mater Res A 91A(4):994–1005

Adv Polym Sci (2012) 246: 213–240
DOI: 10.1007/12_2011_143

Published online: 14 September 2011

Electrospinning of Biocompatible Polymers and Their Potentials in Biomedical Applications

Pitt Supaphol, Orawan Suwantong, Pakakrong Sangsanoh, Sowmya Srinivasan, Rangasamy Jayakumar, and Shantikumar V. Nair

Abstract Electrospinning has been recognized as a versatile method for the fabrication of continuous ultrafine fibers using electrical forces. Various natural and synthetic polymers have been successfully electrospun into non-woven mats or oriented fibrous bundles with high porosity and large surface areas. Despite the numerous reports on the production of electrospun fibers, these fiber mats did not gain much interest for use in the biomedical field until the past decade. This review summarizes the research and development related to the electrospinning of some common biocompatible polymers as well as an overview of their potential in many biomedical applications such as tissue engineering, wound dressing, carriers for drug delivery or controlled release, and enzyme immobilization.

Keywords Biocompatible polymer · Delivery or release control · Electrospinning · Enzyme immobilization · Tissue engineering scaffold · Wound dressing

P. Supaphol (✉) and P. Sangsanoh
The Petroleum and Petrochemical College, Chulalongkorn University, Pathumwan, Bangkok 10330, Thailand

The Center for Petroleum, Petrochemicals, and Advanced Materials, Chulalongkorn University, Pathumwan, Bangkok 10330, Thailand
e-mail: Pitt.S@chula.ac.th

O. Suwantong
School of Science, Mae Fah Luang University, Tasud, Muang, Chiang Rai 57100, Thailand

S. Srinivasan, R. Jayakumar and S.V. Nair
Amrita Center for Nanosciences and Molecular Medicine, Amrita Institute of Medical Sciences and Research Centre, Kochi 682041, India

Contents

1 Electrospinning for Biomedical Applications

Over the past couple of decades, one-dimensional nanostructured materials in the form of fibrous structures have received considerable attention because of their unique properties and highly versatile applicability. There are many practical techniques used for preparing such fibrous structures. Among them, electrospinning has been recognized as the simplest technique and can produce continuous ultrafine fibers from diverse materials, including polymers in solution or molten state. The diameters of these fibers range from a few micrometers down to tens of nanometers, a size range that is otherwise difficult to realize using conventional techniques. The smaller size of the individual fibers results in high ratios of surface area to volume or mass. Because of the simple tooling, the size and shape of the individual fibers, including the porosity of the obtained fiber mat, can be easily tuned. In addition, the chemical compositions of the fibrous matrices can be easily manipulated to achieve desired properties and functionalities. These advantages render electrospinning one of the most versatile fiber-fabrication techniques. In biomedical applications, it is popular because of the ease of fabrication of fibers from biocompatible materials, whether naturally derived or synthetic, and the ability to diversify the properties of the fibers through blending and surface functionalization. The ultrafine fibrous scaffolds produced by electrospinning have been demonstrated to be suitable substrates for promoting the adhesion, proliferation, and differentiation of various types of cultured cells [1–4]. As wound dressing materials, a myriad number of therapeutic agents such as drugs, antibiotic agents, proteins, and genes can be facilely incorporated within the electrospun fibrous framework [5–10]. The main purpose of such structures is not to serve as substrate for tissue regeneration, but as platforms in the delivery of the therapeutic agents.

Due to the high surface area to mass/volume ratio of the electrospun fibers, immobilization of enzymes and other biological catalysts can be done with ease [11–14] and the high porosity of the obtained fibrous membrane, with interconnected porous network, allows the immobilized enzymes and catalysts to

maintain high activities [15]. Despite the wide applicability of electrospinning, the selection of suitable materials is based largely on the requirements of the intended use as well as on the intrinsic properties of the starting materials. Due to the simplicity of the technique, various natural and biocompatible synthetic polymers have been electrospun to satisfy different clinical needs. Some properties of the final fibrous products as submitted by the electrospinning process, such as wettability and mechanical integrity of the obtained fabrics, depend also on the size and morphology of the individual fibers and their organization in the fabrics. Because of the host of biocompatible materials available for selection and the adjustability of the electrospinning setup to achieve the required morphology of the obtained fibers, the physical, physico-chemical, and chemical properties of the electrospun matrices can be easily tailored. This review emphasizes some of the developments in the use of electrospun fibrous matrices (obtained from biocompatible polymers) as substrates for cell and tissue cultures, wound dressings, carriers for drug and gene delivery, and substrates for immobilization of enzymes.

2 Fundamentals of the Electrospinning Process and the Challenges

Electrospinning or electrostatic spinning is an established technique for fiber formation that has recently been rediscovered. It has the ability to fabricate continuous ultrafine fibers with diameters as small as few nanometers in the form of random or aligned non-woven fabrics. The process involves the application of a strong electric field across a conductive capillary, attached to a reservoir containing a polymer solution or melt, and a screen collector. Upon increasing the electric field strength up to a critical value, charges on the surface of a pendant drop destabilize the partially spherical droplet into a conical droplet, which is commonly known as the Taylor cone. Beyond a critical value at which the electric field strength overcomes the surface tension of the polymer solution or melt, a charged polymer jet is eventually ejected from the apex of the cone. The fiber jet undergoes an instability and elongation process, which causes the jet to become very long and thin. During the course of the trajectory of the jet, the solvent evaporates or solidifies, leaving ultrafine fibers on the collector. For a typical electrospinning setup, the major components are: (1) a polymer reservoir attached to a small capillary tube (e.g., a needle), (2) a high voltage power supply, and (3) a screen collector (Fig. 1).

Although conceptually a simple process, electrospinning involves some significant challenges. A number of parameters can greatly influence the formation and structure of the obtained fibers. In principal, these parameters can be divided into two major categories, namely system and process parameters. By appropriately adjusting all or some of these parameters, fibers with desired morphology can be obtained. To understand the electrospinning process, the different parameters that affect the process are briefly considered.

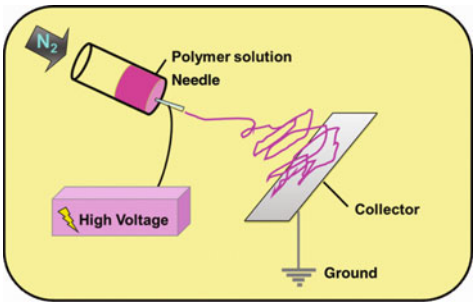

Fig. 1 Typical electrospinning setup

2.1 Process Parameters

Despite the fact that the electrospinning technique is relatively easy to use, there are a number of process parameters that can greatly affect fiber formation and structure. Listed in order of relative impact to the electrospinning process, the most important parameters are applied voltage, polymer flow rate, and capillary–collector distance. All three parameters can influence the formation of nanofibers with bead-like defects.

2.1.1 Applied Voltage

The fiber diameter can be controlled by the applied voltage, but the results vary strongly with the polymer system. The strength of the applied electric field controls the formation of fibers from several micrometers in diameter to tens of nanometers. Suboptimal field strength can lead to bead defects in the electrospun fibers or even failure in jet formation. Based on various previous works [16, 17], it is evident that there is an optimal range of electric field for a certain polymer–solvent system, because either too weak or too strong a field will lead to the formation of beaded fibers.

2.1.2 Polymer Flow Rate

Polymer flow rate also has an impact on fiber size and can influence fiber porosity as well as fiber geometry [18–20]. At high flow rates, significant amounts of bead defects can be observed, largely due to inadequate "drying" of the jet prior to reaching the collector. Incomplete drying also leads to the formation of ribbon-like (or flattened) fibers, because the subsequent drying of the core layer results in collapse of the already-dried skin layer [18, 21].

2.1.3 Capillary–Collector Distance

Playing a much smaller role, the distance between capillary tip and collector can also influence fiber size. The fiber diameter decreases as the distance from the

Taylor cone to the collector increases [22]. Morphological changes can also occur upon decreasing the distance between the capillary tip and the substrate through the formation of beads or the conglutination of adjacent fiber segments, which can be attributed to inadequate drying of the polymer fiber prior to reaching the collector [20].

2.2 System Parameters

In addition to the process parameters, a number of system parameters play an important role in fiber formation and the obtained structure. System parameters include molecular weight, molecular weight distribution, polymer architecture, and solution properties. Solution properties play a particularly important role. In relation to their impact on the electrospinning process, these factors can be ranked as follows: polymer concentration, solvent volatility, and solution conductivity.

2.2.1 Polymer Concentration

The polymer concentration influences both the viscosity and the surface tension of the solution. The formation of fibers through electrospinning is based on uniaxial stretching of the ejected, charged jet. At concentrations that are too low, the ejected jet does not have enough strength to withstand the electrical forces and hence is broken up into discrete beads [23, 24]. As the concentration increases, the morphology of the obtained products changes into fibers with beads, as more entanglements are formed. Further increase in the concentration finally results in the formation of smooth fibers. However, exceedingly high concentrations disrupt the flow of the solutions because the viscosities are exceedingly high [23, 24]. Within the optimal concentration range of the solutions, uniform fibers can be obtained, and their diameters increase with an increase in the concentration. Depending largely on the size of the fibers, smooth fibers with circular or ribbon-like cross-sections can be obtained. Nonetheless, the range within which morphologies would be observed depends on given polymer–solvent systems.

2.2.2 Solvent Volatility

Choice of solvent determines not only the formation ability of the fibers, but also their surface topographies [18, 21]. The very first criterion for choosing a solvent is based on whether it is a good, marginal, or poor solvent for a polymer (i.e., by comparing the solubility parameters of the solvent and the polymer). Once selected, the resulting polymer solution should not phase-separate during the course of the electrospinning. Because the boiling point of a liquid can be related to its ability to evaporate (i.e., the more relevant parameter is vapor pressure), the boiling point should not be so low that the resulting polymer solution would dry out during the

spinning, and hence cause clogging at the tip of the capillary. If the choosing of a solvent with relatively low boiling point is inevitable, a modifying liquid with relatively high boiling point can be added to adjust the evaporation rate of the resulting solvent mixture. Too high a boiling point would, however, cause other adverse effects, such as the flattening and/or conglutination of fibers or fiber segments on the collector. It should be noted that the choosing of a modifying liquid with relatively low boiling point is often intentional so as to impart certain topographies on the surface of the resulting fibers, as the low-boiling-point liquid would cause local phase-separation of the polymer solution at the liquid–air interface.

2.2.3 Solution Conductivity

Solution conductivity can influence fiber size within 1–2 orders of magnitude [18]. Apart from the solubility parameters and the boiling point of the solvent, the dielectric constant (i.e., the tendency of the molecules to be polarized by an external electric field) is another parameter that needs to be considered. The greater the dielectric constant of a solvent, the greater is the conductivity of the resulting solution. Often, it is necessary to add a modifying liquid with a high dielectric constant, an organic or inorganic salt, or a surfactant to improve the conductivity of the solutions. Solutions with high conductivities have greater charge-carrying capacities than solutions with lower conductivities. Therefore, the fiber jets produced from solutions with high conductivities are subjected to greater tensile forces in an electric field than are fiber jets from solutions with low conductivities. In the presence of a strong electric field, on the other hand, the highly conductive solutions are extremely unstable. This could lead to dramatic bending instabilities, and hence fibers with broad diameter distributions could be obtained [25]. It was suggested that the radius of the fiber jet is inversely related to the cube root of the solution conductivity [26].

The above description of the process suggests that many parameters can influence the morphologies of the resulting electrospun fibers. By appropriately varying all or some of these parameters, fibers with desired morphologies can be obtained.

3 Biocompatible Polymers and Surface Functionalization for Enhancement of Biological and Chemical Activity

The field of biomedical application often requires an interdisciplinary approach that combines the life sciences and medicine with materials science and engineering. For a successful application, the material must be biocompatible, meaning that the material has the ability to perform with an appropriate host response in a specific application. Due to the complicated interaction between materials and biological systems, there is no precise definition or accurate measurement of biocompatibility.

Nevertheless, whether a material is accepted by a living body should be the criterion for evaluating the biocompatibility of materials [27]. The requirements of this response vary from application to application; however, toxicity as well as inflammatory and possibly immune responses should typically be minimized. Initial studies on the biocompatibility of materials relied upon the potential use of bioinert substrates to reduce host-specific interactions. While processes such as protein adsorption and the inflammatory response will occur to some degree with any implant, a bioinert material forms no or very little specific interactions with the surrounding environment, including the extracellular fluid or surrounding tissues. The interaction of materials with biological molecules such as proteins, proteoglycan receptors on cell surfaces, and biological molecules normally present in the extracellular matrix (ECM) is largely dependent on the surface chemistry and topography of the materials. Protein adsorption on the material surface is believed to be the initial process when a material comes in contact with a biological environment. These interaction mechanisms will influence the subsequent biological reactions, including cell adhesion and proliferation. However, polymeric materials with different surface properties such as hydrophilicity or hydrophobicity, smooth or rough surfaces, and random or aligned direction may provide different cell responses both in vitro and in vivo. Therefore, understanding the influence of surface properties is crucial, and control of protein–surface interactions continues to be an important factor for consideration in the design of biocompatible surfaces.

Recently, current research has been investigating the incorporation of bioactive materials that can intentionally interact with the biological environment and influence factors such as cell function [28]. These interactions are often accomplished through surface modifications and through functionalization with bioactive molecules such as extracellular proteins (laminin, fibronectin etc.). In addition, the materials must exhibit suitable physical and mechanical properties closely matching the desired requirements, i.e., the modulus of elasticity, strength, structural integrity etc. need to match those of the neighboring tissue. The material selection plays a key role in biomedical application. Synthetic polymers provide many advantages over natural polymers because they can be tailored to give a wider range of properties with predictable lot-to-lot uniformity and reliable source of raw materials. However, naturally occurring polymers normally exhibit better biocompatibility and low immunogenicity.

Synthetic materials can be divided into biodegradable and non-degradable materials. Biodegradable materials are the more popular choice due to the elimination of the need for a second surgical intervention to remove the implanted scaffold [4, 29–41]. It is imperative that the rate of degradation coincides with the rate of new tissue formation. If the rate of degradation is too slow, then new tissue formation will be impeded; however, if the rate of degradation is too fast, then the mechanical stability of the scaffold and developing tissue will be compromised. The rate of degradation can be controlled to some extent by altering parameters such as polymer blend [35, 42] and ratio of amorphous to crystalline segments [18].

In order to more accurately mimic the natural ECM, research has also examined the electrospinning of natural materials such as collagen [43, 44], chitosan [45],

gelatin [46], fibrinogen [47, 48], chitin [49], and hyaluronic acid [50]. However, these materials often lack the desired physical properties or are difficult to electrospin on their own, which has led to the development of hybrid materials consisting of a blend of synthetic and natural materials [50–59].

4 Important Aspects of Biocompatible Polymers in Some Applications

4.1 Tissue Engineering

As defined by Langer and Vacanti in 1993, tissue engineering is "an interdisciplinary field that applies the principles of engineering and life sciences toward the development of biological substitutes that restore, maintain, or improve tissue function" [60]. An important aspect of tissue engineering is the design of polymeric scaffolds with specific mechanical and biological properties similar to native ECM. The ECM is defined as any material that is known broadly as a tissue but is not part of a cell. The main components that make up the ECM are glycoproteins, the most abundant being collagens, proteoglycans, hyaluronic acid, and other molecules depending on the specific tissue, such as fibrin, elastin, fibronectins, laminins, hydroxyapatite (HAp), and even fluids such as serum and bound adhesive motifs [61]. The ECM can also influence cellular function by the physical arrangement of the network of molecules that constitute it [62, 63]. Because fibril arrangements are tissue-specific, it has proven difficult to replicate the physical features of the ECM for regenerative medicine [64]. The complexities of the temporal environment influence phenotypic and other cellular behaviors by providing indirect and direct informational signaling cues [65]. These interactions between cells and ECM can modulate cellular activities such as adhesion, migration, proliferation, differentiation, and gene expression. Thus, the more closely the in vivo environment is recreated, the more likely is the success of the tissue engineering scaffold [66–68].

Electrospun fibers mats function as temporary support for cells to regenerate the cellular matrix that has been destroyed by disease, injury, or congenital defects. Although the desired characteristics of a scaffold vary slightly according to the native tissue, there are general properties that are desirable. First and foremost, the scaffold should be biocompatible, meaning that it will integrate with the host tissue without stimulating any immune response. The scaffold should also be porous to allow for cell attachment and in-growth, as well as for exchange of nutrients during in vitro or in vivo culture [69, 70]. Also, because the scaffold acts as a temporary support for the cells to adhere and proliferate, it should mimic native ECM both architecturally and functionally [69, 71]. In addition, a tissue engineering scaffold should be biodegradable so that a second surgical intervention is not required to remove the implant. The rate of degradation should coincide with the rate of new tissue formation. For these properties, a number of requirements must be considered

that involve the type of material, fiber orientation, porosity, surface modification, and type of tissue that will be replaced.

Materials such as natural or synthetic materials as well as polymer blends can provide optimal mechanical and biological properties of fibrous scaffolds by varying the processing and solution parameters. For the fiber orientation, by using a stationary or rotating collector, either randomly oriented or aligned fibers can be formed, respectively. The degree of anisotropy within an electrospun fibrous mat can greatly affect not only the mechanical properties but also cell adhesion, proliferation, and alignment. In many applications, it is desirable to develop an aligned fibrous mat to replace highly oriented tissue such as the medial layer of a native artery of smooth muscle cells [41] or the axons and glial cells in the peripheral nerve system [31]. These experiments demonstrate the potential applications in which it is desirable to develop a nanofibrous scaffold with a high degree of anisotropy.

Depending on the system parameters and the process parameters, a number of different pore sizes can be obtained. Pore size and the density of pores can also play an important role in the migration and filtration of cells and macromolecules, which can be used to control transport of nutrients and waste products. The pore size of an electrospun scaffold will essentially dictate whether it is viewed as a two-dimensional (2D) mat or a three-dimensional (3D) scaffold by cells; depending on the application either might be desirable. Initially, small pore size was seen as a hindrance in many situations; however, it can actually serve as an advantage in applications where cell infiltration is unwanted, such as skin and the endothelium. Due to the barrier property of electrospun scaffolds, their application in tissue engineered vascular grafts has grown significantly. An electrospun scaffold can provide superior endothelial cell attachment due to the large fraction of surface available for interacting with cells. The small pore size can prevent smooth muscle cell migration into the lumen of the vessel, while still allowing sufficient transport of nutrients and waste removal. However, small pores are not advantageous for all applications. In 3D scaffolds, the cells must be able to infiltrate deep into the scaffold, which require pores of adequate size to allow for cell migration. Recently, researchers have attempted to develop electrospun scaffolds with smaller diameters in order to maximize the surface area. Additionally, it is important to consider the importance of pore size and pore size distribution to allow the use of scaffolds without limiting cell infiltration. Greater enhancement of cellular function can be achieved by attaching bioactive molecules to the surface of the spun scaffolds. Various groups have examined the effects of attaching different bioactive molecules such as RGD peptides [26], gelatin [72], and perlecan (a natural heparan sulfate proteoglycan) [73].

The electrospinning of poly(ε-caprolactone) (PCL) solutions have been reported by Reneker et al. [74]. They varied the PCL solution concentrations between 14 and 18 wt%. The instability in the electrospinning of PCL results in the contact and merging of segments in different loops of the electrospinning jet to form garland-like fibrous structures [74]. Yoshimoto et al. [75] have studied the potential of electrospun PCL fiber mats for use in bone tissue engineering. They found that the

surfaces of the cell–polymer matrixes were covered with mesenchymal stem cell (MSC) multilayers at 4 weeks. Mineralization and type I collagen formation were also observed at 4 weeks [75]. Cardiac nanofibrous meshes have been successfully prepared by electrospinning of PCL solutions in a 1:1 mixture of chloroform and methanol. They found that the cardiomyocytes attached well on the PCL meshes and expressed cardiac-specific proteins such as α-myosin heavy chain, connexin 43 and cardiac troponin I [76]. In 2004, Li et al. [77] fabricated electrospun PCL fiber mats to support in vitro chondrogenesis of MSCs. Since the level of MSC chondrogenesis in the electrospun fiber mats was enhanced compared to the cell pellet culture, they proposed that these fiber mats are candidate bioactive carriers for MSC transplantation in tissue engineering-based cartilage repair. Fujihara et al. [78] fabricated PCL/$CaCO_3$ composite nanofibers with two different PCL to $CaCO_3$ ratios (PCL:$CaCO_3$ of 75:25 and 25:75 wt%) for use as guided bone regeneration membranes. Erisken et al. [79] prepared functionally graded nanocomposite structures of PCL and β-tricalcium phosphate (β-TCP) by using a hybrid twin-screw extrusion electrospinning process. They found that the ability to incorporate the β-TCP nanoparticles into PCL nanofibers enabled better mimicking of the compositional and structural characteristics of bone tissue, particularly at the bone–cartilage interface [79]. Li et al. [80] studied the ability of the electrospun PCL fiber mats to support and maintain multilineage differentiation of bone marrow-derived human MSCs (hMSCs) in vitro. hMSCs were seeded onto these fiber mats and were induced to differentiate along adipogenic, chondrogenic, or osteogenic lineages by specifically differentiating the specialized cell types. These results indicated that these electrospun PCL fiber mats are promising candidate scaffolds for cell-based, multiphasic tissue engineering [80]. A hybrid process incorporating direct polymer melt deposition (DPMD) and an electrospinning process was developed to fabricate a highly functionalized 3D scaffold with an open porous network, a controllable shape, and a biocompatible nanofibrous inner architecture [81]. Each microfibrous layer of the scaffold was built using the DPMD process with computer-aided design modeling data. Between the layers of the 3D structure, PCL/collagen nanofiber matrices were deposited via an electrospinning process. Chondrocytes were seeded and cultured for 10 days to evaluate the potential of these scaffolds for use as an ECM-like tissue engineering scaffold. The results showed that these scaffolds supported cell adhesion and proliferation [81]. Yang et al. [82] developed a facile and efficient process to provide the electrospun PCL scaffold with a bone-like calcium phosphate coating while maintaining its fibrous and porous structure. The biomimetic method including the plasma surface treatment was efficient at mineralizing the electrospun PCL scaffolds with a layer of bone-like apatite. It was concluded that these scaffolds can serve as potential materials for use in bone tissue engineering.

Li et al. [83] fabricated silk fibroin fiber scaffolds containing bone morphogenetic protein 2 (BMP-2) and/or nanoparticles of hydroxyapatite (nHAp) by electrospinning. These scaffolds were used in vitro to study bone formation from hMSCs. The results showed that the incorporation of BMP-2 and/or nHAp into silk

fibroin scaffolds enhanced bone formation significantly and thus suggested that these scaffolds were potential candidates for bone tissue engineering [83].

Chitosan has been considered as one of the most attractive natural polymers for bone tissue engineering due to its biocompatibility, biodegradability, and excellent mechanical properties. A chitosan/PCL nanofibrous scaffold was prepared by a single-step electrospinning technique. The presence of chitosan in the scaffold enhanced the hydrophilicity, bioactivity, and protein adsorption on the scaffold. The cytocompatibility of the chitosan/PCL scaffold was examined using human osteoscarcoma cells (MG63) and was found to be nontoxic and support the attachment and proliferation of various cell lines such as mouse embryo fibroblasts (NIH3T3), murine aneuploid fibro sarcoma (L929), and MG63 cells. These studies demonstrate that a chitosan/PCL nanofibrous scaffold would be useful for bone and skin tissue engineering [84].

Bhattarai et al. [85] reported chitosan/poly(ethylene oxide) (PEO) nanofibrous scaffolds that promoted the attachment of human osteoblasts and chondrocytes and maintained characteristic cell morphology and viability throughout the period of study. This nanofibrous matrix is of particular interest in tissue engineering for controlled drug release and tissue remodeling. Similarly, Subramanian et al. [86] prepared chitosan/PEO nanofibers for cartilage tissue engineering. Chitosan/PEO nanofibers were biocompatible to chondrocytes. Cells attached to the chitosan/PEO nanofiber mats, and the results indicated that the electrospun chitosan/PEO mats could be used for cartilage tissue repair. Mo et al. [87] also reported that smooth muscle cells attached to the electrospun chitosan/collagen nanofibers used for tissue engineering applications. Biocomposite nanofibrous scaffolds were prepared by using chitosan/poly(vinyl alcohol) (PVA) and *N*-carboxyethyl chitosan (N-CECS)/PVA for tissue engineering applications [88]. The cell attachment of the prepared biocomposite nanofibers was studied using mouse fibroblast (L929) cells. The L929 cell culture revealed the attachment and growth of mouse fibroblasts on the surface of biocomposite scaffolds. Similarly, the potential use of the N-CECS/PVA electrospun fiber mats as scaffolding materials for skin regeneration was evaluated in vitro using L929 [89]. Indirect cytotoxicity assessment of the fiber mats indicated that the N-CECS/PVA electrospun mat was nontoxic to the L929 cells. Cell culture results showed that fibrous mats were good at promoting cell attachment and proliferation. This electrospun matrix could be used as potential wound dressing for skin regeneration.

Biomimetic nanocomposite nanofibers of HAp/chitosan were prepared by combining an in situ co-precipitation synthesis approach with an electrospinning process [90]. The incorporation of HAp nanoparticles into chitosan nanofibrous scaffolds induced bone-forming ability as compared to pure chitosan scaffolds due to the excellent osteoconductivity of HAp. Moreover, a carboxymethyl chitin (CMC)/PVA fibrous scaffold was successfully prepared by electrospinning for use as a scaffold for tissue engineering [91]. The results showed that the CMC/PVA fibrous scaffold supported cell attachment and proliferation. Ren et al. [92] fabricated gelatin/siloxane fibrous scaffolds by sol–gel processing and electrospinning to support the growth of hMSCs for bone tissue engineering. Randomly

oriented and aligned poly(lactic-*co*-glycolic acid) (PLGA) and PLGA/gelatin biocomposite scaffolds were successfully prepared by electrospinning for use in bone tissue engineering [93]. The results showed that the elongation of the osteoblast on the aligned nanofibrous scaffolds was parallel to the fiber arrangement, and that the cell number was similar to that of randomly oriented scaffolds. The aligned nanofibrous scaffolds thus provide a beneficial approach for bone regeneration.

A bilayered tubular scaffold composed of a stiff and oriented poly(lactic acid) (PLA) outer fibrous layer and a randomly oriented PCL fibrous inner layer (PLA/PCL) was fabricated through sequential multilayering electrospinning [94]. The rotation speed of the collector was used to control the level of fiber orientation of each layer. The PLA/PCL bilayered scaffolds proved to support the attachment, spread, and growth of mouse fibroblasts and human myofibroblasts. Therefore, these scaffolds could be considered as a candidate scaffolds for blood vessel tissue engineering [94]. Lee et al. [95] fabricated vascular scaffolds composed of PCL and collagen by electrospinning. The results showed that the PCL/collagen composite scaffolds are biocompatible, possess biomechanical properties that resist a high degree of pressurized flow for up to 4 weeks, and provide a favorable environment that supports the growth of vascular cells. Since silk fibroin has unique mechanical properties and good biocompatibility, it is used in biomedical applications. Sato et al. [96] prepared a small diameter graft made of silk fibroin by electrospinning. Moreover, the electrospun silk fibroin graft was coated with a silk sponge in order to improve mechanical strength and water permeation. These results showed that the electrospun silk fibroin graft with the silk sponge is attractive for cardiovascular applications. In addition, silk fibroin/collagen tubular scaffolds were successfully prepared by electrospinning by Zhou et al. [97] for use in vascular tissue engineering.

An electrospun nanofibrous scaffold of the novel poly(*p*-dioxanone-*co*-L-lactide)-*block*-poly(ethylene glycol) (PPDO/PLLA-*b*-PEG) copolymer was prepared by Bhattarai et al. [98]. They studied cell proliferation and the morphology of cell–matrix interaction with the electrospun nanofibrous matrix. The results showed that this scaffold supported cell attachment and proliferation and thus was a candidate scaffold for skin tissue engineering. In 2006, Pan et al. [99] studied the interaction between dermal fibroblasts and an electrospun dextran/PLGA scaffold using cell viability, proliferation, attachment, migration, ECM deposition, cytoskeleton organization, and functional gene expression. The results showed that cells interacted favorably with the scaffold. The collagen gel assay results showed that gel contraction was enhanced by the presence of the scaffold. Therefore, the dextran/PLGA scaffold can be used in enhancing the healing of chronic or trauma wounds [99]. Noh et al. [49] compared the cellular response of the electrospun chitin nanofibers (Chi-N) and commercial chitin microfibers (Chi-M) for potential use in wound healing or tissue engineering applications. Good cell attachment and spreading of all cell types was observed on Chi-N in comparison to Chi-M. The Chi-N treated with type I collagen also promoted the cellular response. These results indicated that Chi-N scaffold was useful for wound healing and regeneration of oral mucosa and skin [49]. Electrospun hexanoyl chitosan scaffolds were prepared by Neamnark et al. [100]. The authors investigated the potential of these scaffolds

for skin tissue engineering in terms of attachment and proliferation of human keratinocytes (HaCaT cells) and human foreskin fibroblasts (HFF). The results showed that these scaffolds supported cell attachment and proliferation of both types of cells, especially HaCaT. Electrospun PLGA fiber matrices of varying fiber diameters were studied for use in skin tissue engineering [101]. The results indicated that the electrospun PLGA fiber matrixes with a diameter range of 350–1,100 nm had a higher proliferation rate than the fiber matrices below and beyond this fiber diameter range. Lowery et al. [102] studied the effect of fiber diameter and pore size on cellular proliferation in tissue engineering scaffolds composed of electrospun PCL. The results showed that the cells proliferated at a faster rate on scaffolds with peak pore diameters greater than 6 μm. Moreover, the cells bridged pores on the surface of fiber mats with 6.5 μm pores, but extended along single fibers in a mat with more than 20 μm pores, showing a pore diameter effect on cell conformation [102].

4.2 Controlled Drug and Gene Delivery

Controlled drug or gene delivery and tissue engineering are closely related areas. Sometimes, release of therapeutic agent can be combined with implantable scaffolds to increase the efficiency of tissue regeneration. Electrospun fibers provide the advantage of increased drug release as compared to cast films due to the high surface area to volume ratio [103]. Due to the great flexibility in material selection, several biocompatible polymeric materials, either biodegradable or non-biodegradable, have been electrospun to produce the fiber matrices for drug or bioactive agent delivery [18]. A number of therapeutic agents including biological active agents (i.e., anticancer drugs, anti-inflammatory drugs, antibiotics, and proteins), herbal extracts, and genes (i.e., DNA) can be loaded and delivered to the desired targets. When selecting a material to be used as a drug delivery device, a number of requirements must be considered. First, the material should protect the drugs from decomposition in the blood stream and, second, it should undergo biodegradation, which eliminates the need for explantation. Third, it should allow controlled release of the therapeutic agent over a time period with a constant release rate and continue as long as necessary for the treatment. It should also ensure that only the drug is released in the targeted tissue.

Materials that undergo biodegradation are generally more popular; however, these materials add an extra level of complexity to drug release as compared to non-degradable materials. Release of the therapeutic molecules can be controlled via diffusion alone or via both diffusion and material degradation. For non-degradable materials, the release profile tends to be primarily controlled by diffusion. In biodegradable systems, the drug may be released by diffusion or by degradation, which can lead to overdosing and local drug concentrations reaching toxic levels. Thus, special care must be taken to tailor both the release rate and the degradation rate if a degradable material is to be used [18].

The drug release profile is dependent on the dispersion of drug in the polymer matrix. Conventionally, the drugs are dissolved or dispersed in the polymer solution before being electrospun into fiber mats, which results in the presence of drug on the fiber surface as well as being encapsulated inside. This can lead to burst release in the initial stages. An alternative method of encapsulating the therapeutic agents inside polymeric nanofibers is by coaxial electrospinning, an advanced electrospinning technique for fabricating core–shell structures [18]. This advanced technique has the advantages of high loading efficiency and controllable release behavior over conventional methods of encapsulating bioactive agents. In coaxial electrospinning, the burst release effect can be suppressed but not eliminated completely. In order to overcome the burst release effect, an extra, protective coating on the drug reservoir of the electrospun fibers has been used. Recently, two-stream electrospinning has been developed to fabricate fibrous composite sheets wherein one component stream provides antibiotic release while the other provides mechanical properties for the desired application.

Zeng et al. [104, 105] used electrospun poly(L-lactic acid) (PLLA) fiber mats as drug carriers. In 2003 [104], the authors studied the influence of surfactants and drugs on the diameter and uniformity of electrospun PLLA fibers. Various types of surfactants, including anionic and cationic surfactants, were used to improve the size distribution of the PLLA fiber diameters. Moreover, various types of drugs including rifampin (a drug for tuberculosis), paclitaxel (PTX, an anticancer drug), and doxorubicin hydrochloride (Dox, an anticancer drug) were also investigated. The results showed that the drugs were encapsulated inside the fibers, and that drug release in the presence of proteinase K followed nearly zero-order kinetics due to the degradation of PLLA fibers. In 2005, Zeng et al. [105] studied the influence of solubility and compatibility of drugs in the drug–polymer system. They also used PLLA fiber mats as carriers to incorporate various types of drugs including the anticancer drugs PTX and Dox. The results showed that there was good compatibility of PTX and Dox with PLLA, whereas Dox was found on the surface of PLLA fibers, resulting in the burst release. Therefore, the compatibility of the drugs in the drug–polymer system is an important factor for controlled release in a drug delivery system. The electrospun amphiphilic PEG-PLLA diblock copolymer fiber mats containing Dox were successfully prepared using water-in-oil emulsion electrospinning [106]. The results showed that the sustained release of Dox was observed for emulsion-electrospun fiber mats in comparison with the suspension-electrospun fiber mats. Both hydrophobic and hydrophilic drugs, PTX and Dox, were also successfully loaded in PEG-PLLA fiber mats by emulsion-electrospinning [107]. The solubility and distribution of both drugs in the drug–polymer system were affected by the release behaviors. Due to the more hydrophilic nature of Dox compared with PTX, Dox was easier to diffuse into buffer solution, leading to a higher release rate. Moreover, the release rate of PTX was accelerated by Dox's release from the same drug-loaded fiber mats, but the release rate of Dox was not affected by PTX. Moreover, PTX-loaded PLGA materials in the form of microfibers, discs, and sheets were prepared by electrospinning [108].

Jiang et al. [5] developed ibuprofen-loaded electrospun PEG-*g*-chitosan with PLGA for controlled drug delivery applications. The presence of PEG-*g*-chitosan significantly moderated the burst release rate of ibuprofen from the electrospun PLGA membranes. Moreover, in this study, ibuprofen was conjugated to the side chains of PEG-*g*-chitosan for prolonged release of more than 2 weeks. These results indicated that chitosan nanofibers could be useful for controlled drug delivery applications.

Kenawy et al. [109] studied the release characteristics of electrospun PVA fiber mats made from partially and fully hydrolyzed PVA containing ketoprofen at a concentration of 5 wt%. Moreover, they studied the stabilization of these fiber mats by treatment with methanol for 1 and 24 h. The authors found that the burst release of ketoprofen was eliminated by the treatment with methanol. Moreover, the higher temperature of the medium showed higher release rates. The degree of hydrolysis of PVA also affected the release rate of ketoprofen. The incorporation of non-steroidal anti-inflammatory drugs (NSAIDs) into electrospun cellulose acetate (CA) fiber mats was investigated by Tungprapa et al. [110]. Four different types of NSAIDs with varying water solubility (naproxen, indomethacin, ibuprofen, and sulindac) at a fixed concentration of 20 wt% based on the weight of CA were used to investigate the release characteristics in acetate buffer solution (pH 5.5) at 37°C. The ability of the drug to release from the polymer matrix depends on many factors such as solubility of the drug in polymer matrix, the solubility of drug in the medium, swelling and solubility of the polymer matrix in the medium, and the diffusion of the drug from the polymer matrix to the medium [110]. Electrospun poly(D,L-lactide) (PDLLA) fiber mats incorporating paracetamol at different loadings (2, 5, and 8 wt%) were fabricated by Cui et al. [111]. The authors studied the drug release characteristics and degradation of fiber mats as a function of fiber characteristics. The effect of different diameters and drug contents on the drug release characteristics and degradation of fiber mats was also studied. The results demonstrated that the release characteristics of paracetamol from these fiber mats showed an initial burst release or steady release phase, followed by a plateau or gradual release. The authors concluded that the drug release behavior from fiber mats can be controlled by fiber size and drug content. Peng et al. [112] also used paracetamol as a model drug. They prepared electrospun PEG-*co*-PDLLA fiber mats with different amounts of PEG (0–20 wt%) and containing paracetamol at a fixed concentration of 5 wt%. The results showed that the drug release rate increased with decreasing PEG content. Moreover, the drug burst release behavior was mainly related to the drug–polymer compatibility, and the sustained release phase depended on polymer degradation. Metoxicam-loaded PVA fiber mats were prepared by electrospinning [113]. The amount of metoxicam loaded in PVA solution was 2.5, 5, 10, and 20 wt% based on the weight of PVA. Comparisons were made against films. The results showed that all the metoxicam-loaded PVA fiber mats exhibited a higher amount of metoxicam permeation than the corresponding films. This could be due to the highly porous structure of the fiber mats that contributed to higher swelling in an aqueous medium.

Kenawy et al. [114] used electrospun fiber mats prepared either from PLA, poly (ethylene-*co*-vinyl acetate) (PEVA), or from a 50:50 blend of the two as carriers to

deliver tetracycline hydrochloride. The release characteristics from the electrospun fiber mats were compared to a commercially available drug delivery system (Actisite) as well as to the films. The electrospinning process was used to fabricate biodegradable amorphous PDLA and semi-crystalline PLLA fiber mats for biomedical applications [115]. The antibiotic drug (mefoxin) was incorporated in these fiber mats to study the release behaviors. The results showed that the burst release of mefoxin was observed within the first 3 h, which is an ideal drug release profile for the prevention of post-operation-induced adhesion, because most infections occur within the first few hours after surgery. The highly water-insoluble drugs itraconazole and ketanserin were incorporated into electrospun segment polyurethane (PU) fiber mats for use in topical drug administration and wound healing [116]. The results showed that both itraconazole and ketanserin were released from the water-insoluble PU fiber mats into an aqueous solution. Moreover, ketanserin was released more rapidly from the PU fiber mats within the first 4 h than itraconazole. The cellulose acetate (CA) fiber mats were used as carriers to deliver the model vitamins, all-*trans* retinoic acid (vitamin A acid) and α-tocopherol (vitamin E) [117]. The release characteristics of these vitamin-loaded CA fiber mats and films were investigated by immersion in acetate buffer solution containing either 0.5 vol% Tween 80 or 0.5 vol% Tween 80 and 10 vol% methanol. The results showed that the vitamin-loaded CA fiber mats exhibited a gradual release over the time periods, whereas the vitamin-loaded CA films exhibited a burst release of the vitamins. PLGA fiber mats were also used as carriers to incorporate all-*trans* retinoic acid [118]. Comparisons were made against the PLGA films. The results showed that the release rate of the vitamin from the PLGA fiber mats exhibited a sustained controlled release and that the PLGA fiber mats preserved their fibrous structure for 4 months.

The encapsulation of human β-nerve growth factor (NGF), which was stabilized in the carrier protein bovine serum albumin (BSA), in a copolymer of ε-caprolactone and ethyl ethylene phosphate (PCLEEP) was achieved by electrospinning [39]. A sustained release of NGF from PCLEEP fiber mats was obtained for up to 3 months. PC12 neurite outgrowth assay also confirmed that the bioactivity of NGF-loaded PCLEEP fiber mats was retained throughout the period of sustained release. Therefore, these fiber mats had the efficiency for use in peripheral nerve regeneration applications. Luong-Van et al. [119] prepared heparin-loaded PCL fiber mats by electrospinning. Heparin is used to prevent vascular smooth muscle cell (VSMC) proliferation, which can lead to graft occlusion and failure, and was loaded at concentrations of 0.5 and 0.05 wt% in PCL solutions. Two model proteins, BSA and lysozyme, were incorporated into core–shell fibers with PCL as shell and protein-containing PEG as core by a coaxial electrospinning method. The obtained diameter of both shell and core was increased with increasing feed rate. The release behavior of protein from the fiber mats were carried out in 0.05 M phosphate buffer solution (pH 7.4) at 37°C. A slight burst release was observed on the first day followed by a relatively steady release. Moreover, the release rate could be controlled by varying the feed rate of the PEG/protein solution: higher feed rate resulted in higher protein release. In addition, Yan et al.

[120] investigated the core–shell structure of fiber mats prepared by coaxial electrospinning from poly(L-lactide-*co*-caprolactone) solution as shell and phosphate buffer saline (pH 7.4) solution containing BSA or/and NGF as core for use in nerve tissue engineering applications. Lu et al. [121] prepared composited fiber mats composed of cationized gelatin (CG)-coated PCL by coaxial electrospinning. CG was used as the shell material for fabricating core–shell fiber mats. They investigated the adsorption behaviors of fluorescein isothiocyanate (FITC)-labeled bovine serum albumin (FITC-BSA) or FITC-heparin onto the fiber mats. Moreover, vascular endothelial growth factor (VEGF) was impregnated into fiber mats through specific interactions with adsorbed heparin in the outer CG layer. Maretschek et al. [122] also prepared cytochrome C (a hydrophilic model protein)-loaded fiber mats based on PLLA by emulsion-electrospinning. Moreover, Yang et al. [123] prepared lysozyme encapsulated within the core–shell structured fibers by emulsion electrospinning. The release of lysozyme loaded in core–shell poly(DL-lactic acid) (PDLLA)/methyl cellulose (MC) fiber mats was carried out in phosphate buffer solution (pH 7.4) containing 0.02% sodium azide as a bacteriostatic agent. The release kinetics for all the fiber mats could be shown to take place in two stages: an initial fast release followed by a constant linear release. An increase of lysozyme loading caused a higher amount of lysozyme release. Thus, the core–shell structured fibers could reduce the initial burst release, sustain the release period dependent on the protein loading, and protect the structural integrity and bioactivity of encapsulated lysozyme during incubation in medium.

4.3 Wound Dressing

Wound healing or wound repair is a native process of regenerating dermal and epidermal tissues in which the skin repairs itself after injury. In normal skin, the epidermis and dermis exist in steady state equilibrium, forming a protective barrier against the external environment. Once the protective barrier is broken, a set of complex biochemical actions occur immediately to repair the damage. The classic model of wound healing is divided into inflammatory, proliferative, and remodeling phases and epithelialization. Normally, the body cannot heal thick burns or deep ulcers because there is no source of cells remaining for regeneration, except from the wound edges. As a result, complete re-epithelialization takes a long time and is complicated, with scarring of the base. Dressings for wound healing function to protect the wound, exude extra body fluids from the wound area, decontaminate the exogenous microorganisms, improve the appearance, and sometimes accelerate the healing process. For these functions, a wound dressing material should provide a physical barrier to a wound, but be permeable to moisture and oxygen. For a full-thickness dermal injury, the adhesion and integration of an artificial dermal layer consisting of a 3D tissue scaffold with well-cultured dermal fibroblasts will considerably assist the re-epithelialization [124].

Recently, an electrospun membrane has been reported to be a good candidate for wound dressing applications because of its unique properties. These include a highly porous membrane structure and well-interconnected pores that are small enough to protect the wound from bacterial penetration via aerosol particle capturing mechanisms [125]. High surface area and high porosity are essential for the exchange of liquids and gases with the environment. They also provide local release of drugs onto the skin. In addition, the electrospinning process provides a simple way to incorporate drugs into the nanofibers for medical treatment and antibacterial purposes, which can then be released into the healing wound in a homogeneous and controlled manner. Usually, the electrospun membrane can also be used for the treatment of wounds or burns of human skin. These kinds of wounds heal particularly fast and without complications if they are covered by a thin web of fiber mats that can let wounds heal by encouraging the formation of normal skin growth and eliminate the formation of scar tissue, which would occur in a traditional treatment [124].

Min et al. [126] fabricated electrospun silk fibroin fiber mats by electrospinning to study the cytocompatibility and cell behavior on these fiber mats. The results showed that these fiber mats supported the attachment and spreading of normal human keratinocytes and fibroblasts. Moreover, electrospun silk fibroin fiber mats containing epidermal growth factor (EGF) to promote the wound healing processes were prepared by electrospinning [127]. The preservation of the structure of these fiber mats during the healing period and the biocompatibility of these fiber mats indicated that these fiber mats are the new type of materials for medical applications, especially for patients suffering from chronic wounds. The collagen nanofibrous matrix produced by electrospinning was investigated for use in wound dressing [128]. The collagen nanofibrous matrix showed good tensile strength, even in aqueous solution. The electrospun collagen nanofibers coated with type I collagen or laminin were found to promote cell adhesion and spreading of normal human keratinocytes. These results indicated that these materials might be good candidates for biomedical applications such as wound dressing and tissue engineering. Gu et al. [129] fabricated electrospun PLLA and gelatin/PLLA fiber mats. The porous structured electrospun gelatin/PLLA fiber mat showed controlled evaporative water loss, promoted fluid drainage ability, and exhibited excellent biocompatibility. Therefore, this fiber mat has a potential for wound dressing application. Electrospun PLGA/collagen fiber mats were prepared by electrospinning [130]. The cytocompatibility and cellular responses to these fiber mats, cell and material interactions, and open wound healing in rats were studied. The results showed that these fiber mats were active in responses in human fibroblasts and were very effective as wound-healing accelerators in early-stage wound healing. These results indicated that the electrospun PLGA/collagen fiber mat might be a good candidate as a wound dressing material [130].

Quaternized chitosan (QCh) derivatives have a high activity against bacteria and thus are potential candidates for wound dressing applications. Electrospun QCh fiber mats were successfully prepared by electrospinning QCh solutions mixed with PVA [131]. The electrospun QCh/PVA fiber mats were stabilized against dissolution in aqueous environment using photomediated crosslinking.

The photo-crosslinked electrospun QCh/PVA fiber mats showed good bactericidal activity against *Staphylococcus aureus* and *Escherichia coli* and thus could serve as potential candidates for wound dressing applications. To achieve continuous defect-free fibers from QCh derivatives, electrospinning of mixed solutions of QCh with poly(vinyl pyrrolidone) (PVP) was carried out [132]. The photo-crosslinked QCh/PVP fibers were irradiated to be water-stable. These fibers showed high antibacterial activity against *S. aureus* and *E. coli* and thus might be used in wound dressing applications. Chen et al. [133–135] developed a composite nanofibrous membrane of chitosan/collagen for wound healing applications. The composite nanofibrous membrane showed enhanced wound healing, and induced cell migration and proliferation. Animal studies also demonstrated that the nanofibrous membrane was better than gauze and commercial collagen sponge for wound healing.

Son et al. [136] prepared electrospun CA fiber mats from a CA solution containing 0.5 wt% of $AgNO_3$. The Ag^+ ions and Ag clusters diffused and aggregated on the surface of the CA fibers during UV irradiation. The Ag nanoparticles with an average size of 21 nm exhibited strong antimicrobial activity. Moreover, electrospun PLLA fiber mats containing nanosilver particles were prepared by electrospinning [137]. These fiber mats had strong antibacterial activities against *S. aureus* and *E. coli* and thus might be used in wound dressings or anti-adhesion membranes. Rujitananroj et al. [138] fabricated electrospun gelatin fiber mats containing 2.5 wt% $AgNO_3$. They studied the potential of these fiber mats as wound dressing materials and found that these fiber mats had greatest antibacterial activity against *Pseudomonas aeroginosa*, followed by *S. aureus*, *E. coli*, and methicillin-resistant *S. aureus*. Electrospun PVA fiber mats containing 1 wt% $AgNO_3$ were prepared and stabilized by heat treatment at 150°C for 10 min [139]. The cytotoxicity of the Ag ions and/or nanoparticles on normal human epidermal keratinocytes (NHEKs) and fibroblasts (NHEFs) was evaluated. The results showed that both Ag ions and Ag nanoparticles had similar cytotoxicity to the NHEK and NHEF cells. Moreover, the NHEFs appeared to be more sensitive to Ag ions or particles than NHEKs. The NHEK cells were more sensitive to the nitrate ions than NHEFs. Therefore, an antimicrobial Ag-containing matrix should be used to minimize the damage to epidermal cells [139]. In addition, electrospun chitosan/gelatin fiber mats containing silver nanoparticles were prepared by electrospinning [140] for use in wound dressing applications. Hang et al. [141] prepared PVA/chitosan fiber mats containing 1 wt% silver nanoparticles by electrospinning. They found that the addition of $AgNO_3$ to the polymer blends improved the electrospinnability of the blends. Moreover, the silver nanoparticles in the polymer blends showed antibacterial activity and acted as a nucleating agent during cold crystallization.

Burn healing is one of the most important problems in modern surgery due to the high percentage of burns among other traumas, and the high lethality and disability after the treatment of burns of high surface area. The problem of covering large burnt surfaces is still a challenge. Recently, a chitosan-based electrospun nanofibrous material was proposed as a new material for burn dressing [142]. Chitosan

nanofiber mats were created and tested as wound dressings for IIIa and IIIb degree burns. The results showed that chitosan nanofiber dressings provide effective absorption of exudate, ventilation of the wound, protection from infection, and stimulation of the process of skin tissue regeneration. Degradation of these materials prevents mechanical damage of the wound during removal. In another work, composite nanofibrous membranes of chitosan and silk fibroin were fabricated by electrospinning [143]. In this study, the antibacterial activities against *E. coli* (Gram negative) and *S. aureus* (Gram positive) were evaluated using turbidity measurements and the results suggested that the antibacterial effect of composite nanofibers varied with the type of bacteria. Furthermore, the biocompatibility of murine fibroblasts on the prepared nanofibrous membranes was investigated by hematoxylin and eosin (H&E) staining and MTT assays in vitro, and the membranes were found to promote cell attachment and proliferation. These results suggested that chitosan/silk fibroin composite nanofibrous membrane could be a promising candidate for wound healing. Shalumon et al. developed sodium alginate (SA)/PVA fibrous mats using an electrospinning technique. ZnO nanoparticles were further prepared, characterized, and introduced (at different concentrations) into SA/PVA fibrous mats through electrospinning to obtain SA/PVA/ZnO composite nanofibers. The prepared composite nanofibers were characterized. Cytotoxicity studies indicated the less toxic nature of composite SA/PVA fibers with low ZnO concentrations. The cell adhesion potential of these mats was further proved by studies with L929 cells for different time intervals. The SA/PVA/ZnO mats showed antibacterial activity against two different bacteria strains, *S. aureus* and *E. coli*, due to presence of ZnO nanoparticles. Hence, these fibrous mats could be ideal biomaterials for wound dressing applications at an optimal concentration of ZnO [144].

4.4 Catalysts, Enzyme Carriers, and Biosensors

Enzymes, which are green catalysts with a high degree of specificity, have received much attention in the fields of fine chemistry, pharmaceutical synthesis, food processing, biosensor fabrication, bioremediation, and protein digestion in proteomic analysis due to several advantages over conventional inorganic catalysts. These advantages include stereo- and regioselectivity, fewer side reactions, and mild reaction conditions [126]. However, some drawbacks limit their use at large industrial scales. Because enzymes are proteins, any changes in reaction conditions could lead to the deformation of their structure and loss of activity. Additionally, the difficultly in removal and recycling of the enzymes after reaction increases the cost of the processes [15]. Enzyme immobilization is an effective way to use enzymatic reactions at the industrial scale. This process is believed to retain the stability of the enzyme. In addition, the immobilized enzyme can be reused throughout several reactions and is easily separated from the product, which decreases the cost problem and also reduces contamination of the product [15].

However, a high loading efficiency of enzyme is a crucial problem in enzyme immobilization due to the loss of enzyme activity after immobilization. Increasing the amount of enzyme immobilized onto the substrate can compensate for the loss of activity [15]. The performance of an immobilized enzyme strongly depends on the properties of the substrate, which usually depend on the material type, composition and structure. Various forms of substrate have been used in enzyme immobilization, including beads, particles, hydrogels, membranes, films, and fibers. However, some of the support materials have disadvantages that are difficult to overcome. For example, mesoporous material usually entraps enzyme molecules on the inner surface, which limits the diffusion and results in lower enzyme activity [12]. Nanoparticles and nanotubes remarkably decrease the mass transfer limitation, whereas their dispersion and recycling are more difficult. By contrast, fiber mats obtained from electrospinning have a great potential to overcome these problems and are promising supports for enzyme immobilization because of the simple and versatile method of fabricating ultrafine fibers. These fibers have an extremely large surface area that provides an enormous number of active sites, thus enhancing the capability to bind more enzymes. Moreover, the interconnected pores of fiber mats provide effective interactions between the reactant and enzyme, which is valuable for continuous-flow chemical reactions or biological, processes [11].

The enzymes can be grafted onto the electrospun fiber surface via surface attachment and encapsulation [15]. Surface attachment refers to physical adsorption or covalent attachment of enzymes on the as-spun supports. However, physical adsorption on a hydrophobic support is often limited because of the poor wettability of the support surface by the enzymes. To improve the performance of the immobilized enzymes, surface modification is crucial for providing reactive groups on the fiber surface. The encapsulation of enzymes in the nanofibers can be achieved by direct co-electrospinning of enzymes with other components. However, the encapsulation approach has several disadvantages, resulting in the loss of enzyme during measurement and storage due to the residual enzyme molecules residing on the surface. Also, the enzyme molecules are confined inside the nonporous fibers, inhibiting the accessibility of the substrate to the enzyme [15].

The immobilization of cellulose in electrospun PVA fiber mats was prepared by electrospinning [14]. These fiber mats were crosslinked by glutaraldehyde vapor, and the catalytic efficiency for biotransformations was studied. The activity of immobilized cellulose in the electrospun PVA fiber mats after crosslinking was over 65% of that of the free enzyme, and fiber mats were superior to casting films for use in immobilization of cellulose. Similarly nanofibrous chitosan/PVA membrane was fabricated for enzyme immobilization [145]. This chitosan/PVA nanofibrous membrane was used as a support for lipase immobilization, with the advantages of high enzyme loading up to 63.6 mg/g and activity retention of 49.8%. The stabilities of the immobilized lipase towards pH, temperature, reuse, and storage were enhanced. These results imply that the chitosan nanofibrous membrane (with excellent biocompatibility) is a potential support for enzyme immobilization and can be used for biosensor applications. Ye et al. [146] fabricated electrospun poly(acrylonitrile-*co*-maleic acid) fiber mats tethered with two natural

biomacromolecules, chitosan and gelatin, to achieve dual-layer biomimetic supports for lipase immobilization. Lipase from *Candida rugosa* was then immobilized on these dual-layer biomimetic supports using glutaraldehyde. After immobilization, the pH, thermal, and reuse stabilities of the immobilized enzyme can be enhanced. Therefore, these immobilized fiber mats could be potential supports in enzyme immobilization technology for industrial applications [59].

Electrospun polysulfone fiber mats containing poly(*N*-vinyl-2-pyrrolidone) (PVP) and PEG as additives were prepared to immobilize *C. rugosa* by physical adsorption [147]. The results showed that the electrospun polysulfone fiber mats were potential supports in enzyme immobilization technology for industrial applications. Blending biopolymers into the fiber mats was a feasible method of improving enzyme activity, whereas the amount of bound enzyme decreased little. Moreover, electrospun polyacrylonitrile (PAN) fiber mats were immobilized with lipase from *C. rugosa* by an amidination reaction [148]. The enzyme molecules are covalently bound to the fiber mats and form aggregates on the fiber surface, which also became more hydrophilic and robust after enzyme immobilization. After enzyme immobilization, the storage stability was improved over that of free enzyme. Lipase enzyme from *C. rugosa* has been successfully immobilized in electrospun PVA fiber mats by electrospinning [149]. The enzyme loading in these fiber mats reached as high as 50 wt%. The lipase-loaded electrospun PVA fiber mats exhibited superior activity to the crude enzyme following exposure to elevated temperatures and humidity.

The immobilization of lipase on electrospun poly(acrylonitrile-*co*-2-hydroxyethyl methacrylate) (PANCHEMA) fiber mats was also achieved [150]. Epoxy-activated PANCHEMA fiber mats seemed to be an almost-ideal system for enzyme immobilization and could preserve relatively high activity of immobilized enzyme. The stabilities of the immobilized lipase were also improved. It was concluded that the lipase-immobilized PANCHEMA fiber mat bioreactor possessing high enzyme loading and catalytic efficiency might have great potential as a biocatalyst for a wide range of reactions including hydrolysis, alcoholysis, aminolysis, and transesterification [150]. To achieve a biofriendly microenvironment for enzyme immobilization, collagen or protein hydrolysate from egg skin was tethered on electrospun poly(acrylonitrile-*co*-acrylic acid) (PANCAA) fiber mats [151]. Lipase from *C. rugosa* was then immobilized on the protein-modified fiber mats by covalent binding using glutaraldehyde as coupling agent, and on the nascent PANCAA fiber mats using EDC/NHS as coupling agent. The enhancement of both the activity retention and stabilities of the immobilized lipase could be found on egg skin hydrolysate-modified and collagen-modified PANCAA fiber mats compared with those on the nascent PANCAA fiber mats. The results indicate that the immobilization of biomacromolecules onto PANCAA fiber mats could provide a biofriendly microenvironment for further tethering of enzymes [64].

Li et al. [152] fabricated electrospun PAN fiber mats immobilized with *C. rugosa* lipase by amidination. Enzyme molecules were covalently bound to the fiber mats and formed small protein aggregates. The immobilized lipase on the electrospun PAN fiber mats showed a good biocatalystic activity for soybean oil

hydrolysis. Moreover, the reusability of immobilized lipase on the electrospun PAN fiber mats was very high. These results implied that the immobilized fiber mats had good potential for industrial applications [152]. *Pseudomonas nitroreducens* LY was immobilized in the electrospun PVA fiber mats by electrospinning [153]. Moreover, theanine was synthesized by the immobilized *P. nitroreducens* LY in fiber mats with a yield of 10.75 g/L. These results indicate that these immobilized fiber mats could be useful in microbial cell immobilizing technology. Stoilova et al. 154] functionalized electrospun styrene-maleic anhydride copolymers by modification with two types of spacers – a polymer with a flexible hydrophilic polyether chain (Jeffamine ED) and a rigid low molecular weight spacer (*p*-phenylenediamine). Acetylcholinesterase was then immobilized onto the modified fiber mats using glutaraldehyde as a binding agent. The results showed that the immobilized acetylcholinesterase had higher thermal and storage stability than the free enzyme.

References

1. Khil MS, Bhattarai SR, Kim HY, Kim SZ, Lee KH (2005) J Biomed Mater Res 72B:117
2. Ma Z, Kotaki M, Inai R, Ramakrishna S (2005) Tissue Eng 11:101
3. Riboldi SA, Sampaolesi M, Neuenschwander P, Cossu G, Mantero S (2005) Biomaterials 26:4606
4. Yang F, Murugan R, Wang S, Ramakrishna S (2005) Biomaterials 26:2603
5. Jiang HL, Fang DF, Hsiao BJ, Chu BJ, Chen WL (2004) J Biomater Sci Polym Ed 15:279
6. Katti DS, Robinson KW, Ko FK, Laurencin CT (2004) J Biomed Mater Res B 70B:286
7. Kim K, Luu YK, Chang C, Fang DF, Hsiao BS, Chu B, Hadjiargyrou M (2004) J Control Release 98:47
8. Kim KS, Chang C, Zong XH, Fang DF, Hsiao BS, Chu B, Hadjiargyrou M (2003) Abstracts of Papers of the American Chemical Society 226:U437
9. Doshi J, Reneker DH (1995) J Electrostat 35:151
10. Luu YK, Kim K, Hsiao BS, Chu B, Hadjiargyrou M (2003) J Control Release 89:341
11. Jia H, Zhu G, Vugrinovich B, Kataphinan W, Reneker DH, Wang P (2002) Biotechnol Prog 18:1027
12. Wang Y, Hsieh YL (2003) Polymer reprints (American Chemical Society, Division of Polymer Chemistry) 44:1212
13. Wang Y, Hsieh YL (2004) J Polym Sci A1 42:4289
14. Wu L, Yuan X, Sheng J (2005) J Membrane Sci 250:167
15. Wang ZG, Wan LS, Liu ZM, Huang XJ, Xu ZK (2009) J Mol Catal B Enzym 56:189
16. Deitzel JM, Kleinmeyer J, Harris D, Tan NCB (2001) Polymer 42:261
17. Meechaisue C, Dubin R, Supaphol P, Hoven VP, Kohn J (2006) J Biomater Sci Polym Ed 17:1039
18. Sill TJ, von Recum HA (2008) Biomaterials 29:1989
19. Taylor G (1969) P Roy Soc Lond A Mat 313:453
20. Megelski S, Stephens JS, Chase DB, Rabolt JF (2002) Macromolecules 22:8456
21. Lannutti J, Reneker D, Ma T, Tomasko D, Farson D (2007) Mater Sci Eng C27:504
22. Jaeger R, Bergshoef MM, Batlle CMI, Schonherr H, Vancso GJ (1998) Macromol Symp 127:141
23. Venugopal J, Zhang YZ, Ramakrishna S (2005) P I Mech Eng N-J Nano 218:35
24. Greiner A, Wendorff JH (2007) Angew Chem Int Ed 46:5670

25. Hayati I, Bailey AI, Tadros TF (1987) J Colloid Interface Sci 117:205
26. Baumgarten P (1971) J Colloid Interface Sci 36:71
27. Chena H, Yuana L, Songa W, Wub Z, Li D (2008) Prog Polym Sci 33:1059
28. Kim TG, Park TG (2006) Tissue Eng 12:221
29. Zhao P, Jiang H, Pan H, Zhu K, Chen W (2007) J Biomed Mater Res A 83:372
30. Yang DJ, Zhang LF, Xu L, Xiong CD, Ding J, Wang YZ (2007) J Biomed Mater Res A 82:680
31. Schnell E, Klinkhammer K, Balzer S, Brook G, Klee D, Dalton P, Mey J (2007) Biomaterials 28:3012
32. Park K, Ju YM, Son JS, Ahn KD, Han DK (2007) J Biomater Sci Polym Ed 18:369
33. Li WJ, Mauck RL, Cooper JA, Yuan X, Tuan RS (2007) J Biomech 40:1686
34. Henry JA, Simonet M, Pandit A, Neuenschwander P (2007) J Biomed Mater Res A 82:669
35. Duan B, Wu L, Li X, Yuan X, Li X, Zhang Y, Yao K (2007) J Biomater Sci Polym Ed 18:95
36. Ashammakhi N, Ndreu A, Piras AM, Nikkola L, Sindelar T, Ylikauppila H, Harlin A, Chiellini E, Hasirci V, Redl H (2007) J Nanosci Nanotechnol 7:862
37. Thomas V, Jose MV, Chowdhury S, Sullivan JF, Dean DR, Vohra YK (2006) J Biomater Sci Polym Ed 17:969
38. Tessmara JK, Göpferich AM (2007) Adv Drug Deliv Rev 59:274
39. Chew SY, Wen J, Yim EK, Leong KW (2005) Biomacromolecules 6:2017
40. Zong X, Li S, Chen E, Garlick B, Kim KS, Fang D, Chiu J, Zimmerman T, Brathwaite C, Hsiao BS, Chu B (2004) Ann Surg 240:910
41. Xu CY, Inai R, Kotaki M, Ramakrishna S (2004) Biomaterials 25:877
42. Kim K, Yu M, Zong X, Chiu J, Fang D, Seo YS, Hsiao BS, Chu B, Hadjiargyrou M (2003) Biomaterials 27:4977
43. Zhong S, Teo WE, Zhu X, Beuerman RW, Ramakrishna S, Yung LY (2006) J Biomed Mater Res A 79:456
44. Matthews JA, Wnek GE, Simpson DG, Bowlin GL (2002) Biomacromolecules 3:232
45. Matsuda A, Kagata G, Kino R, Tanaka J (2007) J Nanosci Nanotechnol 7:852
46. Song JH, Kim HE, Kim HW (2007) J Mater Sci Mater Med 19:95
47. Ayres C, Bowlin GL, Henderson SC, Taylor L, Shultz J, Alexander J, Telemeco TA, Simpson DG (2006) Biomaterials 27:5524
48. McManus MC, Boland ED, Simpson DG, Barnes CP, Bowlin GL (2007) J Biomed Mater Res A 81:299
49. Noh HK, Lee SW, Kim JM, Oh JE, Kim KH, Chung CP, Choid SC, Parkb WH, Min BM (2006) Biomaterials 27:3934
50. Ji Y, Ghosh K, Shu XZ, Li B, Sokolov JC, Prestwich GD, Clark RA, Rafailovich MH (2006) Biomaterials 27:3782
51. Stitzel J, Liu J, Lee SJ, Komura M, Berry J, Soker S, Lim G, Dyke MV, Czerw R, Yoo JJ, Atala A (2006) Biomaterials 27:1088
52. Sui G, Yang X, Mei F, Hu X, Chen G, Deng X, Ryu S (2007) J Biomed Mater Res A 82:445
53. Nie H, Wang CH (2007) J Control Release 120:111
54. Mohammadi Y, Soleimani M, Fallahi-Sichani M, Gazme A, Haddadi Asl V, Arefian E, Kiani J, Moradi R, Atashi A, Ahmadbeigi N (2007) Int J Artif Organs 30:204
55. Meng W, Kim SY, Yuan J, Kim JC, Kwon OH, Kawazoe N, Chen G, Ito Y, Kang IK (2007) J Biomater Sci Polym Ed 18:81
56. Peesan M, Rujiravanit R, Supaphol P (2006) J Biomater Sci Polym Ed 17:547
57. Park KE, Kang HK, Lee SJ, Min BM, Park WH (2006) Biomacromolecules 7:635
58. Li L, Hsieh YL (2006) Carbohydr Res 341:374
59. Huang L, Nagapudi K, Apkarian RP, Chaikof EL (2001) J Biomater Sci Polym Ed 12:979
60. Huang L, Apkarian RP, Chaikof EL (2001) Scanning 23:372
61. Langer R, Vacanti JP (1993) Science 260:920
62. Han D, Gouma PI (2006) Nanomedicine-UK 2:37

63. Murugan R, Ramakrishna S (2007) Tissue Eng 13:1845
64. Berthiaume F, Moghe PV, Toner M, Yarmush ML (1996) FASEB J 10:1471
65. Teo WE, He W, Ramakrishna S (2006) Biotechnol J 1:918
66. Behonick DJ, Werb Z (2003) Mech Develop 120:1327
67. Li WJ, Laurencin CT, Caterson EJ, Tuan RS, Ko FK (2002) J Biomed Mater Res 60:613
68. Mo XM, Xu CY, Kotaki M, Ramakrishna S (2004) Biomaterials 25:1883
69. Smith LA, Ma PX (2004) Colloid Surface B 39:125
70. Liu X, Ma PX (2004) Ann Biomed Eng 32:477
71. Sharma B, Elisseeff JH (2004) Ann Biomed Eng 32:148
72. Rosso F, Marino G, Giordano A, Barbarisi M, Parmeggiani D, Barbarisi A (2005) J Cell Physiol 203:465
73. Ma Z, He W, Yong T, Ramakrishna S (2005) Tissue Eng 11:1149
74. Reneker DH, Kataphinan W, Theron A, Zussman E, Yarin AL (2002) Polymer 43:6785
75. Yoshimoto H, Shin YM, Terai H, Vacanti JP (2003) Biomaterials 24:2077
76. Shin M, Ishii O, Sueda T, Vacanti JP (2004) Biomaterials 25:3717
77. Li WJ, Tuli R, Okafor C, Derfoul A, Danielson KG, Hall DJ, Tuan RS (2005) Biomaterials 26:599
78. Fujihara K, Kotaki M, Ramakrishna S (2005) Biomaterials 26:4139
79. Erisken C, Kalyon DM, Wang H (2008) Biomaterials 29:4065
80. Li WJ, Tuli R, Huang X, Laquerriere P, Tuan RS (2005) Biomaterials 26:5158
81. Park SH, Kim TG, Kim HC, Yang DY, Park TG (2008) Acta Biomater 4:1198
82. Yang F, Wolke JGC, Jansen JA (2008) Chem Eng J 137:154
83. Li C, Vepari C, Jin HJ, Kim HJ, Kaplan DL (2006) Biomaterials 27:3115
84. Shalumon KT, Anulekha KH, Chennazhi KP, Tamura H, Nair SV, Jayakumar R (2011) Int J Biol Macromol 48:571
85. Bhattarai N, Edmondson D, Veiseh O, Matsen FA, Zhang M (2005) Biomaterials 26:6176
86. Subramanian A, Vu D, Larsen GF, Lin HY (2005) J Biomater Sci Polym Ed 7:861
87. Mo X, Chen Z, Weber HJ (2007) Frontier Mater Sci 1:20
88. Yang D, Jin Y, Zhou Y, Ma G, Chen X, Lu F et al (2008) Macromol Biosci 8:239
89. Zhou YS, Yang D, Chen X, Xu Q, Lu F, Nie J (2008) Biomacromolecules 9:349
90. Zhang Y, Venugopal JR, El-Turki A, Ramakrishna S, Su B, Lim CT (2008) Biomaterials 29:4314
91. Shalumon KT, Binulal NS, Selvamurugan N, Nair SV, Menon D, Furuike T, Tamura H, Jayakumar R (2009) Carbohydr Polym 77:863
92. Ren L, Wang J, Yang FY, Wang L, Wang D, Wang TX, Tian MM (2010) Mater Sci Eng C30:437
93. Meng ZX, Wang YS, Ma C, Zheng W, Li L, Zheng YF (2010) Mater Sci Eng C30:1204
94. Vaz CM, Tuijl SV, Bouten CVC, Baaijens FPT (2005) Acta Biomater 1:575
95. Lee SJ, Liu J, Oh SH, Soker S, Atala A, Yoo JJ (2008) Biomaterials 29:2891
96. Sato M, Nakazawa Y, Takahashi R, Tanaka K, Sata M, Aytemiz D, Asakura T (2010) Mater Lett 64:1786
97. Zhou J, Cao C, Ma X, Jin J (2010) Int J Biol Macromol 47:514
98. Bhattarai SR, Bhattarai N, Yi HK, Hwang PH, Cha DI, Kim HY (2004) Biomaterials 25:2595
99. Pan H, Jiang H, Chen W (2006) Biomaterials 27:3209
100. Neamnark A, Sanchavanakit N, Pavasant P, Rujiravanit R, Supaphol P (2008) Eur Polym J 44:2060
101. Kumbar SG, Nukavarapu SP, James R, Nair LS, Laurencin CT (2009) Biomaterials 29:4100
102. Lowery JL, Datta N, Rutlede GC (2010) Biomaterials 31:491
103. Casper CL, Yang W, Farach-Carson MC, Rabolt JF (2007) Biomacromolecules 8:1116
104. Zeng J, Xu X, Chen X, Liang Q, Bian X, Yang L, Jing X (2003) J Control Release 92:227
105. Zeng J, Yang L, Liang Q, Zhang X, Guan H, Xu X, Chen X, Jing X (2005) J Control Release 105:43

106. Xu X, Yang L, Xu X, Wang X, Chen X, Liang Q, Zeng J, Jing X (2005) J Control Release 108:33
107. Xu X, Chen X, Wang Z, Jing X (2009) Eur J Pharm Biopharm 72:18
108. Ranganath SH, Wang CH (2008) Biomaterials 29:2996
109. Kenawy ER, Abdel-Hay FI, El-Newehy MH, Wnek GE (2007) Mater Sci Eng A459:390
110. Tungprapa S, Jangchud I, Supaphol P (2007) Polymer 48:5030
111. Cui W, Li X, Zhu X, Yu G, Zhou S, Weng J (2006) Biomacromolecules 7:1623
112. Peng H, Zhou S, Guo T, Li Y, Li X, Wang J, Weng J (2008) Colloid Surface B 66:206
113. Ngawhirunpat T, Opanasopit P, Rojanarata T, Akkaramongkolporn P, Ruktanonchai U, Supaphol P (2009) Pharm Dev Technol 14:70
114. Kenawy ER, Bowlin GL, Mansfield K, Layman J, Simpson DG, Sanders EH, Wnek GE (2002) J Control Release 81:57
115. Zong X, Kim K, Fang D, Ran S, Hsiao BS, Chu B (2002) Polymer 43:4403
116. Verreck G, Chun I, Rosemblatt J, Peeters J, Dijck AV, Mensch J, Noppe M, Brewster ME (2003) J Control Release 92:349
117. Taepaiboon P, Rungsardthong U, Supaphol P (2007) Eur J Pharm Biopharm 67:387
118. Puppi D, Piras AM, Detta N, Dinucci D, Chiellini F (2010) Acta Biomater 6:1258
119. Luong-Van E, GrØndal L, Chua KN, Leong KW, Nurcombe V, Cool SM (2006) Biomaterials 27:2042
120. Yan S, Xiaoqiang L, Lianjiang T, Chen H, Xiumei M (2009) Polymer 50:4212
121. Lu Y, Jiang H, Tu K, Wang L (2009) Acta Biomater 5:1562
122. Maretschek S, Greiner A, Kissel T (2008) J Control 127:180
123. Yang Y, Li X, Qi M, Zhou S, Weng J (2008) Eur J Pharm Biopharm 69:106
124. Agarwal S, Wendorff JH, Greiner A (2008) Polymer 49:5603
125. Jayakumar R, Prabaharan M, Sudheesh Kumar PT, Nair SV, Tamura H (2011) Biotechnol Adv 29:322
126. Min BM, Lee G, Kim SH, Nam YS, Lee TS, Park WH (2004) Biomaterials 25:1289
127. Schneider A, Wang XY, Kaplan DL, Garlick JA, Egles C (2009) Acta Biomater 5:2570
128. Rho KS, Jeong L, Lee G, Seo BM, Park YJ, Hong SD, Roh S, Cho JJ, Park WH, Min BM (2006) Biomaterials 27:1452
129. Gu SY, Wang ZM, Ren J, Zhang CY (2009) Mater Sci Eng C29:1822
130. Liu SJ, Kau YC, Chou CY, Chen JK, Wu RC, Yeh WL (2010) J Membrane Sci 355:53
131. Ignatova M, Starbova K, Markova N, Manolova N (2006) Carbohydr Res 341:2098
132. Ignatova M, Manolova N, Rashkov I (2007) Eur Polym J 43:1112
133. Chen Z, Mo X, Qing F (2007) Mater Lett 61:3490
134. Chen JP, Chang GY, Chen JK (2008) Colloids Surf A Physicochem Eng Asp 313:183
135. Chen Z, Mo X, He C, Wang H (2008) Carbohydr Polym 72:410
136. Son WK, Youk JH, Park WH (2006) Carbohydr Polym 65:430
137. Xu X, Yang Q, Wang Y, Yu H, Chen X, Jing X (2006) Eur Polym J 42:2081
138. Rujitanaroj P-o, Pimpha N, Supaphol P (2008) Polymer 49:4723
139. Chun JY, Kang HK, Jeong L, Kang YO, Oh JE, Yeo IS, Jung SY, Park WH, Min BM (2010) Colloid Surface B 78:334
140. Zhuang X, Cheng B, Kang W, Xu X (2010) Carbohydr Polym 82:524
141. Hang AT, Tae B, Park JS (2010) Carbohydr Polym 82:472
142. Kossovich LY, Salkovskiy Y, Kirillova IV (2010) World Congr Biomech 31:1212
143. Cai ZX, Mo XM, Zhang KH, Fan LP, Yin AL, He CL, Wang HS (2010) Int J Mol Sci 11:3529
144. Shalumon KT, Anulekha KH, Sreeja VN, Nair SV, Chennazhi KP, Jayakumar R (2011) Int J Biol Macromol. 49(3):247–254. doi:10.1016/j.ijbiomac.2011.04.005
145. Huang XJ, Ge D, Xu ZK (2007) Eur Polym J 43:3710
146. Ye P, Xu ZK, Wu J, Innocent C, Seta P (2006) Biomaterials 27:4169
147. Wang ZG, Wang JQ, Xu ZK (2006) J Mol Catal B Enzym 42:45
148. Li SF, Chen JP, Wu WT (2007) J Mol Catal B Enzym 47:117

149. Wang Y, Hsieh YL (2008) J Memebrane Sci 309:73
150. Huang XJ, Yu AG, Xu ZK (2008) Bioresource Technol 99:5459
151. Huang XJ, Yu AG, Jiang J, Pan C, Qian JW, Xu ZK (2009) J Mol Catal B Enzym 57:250
152. Li SF, Wu WT (2009) Biochem Eng J 45:48
153. Liu B, Li P, Zhang CL, Wang Y, Zhao YS (2010) Process Biochem 45:1330
154. Stoilova O, Ignatova M, Manolova N, Godjevargova T, Mita DG, Rashkov I (2010) Eur Polym J 46:1966

Adv Polym Sci (2012) 246: 241–262
DOI: 10.1007/12_2011_125

Published online: 21 June 2011

Electrospun Nanofibrous Scaffolds-Current Status and Prospects in Drug Delivery

M. Prabaharan, R. Jayakumar, and S.V. Nair

Abstract Controlled delivery systems are used to improve therapeutic efficacy and safety of drugs by delivering them over a period of treatment to the site of action at a rate dictated by the need of the physiological environment. A wide variety of polymeric materials, either biodegradable or non-biodegradable but biocompatible, can be used as delivery matrices. Recently, nanofibrous scaffolds, such as the systems fabricated by electrospinning or electrospraying, have been used in the field of biomedical engineering as wound dressings, scaffolds for tissue engineering, and drug delivery systems. The electrospun nanofibrous scaffolds can be used as carriers for various types of drugs, genes, and growth factors, whereby the release profile can be finely controlled by modulation of the scaffold's morphology, porosity, and composition. The main advantage of this system is that it offers site-specific delivery of any number of therapeutics from the scaffold into the body. The aim of this chapter is to review the recent advances on electrospun nanofibrous scaffolds based on biodegradable and biocompatible polymers for controlled drug and biomolecule delivery applications. The use of electrospun scaffolds as drug carriers is promising for future biomedical applications, particularly in the prevention of post-surgical adhesions and infections, for postoperative local chemotherapy, and for bone and skin tissue engineering.

Keywords Antibiotics · Biomolecules · Cancer · Drug delivery · Electrospinning · Gene delivery · Nanofibers · Scaffolds · Tissue engineering

M. Prabaharan (✉)
Department of Chemistry, Faculty of Engineering and Technology, SRM University, Kattankulathur 603 203, India
e-mail: mprabaharan@yahoo.com

R. Jayakumar and S.V. Nair
Amrita for Nanosciences and Molecular Medicine, Amrita Institute of Medical Sciences and Research Centre, Amrita Viswa Vidyapeetham University, Kochi 682 041, India
e-mail: rjayakumar@aims.amrita.edu

Contents

1 Introduction

In tissue engineering, the scaffold serves as a three-dimensional (3D) template for cell adhesion, proliferation, and formation of an extracellular matrix (ECM), as well as a carrier of growth factors or other biomolecular signals [1]. An ideal scaffold for tissue engineering should have good mechanical properties, suitable biodegradability and, most importantly, good biocompatibility [2, 3]. In particular, the surface properties of the material determine the interactions between the cells and the material and, in consequence, affect cell adhesion [4]. Generally, 3D porous scaffolds can be fabricated from natural and synthetic polymers, ceramics, metals, composite biomaterials, and cytokine-release materials. There are some common methods for fabrication of an emulated scaffold to imitate the structure and functional biology of native ECM. Self-assembly, phase separation, and electrospinning have been utilized to improve nanofiber diameters so that they are similar to the diameter of ECM fibrils, which is in the range 50–500 nm.

Electrostatic spinning is a versatile polymer processing technique in which a stream of a polymer solution or melt is subjected to a high electric field, resulting in the formation of nanodimensional fibers. The collected fibers generate a nonwoven fabric, which can be applied to a number of uses. The application of this technology to drug-based delivery systems has been examined only to a limited extent [5–7]. To generate drug delivery systems based on this approach, a drug is incorporated along with the polymer in the solution to be electrospun. In this process, the diameter and morphology of the filaments is determined by three general types of variable: solution parameters (solution dielectric constant, conductivity, polymer type and concentration, and surface tension), equipment-controlled parameters (flow rate of the solution, hydrostatic pressure in the spinneret, applied electric field, and tip-to-collector distance), and environmental parameters (temperature, humidity, air velocity in the spinning chamber) [8, 9]. Such treatments can give fibers ranging in diameter from 100 nm to several micrometers as well as fibers that range from being highly cylindrical and uniform to beaded fibers that are inhomogeneous in size. Importantly, the large surface area associated with nanospun fabrics allows for fast and efficient solvent evaporation, which gives the incorporated drug

limited time to recrystallize and therefore favors the formation of amorphous dispersions or solid solutions [5]. Due to the special characteristics of electrospun fibers (high surface area-to-volume ratio, flexibility in surface functionalities, and mechanical properties superior to larger fibers), much research [10–16] has been performed to improve some potential applications of nanofibers, including tissue engineering scaffolds, filtration devices, sensors, materials development, and electronic applications.

Electrospun nanofiber meshes have recently emerged as a new generation of scaffold membranes, and possess a number of features suitable for tissue regeneration [17, 18]. They have fibers of the same size-scale as ECM components (fiber diameters ranging from nanometer to submicrometer) and a large surface area, which may improve cellular attachment, morphology, migration, and function. A tissue engineering scaffold should be biocompatible and biodegradable, and the degradation product should be nontoxic. A degradation time of 25 days is suitable for healing acute wounds (burn and skin excision) [19] or about 8 weeks for chronic wounds (diabetic ulcer, pressure ulcer) [20]. Tissue engineering scaffolds can be developed using a variety of materials, including synthetic or natural polymers. Synthetic polyesters, such as lactic acids, glycolic acids and their copolymers with 3-caprolactone, are the most commonly known and used among all biodegradable polymers for fabrication of novel scaffold materials for tissue engineering applications. Among the natural polymers, collagen, chitin, chitosan, fibronectin, and gelatin are the most popular polymers considered for fabrication of scaffolds [21].

Electrospinning techniques offer great flexibility in selecting materials for drug delivery applications. By using suitable polymers, the drug release profile can be tailored either by diffusion alone or diffusion followed by scaffold degradation. Electrospun fibers can be oriented randomly, giving control over both the bulk mechanical properties and the biological response to the scaffold. Recent studies showed that all kinds of drugs such as antibiotics, anticancer agents and proteins, DNA, and RNA can be incorporated into electrospun scaffolds. A number of drug loading methods such as coatings, embedding of drug, and encapsulation of drug (coaxial and emulsion electrospinning) are reported in the literature [22]. These techniques can be used to give precise control over drug release kinetics. Controlled drug delivery systems have gained much attention in the last few decades because of the many advantages compared with conventional dosage forms, such as improved therapeutic efficacy and reduced toxicity. The main advantages of the fibrous scaffold carriers are that they offer site-specific delivery of drugs to the body. Also, more than one drug can be encapsulated directly into the fibers. The utility of a scaffold as a drug delivery carrier can be employed to initiate cellular processes that lead to the creation of a functional tissue that integrates with the body. For example, the release of tissue-specific growth factors can induce differentiation of endogenous or transplanted progenitor cells into the appropriate cell type [23]. The objective of this chapter is to discuss the recent developments on formation of electrospun or electrosprayed nanofibrous scaffolds using biodegradable and biocompatible polymers, and their use in controlled delivery of antibiotic drugs, anticancer drugs, genes, and biomolecules (proteins and growth factors).

2 Mechanism of the Electrospinning Process

The setup for electrospinning consists of three major components: a high-voltage power supply, a spinneret (a metallic needle), and a collector (a grounded conductor) as shown in Fig. 1 [24]. Although the setup for electrospinning is extremely simple, the spinning mechanism is rather complicated due to complex electro-fluid-mechanical issues. In the process of electrospinning, the polymer solution hosted in a syringe can be fed through the spinneret at a constant and controllable rate, and an electrostatic field will exist in the space of the electrospinning device when a high voltage (usually in the range of 1–30 kV) is applied. As shown in Fig. 1, the solution drop at the nozzle of a spinneret is charged, and the induced charges are evenly distributed over the surface. Under the action of electrostatic interactions, the drop is distorted into a conical object that is called a "Taylor cone" [25, 26]. Once the strength of the electrostatic interactions between the external electric field and the surface charges on the Taylor cone has surpassed a threshold value, the electrostatic force can overcome the surface tension of the polymer solution and thus make the solution eject out continuously as a liquid jet from the nozzle. The electrified jet can be attracted by the grounded collectors placed under the spinneret. When the solvent is evaporated, the solid polymer fibers will be deposited as a nonwoven mat on the surface of the collectors.

As for the formation of ultrathin fibers, it is hypothesized that repulsion between surface charges causes the electrified jet to "splay" or "split" into many small fibers of approximately equal diameter and charge per unit length, and the final diameter of the electrospun fibers upon collection is dependent upon how many splays are

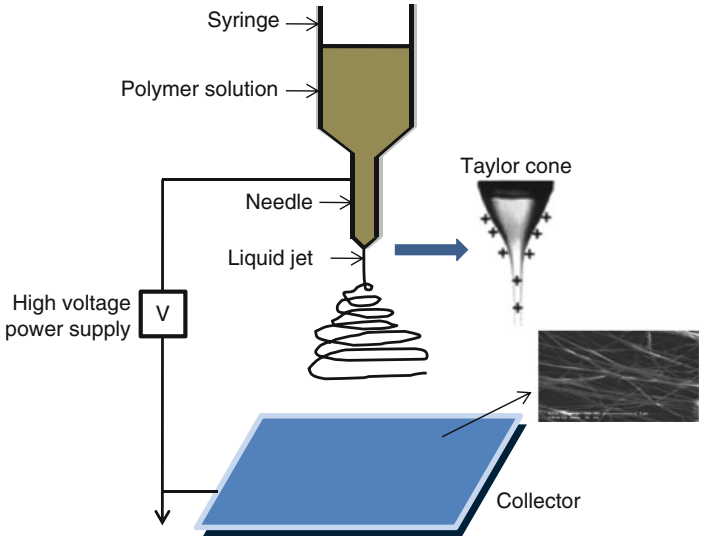

Fig. 1 The electrospinning setup

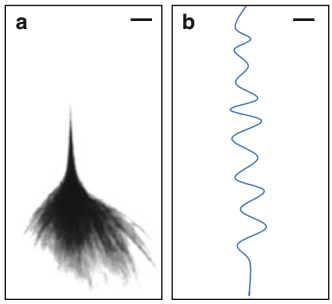

Fig. 2 Jet images of a 2 wt% solution of poly(ethylene oxide) (MW = 2,000,000) in water during electrospinning. (**a**) Unstable jet ($E_\infty = 0.67$ kV/cm, $Q = 0.1$ mL/min, scale bar: 5 mm, 1 ms exposure). (**b**) Close-up of the onset of instability ($E_\infty = 0.67$ kV/cm, $Q = 0.1$ mL/min, scale bar: 1 mm, 18 ns exposure)

created [27]. Recent experimental observations demonstrated that the thinning and electrified jet that appears to splay is actually a single, rapidly whipping jet [28]. The image of this jet using high-speed photography with exposure times as low as 18 ns is shown in Fig. 2. At high fields, after traveling a short distance the jet becomes unstable, begins to whip with a high frequency, and undergoes bending and stretching [28]. The related experimental and theoretical studies [27, 29] clearly demonstrate that the mechanism of electrospinning involves a whipping jet rather than splaying, and its instability is caused by the interaction between the external electric field and the surface charges of the jet. On the basis of these studies, it is conjectured that the diameter of electrospinning fibers mainly depends on the stretching and acceleration of a fluid filament in the instability region, prior to solidification or deposition on the collector. In another study, Feng proposed another model to describe the motion of a highly charged liquid jet in an electric field and discussed the role of nonlinear rheology in the stretching of an electrified jet [30]. All these studies provide a mechanistic understanding of electrospinning processes and thus also the possibility to control the electrospinning process for obtaining an anticipated diameter and structure of the resultant fibers.

3 Properties and Advantages of Electrospun Nanofibrous Scaffolds

Polymeric nanofibers have a diameter in the order of a few nanometers to over 500 nm and possess unique characteristics, such as extraordinary high surface area per unit mass, remarkably high porosity, excellent structural mechanical properties, high axial strength combined with extreme flexibility, and low basis weight. Another interesting aspect of using nanofibers as scaffold materials is that it is feasible to modify not only their morphology and their content but also the surface structure to carry various functionalities. Nanofibers can easily be post-synthetically functionalized by chemical or physical vapor deposition methods. Furthermore, it is even feasible to control secondary structures of nanofibers in order to prepare

nanofibers with core–shell structures, nanofibers with hollow interiors, and porous structures [31].

The electrospinning process is relatively low cost compared to that of most bottom-up nanofiber-fabricating methods. The resulting nanofibers are often uniform, continuous, and do not require expensive purification protocols. Nanofiber production is relatively easy to scale up due to the top-down process and the use of multiple jets for synchronous electrospinning [32]. Moreover, the nanofibers have one dimension at the microscopic scale but another dimension macroscopically. This unique characteristic provides nanofiber mats with the merits possessed by functional materials on the nanometer scale, and these have advantages over conventional solid membranes, such as easy processing and ease of packaging and shipping. These outstanding properties make polymeric nanofibers potential candidates for various applications. For example, nanofibers mats are now being considered for composite material reinforcement, sensors, filtration, catalysis, protective clothing, biomedical applications, space applications such as solar sails, and micro- and nanooptoelectronics.

Electrospinning supplies great flexibility in selecting materials for drug delivery applications. Either biodegradable or nondegradable materials can be used to control whether drug release occurs via diffusion alone or via diffusion and scaffold degradation. Electrospun fibers can be oriented or arranged randomly, giving control over both the bulk mechanical properties and the biological response to the scaffold. There are a number of different drug loading methods, like coatings, embedding the drug, and encapsulating the drug (coaxial and emulsion electrospinning). These techniques can be used to give precise control over drug release kinetics [22]. Controlled drug delivery systems have gained much attention in the last few decades. This is due to the many advantages compared with conventional dosage forms, such as improved therapeutic efficacy and reduced toxicity by delivering drugs at a controlled rate. The main advantages of the electrospun fibrous carriers are that they offer site-specific delivery of drugs to the body. Also, more than one drug can be encapsulated directly into the fibers.

4 Electrospun Nanofibrous Scaffolds in Drug Delivery

4.1 Antibiotic Drug Delivery

Medicated biodegradable poly(lactide-*co*-glycolide) (PLGA)-based nanofibrous scaffolds containing hydrophilic cefoxitin sodium (MefoxinR, an antibiotic drug) were fabricated by electrospinning (Fig. 3) [33]. The drug was successfully incorporated and released from nanofibrous scaffolds without loss of structural integrity or change in functionality. The morphology and the density of the electrospun scaffolds were found to be dependent on the concentration of drug added, which could be attributed to the salt effect during electrospinning. As the concentration of

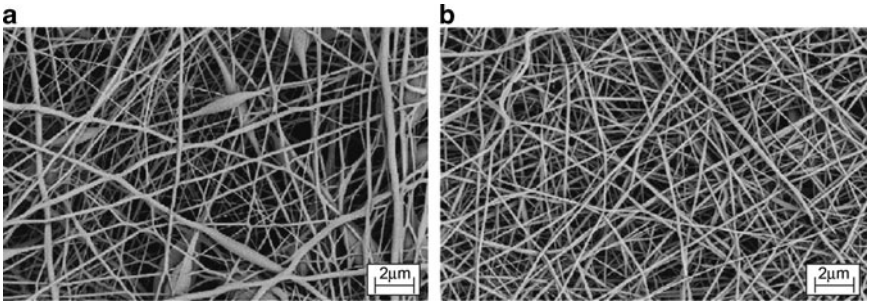

Fig. 3 SEM photographs of electrospun PLGA/PLA/PEG-*b*-PLLA (weight ratio 80:5:15) scaffolds as a function of drug (cefoxitin sodium) concentration: (**a**) without drug and (**b**) with 5 wt% drug

cefoxitin sodium was increased, the morphology of electrospun scaffolds changed from bead-and-string-like to fibrous-like, while at the same time the density of the scaffold gradually decreased. The introduction of an amphiphilic poly(ethylene glycol)-*block*-poly(L-lactic acid) (PEG-*b*-PLLA) block copolymer in the polymer matrix reduced the cumulative amount of the released drug at earlier time points and sustained the drug release profile to longer times (up to 1 week). The released cefoxitin sodium from electrospun scaffolds was found to be structurally intact as well as effective in its ability to inhibit *Staphylococcus aureus* bacteria growth in both static (agar) and dynamic (liquid) environments. From this study, it is clear that these medicated PLGA-based electrospun scaffolds hold a future potential to prevent in vivo post-surgical adhesions and infections.

A localized and temporally controlled delivery system is crucial in order to achieve high local bioactivity and low systemic side effects of antibiotics in the treatment of dental, periodontal, and bone infections. Recently, a 3D porous tissue engineering scaffold was developed with the ability to release antibiotics in a controlled fashion for long-term inhibition of bacterial growth [34]. In this work, the highly soluble antibiotic drug, doxycycline, was successfully incorporated into PLGA nanospheres using a modified water-in-oil-in-oil emulsion method. The PLGA nanospheres were then incorporated into prefabricated nanofibrous PLLA scaffolds with a well-interconnected macroporous structure. Results of in vitro release and antibacterial experiments suggest that the developed drug-containing nanofibrous scaffolds are capable of effectively delivering doxycycline in a controlled fashion with prolonged duration. These biodegradable PLLA scaffolds have a well-interconnected macroporous and nanofibrous structure and can inhibit common bacterial growth for more than 6 weeks with the incorporation of doxycycline-containing PLGA nanospheres. Release kinetics from the scaffolds was found to be determined by PLGA formulation. Incorporation of the nanospheres into scaffolds reduced the burst release. In vitro antibacterial tests of a nanosphere-containing scaffold demonstrated its ability to inhibit common bacterial growth (*S. aureus* and *Escherichia coli*) for a prolonged duration. The successful incorporation of doxycycline into 3D scaffolds and its controlled release from scaffolds extends the usage

of nanofibrous scaffolds from the delivery of large molecules such as growth factors to the delivery of small hydrophilic drugs, allowing for broader application and more complex tissue engineering strategies.

Electrospun fiber mats have been explored as drug delivery vehicles using tetracycline hydrochloride as a model drug [6]. In this study, the mats were made either from PLLA, poly(ethylene-*co*-vinyl acetate) (PEVA), or from a 50:50 blend of the two. The fibers were electrospun from chloroform solutions containing a small amount of methanol to solubilize the antibiotic drug. Release profiles from the electrospun mats were compared to a commercially available drug delivery system, Actisite (Alza Corporation, Palo Alto, CA), as well as to cast films of the various formulations. The results showed that electrospun PEVA and 50:50 PLLA/PEVA mats gave relatively smooth release of drug over about 5 days. The simplicity of the electrospinning process and the wide selection of polymers that can be processed by this means suggest that electrospun polymers matrices may have broad applicability in controlled release technology.

Poly(ε-caprolactone) (PCL) nanofibers containing metronidazole benzoate were successfully electrospun and evaluated for treatment of periodontal disease [35]. In this work, solutions of 10.5% w/v PCL and 5–15% w/w metronidazole benzoate in mixtures of dichloromethane and *N*,*N*-dimethylformamide (DMF) with ratios of 90:10, 80:20 and 70:30 v/v were prepared, and the nanofibers produced by electrospinning. Results showed that decreasing DMF content in the solvent mixture led to a decrease in the solution conductivity and an increase in the solution viscosity as well as in the nanofiber diameter. Increasing metronidazole benzoate concentration in the electrospinning solution caused reverse effects on the viscosity and conductivity and, consequently, on the diameter of the nanofibers. It was demonstrated that the drug release rate was affected by both the solvent ratio and the drug concentration, and that a sustained release of metronidazole benzoate was achieved from the nanofibers for at least 19 days with low burst release. This could be an ideal treatment period for periodontal diseases. All electrospun nanofibers remained smooth and quite flexible, without shrinkage during the period of our treatments, which may offer a desirable texture to be used comfortably. Moreover, the drug release obeyed the Fickian diffusion mechanism. The results suggest that PCL electrospun nanofibers can be used as a locally controlled delivery system for metronidazole benzoate in periodontal disease.

In another work, Zong and coworkers [7] used an electrospinning method to fabricate bioabsorbable amorphous poly (D, L-lactic acid) (PDLA) and semicrystalline PLLA nanofiber nonwoven membranes for biomedical applications. They applied one of the most popular antibiotics, Mexofin, in polymeric solution and electrospun the mixture into nanofibrous nonwoven mats. The resulting membrane exhibits very uniform structures with an average diameter of 160 nm. The release profile of the drug from membranes was determined using UV spectroscopy by measuring the absorbance at 234 nm as a function of time. The authors found over 90% typical loading efficiency of Mefoxin in the PDLA sample by electrospinning and concluded that the drug functionality seems to be completely unaffected by the gentle electrospinning process.

4.2 Anticancer Drug Delivery

In recent years, with the development of electrospinning, the use of electrospun fibers as drug carriers seems to be a promising method for delivery of anticancer drugs, especially in postoperative local chemotherapy, because of their numerous advantages, such as improved therapeutic effect, reduced toxicity, and handling convenience. Xu et al. investigated the utility of electrospun biodegradable PEG–PLLA diblock copolymer fiber carrier for long-term delivery of [1, 3-bis (2-chloroethyl)-1-nitrosourea] (BCNU) [36]. BCNU is one of the most widely used antineoplastic agents for the treatment of malignant gliomas. It can penetrate the blood–brain barrier at potentially tumoricidal concentrations, because of its good lipid solubility and relatively low molecular weight [37]. It is generally accepted that its action mechanism is the formation of interstrand crosslinks in DNA, RNA and protein in a similar way to other alkylating agents [38–40]. The results of this study indicated that the PEG–PLLA fibers were smooth and uniform. BCNU was finely incorporated in the fibers and no BCNU crystals were detected on the fiber surfaces. The release rate of BCNU from the fibers was found to be dependent on the initial BCNU loading. The release of BCNU from the electrospun fibers followed a diffusion mechanism. In vitro cytotoxicity assay showed that the PEG–PLLA fibers themselves did not affect the growth of rat glioma C6 cells. Antitumor activity of the BCNU-loaded fibers against the cells was retained over the whole experiment process, whereas that of pristine BCNU disappeared within 48 h. These results strongly suggest that the BCNU/PEG–PLLA fibers have an effect of controlled release of BCNU and are suitable for postoperative chemotherapy of cancers.

For effective cancer gene therapy, systemic administration of tumor-targeting adenoviral complexes is crucial for delivery to both primary and metastatic lesions. Recently, electrospinning was used to generate nanocomplexes of adenoviral, chitosan, PEG, and folic acid (FA) for effective FA-receptor-expressing tumor-specific transduction [41]. In this study, chitosan–PEG–FA conjugates were generated and processed by electrospinning for adenoviral encapsulation via in situ ionic crosslinking with tripolyphosphate (TPP) (Fig. 4). The electrospinning of adenoviral/chitosan nanocomplexes and ionic crosslinking efficiently coated adenoviral without reducing its biological activity or infectivity. The ionically crosslinked chitosan layer on the adenoviral surface provided chemical conjugation sites for PEG and further for FA, as a targeting moiety at the end of heterofunctional PEG. The results showed that the average size of adenoviral/chitosan–PEG–FA nanocomplexes was approximately 140 nm, and the surface charge was 2.1 mV compared to −4.9 mV for naked adenoviral. Electron microscopy showed well-dispersed, individual adenoviral nanocomplexes without aggregation or degradation. The electrospinning process did not reduce the biological activity of adenoviral, and the transduction of adenoviral/chitosan–PEG–FA nanocomplexes depended on the expression of FA receptor, demonstrating FA receptor-targeted viral transduction. In addition, the transduction efficiency of adenoviral/chitosan–PEG–FA was found

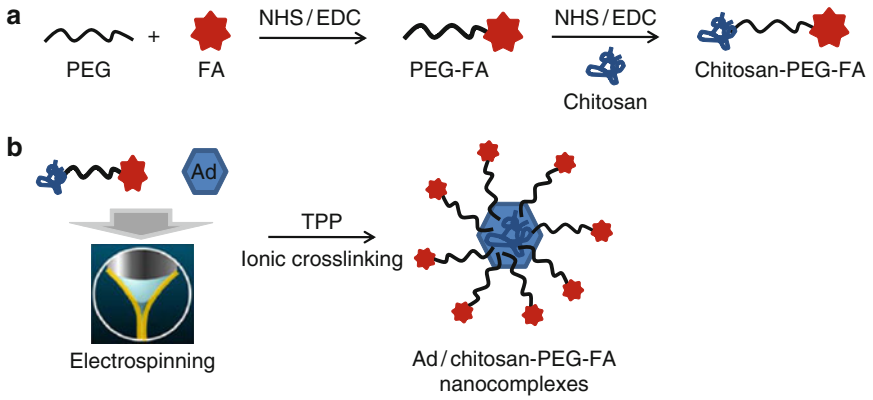

Fig. 4 Synthesis of chitosan–PEG–FA (**a**), and electrospinning process for generating adenoviral (Ad)/chitosan–PEG–FA nanocomplexes (**b**)

to be 57.2% higher than chitosan-encapsulated adenoviral, showing the superiority of FA-receptor-mediated endocytosis for viral transduction. The production of inflammatory cytokine, interleukin-6 from macrophages was significantly reduced by adenoviral/chitosan–PEG–FA nanocomplexes, implying the potential for use in systemic administration. These results clearly demonstrate that cancer cell-targeted viral transduction by adenoviral/chitosan–PEG–FA nanocomplexes can be used effectively for metastatic tumor treatment, with reduced immune reaction against adenoviral.

Biodegradable synthetic polymers can be used to embed drugs in electrospun fibers. The drug release of resultant drug-loaded fibers not only occurs via diffusion alone, but also through loading material degradation. Therefore, the rate of material degradation greatly influences the drug release prolife. Zeng et al. studied the influences of surfactants and anticancer drugs on the diameter size and uniformity of electrospun PLLA fibers by adding various surfactants (cationic, anionic, and nonionic) and anticancer drugs into the PLLA solution [42]. In another study, the influence of the solubility and compatibility of drugs in the drug/polymer/solvent system on the encapsulation of the drug inside the PLLA electrospun fibers and the release behavior of this formulation were also examined by using paclitaxel, doxorubicin hydrochloride, and doxorubicin base as model drugs [43]. The results of these studies showed that the drug release profile of doxorubicin-hydrochloride-embedded PLLA electrospun fibers followed nearly zero-order kinetics in the presence of proteinase K due to the degradation of PLLA fibers. In this procedure, the degradation of PLLA played a key role in the drug release. This gave distinct release properties under different concentrations of proteinase K, similar to biodegradation.

Cellulose acetate fiber mats containing curcumin, widely known for its antitumor, antioxidant, and anti-inflammatory properties, were fabricated from cellulose acetate solution containing curcumin in various amounts (i.e., 5–20 wt% based on

the weight of cellulose acetate powder) by electrospinning [44]. The results showed that incorporation of curcumin in the cellulose acetate solution did not affect the morphology of the resulting fibers, as both the cellulose acetate and the curcumin-loaded cellulose acetate fibers were smooth. The average diameters of the curcumin-loaded cellulose acetate fibers ranged between ~314 and ~340 nm. In this study, the release characteristics of curcumin from the curcumin-loaded cellulose acetate fiber mats was studied by the methods of total immersion and transdermal diffusion through a pig skin in acetate buffer solution containing Tween 80 and methanol at 37 °C. In the total immersion method, almost all of the curcumin loaded in the cellulose acetate fiber mats was released into the medium (~90–95%), while considerably lower values were obtained when the curcumin-loaded cellulose acetate fiber mats were placed on top of pig skin.

Xie et al. developed electrospun PLGA-based nanofibers as implants for the sustained delivery of anticancer drug to treat C6 glioma cells in vitro [45]. Differential scanning calorimetry (DSC) results suggest that the drug was in the solid solution state in the polymeric micro- and nanofibers. In vitro release profiles suggest that sustained release of paclitaxel was achieved for more than 60 days. Cytotoxicity test results suggest that the IC_{50} value of paclitaxel-loaded PLGA nanofibers is comparable to the commercial paclitaxel formulation, Taxol. Electrospun nanofibers often have higher drug encapsulation efficiency than other methods. The electrospun paclitaxel-loaded biodegradable micro- and nanofibers are promising for the treatment of brain tumors as alternative drug delivery devices. Although many types of drug delivery systems have been prepared from electrospun drug-loaded nanofibers, no related clinical experiments have been reported and only few in vivo drug delivery researches have been undertaken, which were mainly associated with cancer research. Ranganath et al. reported the use of paclitaxel-loaded biodegradable implants in the form of microfiber discs and sheets developed using electrospinning to treat malignant glioma in vitro and in vivo [46]. The fibrous matrices not only provided a greater surface area-to-volume ratio for effective drug release rates but also provided needed implantability into the tumor-resected cavity of a post-surgical glioma.

4.3 Gene Delivery

Scaffold-mediated gene delivery or reverse transfection has been studied for DNA delivery. Thus far, the common platforms utilized are typically in the form of hydrogels [19] or porous scaffolding materials formed by gas-forming or particle-leaching techniques [20]. These approaches ensure the localized and prolonged availability of genetic materials to cells. Nanofibrous scaffolds, in contrast, represent a novel class of potent materials for such applications. By providing a good representation of the nanofibrous architecture of the natural extracellular matrix, biomimicking topographical signals are presented to seeded cells. Such added morphological features provide an extra dimension for better control over cellular functions.

Viral gene delivery remains one of the most efficient for achieving transgene expression for tissue engineering applications, although concerns regarding immune response to viral particles persist [47, 48]. Current viral gene therapy approaches in tissue engineering often involve the implantation of in vitro transduced cells with or without the use of scaffolds or hydrogels. Although viral gene transfer is efficient in achieving transgene expression for tissue engineering, the drawbacks of virus dissemination, toxicity, and transient gene expression due to immune response have hindered its widespread application. Many tissue engineering studies thus opt to genetically engineer cells in vitro prior to their introduction in vivo. However, it would be attractive to obviate the need for in vitro manipulation by transducing the infiltrating progenitor cells in situ. Recently, Liao et al. introduced the fabrication of a virus-encapsulating electrospun fibrous scaffold to achieve sustained and localized transduction [49]. In this study, adenovirus encoding the gene for green fluorescent protein was efficiently encapsulated into the core of PCL fibers through coaxial electrospinning. The results showed that the encapsulated viruses were uniformly distributed inside the core of the electrospun fibers and could be released in a porogen-assisted manner. Cells seeded on the virus-encapsulating scaffold exhibited transgene expression for over one month with a reduced proliferation rate. RAW 264.7 cells cultured on the virus-encapsulating fibers produced a lower level of interleukin-1β, tumor necrosis factor-α and interferon-α, suggesting that the activation of macrophage cells by the viral vector was reduced when encapsulated in the core–shell PCL fibers. Prolonged transgene expression, controlled virus exposure, and localized cell transduction are several characteristics shown in this work that suggest that virus-encapsulating coaxial electrospun fibers may advance viral gene transfer for regenerative medicine.

Saraf et al. described the use of coaxial electrospinning as a means for the fabrication of fiber mesh scaffolds and for the encapsulation and subsequent release of a nonviral gene delivery vector over a period of up to 60 days [50]. In this work, various fiber mesh scaffolds containing plasmid DNA (pDNA) within the core, and the nonviral gene delivery vector poly(ethylenimine)-hyaluronic acid (PEI-HA) within the sheath of coaxial fibers, were fabricated on the basis of a fractional factorial design that investigated the effects of four processing parameters at two levels. PCL sheath polymer concentration, PEG core polymer molecular weight and concentration, and the concentration of pDNA were investigated for their effects on average fiber diameter, release kinetics of PEI-HA, and transfection efficiency. It was determined that increasing the values of each of the investigated parameters caused an increase in the average diameter of the fibers. The release kinetics of PEI-HA from the fibers was found to be affected by the loading concentration of pDNA. Two-dimensional (2D) cell culture experiments with model fibroblast-like cells demonstrated that complexes of pDNA with PEI-HA released from fiber mesh scaffolds could successfully transfect cells and induces expression of enhanced green fluorescent protein (EGFP). Peak EGFP expression varied with the investigated processing parameters, and the average transfection observed was a function of PEG molecular weight and concentration. Furthermore, fibroblast-like cells seeded directly onto coaxial fiber mesh scaffolds containing PEI-HA and pDNA

showed EGFP expression over 60 days, which was significantly greater than the EGFP expression observed with scaffolds containing pDNA alone [50]. These results confirmed that electrospun coaxial fiber mesh scaffolds with variable and sustained transfection properties can be applied for tissue engineering and other gene delivery applications involving gene therapy.

Extracellular and intracellular barriers typically prevent nonviral gene vectors from having effective transfection efficiency. Formulation of a gene delivery vehicle that can overcome the barriers is a key step for successful tissue regeneration. Liang et al. have developed a novel core–shelled DNA nanoparticle by invoking solvent-induced condensation of pDNA (β-galactosidase or GFP) in a solvent mixture (94% DMF + 6% Tris/EDTA buffer) and subsequent encapsulation of the condensed DNA globule in a triblock copolymer, PLLA–PEG–PLLA, in the same solvent environment [51]. The results showed that the polylactide shell protects the encapsulated DNA from degradation during electrospinning of a mixture of encapsulated DNA nanoparticles and biodegradable PLGA to form a nanofibrous nonwoven scaffold using the same solution mixture. The bioactive pDNA was found to be released in an intact form from the scaffold with a controlled release rate and transfect cells in vitro.

Small interfering RNA (siRNA) delivery has found useful applications, particularly as therapeutic agent against genetic diseases. Currently, the delivery of siRNA typically takes the form of nanoparticles. In order to expand the applications of these potent but labile molecules for long-term use required by tissue engineering and regenerative medicine, alternative delivery vehicles are required. Recently, a siRNA delivery system using electrospun nanofibers was developed [52]. The results of this study showed that by encapsulating siRNA within PCL nanofibers (300–400 nm in diameter) the controlled release of intact siRNA could be achieved for at least 28 days under physiological conditions. The successful transfection of HEK293 cells with GAPDH-specific siRNA released from fibrous scaffolds at days 5, 15, and 30 demonstrated that the encapsulated molecules remained bioactive throughout the period of sustained release, providing silencing efficiency of 61–81% that was comparable to conventional siRNA transfection. Direct seeding of cells on these biofunctional scaffolds, with and without transfection reagent, demonstrated enhanced cellular uptake and efficient GAPDH gene-silencing. This work demonstrates the potential of nanofibrous scaffold-mediated siRNA delivery for long-term gene-silencing applications. The combination of topographical features provided by nanofibrous scaffolds may provide synergistic contact guidance and biochemical signals to mediate and support cellular development in regenerative medicine.

4.4 Biomolecule Delivery

Currently, two strategies have emerged as the most promising tissue engineering approaches [53]. One is to implant pre-cultured cells and synthetic scaffold

complexes into the defect place. In this approach, the seeded cells are generally isolated from host target tissues, for which they provide the main resource to form newly grown tissue. The synthetic scaffolds, on the other hand, provide porous 3D structures to accommodate the cells to form extracellular matrix (ECMs) and regulate the cell growth in vivo [54, 55]. These synthetic scaffolds are biodegradable and degrade in accordance with the tissue regeneration time frame. The other approach is to place acellular scaffolds immediately after injury. The governing principle of this approach is using scaffolds to deliver appropriate biomolecules to the defect area; the biomolecules are released from the scaffolds in a controlled manner and may recruit progenitor cells towards the defect area and promote their proliferation and differentiation, thereby enhancing tissue regeneration. In recent years, an increasing trend towards the combination of these two approaches is observed [56–59], because the scaffolds with controlled release of biomolecules can induce the seeded cells to proliferate and differentiate during an ex vivo preculture period, thereby encouraging tissue formation after implantation in vivo.

The most frequently used biomolecules are proteins (e.g., growth factors or cytokines) and growth factor coding genes. Growth factors are endogenous proteins capable of binding cell-surface receptors and directing cellular activities involved in the regeneration of new tissue [60]. Localized delivery of exogenous growth factors is suggested to be therapeutically effective for production of cellular components involved in tissue development and the healing process, thus making them important factors for tissue regeneration [61]. Nevertheless, it has to be emphasized that the success of direct growth factor delivery from scaffolds depends on the large-scale production of recombinant growth factors, which is quite expensive. Additionally, protein bioactivity after incorporation within scaffolds also needs to be considered in view of efficacy issues. Instead of growth factor delivery, gene therapy presents a new paradigm in tissue engineering. This concept gives birth to gene-activated scaffolds, which are defined as scaffolds incorporating therapeutic protein-encoding genes [62]. Gene-activated scaffolds ensure the delivery of genes at the desired site [63], after which transfection into target cells is required to produce therapeutic proteins [64]. Compared to growth factor delivery, gene delivery is advantageous in its long-term effect as well as being relatively low cost, which makes it promising for tissue engineering application.

In the last 10 years, huge efforts have been made to explore strategies for the preparation of bioactive scaffolds to deliver therapeutic proteins or genes, and a series of comprehensive reviews has provided detailed information for these strategies [65, 66]. Recently, electrospinning has gained exponentially increasing popularity for the preparation of bioactive scaffolds with biomolecule release. Polymeric nanofiber scaffolds fabricated by electrospinning are particularly suited for tissue engineering due to their structural resemblance to the ECM. The natural ECM is a complex network of protein fibrils having nanodimensions and exhibits gel-like behavior [67, 68]. Collagen I, for example, is the main component of the dermal matrix and is made of a network of fibers with diameter of 50–500 nm [69–71]. The release profiles of biomolecules from these scaffolds are diffusion-controlled and dependent on the dimensions of the nanofibers. Recently, hydrogel

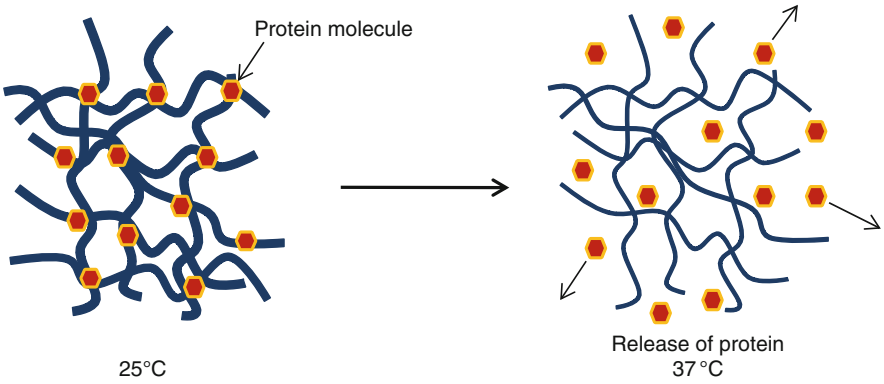

Fig. 5 Representation of temperature-controlled protein release from poly(PEG/PPG/PCL urethane) hydrogel

nanofiber mats based on thermoresponsive multiblock poly(ester urethane)s comprising PEG, poly(propylene glycol) (PPG), and PCL segments were fabricated by electrospinning [72]. The hydrogel nanofiber mats were found to be more water absorbent under cold conditions and shrunk when exposed to higher temperatures. These nanofibers showed temperature-controlled protein release capabilities, providing a significant improvement over conventional PCL nanofibers, which do not have such thermally triggered protein release capabilities (Fig. 5). Studies showed that these nanofiber scaffolds were excellent substrates for cell adhesion and growth, due to their resemblance to the ECM. Additionally, these hydrogel nanofibers degrade much faster than the PCL nanofibers. The mats degrade into small polymer fragments with molecular weight of between 1,000 and 4,000, facilitating the removal of these nanofibers after use through renal filtration [72]. These hydrogel nanofiber scaffolds could potentially be used as thermoresponsive biodegradable supporting structures for skin tissue engineering applications.

Maretschek et al. prepared the highly hydrophobic, protein-loaded nanofiber nonwovens based on PLLA via electrospinning of emulsions [73]. In this study, cytochrome C was chosen as a hydrophilic model protein. The addition of hydrophilic polymers to the aqueous phase of the electrospinning emulsion yielded nanofiber nonwovens composed of polymer blend nanofibers. Mean fiber diameters of these nanofiber nonwovens increased with increasing amounts of hydrophilic polymer in the aqueous phase. To determine the morphology and surface characteristics of the different nanofiber nonwovens, SEM imaging and gas adsorption measurements were also carried out in this study. Transmission electron microscopy (TEM) was used to clarify the localization of the protein within the nanofiber nonwoven. It was observed that the increased fiber diameter of the nanofiber nonwovens composed of polymer blend nanofibers led to a decrease of their specific surface area. PLLA nanofiber nonwovens exhibited a highly hydrophobic surface, which also proved to be the major criterion controlling the protein release. The release rate of PLLA nanofiber nonwovens was rather slow, but nanofiber

nonwovens composed of nanofibers consisting of a polymer blend of PLLA and a hydrophilic polymer (PEG) exhibited adjustable protein release rates depending on the amount of added hydrophilic polymer.

Jiang et al. demonstrated the capabilities of coaxial electrospinning technique for incorporation of water-soluble bioactive agents (bovine serum albumin and lysozyme) into biodegradable core–shell nanofibers with PCL as shell, and protein-containing PEG as core; and their subsequent controlled release [74]. Compared with other methods widely used for encapsulation of proteins, growth factors, and DNA, this technique was found to have the advantages of being facile, high loading efficiency, mild preparation conditions, and relatively steady release characteristics. The results of this study showed that the thickness of the core and shell could be adjusted by the feed rate of the inner dope, which in turn affected the release profiles of the incorporated proteins. It was revealed that the released lysozyme maintained its structure and bioactivity. The nanofiber scaffolds fabricated by coaxial electrospinning technique may find wide applications for controlled release of proteins and tissue engineering. Luu et al. utilized electrospinning to fabricate a synthetic polymer/DNA composite for therapeutic application in gene delivery designed for tissue engineering [75]. The composite was a nonwoven, nanofibrous, membranous structure composed predominantly of PLGA random (PLA–PEG) block copolymer. Release of pDNA from the composite was sustained over a 20-day study period; with maximum release occurring at ~2 h. Cumulative release profiles indicated that amounts released were approximately 68–80% of the initially loaded DNA. Results indicated that DNA released directly from these electrospun fibers was indeed intact, capable of cellular transfection, and successfully expressed the encoded protein β-galactosidase.

Chew et al. investigated the feasibility of encapsulating human β-nerve growth factor (NGF) that was stabilized in the carrier protein, bovine serum albumin in a copolymer of ε-caprolactone and ethyl ethylene phosphate. Partially aligned protein-encapsulating fibers were obtained and the protein was found to be randomly dispersed throughout the electrospun fibrous mesh in an aggregated form. The sustained release of NGF by diffusion was obtained for at least 3 months. PC12 neurite outgrowth assay confirmed that the bioactivity of electrospun NGF was retained throughout the period of sustained release [76]. Patel et al. explored the effects of immobilizing basic fibroblast growth factor (bFGF) onto nanofibers on neurite extension in vitro [77]. The conjugated nanofibers presented several advantages over delivering bFGF in a soluble manner. First, only a small amount of bFGF was required to achieve effects similar to those achieved with soluble bFGF in medium. Second, the electrospun fibrous scaffolds can act as a delivery vehicle for specific targets, without inducing systemic effects. An important consideration when designing such drug delivery systems is to ensure that the process of immobilizing the drug onto the scaffold does not affect the efficacy or the biological activity of the drug itself.

The treatment of challenging fractures and large osseous defects presents a formidable problem for orthopedic surgeons. Tissue engineering and regenerative medicine approaches seek to solve this problem by delivering osteogenic signals within scaffolding biomaterials. Recently, Kolambkar et al. introduced a hybrid

growth factor delivery system that consists of an electrospun nanofiber mesh tube for guiding bone regeneration combined with peptide-modified alginate hydrogel injected inside the tube for sustained growth factor release [78]. In this study, the ability of this system to deliver recombinant bone morphogenetic protein-2 (rhBMP-2) for the repair of critically sized segmental bone defects in a rat model was tested. Longitudinal micro-computed tomography (μ-CT) analysis and torsional testing provided quantitative assessment of bone regeneration. These results indicated that the hybrid delivery system resulted in consistent bony bridging of the challenging bone defects. However, in the absence of rhBMP-2, the use of nanofiber mesh tube and alginate did not result in substantial bone formation. Perforations in the nanofiber mesh accelerated the rhBMP-2-mediated bone repair, and resulted in functional restoration of the regenerated bone. μ-CT-based angiography indicated that the perforations did not significantly affect the revascularization of defects, suggesting that some other interaction with the tissue surrounding the defect (such as improved infiltration of osteoprogenitor cells) contributed to the observed differences in repair. Overall, these results indicate that the hybrid alginate/nanofiber mesh system is a promising growth factor delivery strategy for the repair of challenging bone injuries.

bFGF, an important growth factor involved in tissue repair and mesenchymal stem cell proliferation and differentiation, is a suitable candidate for sustained delivery from scaffolds. Sahoo et al. presented two types of PLGA nanofiber scaffolds incorporated with bFGF. These fibers were fabricated using the facile technique of blending and electrospinning (group I) and by the more complex technique of coaxial electrospinning (group II) [79]. Scaffolds of both groups I and II were observed to be composed of continuous nanofibers with similar morphology to that shown in Fig. 6. Atom force microscopy (AFM) images obtained on scaffolds demonstrated groups of nanofibers with diameters of 500–700 nm. SEM images showed nanofibers with diameters distributed between 100 and 500 nm. It was observed that bFGF was randomly dispersed in group I nanofibers, and distributed as a central core within group II nanofibers. It has been shown that between group I and group II scaffolds, group I scaffolds released the incorporated bFGF in a bioactive form over 1 week, were more hydrophilic, favored bone marrow stem cell (BMSC) attachment and, particularly, proliferation and differentiation into a fibroblastic lineage. However, group II scaffolds could sustain growth factor release for up to 2 weeks. Although both scaffold groups favored BMSC attachment and subsequent proliferation, cells cultured on group I scaffolds demonstrated increased collagen production and upregulated gene expression of specific ECM proteins, indicating fibroblastic differentiation. The study shows that the electrospinning technique could be used to prolong growth factor release from scaffolds.

Nanoscaled PCL and PCL/gelatin fibrous scaffolds with immobilized epidermal growth factor (EGF) were prepared for the purpose of wound-healing treatments [80]. The tissue scaffolds were fabricated by electrospinning and the parameters that affect the electrospinning process were optimized. In this study, the fiber diameters were 488 $\pm$ 114 nm and 663 $\pm$ 107 nm for PCL and PCL/gelatin scaffolds, respectively, and the porosities were calculated as 79% for PCL and 68% for

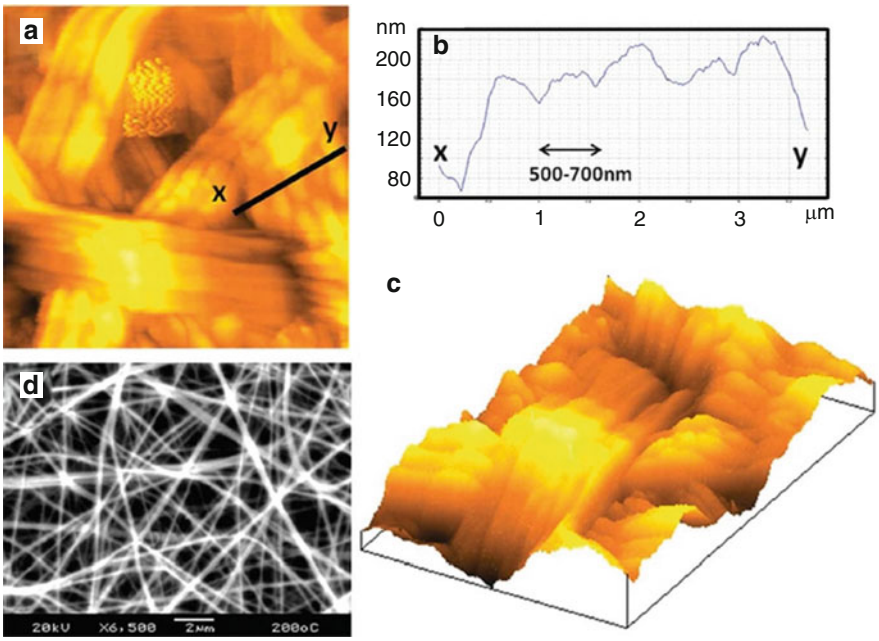

Fig. 6 AFM images in 2D (**a**) and 3D (**c**) showing group I nanofibers of 500–700 nm diameter, as measured by profiling along the line $x-y$ (**b**). SEM image (**d**) shows fibers ranging in diameter from 100 to 500 nm [62]

PCL/gelatin scaffolds. Electrospun PCL and PCL/gelatin scaffolds were modified with 1,6-diaminohexane to introduce amino groups on the surface, then EGF was chemically conjugated to the surface of nanofibers. The results obtained from attenuated total reflectance Fourier transform infrared (ATR-FTIR) spectroscopy and quantitative measurements showed that EGF was successfully immobilized on the nanofibrous scaffolds. In order to investigate the effect of the immobilized EGF on cell spreading and proliferation, L929 mouse fibroblastic cells were cultivated on both unmodified scaffolds and on scaffolds with immobilized EGF. According to the results, EGF immobilized on PCL/gelatin scaffolds exerted early cell spreading and superior and rapid proliferation compared to EGF immobilized on PCL scaffolds and compared to neat PCL or PCL/gelatin scaffolds. These results confirmed that PCL/gelatin scaffolds with immobilized EGF could potentially be employed as novel scaffolds for skin tissue-engineering applications.

5 Conclusions and Future Directions

In the past few years, remarkable progress has been made in the field of electrospinning for the preparation of various types of scaffolds. The development of electrospun nanofibers has enhanced the scope of fabricating scaffolds that can

potentially mimic the architecture of natural human tissue at the nanometer scale. The high surface area-to-volume ratio of the electrospun nanofibers combined with their microporous structure favors cell adhesion, proliferation, migration, and differentiation, all of which are highly desired properties for tissue engineering and drug delivery applications. Because of the ultrathin fiber diameter, electrospun scaffolds are considered to be an effective delivery system for drugs, genes, and biomolecules due to the stereological porous structure and high specific surface area. Drugs and biomolecules can be incorporated within electrospun scaffolds by physical adsorption, blend electrospinning or coaxial electrospinning as well as via covalent immobilization after scaffold fabrication.

Although there have been a substantial number of studies dedicated to the methodology of preparing electrospun scaffolds to achieve biomolecule delivery, further studies are needed to improve the stability of incorporated protein, gene transfection efficiency, and the accuracy of release kinetics control. Since only a limited number of research efforts so far have focused on in vivo applications of electrospun nanofibrous scaffolds with protein or gene delivery, more animal studies are needed to fully explore the potential of these scaffolds for clinical applications. Close cooperation between laboratories and clinics might eventually help to translate this promising technique from bench to bed, and it is likely that biomolecule delivery from electrospun scaffolds will provide therapeutic benefit in regenerative medicine in the near future.

To date, most of the drug release studies have been done in vitro using electrospun scaffolds. In this line, several problems must be resolved, such as drug loading, the initial burst effect, residual organic solvent, stability of active agents, and the combined usage of new biocompatible polymers. The drug release characteristics of electrospun nanofibrous scaffolds rely on the drug being encapsulated within the nanofibers. However, due to surface effects the drug particles in the nanofibers tend to accumulate on the fiber surface. Thus, a burst release at an initial stage is inevitable unless the blend of drug and polymer carrier is fully integrated into the nanofiber at a molecular level. The solubility and compatibility of the drug in the drug/polymer/solvent system are the decisive factors for the preparation of an electrospun fiber formulation with constant release of the drug. Therefore, in order to encapsulate most of the drug inside the polymer fibers, and thus to acquire a constant and stable drug release profile, a lipophilic polymer should be chosen as the fiber material for a lipophilic drug whereas a hydrophilic polymer should be employed for a hydrophilic drug, and the solvents used should be suitable for both drug and polymer.

In future studies, it is important to focus research on gaining a better fundamental understanding of the electrospinning process, particularly on exploiting new techniques or systems that can precisely control drug release profile so that any possibility of dose dumping and subject-to-subject variability can be minimized. The relationships between the drug controlled release profile and the electrospinning parameters should be elucidated. It is critically important to provide controlled and sequential drug release in tissue engineering applications, and further progress in drug-loaded electrospun fibers with core–shell structures may provide the possibility

to encapsulate two different drugs or biologically active agents within the core–shell structure at the same time. A controllable release profile and sequential release could be achieved by properly selecting bioabsorbable polymers with desired degradation rates.

Acknowledgments One of the authors, R. Jayakumar, is grateful to SERC Division, Department of Science and Technology (DST), India, for providing funding under the scheme of "Fast Track Scheme for Young Investigators" (Ref. No. SR/FT/CS-005/2008). The author R. Jayakumar is also thankful to the Department of Biotechnology (DBT), Government of India for providing financial support to carry out research work under the Bioengineering Program (Ref. No. BT/PR13885/MED/32/145/2010). S.V. Nair is also grateful to DST, India, which partially supported this work under the Nanoscience and Nanotechnology Initiative program monitored by C.N.R. Rao.

References

1. Chen GP, Ushida T, Tateishi T (2001) Biomaterials 18:2563
2. Thomson RC, Wake MC, Yaszemski MJ, Mikos AG (1995) Adv Polym Sci 122:245
3. Langer R (1995) Ann Biomed Eng 23:101
4. Dobkowski J, Kolos R, Kaminski J, Kowalczynska HM (1999) J Biomed Mater Res 47:234
5. Verreck G, Chun I, Peeters J, Rosenblatt J, Brewster ME (2003) Pharm Res 20:810
6. Kenawy ER, Bowlin GL, Mansfield K, Layman J, Simpson DG, Sanders EH, Wnek GE (2002) J Control Release 81:57
7. Zong X, Kim K, Fang D, Ran S, Hsiao BS, Chu B (2002) Polymer 43:4403
8. Lee KH, Kim HY, Khil MS, Ra YM, Lee DR (2003) Polymer 44:1287
9. Shin YM, Hohman MM, Brenner MP, Rutledge GC (2001) Polymer 42:9955
10. Zhang Y, Lim CT, Ramakrishna S, Huang ZM (2005) J Mater Sci Mater Med 16(10):933
11. Li L, Hsieh YL (2006) Carbohydr Res 341:374
12. Subbiah TH, Bhat GS, Tock RW, Parameswaran S, Ramkumar SS (2005) J Appl Polym Sci 96:557
13. Kwon IK, Kidoaki S, Matsuda T (2005) Biomaterials 26(18):3929
14. Van EL, Grondahl L, Chua KN, Leong KW, Nurcombe V, Cool SM (2006) Biomaterials 27 (9):2042
15. Deitzel JM, Kleinmeyer J, Harris D, Becletan NC (2001) Polymer 42:261
16. Huang ZM, Zhang YZ, Kotaki M, Ramakrishna S (2003) Comp Sci Technol 63:2223
17. Pham QP, Sharma U, Mikos AG (2006) Tissue Eng 12(5):1197
18. Jayakumar R, Prabaharan M, Nair SV, Tamura H (2010) Biotechnol Adv 28(1):142
19. Yannas V, Burke JF (1980) J Biomed Mater Res 14:65
20. Galassi G, Brun P, Radice M, Cortivo R, Zanon GF, Genovese P, Abatangelo G (2000) Biomaterials 21:2183
21. Naira LS, Laurencin CT (2007) Prog Polym Sci 32:762
22. Sill TJ, Recum HA (2008) Biomaterials 29:1989
23. Prabaharan M, Rodriguez-Perez A, de Saja JA, Mano JF (2007) J Biomed Mater Res Part B 81B:427
24. Li D, Xia Y (2004) Adv Mater 16:1151
25. Frenot A, Chronakis IS (2003) Curr Opin Colloid Interface Sci 8:64
26. Huang ZM, Zhang YZ, Kotaki M, Ramakrishna S (2003) Compos Sci Technol 63:2223
27. Reneker DH, Chun I (1996) Nanotechnology 7:216
28. Shin YM, Hohman MM, Brenner MP, Rutledge GC (2001) Appl Phys Lett 78:1149
29. Hohman MM, Shin M, Rutledge G, Brenner MP (2001) Phys Fluids 13:2201
30. Feng JJ (2002) Phys Fluids 14:3912

31. Chronakis IS (2005) J Mater Process Technol 167:283
32. Varabhas JS, Chase GG, Reneker DH (2008) Polymer 49:4226
33. Kwangsok K, Yen KL, Charles C, Dufei F, Benjamin SH, Benjamin C, Michael H (2004) J Control Release 98:47
34. Kai F, Hongli S, Mark AB, Ellen JD, William VG, Peter XM (2010) J Control Release 146:363
35. Zamani M, Morshed M, Varshosaz J, Jannesari M (2010) Eur J Pharm Biopharm 75:179
36. Xu X, Chen X, Xu X, Lu T, Wang X, Yang L, Jing X (2006) J Control Release 114:307
37. Loo TL, Dion RL, Dixon RL, Rall DP (1966) J Pharm Sci 55:492
38. Colvin M, Brundrett RB, Cowens W, Jardine I, Ludlum DB (1976) Biochem Pharmacol 25:695
39. Erickson LC, Laurent G, Sharkey NA, Kohn KW (1980) Nature 288:727
40. Pieper RO, Noftz SL, Erickson SL (1995) Mol Pharmacol 47:290
41. Park Y, Kang E, Kwon OJ, Hwang T, Park H, Lee JM, Kim JH, Yun CO (2010) J Control Release 148:75
42. Zeng J, Xu XY, Chen XS, Liang QZ, Bian XC, Yang LX, Jing XB (2003) J Control Release 92:227
43. Zeng J, Yang LX, Liang QZ, Zhang XF, Guan HL, Xu XL, Chen XS, Jing XB (2005) J Control Release 105:43
44. Suwantong O, Opanasopit P, Ruktanonchal U, Supaphol P (2007) Polymer 48:7546
45. Xie J, Wang CH (2006) Pharm Res 23:1817
46. Ranganath SH, Wang CH (2008) Biomaterials 29:2996
47. Zhang X, Godbey WT (2006) Adv Drug Deliv Rev 58:515
48. Wang Y, Yuan F (2006) Ann Biomed Eng 34:114
49. Liao IC, Chen S, Liu JB, Leong KB (2009) J Control Release 139:48
50. Saraf A, Baggett LS, Raphael RM, Kasper FK, Mikos AG (2010) J Control Release 143:95
51. Liang D, Luu YK, Kim K, Siao BS, Hadjiargyrou M, Chu B (2005) Nucl Acids Res 33:170
52. Cao H, Jiang X, Chai C, Chew SY (2010) J Control Release 144:203
53. Langer R, Vacanti JP (1993) Science 260(5110):920
54. Rosenberg MD (1963) Science 139:411
55. Ma Z, Kotaki M, Inai R, Ramakrishna S (2005) Tissue Eng 11(1–2):101
56. Martins A, Duarte ARC, Faria S, Marques AP, Reis RL, Neves NM (2010) Biomaterials 31 (22):5875
57. Wang F, Li ZQ, Khan M, Tamama K, Kuppusamy P, Wagner WR, Sen CK, Guan JJ (2010) Acta Biomater 6(6):1978
58. Murphy WL, Peters MC, Kohn DH, Mooney DJ (2000) Biomaterials 21(24):2521
59. Moioli EK, Clark PA, Xin X, Lal S, Mao JJ (2007) Adv Drug Deliv Rev 59(4–5):308
60. Varkey M, Gittens SA, Uludag H (2004) Expert Opin Drug Deliv 1(1):19
61. Chen FM, Zhang M, Wu ZF (2010) Biomaterials 31(24):6279
62. Lu Z, Zreiqat H (2010) Tissue Eng A 16(10):3075
63. Roy K, Wang D, Hedley ML, Barman SP (2003) Mol Ther 7(3):401
64. Storrie H, Mooney DJ (2006) Adv Drug Deliv Rev 58(4):500
65. Babensee JE, McIntire LV, Mikos AG (2000) Pharm Res 17(5):497
66. De Laporte L, Shea LD (2007) Adv Drug Deliv Rev 59(4–5):292
67. Lutolf MP, Hubbell JA (2005) Nat Biotechnol 23(1):47
68. Abrams GA, Murphy CJ, Wang ZY, Nealey PF, Bjorling DE (2003) Urol Res 31(5):341
69. Elsdale T, Bard J (1972) J Cell Biol 54:626
70. Nisbet DR, Crompton KE, Horne MK, Finkelstein DI, Forsythe JS (2008) J Biomed Mater Res B 87B(1):251
71. Chew SY, Mi RF, Hoke A, Leong KW (2007) Adv Funct Mater 17(8):1288
72. Loh XJ, Peh P, Liao S, Sng C, Li J (2010) J Control Release 143:175
73. Maretschek S, Greiner A, Kissel T (2008) J Control Release 127:180
74. Jiang H, Hu Y, Li Y, Zhao P, Zhu K, Chen W (2005) J Control Release 108:237

75. Luu YK, Kim K, Hsiao BS, Chu B, Hadjiargyrou M (2003) J Control Release 89:341
76. Chew SY, Wen J, Yim EKF, Leong KW (2005) Biomacromolecules 6:2017
77. Patel S, Kurpinski K, Quigley R, Gao H, Hsiao BS, Poo MM (2007) Nano Lett 7:2122
78. Kolambkar YM, Dupont KM, Boerckel JD, Huebsch N, Mooney DJ, Hutmacher DW, Guldberg RE (2011) Biomaterials 32:65
79. Sahoo S, Ang LT, Goh JCH, Toh SL (2010) J Biomed Mater Res 93A:1539
80. Seda TR, Kazaroglu N, Merve M, Bora M, Gumusderelioglu M (2011) J Biomat Sci Polym Ed 22:207

Adv Polym Sci (2012) 246: 263–282
DOI: 10.1007/12_2011_123

Published online: 14 May 2011

Biomedical Applications of Polymer/Silver Composite Nanofibers

R. Jayakumar, M. Prabaharan, K.T. Shalumon, K.P. Chennazhi, and S.V. Nair

Abstract Electrospinning is a very attractive method for preparing polymer or composite nanofibers. Electrospun nanofibers with a high surface area-to-volume ratio have received much attention because of their biomedical applications. Recently, the incorporation of metal nanoparticles into polymer nanofibers has drawn a great deal of attention because these metal nanoparticles can endow the polymer nanofibers with distinctive properties, such as optical, electronic, catalytic, and antimicrobial properties. These properties enable nanofibers to be used in variety of novel applications such as biosensors, catalysts, nanoelectronic devices, etc. Nanofibers containing silver nanoparticles have a wide range of application potential such as for filtration, wound dressings, tissue engineering, biosensors, and catalysts. This review summarizes the preparation and applications of silver nanoparticles incorporated into polymeric nanofibers.

Keywords Silver nanoparticles · Electrospinning · Filtration · Nanofibers · Polymers · Tissue engineering · Wound dressing

Contents

R. Jayakumar (✉), K.T. Shalumon, K.P. Chennazhi, and S.V. Nair
Amrita Center for Nanosciences and Molecular Medicine, Amrita Institute of Medical Sciences and Research Centre, Amrita Vishwa Vidhyapeetham University, Cochin 682 041, India
e-mail: rjayakumar@aims.amrita.edu; jayakumar77@yahoo.com

M. Prabaharan
Department of Chemistry, Faculty of Engineering and Technology, SRM University, Kattankulathur 603 203, India

1 Introduction

Electrospinning is a very attractive method for preparing polymer or composite nanofibers. During electrospinning, a high voltage is applied to a polymer solution to produce a polymer jet. With the fast evaporation of solvent, the charge density in the polymer jet is increased, which results in the formation of nanofibers [1]. In recent years, the electrospinning technique has been proven to be a versatile and effective method for fabricating nanofibers with exceptionally long length, uniform diameter, diverse composition and high surface-to-volume ratio [1]. These nanofibers can be applied in membrane technology [2], optical and biosensors [3], superhydrophobic surfaces [4], tissue engineering [5, 6], and drug delivery [7, 8].

Development in electrospinning in terms of fiber construction and organization, material selection and incorporation, and postspinning modifications have paved the way for future developments in advanced composite systems. A nanocomposite system with up to five distinct levels of organization can be constructed using electrospun fibers. At the first level is a composite nanofiber. The second level is a second layer of composite material coated over the core composite nanofiber. Surface modification of the nanofiber will give the third level. The fourth level of organization is by arranging the nanofibers to form an assembly. Finally at the last level, the nanofiber assembly can be encapsulated within a matrix or form a bulk structure of a predetermined shape. Recently, more and more people have devoted themselves to the study of inorganic/organic composite nanofibers prepared by the electrospinning method. Numerous inorganic/organic polymer composite nanofibers have been prepared [8].

Nanoparticles are clusters of atoms in the size range of 1–100 nm. The use of nanoparticles is gaining impetus in the present century because they posses defined chemical, optical, and mechanical properties. The metallic nanoparticles are most

promising as they show good antibacterial properties due to their large surface area-to-volume ratio. This is of increasing interest because of the growing microbial resistance to metal ions and antibiotics, and to the development of resistant strains [9]. Different types of nanomaterials like copper, zinc, titanium [10], magnesium, gold [11], and silver (Ag) [12–14] have been studied but Ag nanoparticles have proved to be most effective because of their good antimicrobial efficacy against bacteria, viruses, and other eukaryotic microorganisms [9].

Polymer-supported Ag nanoparticles have been widely investigated and provide potential applications as catalysts, photonic and electronic sensors, wound dressings, body wall repairs, augmentation devices, tissue scaffolds, and antimicrobial filters [15–22]. For these applications, Ag nanoparticles have to be supported in a biocompatible polymer system [23–26]. The electrospinning technique has often been adopted for the incorporation of Ag nanoparticles into polymer porous media. In this chapter, we review the preparation methods and properties of Ag nanoparticles incorporated into polymeric nanofibers and their applications in the fields of filtration, catalysis, tissue engineering and wound dressing.

2 Preparation Methods and Properties

2.1 Ag–Alginate Nanofibers

High molecular weight poly(vinyl alcohol) (PVA)/sodium alginate (SA)/Ag nanocomposite fiber was prepared using the electrospinning technique [27]. The effect of the addition of Ag colloidal solution on the PVA/SA/Ag nanocomposite was investigated through a series of experiments by varying the molecular weight of PVA and electrospinning processing parameters such as concentration of PVA solution, PVA/SA blend ratio, applied voltage, and tip-to-collector distance. In the case of PVA with number-average degree of polymerization of 1,700, by increasing the amount of SA in the spinning solution, the morphology was changed from fine uniform fiber to beaded fiber or to bead-on-string fiber structure. Increasing the amount of Ag colloidal solution resulted in higher charge density on the surface of the ejected jet during spinning, thus more electric charge was carried by the electrospinning jet. As the charge density increased, the diameter of the nanocomposite fibers became smaller. Energy-disperse X-ray (EDX) analysis indicated that carbon, oxygen, and Ag were the principle elements of PVA/SA/Ag nanocomposites [27].

Antibacterial nanofiber mats have been prepared by mixing the biocompatible poly(ethylene oxide) (PEO), gelatin, and nanometer Ag colloid with the electrospinning solution of sodium alginate [28]. In this work, smooth fibers with diameters of around 300 nm were obtained from 4.0% solutions of varied alginate/PEO/gelatin proportion. The wetability of the prepared mats was decreased by crosslinking the mats with glutaraldehyde/acetone and aqueous calcium chloride/ethanol solutions [28].

2.2 Ag–Cellulose Acetate Nanofibers

Electrospun Ag-loaded cellulose acetate nanofibers were prepared from cellulose acetate solutions with 0.5 wt% of $AgNO_3$ in presence of UV light at 245 nm. During the exposure to UV light, Ag nanoparticles were predominantly generated on the surface of the cellulose acetate nanofibers [25]. The number and size of the Ag nanoparticles were continuously increased up to 240 min. The Ag^+ ions and Ag clusters diffused and aggregated on the surface of the cellulose acetate nanofibers during the UV irradiation. Recently, a facile method was developed for loading a large amount of Ag nanoparticles into a biodegradable and biocompatible cellulose acetate nanofibrillar aerogel in a controlled manner [29]. In this work, the microsized cellulose acetate fibrils were first separated into nanosized fibrils by salt-assisted chemical treatment in water–acetone co-solvent to give a nanofibrillar structure. Using the high electron-rich oxygen density in the cellulose acetate macromolecules and the large surface area of the cellulose acetate nanoporous structure as an effective nanoreactor, the in-situ direct metallization technique was successfully used to synthesize Ag nanoparticles with an average diameter of 2.8 nm and a loading content of up to 6.98 wt%, which is difficult to achieve by other methods. This novel procedure provides a facile and economic way to manufacture Ag nanoparticles supported on a porous membrane for various biomedical applications [29]. Ag nanoparticles incorporated into bacterial cellulose nanofibers have also been reported in the literature for wound-dressing applications [30].

2.3 Ag–Gelatin Nanofibers

Gelatin is a novel promising biomaterial due to its excellent biocompatibility and biodegradability [31]. Ag nanoparticles first appeared in a $AgNO_3$-containing gelatin solution after it had been aged for at least 12 h. Electrospinning of both the base and the 12 h-aged $AgNO_3$-containing gelatin solutions resulted in the formation of smooth fibers, with average diameters of ~230 and 280 nm, respectively. The average diameter of the as-formed Ag nanoparticles in the electrospun fibers from the 12 h-aged $AgNO_3$-containing gelatin solution was 13 nm. The Ag-containing gelatin fiber mats were further crosslinked with moist glutaraldehyde vapor to improve their stability in an aqueous medium. Both the weight loss and the water retention of the Ag-containing gelatin fiber mats in acetate buffer (pH 5.5), distilled water (pH 6.9) or simulated body fluid (SBF; pH 7.4) decreased with increasing crosslinking time. The release of Ag ions from both the 1 h- and 3 h-crosslinked Ag-containing gelatin fiber mats by the total immersion method in acetate buffer and distilled water (both at a skin temperature of 32°C) occurred rapidly during the first 60 min, and increased gradually afterwards; whereas that in SBF (at the physiological temperature of 37°C) occurred more gradually over the testing period.

In order to improve the antimicrobial activity of gelatin, gelatin nanofibers containing Ag nanoparticles were prepared by electrospinning a gelatin/$AgNO_3$/formic acid system, followed by UV irradiation [32]. It was observed that the Ag nanoparticles, which presented a quasi-spherical shape and 9–20 nm average diameter, were generated on the surface of the gelatin nanofibers. The size of the Ag particles can be adjusted by changing the content of $AgNO_3$. With an increased amount of $AgNO_3$, the average fiber diameter decreased [32]. The gelatin nanofibers functionalized with Ag nanoparticles were prepared by electrospinning using solutions of gelatin mixed with $AgNO_3$ [33]. The common solvent used for gelatin and $AgNO_3$ was selected as a mixture of formic acid and acetic acid in the ratio 4:1 (v/v). In this system, formic acid was used as a solvent of gelatin, but also as reducing agent for Ag ions in solution. Ag nanoparticles were stabilized through a mechanism that involves an interaction with the oxygen atoms of gelatin carbonyl groups [33]. The results of investigations by transmission electron microscopy (TEM) and X-ray diffraction (XRD) confirmed the presence of Ag nanoparticles with diameters of less than 20 nm, which were uniformly distributed over the surface of smooth nanofibers with an average diameter of 70 nm.

A new method for making chitosan/gelatin nanofibers containing Ag nanoparticles was developed by Zhuang et al. [34]. In this work, Ag nanoparticles with sizes ranging from 1 nm to 5 nm were synthesized at room temperature using microcrystalline chitosan as the reducing agent and stabilizer. The Ag nanoparticle/chitosan composites were then dissolved in acetic acid solution containing gelatin and the prepared solution then electrospun into chitosan/gelatin nanofibers containing Ag nanoparticles. The structure of the resultant nanofibers was examined with SEM, TEM, and XPS. The results indicated that the nanofibers, having a diameter range of 220–400 nm, were apparently smooth and that the Ag nanoparticles, with size distribution of 2–10 nm, were successfully incorporated into the electrospun nanofibers [34].

2.4 Ag–Nylon 6 Nanofibers

Nylon 6 nanofibers containing Ag nanoparticles were prepared by electrospinning [35]. Assembly of Ag nanoparticles onto nylon 6 nanofibers by controlling the interfacial hydrogen-bonding interactions has also been demonstrated [36]. Ag nanoparticles were synthesized in aqueous media using sodium citrate as a stabilizer. Nylon 6 nanofiber mats, produced by electrospinning, were immersed into pH-adjusted solutions of metal nanoparticles. The key factor determining the assembly phenomena was identified as the hydrogen-bonding interactions between the amide groups in the nylon 6 backbone and the carboxylic acid groups capped on the surface of the metal nanoparticles. The assembly was strongly dependent on the pH of the media, which affected the protonation of the carboxylate ions on the metal nanoparticles, hence influencing the hydrogen-bonding interactions between nanofibers and nanoparticles. High surface coverage of the nanofibers by the Ag

nanoparticles was found at pH 3–6, whereas only a few Ag nanoparticles were found on the surface of the fibers when the pH was greater than 7 [36].

Ag nanoparticles were also synthesized using $AgNO_3$ as the starting precursor, ethylene glycol as solvent, and poly(*N*-vinylpyrrolidone) (PVP) introduced as a capping agent [37]. These Ag nanoparticles were reinforced in the nylon matrix by electrospinning of nylon-6/Ag solution in 2,2,2-trifluoroethanol. The effects of solution concentration and relative humidity on the resultant fibrous membranes were studied. It was observed that concentration and relative humidity could be used to modulate the fiber diameter. The composite membranes showed higher strength (~two- to threefold increase in strength) compare to as-synthesized nylon fibers [37].

2.5 Ag–Poly(acrylonitrile) Nanofibers

Ag nanoparticles dispersed in poly(acrylonitrile) (PAN) nanofibers were prepared by electrospinning [24]. UV spectra and TEM showed that the average diameter of Ag nanoparticles was 10 nm and that these particles were dispersed homogeneously in PAN nanofibers. Surface enhanced Raman scattering (SERS) indicated that the structure of PAN was changed after Ag nanoparticles were dispersed in PAN. A new route based on electrospinning was designed for the preparation of AgCl/PAN composite nanofibers [38]. In this study, the AgCl nanoparticles were found to be uniform in size and uniformly dispersed on the surface of the composite nanofibers (Fig. 1). In another study, $AgNO_3$/PAN hybrid nanofibers were prepared by using the electrospinning technique. These hybrid nanofibers were then treated with pyrrole in boiling toluene medium to obtain Ag/polypyrrole/PAN composite fibrous mats [39]. The Ag/polypyrrole composite dispersed in the fibrous mats exhibited a core–shell structure, and the conductivity of the optimum Ag/polypyrrole/PAN composite fibrous mats was found to be relatively high.

Fibrous membranes with antibacterial activity were prepared from PAN (10% w/v) solutions containing $AgNO_3$ (0.5–2.5% by weight of PAN) by electrospinning [40]. In this study, *N*,*N*-dimethylformamide (DMF) was used as both the solvent for PAN and reducing agent for Ag^+ ions. The enhancement in the reduction process was achieved with UV irradiation, which resulted in the formation of larger Ag nanoparticles in areas adjacent to and at the surface of the fibers. Without the UV treatment, the size of the Ag nanoparticles was smaller than 5 nm on average. With 10 min of UV treatment, the size of the particles increased and there was an increase in the initial $AgNO_3$ concentration in the solution to 5.3–7.8 nm on average. Without or with the UV treatment, the diameters of the obtained PAN/Ag nanoparticle composite fibers decreased with an increase in the initial $AgNO_3$ concentration in the solution, with the diameters of the obtained composite fibers that had been subjected to UV irradiation exhibiting lower values. Both the cumulative amounts of the released Ag and the bactericidal activities of the PAN/Ag nanoparticle composite fibrous materials against two commonly studied bacteria

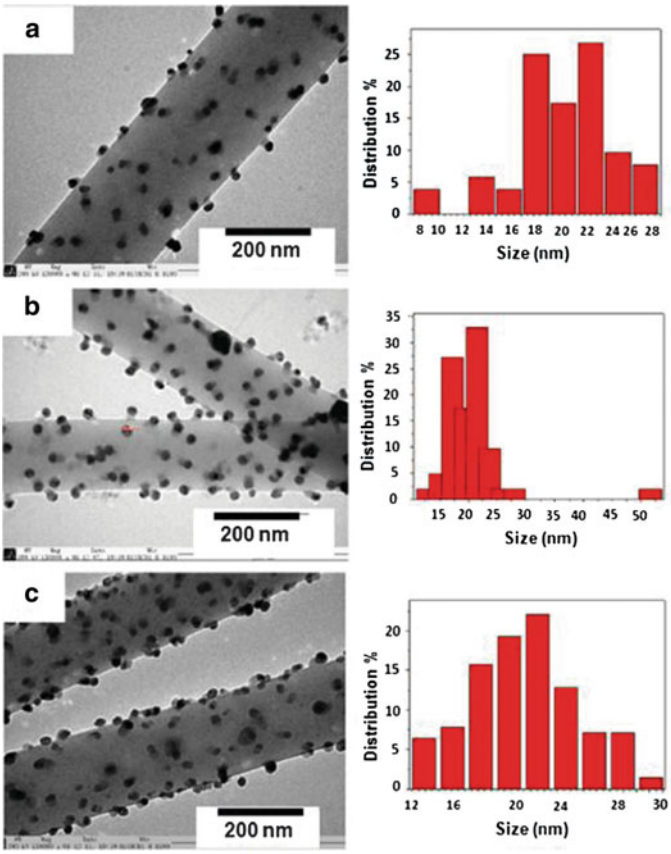

Fig. 1 TEM images and size distributions of AgCl nanoparticles in electrospun PAN/AgCl composite fibers. Molar ratio of AgCl to acrylonitrile was (**a**) 1:20, (**b**) 1:10, and (**c**) 1:5

(i.e., Gram-positive *S. aureus* and Gram-negative *Escherichia coli*) increased with increases in both the initial $AgNO_3$ concentration in the solutions and the UV irradiation time interval [40].

2.6 Ag–Poly(ε-caprolactone) Nanofibers

Antimicrobial nanofibers of poly(ε-caprolactone) (PCL) were prepared by electrospinning of a PCL solution with small amounts of Ag-loaded zirconium phosphate (AgZ) nanoparticles for potential use in biomedical applications [41]. SEM, EDX, and XRD investigations of the electrospun fibers confirmed that Ag-containing nanoparticles were incorporated and well-dispersed in smooth PCL nanofibers [41]. In another study, PCL-based polyurethane (PCL-PU) nanofibers containing Ag nanoparticles for use in antimicrobial nanofilter applications were prepared by

electrospinning 8 wt% PCL-PU solutions containing different amounts of $AgNO_3$ in a mixed solvent consisting of DMF and THF (7:3 w/w) [42]. The average diameter of the pure PCL-PU nanofibers was 560 nm and decreased with increasing concentration of $AgNO_3$. The PCL-PU nanofiber mats electrospun with $AgNO_3$ exhibited higher tensile strength, tensile modulus, and lower elongation than the pure PCL-PU nanofiber mats. The average size and number of the Ag nanoparticles in the PCL-PU nanofibers were considerably increased after being annealed at 100°C for 24 h. Particles were all spherical and evenly distributed in the PCL-PU nanofibers, indicating that the PCL-PU chains stabilized the Ag nanoparticles well [42].

Recently, PCL containing bovine bone hydroxyapatite (HA) and hydroxyapatite/Ag (HA-Ag) composite nanofibers were prepared via an electrospinning process [43]. The morphology, structure and thermal properties of the PCL, PCL/HA, and PCL/HA-Ag composite nanofibers before and after immersion in SBF were characterized. SEM images revealed that the nanofibers were well-oriented and incorporated the HA-Ag nanoparticles well. Mechanical study revealed that the yield stress of PCL/HA-Ag composite nanofibers showed a higher value than that of PCL/HA composite, possibly due to the addition of metallic Ag nanoparticles [43].

2.7 Ag–Poly(ethylene oxide) Nanofibers

Biodegradable poly(ethylene oxide) (PEO) nanofibers containing Ag nanoparticles were prepared by electrospinning [44]. TEM showed that the Ag nanoparticles were dispersed in PEO nanofibers without aggregation. In another study, PEO solutions containing various amounts of poly(ethylene glycol) (PEG) and Ag nanoparticles were prepared [45]. The occurrence of Ag nanoparticles was by a direct reduction of Ag^+ ions from the addition of $AgNO_3$ in the PEO/PEG solutions. The average diameter of the Ag nanoparticles was found to increase with increasing PEG molar mass and with decreasing PEG concentration. The average diameters of the as-spun fibers were generally found to increase with increasing concentration and molar mass of PEG and increasing amount of added $AgNO_3$. The amount of elemental Ag observed was found to increase with increasing PEG content and increasing amount of $AgNO_3$ added, and the amount of elemental Ag was also found to be greater when PEG with lower molar mass was used as the reducing agent [45].

A facile approach to the synthesis and incorporation of Ag nanoparticles into electrospun polymer nanofibers has been reported, wherein the electrospinning polymer acts as both a reducing agent for the metal salt precursor, as well as a protecting and templating agent for the ensuing nanoparticles [46]. This one-step process at ambient conditions and free of organic solvents was demonstrated using a system comprising $AgNO_3$ and PEO (600, 1,000, and 2,000 kDa). The PEO transforms Ag^+ into Ag nanoparticles, a phenomenon that has not been previously possible at PEO molecular weights less than 20 kDa without the addition of a separate reducing agent and stabilizer or the application of heat. The Ag

nanoparticles reduce fiber diameter and enhance fiber quality due to increased electrical conductivity. Interestingly, several of the nanofibers exhibit Ag nanoparticle-localized nanochain formation and protrusion from the nanofiber surface that can be attributed to the combined effect of applied electrical field on the polymer and the differences between the electrical conductivity and polarizability of the polymer and Ag nanoparticles [46].

2.8 Ag–Poly(methyl methacrylate) Nanofibers

Poly(methyl methacrylate) (PMMA) nanofibers containing Ag nanoparticles were synthesized by radical-mediated dispersion polymerization. UV-visible spectroscopic analysis indicated that the Ag nanoparticles were continually released from the polymer nanofiber in aqueous solution [47]. In another study, the electrospinning conditions for PMMA were studied [48]. In this work, conductivity of the polymer solution containing Ag nanoparticles and its effect on fiber diameter were also studied. As the results showed, the maximum concentration for the electrospinning of PMMA was found to be 18 wt%, and the ratio of DMF to THF was 7:3 (v/v). The diameter of nanofibers obtained was found to be 100–400 nm when the PMMA solution contained 1,000 ppm of Ag nanoparticles [48].

The first use of electrospun nanofibrous materials as highly responsive fluorescence quenching-based optical Ag sensors was reported by Kacmaz and coworkers [49]. PMMA and ethyl cellulose were used as polymeric support materials. Sensors were based on the change in the fluorescence signal intensity of methoxy azomethine ionophore. The preliminary results of Stern–Volmer analysis showed that the sensitivities of electrospun nanofibrous membranes to detect Ag ions were ten- to 100-fold higher than those of the thin-film-based sensors. The extraordinary sensitivities could be attributed to the high surface area of the nanofibrous membrane structures. It was found that the stability of the sensing agent in the employed matrix materials was excellent, and when stored in the ambient air there was no significant drift in signal intensity after 5 months [49].

2.9 Ag–Poly(L-lactide) Nanofibers

Biodegradable poly(L-lactide) (PLA) nanofibers containing Ag nanoparticles were prepared via electrospinning [50]. The prepared composite nanofibers were characterized by SEM, TEM, and XRD. The fiber diameter was found to increase with increasing amount of $AgNO_3$ added. The diameter of the Ag nanoparticles was found to be about 30 nm in the fibers. In this study, the release of Ag ions from the Ag-containing PLA fibers and their antibacterial activities were also investigated. In another work using a similar approach, biodegradable poly(lactide-*co*-glycolide) (PLGA) antimicrobial nanofibers containing Ag nanoparticles were prepared by electrospinning for biomedical applications [51].

2.10 Ag–Poly(pyrrole) Nanofibers

Ag–polypyrrole composite nanofibers were synthesized in one step by the redox reaction between $AgNO_3$ and pyrrole monomer in dilute mixed cetyltrimethylammonium bromide (CTAB)/sodium dodecyl sulfate (SDS) aqueous solution [52]. The composite nanofibers showed uniform nanofiber morphology. FT-IR, Raman and XRD spectra confirmed the interaction between poly(pyrrole) nanofibers and Ag nanoparticles. The co-guidance of the mixed surfactants and the interaction between $AgNO_3$ and the surfactants were found to be responsible for the formation of the nanofibers; however, excess usage of SDS resulted in the generation of globular particles. The interaction between $AgNO_3$ and the surfactants was found to be the reason for the ordered growth of the poly(pyrrole) [52].

2.11 Ag–Poly(urethane) Nanofibers

Polyurethane (PU) nanofibers containing Ag nanoparticles were synthesized by electrospinning [53]. A simple method that did not depending on additional foreign chemicals was used to self-synthesize the Ag nanoparticles in/on PU nanofibers. The synthesis of Ag nanoparticles was carried out by exploiting the reduction ability of DMF, which is used mainly to decompose $AgNO_3$ to Ag nanoparticles. Typically, a sol–gel consisting of $AgNO_3$/PU was electrospun and aged for 1 week. Ag nanoparticles were created in/on PU nanofibers. SEM confirmed the well-oriented nanofibers and good dispersion of pure Ag nanoparticles. TEM indicated that the Ag nanoparticles were 5–20 nm in diameter. XRD demonstrated the good crystalline features of Ag metal. The mechanical properties of the nanofiber mats showed improvement with increasing Ag nanoparticle content. Similarly, polyurethane cationomers (PUCs) containing different amounts of quaternary ammonium groups were synthesized and successfully electrospun into non-woven nanofiber mats for use in antimicrobial nanofilter applications [54]. In a similar approach, Ag nanoparticles were incorporated into electrospun PU nanofibers to enhance the antibacterial and wound-healing properties [55]. In this study, the electrospinning parameters were optimized for PU with and without Ag nanoparticles.

2.12 Ag–Poly(vinyl alcohol) Nanofibers

Ag nanoparticles embedded in poly(vinyl alcohol) (PVA)–PMMA nanofibers were fabricated by one-step radical-mediated dispersion polymerization using 2,2′-azobis(isobutyronitrile) (AIBN) [56]. The AIBN radical acted as a reductant and initiator during the polymerization process, and PVA played a role both in protecting the Ag nanoparticles from aggregation and in producing the polymer

nanofibers. This novel approach could be expanded to the synthesis of other metal nanoparticles and diverse polymer nanofibers [56].

In another study, two methods for the facile and controlled preparation of PVA nanofibers containing Ag nanoparticles were investigated for use in antimicrobial applications [57]. In the first method, PVA nanofibers containing Ag nanoparticles were electrospun from PVA/$AgNO_3$ aqueous solutions after first refluxing. The Ag nanoparticles in the PVA/$AgNO_3$ aqueous solutions were generated after refluxing. It was found that the Ag nanoparticles were also spontaneously generated during the electrospinning process. In the second method, Ag nanoparticles were generated by annealing the PVA nanofibers electrospun from PVA/$AgNO_3$ aqueous solutions. Residual Ag^+ ions and the Ag nanoparticles generated during the electrospinning process in the PVA nanofibers were diffused and aggregated into larger Ag nanoparticles during the annealing process. All of the Ag nanoparticles were spherical and evenly distributed in the PVA nanofibers prepared by the both methods [57].

PVA nanofibers containing Ag nanoparticles have been produced by electrospinning a sol–gel consisting of PVA and $AgNO_3$ [58]. In this work, the dried nanofiber mats were calcined at 850°C in an argon atmosphere. The produced nanofibers had distinct plasmon resonance compared with the reported Ag nanoparticles. In contrast to the shape of Ag nanoparticles, the nanofibers had a blue-shifted plasmon resonance at 330 nm. Moreover, a study of optical properties indicated that the synthesized nanofibers have two band gap energies of 0.75 and 2.34 eV. An investigation of the electrical conductivity behavior of the obtained nanofibers showed thermal hystersis. These privileged physical features greatly widen the applications of the prepared nanofibers in various fields [58]. PVA/$AgNO_3$ composite nanofibers were also reported [59, 60].

A heat-treated PVA nanofibrous matrix containing Ag nanoparticles was prepared by electrospinning an aqueous 10 wt% PVA solution and followed by heat treatment at 150°C for 10 min [61]. The average diameter of the as-spun and heat-treated PVA nanofibers was 330 nm. The heat-treated PVA nanofibrous matrix was irradiated with UV light to transform the Ag ions in the nanofibrous matrix into Ag nanoparticles. The in vitro cytotoxicity of the Ag ions and/or nanoparticles on normal human epidermal keratinocytes (NHEK) and fibroblasts (NHEF) cultures was examined [61].

*2.13 Ag–Poly(*N*-vinyl pyrrolidone) Nanofibers*

Poly(*N*-vinylpyrrolidone) (PVP) was used in two methods for preparing polymer nanofibers containing Ag nanoparticles [62]. The first method involved electrospinning the PVP nanofibers containing Ag nanoparticles directly from the PVP solutions containing the Ag nanoparticles. DMF was used as a solvent for the PVP as well as a reducing agent for the Ag^+ ions in the PVP solutions. In the second method, PVA aqueous solutions were electrospun with 5 wt% of the PVP

containing Ag nanoparticles. PVP containing Ag nanoparticles could be used to introduce Ag nanoparticles to other polymer nanofibers that are miscible with PVP [62]. Heat treatment of various compositions of $AgNO_3$-doped PVP composite nanofibers fabricated by electrospinning produced two kinds of Ag species: (1) Ag nanoparticles dispersed in PVP nanofibers, when the loading of $AgNO_3$ was 5 wt%, and (2) a net-like Ag nanofiber film, when the loading of $AgNO_3$ was five times greater than that of PVP in the composite nanofibers [63].

A new synthetic route was adapted to prepare hybrid nanofibers using AgBr nanoparticles and PVP [64]. In this method, first $AgNO_3$ was added to the PVP solution and then bromide ions reacted with Ag ions to form AgBr nanoparticles by the sol–gel technique. Finally, PVP nanofibers containing AgBr nanoparticles were formed by electrospinning the composite solution [64]. Incorporation of AgCl nanoparticles into PVP nanofibers has been successfully achieved using electrospinning technology [65]. The Ag ions interacted with the carbonyl groups in the PVP molecules. The formation of AgCl nanoparticles inside the PVP was carried out via the reaction of Ag ions and HCl. TEM proved that most of the AgCl nanoparticles were uniformly dispersed in the PVP fibers, as shown in Fig. 2 [65].

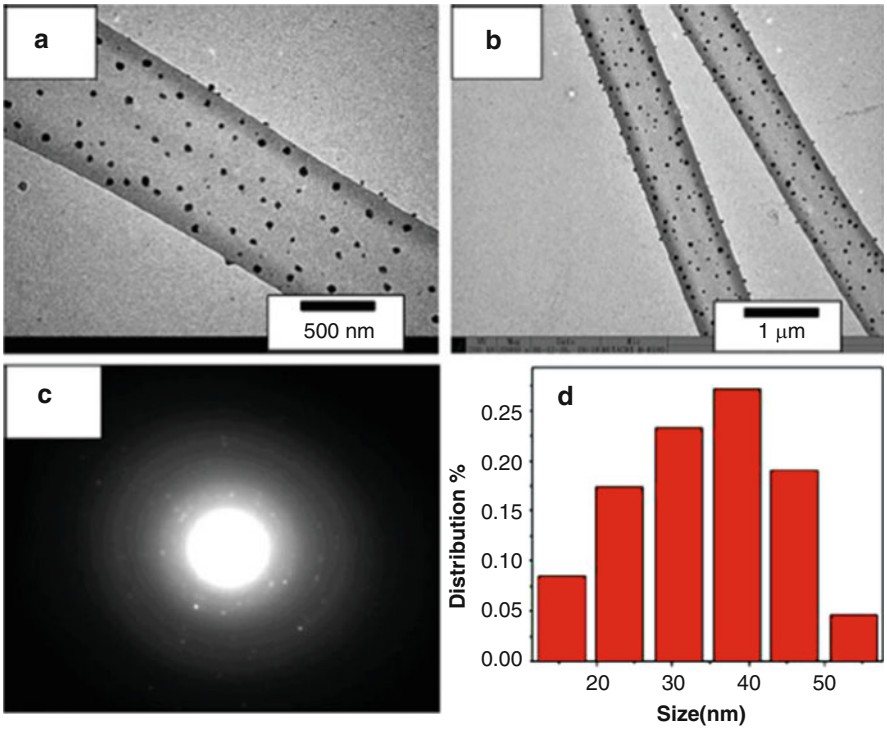

Fig. 2 (**a**, **b**) TEM images of AgCl/PVP nanocomposite fibers. (**c**) Electron diffraction patterns of composite nanofibers. (**d**) Size distributions of AgCl nanoparticles in composite nanofibers

Oligoaniline derivative/PVP nanofibers containing Ag nanoparticles have been prepared by electrospinning [66]. Here, Ag nanoparticles were prepared through reduction of Ag^+ by an oligoaniline derivative. In another study, a new series of PVP and AgCl nanoparticle composite fibers were synthesized by electrospinning and gel–sol technology [67]. In this work, the sol–gel process was used to prepare AgCl nanoparticles in the PVP solution, and then this solution was electrospun to obtain AgCl/PVP composite nanofibers.

3 Applications of Ag-Loaded Polymeric Nanofibers

3.1 Catalysts

For metal nanocomposites to perform as good catalysts, they should possess the following three important characteristics: (1) the substrate should have high surface area [68, 69] (2) the nanoparticles present inside the substrate should be easily accessible to various chemical reagents [69], and (3) the size and distribution of the nanoparticles in the substrate should be uniform. The substrates used for metal particle encapsulation include metal oxides [69], organically modified silicates [70], polymers shaped as thin films [71, 72], spheres [73, 74], fibers [75, 76], dendrimers [77] and so forth. Among these substrates, fibrous materials show unique properties suitable for use as catalysts. Some of the main benefits of fibrous catalysts include flexibility of form, low resistance to flow of gas and liquids through a bundle of fibers, high surface area, safer operation, easy scale-up, and reusability [78]. Some specific examples of fibrous material include metal wires in the form of gauzes [79], fiberglass materials [80], and carbon fibers [81]. These materials act as excellent carriers for supporting catalytic particles.

Electrospinning is a widely employed method that has been used in recent years to produce polymer nanofiber mats with high surface area, which could be used as metal-supporting substrates for catalytic applications [75]. Recently, nanoribbons with catalytic activity have been successfully synthesized via electrospinning of a sol composed of tetraethyl orthosilicate, PVP, Pluronic P123, and $AgNO_3$. The fibers were thermally treated to remove PVP and P123 (pyrolysis), and $AgNO_3$ was reduced to create Ag nanoparticles [82]. The prepared silica fibers had an average diameter of 750–800 nm and worm-like mesoporous structure. The composite nanoribbons presented a width of approximately 10 μm. It was found that varying the concentration of $AgNO_3$ and the thermal treatment conditions can readily control the content and size of Ag nanoparticles encapsulated in ribbons. The Ag nanoparticles in the ribbons exhibited good catalytic activity on the reduction of methylene blue dye with $NaBH_4$ as a reducing agent, which was given by the ultrahigh surface area of the ribbons and their very small thickness. The above research on composite nanofibers is a promising step in the preparation of a novel catalyst with relatively simple production and good catalytic efficiency. In another

study, the mechanism of formation of Ag-loaded PVP nanofibers was discussed on the basis of the redox reaction between $AgNO_3$ and PVP [63]. During heat treatment, $AgNO_3$ oxidizes the organic groups of PVP, while $AgNO_3$ is itself simultaneously reduced to metallic Ag nanoparticles, which are dispersed throughout the body of the PVP nanofiber. When the ratio of $AgNO_3$ to PVP was high, the nanoparticles obtained were sufficiently abundant in the nanofiber. The Ag-loaded PVP nanofiber films showed a net-like structure and good electrical conductivity. We expect that this facile and effective method for the preparation of Ag nanoparticle-doped PVP nanofibers will find applications in the areas of catalysis and electronics [63].

3.2 Filtration

Membranes have been widely used in water treatment to remove contaminants such as particles, hazardous chemicals, and organisms from the water. Although electrospun non-woven membranes have already been used commercially for a few decades as air filtration membranes, it is only recently that they have been investigated for use in water treatment [8]. Concerns on the ability of nanofibrous membranes to withstand the high pressures commonly used in water treatment may have contributed to the lack of research in this area until now. This concern has been alleviated recently when electrospun membranes were successfully shown to be effective as microfilters. There are also many studies on incorporating antimicrobial properties into membranes. This might be able to reduce the formation of biofilm on the surface of membranes, which is a common source of membrane fouling. Ag nanoparticles are the most commonly used antimicrobial agent to be attached or embedded in electrospun nanofibers [25, 32, 50, 51, 54, 56, 83–85]. Leaching of Ag(I)–imidazole cyclophane gem–diol complexes encapsulated in electrospun Tecophilic nanofibers have been shown to inhibit bacterial and fungal growth [86]. However, care must be taken to ensure that the antimicrobial additives do not unintentionally leach out of the nanofiber and pollute the water instead. Advances in other complimentary areas such as detection of membrane fouling and fiber organization could lead to an effective multi-tiered composite water filtration membrane. PUCs containing different amounts of quaternary ammonium groups were synthesized and successfully electrospun into non-woven nanofiber mats for use in antimicrobial nanofilter applications [54]. The PUCs showed very strong antimicrobial activities against *S. aureus* and *E. coli*.

3.3 Tissue Engineering

Functional nanofibrous scaffolds produced by electrospinning have great potential in many biomedical applications, especially tissue engineering and regenerative

medicine. Many kinds of polymers such as PLA, PLGA, PCL, and natural biomaterials like collagen, elastin, silk fibroin etc are often used for preparing 3D scaffolds. One of the major hurdles is infection upon implantation, which can be potentially avoided by incorporating an antibacterial function with low cytotoxicity. Ag nanoparticles, due to their high antibacterial property coupled with low cytotoxicity are promising candidates to impart this functionality. Various research groups are investigating the feasibility of incorporating Ag nanoparticles within the 3D composite scaffolds to protect tissue engineering constructs from infection. Bioactivity studies of electrospun PCL/HA and PCL/HA-Ag composite nanofibers were carried out by Nirmala et al. [43] for tissue engineering applications. The SBF incubation test confirmed that the fast formation of apatite-like materials suggests in vitro bioactive behavior of the nanofibers. This study demonstrated that electrospun PCL/HA and PCL/HA-Ag composite nanofibers activate bioactivity and support growth of apatite-like materials. These results demonstrated that PCL/HA-Ag composite nanofibers can be used for tissue engineering applications. In an another work, the PVA nanofibrous matrix containing Ag showed slightly higher level of attachment and spreading in the early stage culture (1 h) than the PVA nanofibers without Ag (control) [61]. However, compared with the PVA nanofibers without Ag, the heat-treated and UV-irradiated PVA nanofibers, containing mainly Ag ions and nanoparticles, respectively, showed reduced cell attachment and spreading. This shows that both Ag ions and Ag nanoparticles are cytotoxic to normal human epidermal keratinocytes (NHEK) and normal human epidermal fibroblasts (NHEF). There was no significant difference in cytotoxicity to NHEK and NHEF between Ag ions and Ag nanoparticles. NHEF appeared to be more sensitive to Ag ions or particles than NHEK. In addition, the residual nitrate ions (NO_3^-) in the PVA nanofibers had an adverse effect on the culture of both cells [61]. These results indicated that Ag nanoparticles incorporated into nanofibers have applications in tissue engineering.

3.4 Wound Dressings

Electrospinning could generate scaffold with more homogeneity, besides meeting other requirements for use as a wound-dressing material such as oxygen permeation and protection of wounds from infection and dehydration. As we know, Ag has long been recognized as a broad-spectrum and highly effective antimicrobial agent for treating wounds and burns. Ag ion works by denaturing the proteins and nucleic acids of the bacteria by binding to their negatively charged components. In addition, Ag acts in generating oxygen, which in turn destroys the cell wall membranes of bacteria [41]. Metallic Ag is used commercially in wound dressings such as Acticoat (Smith & Nephew Health), in which Ag is applied to the polymer mesh by a vapor deposition process. It shows an excellent antibacterial activity of above 99.9%. However, there are some disadvantages; for instance, the metallic Ag of the wound dressing leads to gray-blue discoloration on the skin and moisture supplies

are regularly necessary to dissolve the metallic Ag. The manufacturing cost is also relatively high. To avoid these problems, non-woven wound-dressing material was recently developed by electrospinning of PVA/$AgNO_3$ aqueous solution [60]. These electrospun PVA/$AgNO_3$ fiber webs were found to be promising materials for wound-dressing applications.

Duan et al. [41] have produced antimicrobial nanofibers of PCL by electrospinning of a PCL solution with small amounts of AgZr nanoparticles for potential use in wound-dressing applications. The results of the antimicrobial tests showed that these fibers maintained the strong killing abilities of Ag in the AgZr nanoparticles against the tested bacteria strains (Gram-positive *S. aureus* (ATCC 6538) and Gram-negative *E. coli* (ATCC 25922). Discoloration has not been observed in the nanofibers. To test the biocompatibility of nanofibers as potential wound dressings, primary human dermal fibroblasts (HDFs) were cultured on the nanofibrous mats. The cultured cells were evaluated in terms of cell proliferation and morphology. The results indicated that the cells attached and proliferated as continuous layers on the AgZr-containing nanofibers and maintained the healthy morphology of HDFs (Fig. 3).

The Ag nanoparticles containing bacterial cellulose nanofibers exhibited strong antimicrobial activity, indicating wound-dressing applications [25]. Gelatin fiber mats with antibacterial activity against some common bacteria found on burn

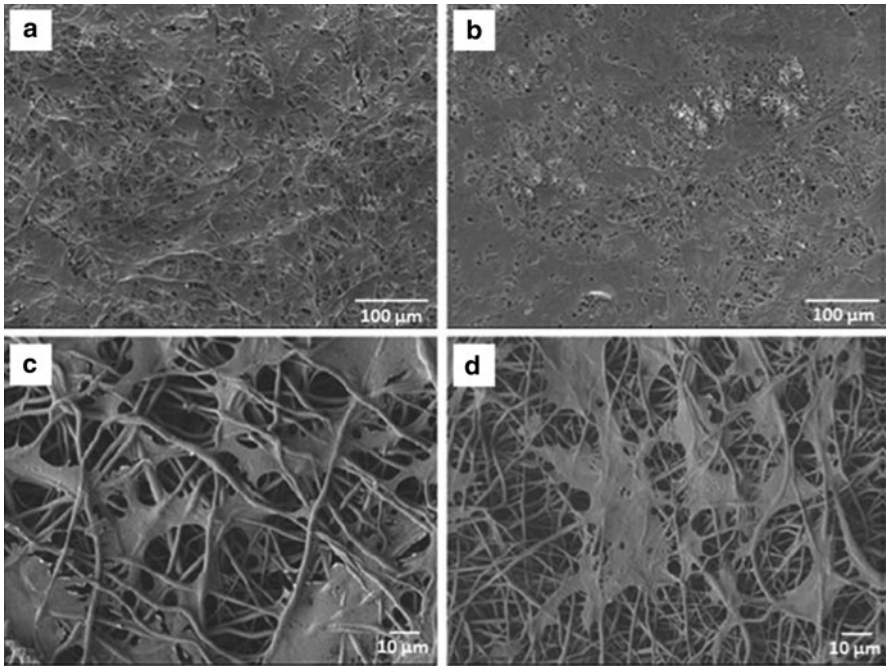

Fig. 3 SEM photographs of HDFs on the neat electrospun PCL fibers (**a**, **c**) and the nanoAgZ-containing composite fibers (**b**, **d**)

wounds were prepared from a gelatin solution containing 2.5 wt% $AgNO_3$ [31]. The antibacterial activity of these materials, regardless of the sample types, was greatest against *Pseudomonas aeroginosa*, followed by *S. aureus*, *E. coli*, and methicillin-resistant *S. aureus* [31]. Similarly, the Ag-loaded gelatin nanofibers were found to have good antibacterial activity [32, 33]. The gelatin nanofibers with incorporated Ag nanoparticles exhibited strong antimicrobial activity, which suggested that the gelatin nanofibers containing Ag nanoparticles could effectively suppress bacterial proliferation and protect wounds from bacterial invasion.

The antibacterial activities of the Ag-loaded nylon 6 nanofiber mats were investigated in a broth dilution test against *S. aureus* (Gram-positive) and *Klebsiella pneumoniae* (Gram-negative) bacteria. It was revealed that nylon 6 fibers with Ag nanoparticles possessed excellent antibacterial properties and an inhibitory effect on the growth of *S. aureus*, *E. coli*, and *K. pneumoniae*. By contrast, nylon 6 fibers without Ag nanoparticles did not show any such antibacterial activity. Therefore, electrospun nylon 6/Ag nanocomposites could be used in wound dressings, or in anti-adhesion membranes [35, 36]. The Ag nanoparticles embedded in PEO nanofibers showed better antibacterial activities against *S. aureus*, *E. coli* and *K. pneumoniae* [45, 48]. Therefore, it is expected that the Ag nanoparticle/PEO nanocomposites can be used for practical applications as a wound-dressing material [45, 48].

The antibacterial properties of Ag/PMMA nanofibers against both Gram-negative (*E. coli*) and Gram-positive (*S. aureus*) bacteria were evaluated using minimum inhibitory concentration (MIC), the modified Kirby–Bauer method, and a kinetic test. The MIC test demonstrated that the Ag/PMMA nanofibers had enhanced antimicrobial efficacy compared to that of silver sulfadiazine and $AgNO_3$ at the same Ag concentration [47, 48]. PLA/Ag composite nanofibers showed antibacterial activities of 98.5% and 94.2% against *S. aureus* (Fig. 4) and *E. coli*, respectively, because of the presence of the Ag nanoparticles [50]. The antibacterial efficacy of the composites mats made of Ag nanoparticles and PLGA fibers was measured. The antimicroorganization efficacy of Ag nanoparticles along with the biodegradability of the PLGA fibers can be combined in practical medical applications [51].

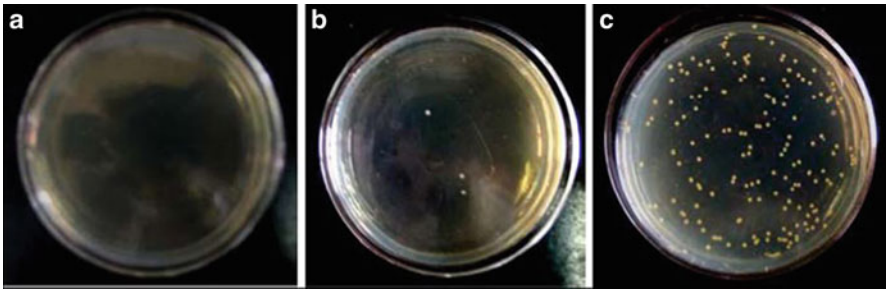

Fig. 4 Antibacterial activity against *S. aureus* after 12 h of incubation with (a) $AgNO_3$ (b) Ag/PLA fibers (the $AgNO_3$ content in the spinning solution with respect to PLA was 32 wt%); (**c**) *S. aureus* was blank control

Ag/polyrhodanine nanofibers were found to have excellent antimicrobial activity against Gram-negative *E. coli*, Grain-positive *S. aureus*, and *Candida albicans*. The modified Kirby–Bauer test demonstrated that Ag/polyrhodanine nanofibers had better antimicrobial efficacy than Ag [47]. Similarly, the PVA nanofibers containing Ag nanoparticles showed very strong antimicrobial activity [59]. Two model organisms, *E. coli* and *S. typhimurium*, were used to check the antimicrobial influence of PU/Ag composite nanofiber mats [53]. Subsequently, antimicrobial tests indicated that the prepared nanofibers had a high bactericidal effect. Accordingly, these results highlight the potential use of these nanofiber mats as antimicrobial agents [53].

4 Conclusion and Future Prospects

In summary, different types of Ag nanoparticles incorporated into polymeric nanofibers have been extensively studied for biomedical applications. The Ag-incorporated polymeric nanofibers showed good catalytic and electric properties, so they can be used in chemical and electronic industries. The antibacterial and antifungal properties of Ag-incorporated polymeric nanofibers have been extensively studied for filtration, tissue engineering, and wound-healing applications. Since Ag ions release continuously from Ag-loaded nanofibers, these materials have an improved antimicrobial efficacy during their application as scaffolds in tissue engineering. The burn wounds treated with Ag nanoparticles showed better cosmetic appearance and scarless healing. However, with the advent of Ag nanoparticles and its major use as an antimicrobial agent, many experimental trials are needed to understand the toxicity. In addition, the exact mechanism of interaction of Ag nanoparticles with bacterial cells and how the surface area of nanoparticles influences their killing activity need to be studied. To get a better understanding of the antimicrobial efficiency of Ag dressings, more use of animal models and clinical studies are obligatory.

Acknowledgments One of the authors, R. Jayakumar, is grateful to SERC Division, Department of Science and Technology (DST), India, for providing the fund under the scheme of "Fast Track Scheme for Young Investigators" (Ref. No. SR/FT/CS-005/2008). S.V. Nair is grateful to DST, India, which partially supported this work, under a center grant of the Nanoscience and Nanotechnology Initiative program monitored by C.N.R. Rao. R. Jayakumar is also grateful to the Department of Biotechnology (DBT), Govt. of India for providing research support.

References

1. Reneker DH, Chun I (1996) Nanotechnology 7:216
2. Zong XH, Ran SF, Kim KS, Fang DF, Hsiao BS, Chu B (2003) Biomacromolecules 4:416
3. Wang XY, Drew C, Lee SH, Senecal KJ, Kumar J, Samuelson LA (2002) Nano Lett 2:1273
4. Jiang L, Zhao Y, Zhai J (2004) Angew Chem Int Ed 43:4338

5. Wnek GE, Carr ME, Simpson DG, Bowlin GL (2003) Nano Lett 3:213
6. Shalumon KT, Binulal NS, Selvamurugan N, Nair SV, Menon D, Furuike T, Tamura H, Jayakumar R (2009) Carbohydr Polym 77:863
7. Sanders EH, Kloefkorn R, Bowlin GL, Simpson DG, Wnek GE (2003) Macromolecules 36:3803
8. Jayakumar R, Prabaharan M, Nair SV, Tamura H (2010) Biotech Adv 28:142
9. Gong P, Li H, He X, Wang K, Hu J, Tan W, Zhang S, Yang X (2007) Nanotechnology 18:285604
10. Retchkiman SPS, Canizal G, Becerra HR, Zorrilla C, Liu HB, Ascencio JA (2006) Opt Mater 29:95
11. Gu H, Ho PL, Tong E, Wang L, Xu B (2003) Nano Lett 3:1261
12. Madhumathi K, Sudhessh Kumar PT, Abilash S, Sreeja V, Tamura H, Manzoor K, Nair SV, Jayakumar R (2010) J Mater Sci Mater Med 21:807
13. Sudheesh Kumar PT, Abilash S, Manzoor K, Nair SV, Tamura H, Jayakumar R (2010) Carbohydr Polym 80:761
14. Jayakumar R, Prabaharan M, Sudheesh Kumar PT, Nair SV, Tamura H (2011) Biotechnol Adv 29:322
15. Jansen B, Rinck M, Wolbring P, Strohmeier A, Jahnns T (1994) J Biomater Appl 9:55
16. Feng QL, Wu J, Chen GQ, Cui FZ, Kim TN, Kim JO (2000) J Biomed Mater Res 52:662
17. Kang HY, Jung MJ, Jeong YK (2000) Korean J Biotechnol Bioeng 15:521
18. Klueh U, Wagner V, Kelly S, Johnson A, Bryers JD (2000) J Biomed Mater Res 53:621
19. Clupper DC, Hench LL (2001) J Mater Sci Mater Med 12:917
20. Guggenbichler JP (2003) Mat Wiss Werkstofftech 34:1145
21. Son WK, Youk JH, Lee TS, Park WH (2004) Macromol Rapid Commun 25:1632
22. Sondi I, Salopek SB (2004) J Coll Interface Sci 275:177
23. Yang QB, Li DM, Hong YL, Li ZY, Wang C, Qiu SL, Wei Y (2003) Synth Met 137:973
24. Wang Y, Yang Q, Shan G, Wang C, Du J, Wang S, Li Y, Chen X, Jing X, Wei Y (2005) Mater Lett 59:3046
25. Son WK, Youk JH, Park WH (2006) Carbohydr Polym 65:430
26. Lee HY, Park HK, Lee YM, Kim K, Park SB (2007) Chem Commun 28:2959–2961
27. Lee YJ, Lyoo WS (2009) J Polym Sci Polym Phys 47:1916
28. Gu Z, Han Y, Pan F, Wang X, Weng D, Zhou S (2009) Mat Sci Forum 610:1188
29. Luong ND, Lee Y, Nam JD (2008) Eur Polym J 44:3116
30. Ifuku S, Tsuji M, Morimoto M, Saimoto H, Yano H (2009) Biomacromolecules 10:2714
31. Rujitanaroj P, Pimpha N, Supaphol P (2008) Polymer 49:4723
32. Xu X, Zhou M (2008) Fibre Polym 9:685
33. Tofoleanu F, Balau Mindru T, Brinza F, Sulitanu N, Sandu IG, Raileanu D, Floristean V, Hagiu BA, Ionescu C, Sandu I, Tura V (2008) J Optoelec Adv Mater 10:3512
34. Zhuang X, Cheng B, Kanga W, Xu X (2010) Carbohydr Polym 82:524
35. Park SW, Bae HS, Xing ZC, Kwon OH, Huh MW, Kang IK (2009) J Appl Polym Sci 112:2320
36. Dong H, Wang D, Sun G, Hinestroza JP (2008) Chem Mater 20:6627
37. Francis L, Giunco F, Balakrishnan A, Marsano E (2010) Curr Appl Phys 10:1005
38. Bai J, Li Y, Yang S, Du J, Wang S, Zhang C, Yang O, Chen X (2007) Nanotechnology 18:305601
39. Chen R, Zhao S, Han G, Dong J (2008) Mater Lett 62:4031
40. Rujitanaroj PO, Pimpha N, Suphapol P (2010) J Appl Polym Sci 116:1967
41. Duan YY, Jia J, Wang SH, Yan W, Jin L, Wang ZY (2007) J Appl Polym Sci 106:1208
42. Jeon HJ, Kim JS, Kim TG, Kim JH, Yu WR, Youk JH (2008) Appl Surf Sci 254:5886
43. Nirmala R, Nam KT, Park DK, Woo-ilb B, Navamathavan R, Kim HY (2010) Surf Coat Technol 205:174
44. Kim CN, Xing ZC, Baek YJ, Bae HS, Kang IK (2009) Polymer 33:429
45. Rujitanaroj PO, Pimpha N, Suphapol P (2007) Preparation of ultrafine poly(ethylene oxide)/poly/ethylene glycol) fibers containing silver nanoparticles as antibacterial coating.

In: Proceedings of the 2nd IEEE international conference on nano/micro engineered and molecular systems (IEEE NEMS 2007) Bangkok, Thailand, pp 1065–1070
46. Saquing CD, Manasco JL, Khan AK (2009) Small 5:944
47. Kong H, Jang J (2008) Langmuir 24:2051
48. Kim J, Lee J, Kwon S, Jeong S (2009) J Nanosci Nanotech 9:1098
49. Kacmaz S, Ertekin K, Suslu A, Ozdemir M, Ergun Y, Celik E, Cocen U (2010) Sens Actuators B chem. 153:205
50. Xu X, Yang Q, Wang Y, Yu H, Chen X, Jing X (2006) Eur Polym J 42:2081
51. Xu X, Yang O, Bai J, Lu T, Li Y, Jing X (2008) J Nanosci Nanotech 8:5066
52. Xing S, Zhao G (2007) Mater Lett 61:2040
53. Sheikh FA, Barakat NAM, Kanjwal MA, Chaudhari MA, Jung IH, Lee JH, Kim HY (2009) Macromol Res 17:688
54. Jeong EH, Yang J, Youk J (2007) Mater Lett 61:3991
55. Lakshman LR, Shalumon KT, Sreeja VN, Jayakumar R, Nair SV (2009) J Macromol Sci Pre Appl Chem A47:1012
56. Kong H, Jang J (2006) Chem Commun 28:3010
57. Jin WJ, Jeon HJ, Kim JH, Youk JH (2007) Syn Metals 157:454
58. Barakat NAM, Woo KD, Kanjwal MA, Choi KE, Khil MS, Kim HY (2008) Langmuir 24:11982
59. Hong KH, Park JL, Hwan Sul IN, Youk JH, Kang TJ (2006) J Polym Sci Polym Phys 44:2468
60. Hong KH (2007) Polym Eng Sci 47:43
61. Chun JY, Kang HK, Jeong L, Kanga YO, Oh JE, Yeo IS, Jung SY, Park WH, Min BM (2010) Coll Surf B: Biointerfaces 78:334
62. Jin WJ, Lee HK, Jeong RH, Park WH, Youk JH (2005) Macromol Rapid Commun 26:1903
63. Jin M, Zhang X, Nishimoto S, Liu Z, Tryk DA, Murakami T, Fujishima A (2007) Nanotechnology 18:075605
64. Bai J, Li Y, Zhang C, Liang X, Yang Q (2008) Colloids Surf A Physicochem Eng Asp 329:1650
65. Bai J, Li Y, Li M, Wang S, Zhang C, Yang Q (2008) Appl Surf Sci 254:4520
66. Chao D, Cui L, Zhang J, Liu X, Li Y, Zhang W, Wang C (2009) Syn Metals 159:537
67. Jie B, Yaoxian L, Lei S, Chaoqun Z, Quingbiao Y (2009) Bicomponent AgCl/PVP nanofibre fabricated by electrospinning with gel-sol method. Bull Mater Sci 32:161
68. Bronstein LM, Polarz S, Smarsly B, Antonietti M (2001) Adv Mater 13:1333
69. Khushalani D, Hasenzahl S, Mann S (2001) J Nanosci Nanotechnol 1:129
70. Chakrabarti K, Whang CM (2002) Mater Sci Eng B88:26
71. Zheng M, Gu M, Jin Y, Jin G (2001) Mater Res Bull 36:853
72. Bharathi S, Nogami M, Ikeda S (2001) Langmuir 17:7468
73. Jiang T, Chen W, Zhao F, Liu Y, Wang R, Du H, Zhang T (2005) J Appl Polym Sci 98:1296
74. Lin KJ, Chen LJ, Prasad MR, Cheng CY (2004) Adv Mater 16:1845
75. Demir MM, Gulgun MA, Menceloglu YZ, Erman B, Abramchuk SS, Makhaeva EE, Khokhlov AR, Matveeva VG, Sulman MG (2004) Macromolecules 37:1787
76. Huang ZM, Zhang YZ, Kotaki M, Ramakrishna S (2003) Compos Sci Technol 63:2223
77. Hayakawa K, Yoshimura T, Esumi K (2003) Langmuir 19:5517
78. Matatov MY, Sheintuch M (2002) Appl Catal A231:1
79. Horner BT (1993) Platinum Met Rev 37:76
80. Neyestanaki AK, Lindfors LE (1994) Sci Technol 97:121
81. Serp P, Corrias M, Kalck P (2003) Appl Catal A253:337
82. Kang H, Zhu Y, Yang X, Jing Y, Lengalova A, Li C (2010) J Coll Interface Sci 341:303
83. Yao C, Li X, Neoh K, Shi Z, Kang E (2008) J Membr Sci 320:259
84. Lala N, Ramaseshan R, Bojun L, Sundarrajan S, Barhate R, Ying-Jun L, Ramakrishna S (2007) Biotechnol Bioeng 97:1357
85. Ag S (2003) FEMS Microbiol Rev 27:341
86. Melaiye A, Sun Z, Hindi K, Milsted A, Ely D, Reneker D, Tessier C, Youngs W (2005) J Am Chem Soc 127:2285

Index